PGC-1α modulates skeletal muscle regeneration by affecting immune response and satellite cell behavior

Inauguraldissertation

zur
Erlangung der Würde eines Doktors der Philosophie
vorgelegt der
Philosophisch-Naturwissenschaftlichen Fakultät
der Universität Basel

von

Ivana Dinulović

aus Serbien

Basel, 2014

Genehmigt von der Philosophisch-Naturwissenschaftlichen Fakultät
auf Antrag von

Prof. Dr. Christoph Handschin

Prof. Dr. Markus Rüegg

Basel, den 11.11.2014

Prof. Dr. Jörg Schibler, Dekan

Table of Contents

1 Abbreviations

AAV	adeno-associated virus
Ad	adenovirus
Akt (PKB)	protein kinase B
ALS	amyotrophic lateral sclerosis
Amp	ampicillin
AMPK	5' AMP-activated protein kinase
Anxa1	annexin A1
Anxa6	annexin A6
Arg-1	arginase 1
ATF2	activating transcription factor 2
ATP	adenosine triphosphate
AV	average
BAT	brown adipose tissue
bFGF (FGF2)	basic fibroblast growth factor
BSA	bovine serum albumin
CaMKIV	calcium/calmodulin-dependent protein kinase type IV
CBP	CREB-binding protein
CD133	prominin-1
CEE	chicken embryo extract
ChIP-Seq	chromatin immunoprecipitation- sequencing
CK	creatine kinase
c-Met (HGFR)	hepatocyte growth factor receptor
CMV	cytomegalovirus
CnA	calcineurin A
Cox5b	cytochrome c oxidase subunit 5B, mitochondrial
CREB	cAMP response element-binding protein
CT	X-ray computed tomography
CTX	cardiotoxin
CycS	cytochrome c, somatic
d	day(s)
D2R	dopamine type 2 receptor
DAPI	4',6-diamidino-2-phenylindole
db	diabetic
DHR	downhill running
DMD	Duchenne muscular dystrophy

DMEM	Dulbecco's modified Eagle's medium
DTT	dithiothreitol
Dysf	dysferlin
EBD	Evans blue dye
ECM	extracellular matrix
EDL	extensor digitorum longus muscle
EDTA	ethylene diamine tetraacetic acid
EGTA	ethylene glycol tetraacetic acid
e	embryonic
ER	estrogen receptor
ERR	estrogen-related receptor
FACS	fluorescence-activated cell sorting
FAO	fatty acid oxidation
FAP	fibro/adipogenic progenitor
FBS	fetal bovine serum
FDG	2-deoxy-2-[18F]-fluoro-D-glucose
FGF-2 (bFGF)	fibroblast growth factor 2
FGFR1	fibroblast growth factor receptor 1
FI	fusion index
FMISO	[18F]-fluoroiminidasole
FN	fibronectin
FoxO	forkhead box protein O
Fzd7	frizzled-7
G0	resting phase
GABP (NRF2)	GA-binding protein
GAlert	alerted state of resting phase
Gastro	gastrocnemius muscle
GCN5	histone acetyltransferase GCN5
GFP	green fluorescent protein
Glut4	glucose transporter type 4
GOI	gene of interest
h	hour(s) or human
H&E	hematoxylin and eosin stain
HA	influenza hemagglutinin
HEPES	2-[4-(2-hydroxyethyl)piperazin-1-yl]ethanesulfonic acid
HFD	high-fat diet
HGF	hepatocyte growth factor

hMPCs	human muscle precursor cells
HNF4α	hepatocyte nuclear factor 4 alpha
HS	horse serum
HSA	human α-skeletal actin
HSC	hematopoietic stem cell
Hz	hertz
Ig	immunoglobulin
IGF-1	insulin-like growth factor 1
IHC	immunohistochemistry
IL-1	interleukin 1
IL-10	interleukin 10
IL-4Rα	interleukin 4 receptor alpha
IL-6	interleukin 6
im	intramuscular
inj	injection
ip	intraperitoneal
Itga7	integrin 7alpha
KD	knock-down
KifC3	kinesin family member C3
LA	Luria-Bertani Agar
LARGE	like-acetylglucosaminyltransferase
LB	Luria-Bertani broth
LDH	lactate dehydrogenase
LGMD 2B	limb-girdle muscular dystrophy type 2B
LKB1	liver kinase B1
M	macrophage
MAPK	mitogen-activated protein kinase
MB	myoblast
MCK	muscle creatine kinase
MCOLN1	mucolipin-1
MCP-1 (CCL2)	monocyte chemotactic protein 1
Mdx	mouse model of DMD
MEF2	myocyte enhancer factor 2
MG53 (TRIM72)	mitsugumin 53
min	minute(s)
MIP-1α (CCL3)	macrophage inflammatory protein 1alpha
MIP-1β (CCL4)	macrophage inflammatory protein 1beta

mKO	muscle-specific knock-out
MMP	matrix metalloproteinase
MOI	multiplicity of infection
MRF-4 (Myf6)	myogenic regulatory factor 4, herculin
mRFP	monomer red fluorescent protein
MRFs	myogenic regulatory factors
ms	millisecond(s)
Mstn (GDF-8)	myostatin
MT	myotube
mTG	muscle-specific transgenic
mTORC1	mammalian target of rapamycin complex 1
Myc	avian myelocytomatosis viral oncogene homolog
Myd	myodystrophy
Myf5	myogenic factor 5
MyHC	myosin heavy chain
Na3VO4	sodium orthovanadate
Na4P2O7x10H2O	sodium pyrophosphate decahydrate
NADH	nicotinamide adenine dinucleotide (reduced)
NaF	sodium fluoride
NFκB	nuclear factor kappa B
NMJ	neuromuscular junction
NO	nitrogen monoxide
NRF1	nuclear respiratory factor 1
ob	obese
OCT	optimal cutting temperature compound
OE	overexpression
OXPHOS	oxidative phosphorylation
p16 (CDKN2A)	cyclin-dependent kinase inhibitor 2A
p300	E1A binding protein p300
PAGE	polyacrylamide gel electrophoresis
Pax7	paired box 7
PBS	phosphate buffered saline
PET	positron emission tomography
PFA	paraformaldehyde
PGC-1	peroxisome proliferator-activated receptor γ coactivator 1
PI3K	phosphatidylinositol-4,5-bisphosphate 3-kinase
PIP3	phosphatidylinositol (3,4,5)-trisphosphate

PKA	cAMP-dependent protein kinase
PML	promyelocytic leukemia protein
PPAR	peroxisome proliferator-activated receptor
PRC	PGC-1-related coactivator
pS6	phospho-S6 ribosomal protein
PVDF	polyvinylidene difluoride
QU	quadriceps muscle
Rab27b	Ras-related protein Rab-27B
Rab3a	Ras-related protein Rab-3A
RER	respiratory exchange ratio
RFP	red fluorescent protein
ROS	reactive oxygen species
RT	room temperature
s	second(s)
SC	satellite cell
sc	subcutaneous
Sdc4	syndecan-4
SDM	site-directed mutagenesis
SDS-PAGE	sodium dodecyl sulfate polyacrylamide gel electrophoresis
SEM	standard error of the mean
Sirt1	NAD-dependent deacetylase sirtuin-1
SNAP	soluble N-ethylmaleimide-sensitive factor (NSF) attachment protein
SNARE	SNAP receptor
SOL	soleus muscle
Spry1	sprouty 1
SRC-1	steroid receptor coactivator 1
Syt7	synaptotagmin VII
Sytl2	synaptotagmin-like 2
T0	time point zero
T3	time point 3 days
TA	tibialis anterior muscle
TBP	TATA box binding protein
TFAM	mitochondrial transcription factor A
TGF-β	transforming growth factor beta
TNC	tenascin-C
TNF-α	tumor necrosis factor alpha, cachexin
TR	thyroid hormone receptor

TrisHCl	2-Amino-2-hydroxymethyl-propane-1,3-diol hydrochloride
Vamp1	vesicle-associated membrane protein 1
VEGF	vascular endothelial growth factor
Vis	visceral
WAT	white adipose tissue
Wnt7a	wingless-type MMTV integration site family, member 7A
WT	wild type
YFP	yellow fluorescent protein
α-SMA (ACTA2)	alpha smooth muscle actin

2 Summary

The benefits of exercise on wellbeing have been known to mankind for thousands of years, yet the underlying mechanisms of exercise have been explained only relatively recently. Today we know that lack of exercise is associated with many chronic pathologies, and that regular moderate exercise, on the other hand, can improve human health. Signaling pathways activated by endurance exercise lead to skeletal muscle adaptations, and at the core of these adaptations lies peroxisome proliferator-activated receptor γ coactivator 1α (PGC-1α). These modulations brought about by PGC-1α enhance muscle endurance, and protect against several atrophic conditions. In addition, endurance exercise has been shown to increase the number of satellite cells and regenerative potential of skeletal muscle. However, in some pathologies, exercise is not an option for improvement of systemic and muscle phenotype.

Interestingly, experiments in mice have revealed that overexpressing PGC-1α mimics the effects of exercise, and that this is associated with a fiber type switch towards a more oxidative phenotype. Although PGC-1α was shown to palliate dystrophic condition by protecting muscles from damaging effects of contractions, PGC-1α's effects on satellite cells and regeneration have not been investigated. In addition, the causes of the protective role of PGC-1α in muscle have not been elucidated.

Using mouse models with overexpression and deletion of PGC-1α specifically in skeletal muscle, in combination with cardiotoxin injury, we have investigated the contribution of PGC-1α to skeletal muscle regeneration. Our results indicate that PGC-1α improves muscle's initial response to injury resulting in a faster removal of necrotic tissue. Additionally, PGC-1α reduces fibrosis development in a model of chronic damage. Considering the PGC-1α levels in regenerating muscles, these differences were probably driven by the preexisting milieu of muscle residing inflammatory cells dependent on PGC-1α expression in myofibers, and were associated with myostatin and insulin-like growth factor 1 (IGF-1) levels prior and after injury, respectively. However, overall regeneration was neither impaired nor improved with PGC-1α deletion or overexpression.

We detected a reduction in satellite cell numbers in PGC-1α overexpressing mice. This was surprising, given that oxidative fibers contain more satellite cell. *Ex vivo* experiments further revealed that PGC-1α levels also influence satellite cell response to activating stimuli, and that increased PGC-1α in the fiber (satellite cell niche) results in faster activation and proliferation of these cells. The effect on satellite cell behavior was at least partially due to reduced fibronectin levels in the basal lamina of transgenic mice. Deletion of PGC-1α from satellite cells and their niche resulted in the opposite phenotype.

We also sought to explore the mechanism through which PGC-1α increases protection in dystrophic skeletal muscle. In transgenic mice, we detected increased synaptotagmin VII, the deletion of which results in myopathy. On the other hand, knocking-down PGC-1α in C2C12 myoblasts reduced the resealing capacity of the sarcolemma. In addition, an increase in integrin 7α observed after exercise was absent in PGC-1α knock-out mice. These results suggest increased sarcolemma stability and propensity for repair dependent on PGC-1α levels in muscles.

Finally, in a proof-of-principal study addressing applications in regenerative medicine, we wanted to explore whether adenoviral delivery and induction of PGC-1α in human myoblasts can improve skeletal muscle formation after myoblast transplantation. Apart from the foreseen benefits based on previously published research, we can speculate that PGC-1α might surpass our expectations and significantly improve not just the survival and function of newly-formed tissue, but also, based on the data presented here, improve the regenerative capabilities of skeletal muscle.

The results reported here could potentially expand the therapeutic benefits of PGC-1α induction in skeletal muscle myopathies. However, further research is necessary in order to fully understand these effects before using PGC-1α to facilitate skeletal muscle repair and regeneration, especially having in mind the discrepancies in PGC-1α induction and oxidative fiber phenotypes in relation to satellite cell numbers.

3 Introduction

3.1 PGC-1α – structure, regulation and function

A balanced metabolism is essential for normal functioning of living organisms. Varying conditions require high plasticity in regulating metabolic processes and adaptation to changes such as food availability or deprivation, or high physical activity and rest. In the past years, it has become clear that adaptations to ever changing conditions are regulated on the transcriptional level (1), which drew much attention to transcription factors and their role in controlling gene expression. However, recently, coactivators took center stage in regulating metabolic equilibrium, as they were recognized as integrating factors that are able to detect and react to various stimuli and in turn control multiple downstream signaling pathways though interaction with a plethora of transcription factors (2). An excellent example of one such factor is the peroxisome proliferator-activated receptor γ coactivator 1α (PGC-1α).

PGC-1α was first detected in brown adipose tissue as a factor controlling the transcription program of adaptive thermogenesis (3). It was the first member of the coactivator family to be discovered. Two other members, peroxisome proliferator-activated receptor γ coactivator 1β (PGC-1β) and PGC-1-related coactivator (PRC), have similarity in sequence and therefore some overlapping functions with PGC-1α, but they remain less studied (4, 5). Although primarily known for its pivotal role in mitochondrial biogenesis and oxidative metabolism, PGC-1α has many other tissue-specific roles (6). It is highly expressed in metabolically active organs such as brain, heart, brown adipose tissue (BAT), muscle, kidney, liver. In general, PGC-1α is induced in energy demanding conditions. Therefore, stimuli such as fasting, cold or exercise increase its expression in liver, BAT, and skeletal muscle, respectively. In turn, in addition to increased mitochondrial biogenesis and respiration, PGC-1α induces gluconeogenesis in liver, adaptive thermogenesis in BAT and a fiber type switch in skeletal muscle tissue (7). In this text, aspects of PGC-1α's structure, regulation and function in skeletal muscle compared to other organs are emphasized.

3.1.1 Structure of PGC-1α

Sequencing of PGC-1α has revealed several distinct regions (Figure 1). PGC-1α does not possess histone modifying abilities, but its N-terminus contains an activation domain through which it is able to bind histone acetyl-transferases (HAT) cAMP response element-binding protein-binding protein/E1A binding protein p300 (CBP/p300) and steroid receptor coactivator 1 (SRC-1) (8). These enzymes induce structural changes in chromatin, making it more accessible to different DNA binding proteins, thereby facilitating transcription. The transcriptional repression domain contains a binding site for p160 myb binding protein, which attenuates its transcriptional activity (9). The C-terminus of PGC-1α contains an Arg/Ser rich domain and an RNA binding domain. Through these regions PGC-1α binds mediator complex (10) and processes RNA during transcription (11). In addition, PGC-1α is able to bind and coactivate a multitude of transcription factors, some of which bind through the three LXXLL motives present in the PGC-1α sequence. After the discovery of the first binding partners of PGC-1α, the nuclear receptors peroxisome proliferator-activated receptor γ (PPARγ) and thyroid hormone receptor (TR) (3), many other transcription factors were found to interact with PGC-1α. Those include additional nuclear receptors such as peroxisome proliferator-activated receptor α (PPARα), peroxisome proliferator-activated receptor β/δ (PPARβ/δ), estrogen receptor α (ERα), estrogen-related receptor α (ERRα), estrogen-related receptor γ (ERRγ), hepatocyte nuclear factor 4 α (HNF4α), but also non-nuclear receptors such as forkhead box protein O1 (FoxO1), forkhead box protein O3a (FoxO3a), nuclear respiratory factor 1(NRF1), nuclear respiratory factor 2 (NRF2, also known as GABP) and myocyte enhancer factor 2 (MEF2).

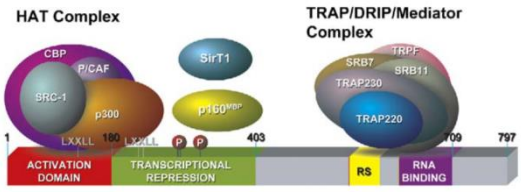

Figure 1 Structure of PGC-1α; adapted from (6)

Long after the discovery of PGC-1α, different splice variants of this coactivator started to emerge (Figure 2). Today, we are aware of the existence of seven isoforms (12); the nomenclature has not been agreed upon, and is somewhat simplified in the text below. Apart from the full length PGC-1α described initially (now known as PGC-1αa), the discovery of an alternative promoter (13-15) unveiled two additional isoforms: PGC-1αb and PGC-1αc, transcribed from different start sites. The NT-PGC-1α isoform is transcribed from the proximal promoter as PGC-1αa, yet is much shorter due to stop codon formation due to an alternative splicing event (16). Recently, three new PGC-1α splice variants have been described: PGC-1α2, PGC-1α3 and PGC-1α4 (17). Unlike the full length splice variant, PGC-1α4 was shown to induce skeletal muscle hypertrophy but not mitochondrial biogenesis (17). However, apart from PGC-1α4, specific functions of the other isoforms are not known. Specificity in expression patterns has been described for some of these. For example, exercise in skeletal muscle tissue induces expression of isoforms transcribed from the alternative promoter, and these isoforms can also be found in BAT and heart, but not liver (13).

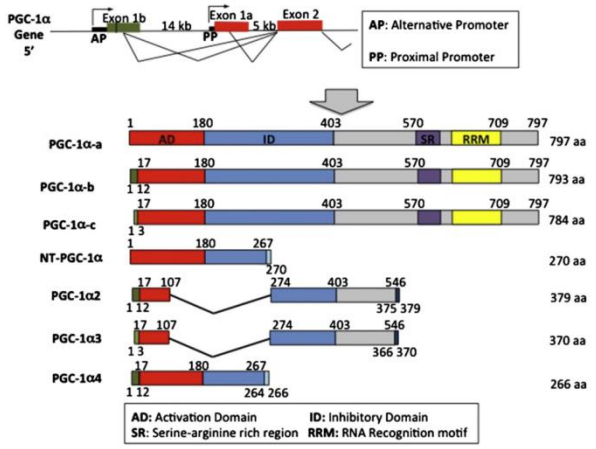

Figure 2 Different isoforms of PGC-1α; adapted from (12)

3.1.2 Regulation of PGC-1α

PGC-1α is extensively regulated both on transcriptional and post-translational levels (Figure 3). A wide diapason of stimuli activates several signal transduction pathways that

converge on regulating the levels and activity of PGC-1α, and some of the most important ones are described below.

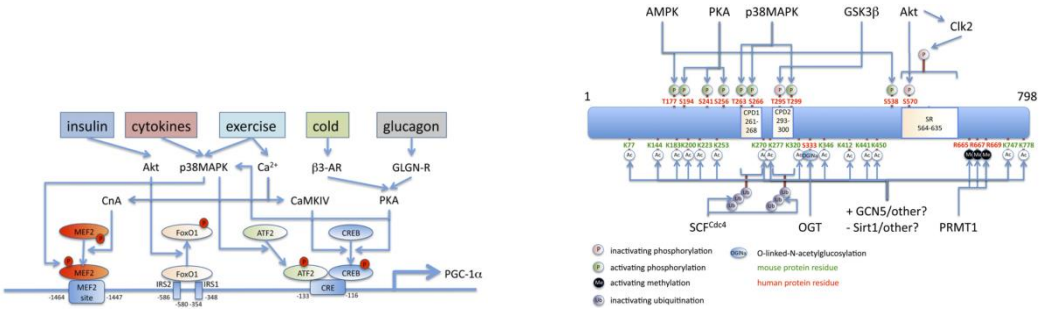

Figure 3 Transcriptional and post-translational regulation of PGC-1α; from (7)

In the liver, glucagon signals low levels of plasma glucose and activates PKA, which in turn by phosphorylating cAMP response element-binding protein (CREB) induces PGC-1α expression (18). In response, PGC-1α induces the gluconeogenic program. In BAT, cold triggers a similar signaling cascade to induce PGC-1α expression, resulting in activation of the adaptive thermogenic program (3, 19).

In skeletal muscle, PGC-1α is induced by exercise, cold and low energy status. Contractions on one hand increase Ca^{2+} signaling and, through the calcineurin A (CnA)-MEF2 axis or the calcium/calmodulin-dependent protein kinase type IV (CaMKIV)-CREB axis, boost PGC-1α levels (19, 20). On the other hand, exercise results in p38 mitogen-activated protein kinase (p38MAPK) activation through β2-adrenergic signaling, which leads to increased PGC-1α expression through phosphorylation of MEF2 (21) and activating transcription factor 2 (ATF2) (22). 5' AMP-activated protein kinase (AMPK) gets activated in low energy states (e.g. during exercise), and increases PGC-1α levels through a yet unknown mechanism (23, 24). Another regulator of PGC-1α expression in muscle is protein kinase B (PKB, also known as Akt) , which reduces PGC-1α levels through phosphorylation of FoxO1 upon insulin signaling (25). In addition, p38MAPK and AMPK control PGC-1α activity through direct phosphorylation events, which increase its activity (9, 26, 27). Besides phosphorylation, other post-translational modifications such as acetylation and methylation are also employed in controlling PGC-1α activity or protein stability. Therefore, for example, in low energy states, nicotinamide adenine

dinucleotide- dependent deacetylase sirtuin-1 (Sirt1) will deacetylate and activate PGC-1α, a step that is counteracted by the histone acetyltransferase GCN5 (28, 29).

3.1.3 Function of PGC-1α

Besides being a major driver of oxidative metabolism through increased mitochondrial biogenesis (30) and fatty acid oxidation (31, 32), PGC-1α has many other tissue-specific roles (Figure 4). Many of these additional roles are also metabolic – like fasting-induced gluconeogenesis in liver (33) or adaptive thermogenesis in BAT (3).

In skeletal muscle, PGC-1α induces glucose uptake, glycogen synthesis and lipogenesis (34, 35). In addition, it induces vascularization (36) and oxidative fiber type predominance (37). All these adaptations result in increased endurance capacity of muscle tissue. This knowledge has been gathered through the use of muscle-specific knock-out and transgenic animals that result in loss or overexpression of PGC-1α, respectively.

However, many of PGC-1α's roles in skeletal muscle are not primarily metabolic. For example, in addition to an oxidative fiber type switch and vascularization, PGC-1α increases anti-oxidative defense, reduces inflammation and induces neuromuscular junction (NMJ) remodeling (38-42). These adaptations have proven important for skeletal muscle and whole body maintenance in aging (42). One possible explanation, that recently drew much attention, for the effects of PGC-1α levels in muscle on whole body metabolism and wellbeing, is secretion of myokines (43, 44). Skeletal muscle PGC-1α has a protective role in some forms of atrophy and dystrophy as well, although the mechanisms behind this are not thoroughly elucidated (39, 41, 45-49).

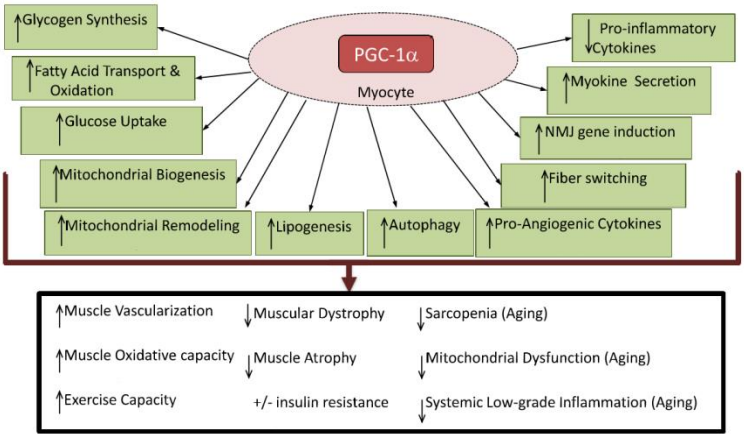

Figure 4 Roles of PGC-1α in skeletal muscle; adapted from (12)

PGC-1α regulates different pathways in combination with various transcription factors. For example, mitochondrial biogenesis and oxidative phosphorylation are induced through increase in electron transport chain proteins and mitochondrial transcription factor A (TFAM), whose expression PGC-1α drives together with the NRF1, NRF2 and ERRα transcription factors (30). On the other hand, vascularization is accomplished partially through increased vascular endothelial growth factor (VEGF) production in cooperation with ERRα (36), and a fiber type switch, through regulation of troponin I (slow) and myoglobin expression in combination with MEF2 (37). However, some pathways regulated by PGC-1α remain vaguely defined, such as ones that result in phenotypic alleviation in dystrophy or aging.

3.2 Skeletal muscle regeneration and repair

Skeletal muscle tissue is essential for voluntary activities and enables breathing, posture and movement. In addition, it is a very important metabolic organ that comprises ~40% of the human body (50). Due to its high significance, it is not surprising that it has a great capacity for regeneration. Skeletal muscle is a relatively stable tissue, measured by infrequent turnover of myonuclei (51). Yet, upon injury, it will quickly respond to compensate for the loss of damaged myofibers.

Skeletal muscle regeneration is a complex processes that requires the cooperation of a multitude of cell types. Apart from auxiliary cells types, such as immune cells (mast cells, neutrophils, macrophages) and fibroblasts, many cells with myogenic potential can participate in skeletal muscle regeneration (satellite cells, side population cells, perycites, mesoangioblasts, bone marrow cells, $CD133^{+}$ cells) (52, 53). In addition, secreted factors coming from degenerating/regenerating fibers and immune cells, but also blood vessels and motor neurons, actively participate in skeletal muscle regeneration through autocrine, paracrine and endocrine signaling.

Skeletal muscle regeneration can be roughly separated into three phases: 1) skeletal muscle degeneration and inflammation, 2) precursor proliferation and myotube formation and 3) skeletal muscle maturation and functional recovery (54). This process is triggered by a harmful event that results in myotube necrosis; for example, due to damage to the skeletal muscle membrane, the sarcolemma, which overwhelms the cell's capacity for quick resealing. However, if the impact of the damage is not too pronounced and affects only a small portion of the sarcolemma, repair can prevent myotube death, and consequently, the complex and energy consuming process of regeneration (Figure 5) (55).

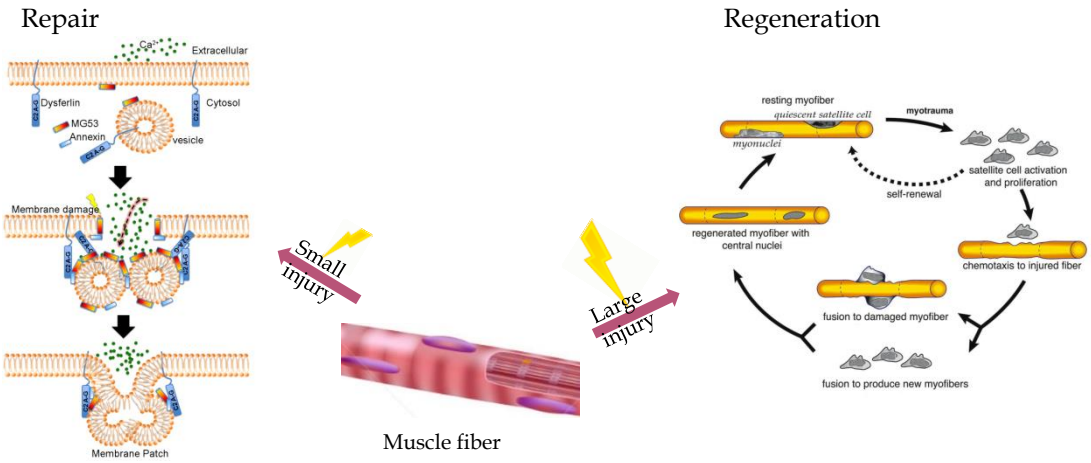

Figure 5 Skeletal muscle regeneration and repair: adapted from (56, 57) and www.shutterstock.com and www.clipartpal.com

3.2.1 Repair of muscle fibers – membrane resealing

The sarcolemma is exposed to everyday mechanical tensions due to contractions of skeletal muscles. Therefore, its stability and capacity for self-repair is a prerequisite for unimpeded muscle function. Many cell types have the ability to reseal ruptures in their membranes, and this process becomes especially important for mechanically active tissues, such as skeletal muscle (55). Tears in the sarcolemma initiate a series of events that leads to the recruitment and dispatching of internal membrane structures to the site of the damage, resulting in patch formation and membrane resealing (58). These processes are not fully delineated. Current research suggests that membrane opening results in changes in redox state sensed by the mitsugumin 53 (MG53) protein present in membranes (59). This protein participates in membrane patch creation and vesicle translocation through an oxidation-dependent oligomerization event. In the end, dysferlin and auxiliary proteins participate in Ca^{2+} dependent resealing (60, 61).

Inability to repair membrane damage results in the leaky membrane phenotype, and can be detected with membrane impermeable fluorescent dyes, both *in vitro* and *in vivo*, as well as by measuring serum levels of muscle-specific proteins (e.g. creatine kinase). However, the leaky phenotype can also be the outcome of membrane instability, and therefore is not *per se* a readout for resealing problems (62). In that regard, current data indicate that the absence of dystrophin

leads to a destabilized sarcolemma due to Ca^{2+} entry through the stretch-induced channels that can become leaky with increased reactive oxygen species (ROS) production (60, 62). However, these events are also poorly understood.

3.2.2 Degeneration of muscle fibers – necrosis and inflammation

When damage to the fiber or sarcolemma surpasses the cell's capacity for repair, either partial or full necrosis will follow. Limited muscle insults will result in partial fiber necrosis. In these circumstances, the membrane will reestablish at the damaged site and regeneration will enable recovery of the fibers. In the event of severe injury, complete necrosis will occur, leaving an empty fiber scaffold comprised of extracellular matrix components. Regeneration in this case designates *de novo* myogenesis (53, 57).

The first step in muscle regeneration is muscle degeneration, comprised of necrosis and inflammation. Necrosis is uncontrolled, pro-inflammatory cell death (63). It is characterized by increased Ca^{2+} cytosolic concentration, leading to activation of calcium-dependent proteases (e.g. calpains) and disintegration of cellular components (53). Within seconds to minutes, the first cells to respond to the changes in environment caused by cell debris formation are skeletal muscle resident mast cells and macrophages (64, 65). They start to secrete pre-synthesized chemokines (e.g. tumor necrosis factor α (TNF-α), interleukin 1 (IL-1), IL-6) in order to attract immune cells from the bloodstream (66). The initial recruitment involves neutrophils, which invade the muscle within minutes to hours. They secrete more chemokines (e.g. monocyte chemotactic protein 1 (MCP-1), macrophage inflammatory protein 1α (MIP-1α), MIP-1β) and therefore amplify the inflammatory signal (67, 68). The neutrophils are slowly replaced with monocytes after the first day of injury. The recruited monocytes differentiate into macrophages once they enter the damaged muscle tissue (64). These cells are very plastic, and depending on their environment they can act as more classically activated (proinflammatory, M1), alternatively activated (M2a) or anti-inflammatory (M2b and M2c) macrophages (69). Their phenotypic make-up is characterized by synthesis and secretion of specific cytokines that can further propagate inflammation, favor engulfment of cell debris, or signal reduction in the inflammatory phase, respectively (65). In addition, the resulting environment is conductive to progenitor

activation and proliferation (M1 macrophage-driven), or differentiation (M2 macrophage-driven) (70).

Inflammation is a necessary step for successful skeletal muscle regeneration, with the timing and duration of each wave of inflammation being tightly controlled (71, 72). In that respect, delayed or reduced inflammation as well as prolonged or excessive inflammation, can be equally detrimental (73, 74). While a hindered inflammatory response slows or blocks the regenerative process due to inability to clear necrotic tissue, sustained inflammation leads to fibrotic tissue formation and prevention of full functional recovery of muscle tissue (75-77).

3.2.3 Satellite cells

Satellite cells (SCs) are mitotically quiescent and transcriptionally inactive adult muscle stem cells located at the myofiber periphery, as the name suggests, between the sarcolemma and basal lamina (78, 79). When dormant, SCs are characterized by a thin rim of cytoplasm, small number of organelles and condensed state of chromatin (80). They represent only 2-5% of myonuclei, yet can provide a life-long supply of precursor cells for skeletal muscle regeneration and postnatal muscle growth (81). The initial method for their detection was electron microscopy. Today, thanks to the discovery of several markers, SCs can be easily observed using fluorescence microscopy. A widely used marker is paired-box transcriptional factor Pax7, which is specifically expressed only by SCs in skeletal muscle and is essential for SC lineage formation and function (82, 83).

Although a variety of precursors both from and outside of muscle tissue can contribute to muscle regeneration, SCs are recognized as cells necessary for this process (84-87). As true stem cells, they: 1) can become activated and proliferate in order to regenerate damaged tissue, 2) are multipotent and apart from skeletal muscle, can be induced towards adipogenic and osteogenic lineages, and 3) have the potential to self-renew, ensuring a constant supply of stem cells for future rounds of degeneration/regeneration (88-92).

3.2.3.1 Satellite cell niche

The satellite cell niche represents a local microenvironment that supports SC quiescence and controls the behavior of satellite cells (93). Due to their specific location, just outside of the muscle fiber, SCs are in a position to receive various signals coming from different environments (Figure 6). They can sense changes in the muscle fiber, basal lamina of extracellular matrix (ECM) and respond to secreted factors from motor neurons, blood vessels, fibroblasts, immune and other cells.

The immediate niche of SCs is comprised of the basal lamina and myofiber (80), and its effects can be explored *ex vivo*, using isolated fibers. SCs expose α7β1 integrins on the basal lamina side of the membrane, through which they bind laminin (94). The apical membrane of SCs, on the other hand, expresses the docking molecule M-Cadherin and Notch receptor, through which SCs can bind Delta ligand expressed by myofibers upon injury (95-97). This differential expression of cell surface receptors forms the basis for cell polarity and asymmetric cell expansion (98).

Many growth factors, synthesized and secreted primarily by fibroblasts, reside in the ECM in a bound, and therefore inactive form. Once liberated (e.g. by contraction-induced shedding), they can bind to receptors in the SC membrane and induce an appropriate response (80). In addition, basal lamina components themselves can influence SC activation and proliferation, and therefore their myogenic potential. In that respect, the basal lamina thickening observed in aging reduces SCs' propensity to activate (99).

Interestingly, SCs are not uniformly present throughout muscle fibers, but rather demonstrate a tendency to congregate around blood vessels and the NMJ, suggesting that signals coming from these entities are important for SC behavior (100, 101). In addition, they are present in higher numbers in oxidative fibers and muscles, compared to glycolytic ones (102). However, how the metabolic status of the fiber might influence SCs is not known (103). It is also unclear whether there are some intrinsic differences between SCs from glycolytic vs. oxidative fibers, and what the reason for the differences in SC numbers might be. Endurance exercise, which induces a fast-to-slow fiber type switch, was shown to increase SC numbers (104).

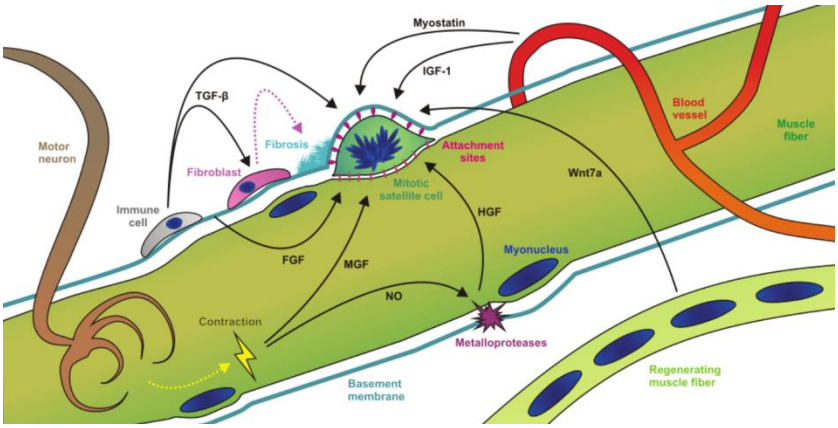

Figure 6 Satellite cell niche (105)

3.2.3.2 Quiescence and activation

As previously mentioned, SCs are metabolically quiescent under homeostatic conditions and reside in the resting (G_0) state. However, damage and contraction elicit their activation, after which they enter the cell cycle. Depending on the stimulus, SCs can just be transiently activated, or they can proliferate and fuse in order to repair damaged fibers or contribute to fiber growth (106). A very useful marker to detect SC activation vs. quiescence is Ki67, which is expressed in all stages of the cell cycle except for G_0 (107, 108). However, recent research has challenged our understanding of SC dormancy and indicated that the situation is more complex.

Currently, we can differentiate between two stages of quiescence – full quiescence (G_0) and alertness (G_{Alert}) (109). It has been demonstrated that SCs in G_{Alert} do not express Ki67, yet they are able to respond to injury in a much faster manner compared to cells in G_0, and as a consequence, regenerate skeletal muscle faster. Interestingly, factors coming from other muscles or even other tissues can provoke a transition in SC state, confirming the importance of endocrine secreted factors in SC behavior. Mammalian target of rapamycin complex 1 (mTORC1) signaling and the upstream hepatocyte growth factor (HGF)/c-Met axis of signal reception have proven essential for this switch.

c-Met is a receptor tyrosine kinase present on SCs of the muscle fiber, and together with its ligand HFG, initiates the pathway of initial SC activation (110). Upon contraction, Ca^{2+} signaling leads to increased nitrogen monoxide (NO) levels in myofibers and consequently to

activation of matrix metalloproteinases (MMPs), which cleave ECM-bound HGF and allow its binding to c-Met (111). Another important modulator of SC activation is myostatin (Mstn), which keeps SCs in a quiescent state (112). Interestingly, not only Mstn levels in SCs, but also in the SC niche (myofiber) influence SC behavior (113).

3.2.3.3 Proliferation and maintenance

Upon injury, quiescent SCs become activated and start proliferating in order to provide precursor cells for muscle regeneration. SCs' return to quiescence is as important as SC activation. Repeating rounds of degeneration/regeneration of muscle tissue, or otherwise induced constant activation of SCs, or their inability to return to quiescence, all lead to SC depletion and skeletal muscle deterioration. Apart from constant injury observed in dystrophy, aging can also lead to chronic activation of SCs, resulting in a reduction in SCs numbers (114).

SCs represent a heterogeneous population of cells according to their marker expression, but also to their myogenic and self-renewal potential. Myf5 is the earliest myogenic regulatory factor that predisposes SCs to the myogenic commitment (115). Lineage tracing experiments using Myf5-Cre/ROSA-YFP mice have demonstrated that ~90% of the SC population are $Pax7^{+}/YFP^{+}$ – cells that are expressing, were at some point in their life expressing, or are derived from progenitors that expressed Myf5. It has been demonstrated *in vivo* that while both $Pax7^{+}/YFP^{+}$ and $Pax7^{+}/YFP^{-}$ cells can terminally differentiate, only $Pax7^{+}/YFP^{-}$ cells can significantly repopulate the SC niche (89). Furthermore, although both SC subpopulations can divide symmetrically, asymmetrical division was detected only in $Pax7^{+}/YFP^{-}$ cells, and is dependent on the SC niche. Skeletal muscle maintenance may rely primarily on asymmetric division. However, symmetrical division is the preferred choice of self-renewal in response to acute damage, such as after cardiotoxin injection, when stem cells needs to replenish and expand in order to regenerate muscle (98, 116).

In addition to SC renewal through asymmetric and symmetric division, myoblasts' return to quiescence is another way of maintaining the SC pool. This was first reported in *ex vivo* settings, where it was noticed that all $Pax7^{+}$ cells on isolated myofibers start expressing MyoD, but then a certain proportion of them downregulate it and return to quiescence. However, lineage regression was also observed *in vivo*, where sprouty 1 (Spry1), a negative regulator of receptor

tyrosine kinase signaling, proved essential for returning a subset of myogenic progenitors to a quiescent state (117).

3.2.4 Myotube formation – adult myogenesis

Once SCs become activated, they begin expressing myogenic regulatory factors (MRFs). The first to be expressed are Myf5 and MyoD, which destine SCs toward the myogenic lineage. Actively proliferating SCs are called myoblasts, and as they progress further down the myogenesis pathway, they reduce expression of Pax7 and induce expression of myogenin. However, one portion of cells will reduce MyoD and increase Pax7 expression, returning to the dormant state (50, 118).

Once the proliferation phase in over, myoblasts will exit the cell cycle, becoming postmitotic mononuclear myocytes (Figure 7). These cells will fuse together in order to form multinucleated myofibers, the stage for which myogenin and MRF-4 (myogenic regulatory factor 4, also known as Myf6 or herculin) expression is characteristic (50). Newly formed muscle fibers are initially of small caliber, basophilic due to increased protein synthesis, and with centrally located nuclei. Later on, these fibers grow to their original size and the nuclei relocate to the periphery. In the absence of pathology, regenerated muscle is morphologically and physiologically indistinguishable from uninjured muscle (80).

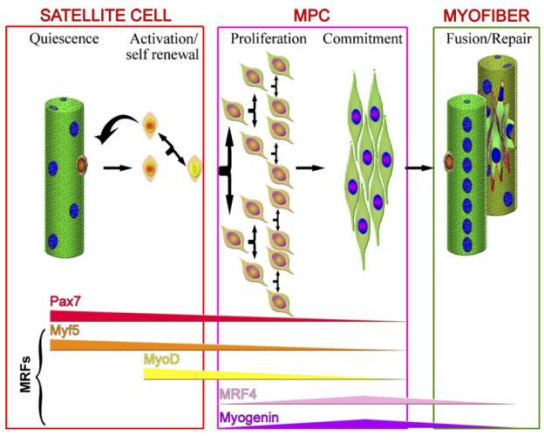

Figure 7 Adult myogenesis (119)

These steps represent adult myogenesis in a nutshell, and are in many ways similar to embryonic events in skeletal muscle tissue formation. The described sequential expression of Pax7 and MRFs enables tracking of myogenesis progression and assessment of the regenerative stage after induced injury (120).

3.2.5 Functional recovery and fibrosis

After myocyte fusion, the newly formed myotubes will continue to grow until they reach their pre-injury size. This process is dependent on protein synthesis, and can be followed using histology through assessment of cross-sectional area (CSA). Myotube size also corresponds to ability to generate force, and therefore the stages of regeneration can also be evaluated through muscle contractility measurements (121).

Another characteristic of skeletal muscle regeneration is scar tissue formation (54). It is comprised of extracellular matrix components, for example various collagens, fibronectin and tenascin-C (122). These components are primarily secreted by muscle resident fibroblasts, and they provide the initial scaffold on which the skeletal muscle is rebuilt after injury. However, this formation of fibrotic tissue needs to be limited in size and duration for successful skeletal muscle regeneration to occur (Figure 8).

Excessive fibrous tissue formation results in the replacement of functional muscle tissue with scar tissue, and therefore reduces skeletal muscle performance (123). Fibrosis is characterized by sustained transforming growth factor β (TGF-β) signaling, which through activated Smad transcription factors leads to overproduction and accumulation of fibronectin and other ECM components (77). Imbalances in communication between myoblasts and fibroblasts, as well as prolonged inflammation, are recognized as driving forces in this pathology (86, 123).

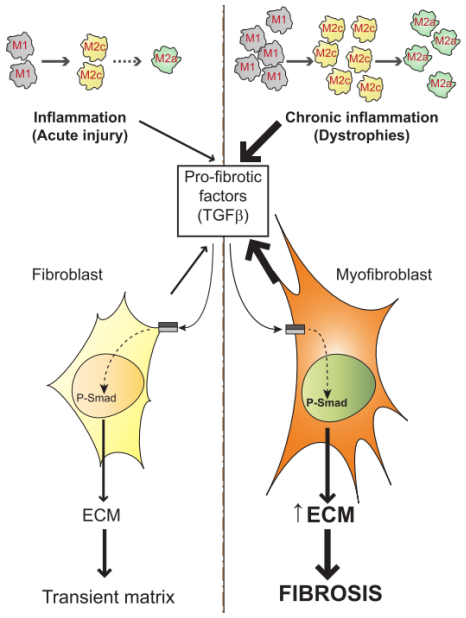

Figure 8 Imbalance in inflammation results in fibrosis (77)

3.2.6 Skeletal muscle regeneration and repair in chronic degenerative diseases, acute traumatic injuries and aging

Skeletal muscle tissue has a vast, albeit not limitless propensity for regeneration. Dystrophic conditions and aging are characterized by chronic changes that drive the loss in regenerative capacity. This might be due to the SC depletion caused by repetitive activation/proliferation, poorer myogenic potential, and SC death (114). The causes might be SC intrinsic or extrinsic, such as changes in the SC niche or circulatory systemic factors (124). In addition, reduced regeneration can also be observed in acute injuries in humans when a large portion of muscle tissue is damaged, without pathological changes affecting SCs (54).

Muscular dystrophies are a heterogeneous group of muscle disorders characterized by skeletal muscle weakness and wasting. Many arise due to various genetic mutations that in most cases affect cytoskeletal proteins. Lack of these proteins makes muscles more prone to the damaging effects of wear-and-tear stemming from everyday contractions, resulting in repetitive cycles of degeneration and regeneration (125). This constant damage is a great burden on the SC population, culminating in SC loss and diminished proliferative capacity resulting in reduced ability to regenerate. It is thought that SC senescence and apoptosis, due to telomere shortening

with every division, but also extrinsic factors such as reduced availability of insulin-like growth factor 1 (IGF-1), are responsible for the pathology (114).

Aging is accompanied by sarcopenia – a decline in skeletal muscle mass and performance, which leads to frailty, morbidity and reduced regenerative capacity. Reduced SC numbers and proliferation have been detected in aged animals, and changes in the environment probably contribute to this muscle phenotype (124, 126). In that regard, recent discoveries have identified several intrinsic and extrinsic factors contributing to diminished SC renewal and SC senescence: fibroblast growth factor 2 (FGF-2) from the niche increases with aging and draws satellite cells out of quiescence, while Spry1, an inhibitor of FGF signaling, maintains SC dormancy. The negative effect of FGF-2 on SC maintenance can be overcome by reducing FGF signaling or overexpressing Spry1 in SCs (127), which decreases with aging. In addition, an increase in p38MAPK signaling accompanied by altered fibroblast growth factor receptor 1 (FGFR1) signaling was observed in SCs of aged mice and resulted in reduced SC self-renewal. These defects could not be overcome in a heterochronic culture experiment, signifying the contribution of SC intrinsic changes in the pathology (128).

Apart from aging and various pathologic conditions, limited regenerative capacity is also observed in acute traumatic injuries. This is not due to changes in SC numbers or behavior, but simply due to the size of the muscle affected, with fibrosis proceeding faster than myogenesis (54). These limitations can be alleviated with transplantation techniques, using biomaterials to bridge the gap resulting from the damaged tissue and providing a scaffold for cells participating in regeneration. These approaches can be combined with cell therapies and growth factors in order to boost vascularization of the nascent tissue (129).

Loss of SC numbers was also observed in other atrophic conditions, such as denervation or immobilization (114). Contrary to that, endurance exercise was shown to increase SC numbers and their myogenic potential in aging (104).

3.3 PGC-1α in skeletal muscle regeneration and repair

PGC-1α has emerged as a junction point of many transduction pathways initiated by various stimuli that signal alterations in the environment to which muscle needs to adapt (6). At the core of these adaptations is increased oxidative metabolism (30-32). Interestingly, oxidative metabolism seems to be central to adult myogenesis (130-132), as illustrated by experiments performed on ERRα and ERRγ mutants (133-135).

Muscle-specific overexpression of PGC-1α leads to increased vascularization and adaptations in NMJ gene expression, which together with mitochondrial biogenesis and slow contractile protein expression result in an oxidative fiber type switch (36, 37, 41). Slow oxidative fibers are more resistant to various atrophic conditions (e.g. fasting, glucocorticoids, sepsis, cancer cachexia, diabetes) compared to glycolytic fibers, and this protection might result from higher expression of PGC-1α in oxidative muscles (45, 136). In addition, vascularization and innervation are essential for the proper functioning and survival of muscle tissue upon cell transplantation, and are one of the major limiting factors in regenerative medicine (137).

The major stimulus that initiates PGC-1α induction and consequently the aforementioned adaptations in skeletal muscle under physiological conditions is endurance exercise (138, 139). Interestingly, such an exercise regimen increases SC numbers and also improves SC myogenic capacity in aging rats (104). In addition, it has been long known that oxidative muscles and fibers contain higher numbers of SCs than glycolytic ones (102). However, in which way metabolic properties of fibers affect SC numbers and behavior is underexplored (103).

Contrary to PGC-1α transgenic mice, muscle-specific knock-out mice exhibit a mirrored phenotype and are prone to mild myopathy (39). Due to the beneficial muscle features driven by PGC-1α expression, in addition to exploring its metabolic roles, research has also been directed towards evaluating PGC-1α's effects on muscle pathologies. For example, on several occasions researches have assessed the outcome of PGC-1α overexpression in Duchenne muscular dystrophy (DMD) mouse model (*mdx*) (41, 46-48). Oxidative fiber type switch, induced expression of markers of regeneration and dystophin-glycoprotein complex components are some modulations that were reported to alleviate the dystrophic phenotype. There was even some speculation regarding improvement in regenerative potential (47), although most of their

conclusions were based on increased protection to muscle tissue (41). This protective effect indicates improved membrane stability and/or membrane resealing after damage.

Protective effects of PGC-1α on muscle tissue were also demonstrated in other pathologies, such as mitochondrial myopathy (49), statin induced myopathy (140) and amyotrophic lateral sclerosis (ALS) (141). Additionally, PGC-1α was shown to reduce muscle loss in fasting and denervation induced atrophy (45) as well as in sarcopenia, where systemic effects of overexpressed PGC-1α in muscle tissue were reported, increasing the longevity of these mice (42).

3.4 References

1. Chawla, A., Repa, J. J., Evans, R. M., and Mangelsdorf, D. J. (2001) Nuclear receptors and lipid physiology: opening the X-files. *Science* **294**, 1866-1870
2. Spiegelman, B. M., and Heinrich, R. (2004) Biological control through regulated transcriptional coactivators. *Cell* **119**, 157-167
3. Puigserver, P., Wu, Z., Park, C. W., Graves, R., Wright, M., and Spiegelman, B. M. (1998) A cold-inducible coactivator of nuclear receptors linked to adaptive thermogenesis. *Cell* **92**, 829-839
4. Lin, J., Puigserver, P., Donovan, J., Tarr, P., and Spiegelman, B. M. (2002) Peroxisome proliferator-activated receptor gamma coactivator 1beta (PGC-1beta), a novel PGC-1-related transcription coactivator associated with host cell factor. *J Biol Chem* **277**, 1645-1648
5. Andersson, U., and Scarpulla, R. C. (2001) Pgc-1-related coactivator, a novel, serum-inducible coactivator of nuclear respiratory factor 1-dependent transcription in mammalian cells. *Mol Cell Biol* **21**, 3738-3749
6. Lin, J., Handschin, C., and Spiegelman, B. M. (2005) Metabolic control through the PGC-1 family of transcription coactivators. *Cell metabolism* **1**, 361-370
7. Fernandez-marcos, P. J., and Auwerx, J. (2011) Regulation of PGC-1a , a nodal regulator of mitochondrial biogenesis 1 – 4. 1-7
8. Puigserver, P., Adelmant, G., Wu, Z., Fan, M., Xu, J., O'Malley, B., and Spiegelman, B. M. (1999) Activation of PPARgamma coactivator-1 through transcription factor docking. *Science* **286**, 1368-1371
9. Fan, M., Rhee, J., St-Pierre, J., Handschin, C., Puigserver, P., Lin, J., Jaeger, S., Erdjument-Bromage, H., Tempst, P., and Spiegelman, B. M. (2004) Suppression of mitochondrial respiration through recruitment of p160 myb binding protein to PGC-1alpha: modulation by p38 MAPK. *Genes Dev* **18**, 278-289
10. Wallberg, A. E., Yamamura, S., Malik, S., Spiegelman, B. M., and Roeder, R. G. (2003) Coordination of p300-mediated chromatin remodeling and TRAP/mediator function through coactivator PGC-1alpha. *Mol Cell* **12**, 1137-1149
11. Monsalve, M., Wu, Z., Adelmant, G., Puigserver, P., Fan, M., and Spiegelman, B. M. (2000) Direct coupling of transcription and mRNA processing through the thermogenic coactivator PGC-1. *Mol Cell* **6**, 307-316
12. Chan, M. C., and Arany, Z. (2014) The Many roles of PGC-1α in Muscle – Recent Developments. *Metabolism*, 1-11
13. Chinsomboon, J., Ruas, J., Gupta, R. K., Thom, R., Shoag, J., Rowe, G. C., Sawada, N., Raghuram, S., and Arany, Z. (2009) The transcriptional coactivator PGC-1alpha mediates exercise-induced angiogenesis in skeletal muscle. *Proceedings of the National Academy of Sciences of the United States of America* **106**, 21401-21406
14. Yoshioka, T., Inagaki, K., Noguchi, T., Sakai, M., Ogawa, W., Hosooka, T., Iguchi, H., Watanabe, E., Matsuki, Y., Hiramatsu, R., and Kasuga, M. (2009) Identification and characterization of an alternative promoter of the human PGC-1alpha gene. *Biochem Biophys Res Commun* **381**, 537-543
15. Miura, S., Kai, Y., Kamei, Y., and Ezaki, O. (2008) Isoform-specific increases in murine skeletal muscle peroxisome proliferator-activated receptor-gamma coactivator-1alpha

(PGC-1alpha) mRNA in response to beta2-adrenergic receptor activation and exercise. *Endocrinology* **149**, 4527-4533

16. Zhang, Y., Huypens, P., Adamson, A. W., Chang, J. S., Henagan, T. M., Boudreau, A., Lenard, N. R., Burk, D., Klein, J., Perwitz, N., Shin, J., Fasshauer, M., Kralli, A., and Gettys, T. W. (2009) Alternative mRNA splicing produces a novel biologically active short isoform of PGC-1alpha. *J Biol Chem* **284**, 32813-32826
17. Ruas, J. L. L., White, J. P. P., Rao, R. R. R., Kleiner, S., Brannan, K. T. T., Harrison, B. C. C., Greene, N. P. P., Wu, J., Estall, J. L. L., Irving, B. A. A., Lanza, I. R. R., Rasbach, K. A. A., Okutsu, M., Nair, K. S. S., Yan, Z., Leinwand, L. A. A., and Spiegelman, B. M. M. (2012) A PGC-1α Isoform Induced by Resistance Training Regulates Skeletal Muscle Hypertrophy. *Cell* **151**, 1319-1331
18. Herzig, S., Long, F., Jhala, U. S., Hedrick, S., Quinn, R., Bauer, A., Rudolph, D., Schutz, G., Yoon, C., Puigserver, P., Spiegelman, B., and Montminy, M. (2001) CREB regulates hepatic gluconeogenesis through the coactivator PGC-1. *Nature* **413**, 179-183
19. Handschin, C., Rhee, J., Lin, J., Tarr, P. T., and Spiegelman, B. M. (2003) An autoregulatory loop controls peroxisome proliferator-activated receptor gamma coactivator 1alpha expression in muscle. *Proc Natl Acad Sci U S A* **100**, 7111-7116
20. Wu, H., Kanatous, S. B., Thurmond, F. A., Gallardo, T., Isotani, E., Bassel-Duby, R., and Williams, R. S. (2002) Regulation of mitochondrial biogenesis in skeletal muscle by CaMK. *Science* **296**, 349-352
21. Zhao, M., New, L., Kravchenko, V. V., Kato, Y., Gram, H., di Padova, F., Olson, E. N., Ulevitch, R. J., and Han, J. (1999) Regulation of the MEF2 family of transcription factors by p38. *Mol Cell Biol* **19**, 21-30
22. Akimoto, T., Pohnert, S. C., Li, P., Zhang, M., Gumbs, C., Rosenberg, P. B., Williams, R. S., and Yan, Z. (2005) Exercise stimulates Pgc-1alpha transcription in skeletal muscle through activation of the p38 MAPK pathway. *J Biol Chem* **280**, 19587-19593
23. Suwa, M., Nakano, H., and Kumagai, S. (2003) Effects of chronic AICAR treatment on fiber composition, enzyme activity, UCP3, and PGC-1 in rat muscles. *J Appl Physiol (1985)* **95**, 960-968
24. Jorgensen, S. B., Wojtaszewski, J. F., Viollet, B., Andreelli, F., Birk, J. B., Hellsten, Y., Schjerling, P., Vaulont, S., Neufer, P. D., Richter, E. A., and Pilegaard, H. (2005) Effects of alpha-AMPK knockout on exercise-induced gene activation in mouse skeletal muscle. *FASEB J* **19**, 1146-1148
25. Southgate, R. J., Bruce, C. R., Carey, A. L., Steinberg, G. R., Walder, K., Monks, R., Watt, M. J., Hawley, J. A., Birnbaum, M. J., and Febbraio, M. A. (2005) PGC-1alpha gene expression is down-regulated by Akt- mediated phosphorylation and nuclear exclusion of FoxO1 in insulin-stimulated skeletal muscle. *FASEB J* **19**, 2072-2074
26. Jäger, S., Handschin, C., St-Pierre, J., and Spiegelman, B. M. (2007) AMP-activated protein kinase (AMPK) action in skeletal muscle via direct phosphorylation of PGC-1alpha. *Proceedings of the National Academy of Sciences of the United States of America* **104**, 12017-12022
27. Puigserver, P., Rhee, J., Lin, J., Wu, Z., Yoon, J. C., Zhang, C. Y., Krauss, S., Mootha, V. K., Lowell, B. B., and Spiegelman, B. M. (2001) Cytokine stimulation of energy expenditure through p38 MAP kinase activation of PPARgamma coactivator-1. *Mol Cell* **8**, 971-982

28. Lerin, C., Rodgers, J. T., Kalume, D. E., Kim, S. H., Pandey, A., and Puigserver, P. (2006) GCN5 acetyltransferase complex controls glucose metabolism through transcriptional repression of PGC-1alpha. *Cell Metab* **3**, 429-438
29. Gerhart-Hines, Z., Rodgers, J. T., Bare, O., Lerin, C., Kim, S. H., Mostoslavsky, R., Alt, F. W., Wu, Z., and Puigserver, P. (2007) Metabolic control of muscle mitochondrial function and fatty acid oxidation through SIRT1/PGC-1alpha. *EMBO J* **26**, 1913-1923
30. Wu, Z., Puigserver, P., Andersson, U., Zhang, C., Adelmant, G., Mootha, V., Troy, A., Cinti, S., Lowell, B., Scarpulla, R. C., and Spiegelman, B. M. (1999) Mechanisms controlling mitochondrial biogenesis and respiration through the thermogenic coactivator PGC-1. *Cell* **98**, 115-124
31. Vega, R. B., Huss, J. M., and Kelly, D. P. (2000) The coactivator PGC-1 cooperates with peroxisome proliferator-activated receptor alpha in transcriptional control of nuclear genes encoding mitochondrial fatty acid oxidation enzymes. *Mol Cell Biol* **20**, 1868-1876
32. Wende, A. R., Huss, J. M., Schaeffer, P. J., Giguere, V., and Kelly, D. P. (2005) PGC-1alpha coactivates PDK4 gene expression via the orphan nuclear receptor ERRalpha: a mechanism for transcriptional control of muscle glucose metabolism. *Mol Cell Biol* **25**, 10684-10694
33. Yoon, J. C., Puigserver, P., Chen, G., Donovan, J., Wu, Z., Rhee, J., Adelmant, G., Stafford, J., Kahn, C. R., Granner, D. K., Newgard, C. B., and Spiegelman, B. M. (2001) Control of hepatic gluconeogenesis through the transcriptional coactivator PGC-1. *Nature* **413**, 131-138
34. Wende, A. R., Schaeffer, P. J., Parker, G. J., Zechner, C., Han, D.-H., Chen, M. M., Hancock, C. R., Lehman, J. J., Huss, J. M., McClain, D. a., Holloszy, J. O., and Kelly, D. P. (2007) A role for the transcriptional coactivator PGC-1alpha in muscle refueling. *The Journal of biological chemistry* **282**, 36642-36651
35. Summermatter, S., Baum, O., Santos, G., Hoppeler, H., and Handschin, C. (2010) Peroxisome proliferator-activated receptor {gamma} coactivator 1{alpha} (PGC-1{alpha}) promotes skeletal muscle lipid refueling in vivo by activating de-novo lipogenesis and the pentose phosphate pathway. *The Journal of biological chemistry* **285**, 32793-32800
36. Arany, Z., Foo, S.-Y., Ma, Y., Ruas, J. L., Bommi-Reddy, A., Girnun, G., Cooper, M., Laznik, D., Chinsomboon, J., Rangwala, S. M., Baek, K. H., Rosenzweig, A., and Spiegelman, B. M. (2008) HIF-independent regulation of VEGF and angiogenesis by the transcriptional coactivator PGC-1alpha. *Nature* **451**, 1008-1012
37. Lin, J., Wu, H., Tarr, P. T., Zhang, C.-Y., Wu, Z., Boss, O., Michael, L. F., Puigserver, P., Isotani, E., Olson, E. N., Lowell, B. B., Bassel-Duby, R., and Spiegelman, B. M. (2002) Transcriptional co-activator PGC-1 alpha drives the formation of slow-twitch muscle fibres. *Nature* **418**, 797-801
38. St-Pierre, J., Drori, S., Uldry, M., Silvaggi, J. M., Rhee, J., Jager, S., Handschin, C., Zheng, K., Lin, J., Yang, W., Simon, D. K., Bachoo, R., and Spiegelman, B. M. (2006) Suppression of reactive oxygen species and neurodegeneration by the PGC-1 transcriptional coactivators. *Cell* **127**, 397-408
39. Handschin, C., Chin, S., Li, P., Liu, F., Maratos-Flier, E., Lebrasseur, N. K., Yan, Z., and Spiegelman, B. M. (2007) Skeletal muscle fiber-type switching, exercise intolerance, and myopathy in PGC-1alpha muscle-specific knock-out animals. *The Journal of biological chemistry* **282**, 30014-30021

40. Eisele, P. S., Salatino, S., Sobek, J., Hottiger, M. O., and Handschin, C. (2013) The peroxisome proliferator-activated receptor γ coactivator 1α/β (PGC-1) coactivators repress the transcriptional activity of NF-κB in skeletal muscle cells. *The Journal of biological chemistry* **288**, 2246-2260
41. Handschin, C., Kobayashi, Y. M., Chin, S., Seale, P., Campbell, K. P., and Spiegelman, B. M. (2007) PGC-1alpha regulates the neuromuscular junction program and ameliorates Duchenne muscular dystrophy. *Genes & development* **21**, 770-783
42. Wenz, T., Rossi, S. G., Rotundo, R. L., Spiegelman, B. M., and Moraes, C. T. (2009) Increased muscle PGC-1alpha expression protects from sarcopenia and metabolic disease during aging. *Proc Natl Acad Sci U S A* **106**, 20405-20410
43. Boström, P., Wu, J., Jedrychowski, M. P., Korde, A., Ye, L., Lo, J. C., Rasbach, K. a., Boström, E. A., Choi, J. H., Long, J. Z., Kajimura, S., Zingaretti, M. C., Vind, B. F., Tu, H., Cinti, S., Højlund, K., Gygi, S. P., and Spiegelman, B. M. (2012) A PGC1-α-dependent myokine that drives brown-fat-like development of white fat and thermogenesis. *Nature* **481**, 463-468
44. Catoire, M., Mensink, M., Kalkhoven, E., Schrauwen, P., and Kersten, S. (2014) Identification of human exercise-induced myokines using secretome analysis. *Physiological genomics*, 256-267
45. Sandri, M., Lin, J., Handschin, C., Yang, W., Arany, Z. P., Lecker, S. H., Goldberg, A. L., and Spiegelman, B. M. (2006) PGC-1alpha protects skeletal muscle from atrophy by suppressing FoxO3 action and atrophy-specific gene transcription. *Proceedings of the National Academy of Sciences of the United States of America* **103**, 16260-16265
46. Selsby, J. T., Morine, K. J., Pendrak, K., Barton, E. R., and Sweeney, H. L. (2012) Rescue of dystrophic skeletal muscle by PGC-1α involves a fast to slow fiber type shift in the mdx mouse. *PloS one* **7**, e30063-e30063
47. Hollinger, K., Gardan-Salmon, D., Santana, C., Rice, D., Snella, E., and Selsby, J. T. (2013) Rescue of dystrophic skeletal muscle by PGC-1α involves restored expression of dystrophin-associated protein complex components and satellite cell signaling. *American journal of physiology. Regulatory, integrative and comparative physiology* **305**, R13-23
48. Chan, M. C., Rowe, G. C., Raghuram, S., Patten, I. S., Farrell, C., and Arany, Z. (2014) Post-natal induction of PGC-1alpha protects against severe muscle dystrophy independently of utrophin. *Skeletal Muscle* **4**, 2-2
49. Wenz, T., Diaz, F., Spiegelman, B. M., and Moraes, C. T. (2008) Activation of the PPAR/PGC-1alpha pathway prevents a bioenergetic deficit and effectively improves a mitochondrial myopathy phenotype. *Cell metabolism* **8**, 249-256
50. Bentzinger, C. F., Wang, Y. X., and Rudnicki, M. a. (2012) Building muscle: molecular regulation of myogenesis. *Cold Spring Harbor perspectives in biology* **4**
51. Schmalbruch, H., and Lewis, D. M. (2000) Dynamics of nuclei of muscle fibers and connective tissue cells in normal and denervated rat muscles. *Muscle Nerve* **23**, 617-626
52. Péault, B., Rudnicki, M., Torrente, Y., Cossu, G., Tremblay, J. P., Partridge, T., Gussoni, E., Kunkel, L. M., and Huard, J. (2007) Stem and progenitor cells in skeletal muscle development, maintenance, and therapy. *Molecular therapy : the journal of the American Society of Gene Therapy* **15**, 867-877
53. Ciciliot, S., and Schiaffino, S. (2010) Regeneration of Mammalian Skeletal Muscle: Basic Mechanisms and Clinical Implications. *Current Pharmaceutical Design* **16**, 906-914

54. Turner, N. J., and Badylak, S. F. (2012) Regeneration of skeletal muscle. *Cell and tissue research* **347**, 759-774
55. McNeil, P. L., and Kirchhausen, T. (2005) An emergency response team for membrane repair. *Nat Rev Mol Cell Biol* **6**, 499-505
56. Han, R. (2011) Muscle membrane repair and inflammatory attack in dysferlinopathy. *Skelet Muscle* **1**, 10
57. Hawke, T. J., and Garry, D. J. (2001) Myogenic satellite cells: physiology to molecular biology. *J Appl Physiol (1985)* **91**, 534-551
58. McNeil, P. L. (2002) Repairing a torn cell surface: make way, lysosomes to the rescue. *Journal of cell science* **115**, 873-879
59. Cai, C., Masumiya, H., Weisleder, N., Matsuda, N., Nishi, M., Hwang, M., Ko, J.-K., Lin, P., Thornton, A., Zhao, X., Pan, Z., Komazaki, S., Brotto, M., Takeshima, H., and Ma, J. (2009) MG53 nucleates assembly of cell membrane repair machinery. *Nature cell biology* **11**, 56-64
60. Bansal, D., Miyake, K., Vogel, S. S., Groh, S., Chen, C. C., Williamson, R., McNeil, P. L., and Campbell, K. P. (2003) Defective membrane repair in dysferlin-deficient muscular dystrophy. *Nature* **423**, 168-172
61. Cai, C., Weisleder, N., Ko, J. K., Komazaki, S., Sunada, Y., Nishi, M., Takeshima, H., and Ma, J. (2009) Membrane Repair Defects in Muscular Dystrophy Are Linked to Altered Interaction between MG53, Caveolin-3, and Dysferlin. *Journal of Biological Chemistry* **284**, 15894-15902
62. Allen, D. G., and Whitehead, N. P. (2011) Duchenne muscular dystrophy - What causes the increased membrane permeability in skeletal muscle? *The international journal of biochemistry & cell biology* **43**, 290-294
63. Dorn, G. W. (2013) Molecular mechanisms that differentiate apoptosis from programmed necrosis. *Toxicologic pathology* **41**, 227-234
64. Tidball, J. G. (2005) Inflammatory processes in muscle injury and repair. 345-353
65. Ceafalan, L. C., Popescu, B. O., and Hinescu, M. E. (2014) Cellular Players in Skeletal Muscle Regeneration. *BioMed research international* **2014**, 957014-957014
66. Wang, Y., and Thorlacius, H. (2005) Mast cell-derived tumour necrosis factor-alpha mediates macrophage inflammatory protein-2-induced recruitment of neutrophils in mice. *British journal of pharmacology* **145**, 1062-1068
67. Chiba, K., Zhao, W., Chen, J., Wang, J., Cui, H. Y., Kawakami, H., Miseki, T., Satoshi, H., Tanaka, J., Asaka, M., and Kobayashi, M. (2004) Neutrophils secrete MIP-1 beta after adhesion to laminin contained in basement membrane of blood vessels. *Br J Haematol* **127**, 592-597
68. Silva, M. T. (2010) When two is better than one: macrophages and neutrophils work in concert in innate immunity as complementary and cooperative partners of a myeloid phagocyte system. *J Leukoc Biol* **87**, 93-106
69. Kharraz, Y., Guerra, J., Mann, C. J., Serrano, A. L., and Munoz-Canoves, P. (2013) Macrophage plasticity and the role of inflammation in skeletal muscle repair. *Mediators Inflamm* **2013**, 491497
70. Bentzinger, C. F., Wang, Y. X., Dumont, N. a., and Rudnicki, M. a. (2013) Cellular dynamics in the muscle satellite cell niche. *EMBO reports* **14**, 1062-1072
71. Lu, H., Huang, D., Ransohoff, R. M., and Zhou, L. (2011) Acute skeletal muscle injury: CCL2 expression by both monocytes and injured muscle is required for repair. *FASEB*

journal : official publication of the Federation of American Societies for Experimental Biology **25**, 3344-3355
72. Warren, G. L., O'Farrell, L., Summan, M., Hulderman, T., Mishra, D., Luster, M. I., Kuziel, W. A., and Simeonova, P. P. (2004) Role of CC chemokines in skeletal muscle functional restoration after injury. *Am J Physiol Cell Physiol* **286**, C1031-1036
73. Senf, S. M., Howard, T. M., Ahn, B., Ferreira, L. F., and Judge, A. R. (2013) Loss of the inducible Hsp70 delays the inflammatory response to skeletal muscle injury and severely impairs muscle regeneration. *PLoS One* **8**, e62687
74. van der Poel, C., Gosselin, L. E., Schertzer, J. D., Ryall, J. G., Swiderski, K., Wondemaghen, M., and Lynch, G. S. (2011) Ageing prolongs inflammatory marker expression in regenerating rat skeletal muscles after injury. *J Inflamm (Lond)* **8**, 41
75. Mounier, R., Théret, M., Arnold, L., Cuvellier, S., Bultot, L., Göransson, O., Sanz, N., Ferry, A., Sakamoto, K., Foretz, M., Viollet, B., and Chazaud, B. (2013) AMPKα1 regulates macrophage skewing at the time of resolution of inflammation during skeletal muscle regeneration. *Cell metabolism* **18**, 251-264
76. Segawa, M., Fukada, S., Yamamoto, Y., Yahagi, H., Kanematsu, M., Sato, M., Ito, T., Uezumi, A., Hayashi, S., Miyagoe-Suzuki, Y., Takeda, S., Tsujikawa, K., and Yamamoto, H. (2008) Suppression of macrophage functions impairs skeletal muscle regeneration with severe fibrosis. *Exp Cell Res* **314**, 3232-3244
77. Mann, C. J., Perdiguero, E., Kharraz, Y., Aguilar, S., Pessina, P., Serrano, A. L., and Muñoz-Cánoves, P. (2011) Aberrant repair and fibrosis development in skeletal muscle. *Skeletal Muscle* **1**, 21-21
78. Mauro, a. (1961) Satellite cell of skeletal muscle fibers. *The Journal of biophysical and biochemical cytology* **9**, 493-495
79. Schultz, E., Gibson, M. C., and Champion, T. (1978) Satellite cells are mitotically quiescent in mature mouse muscle: an EM and radioautographic study. *J Exp Zool* **206**, 451-456
80. Yin, H., Price, F., and Rudnicki, M. a. (2013) Satellite cells and the muscle stem cell niche. *Physiological reviews* **93**, 23-67
81. Chargé, S. B. P., and Rudnicki, M. a. (2004) Cellular and molecular regulation of muscle regeneration. *Physiological reviews* **84**, 209-238
82. Kuang, S., and Rudnicki, M. a. (2008) The emerging biology of satellite cells and their therapeutic potential. *Trends in molecular medicine* **14**, 82-91
83. Seale, P., Sabourin, L. a., Girgis-Gabardo, a., Mansouri, a., Gruss, P., and Rudnicki, M. a. (2000) Pax7 is required for the specification of myogenic satellite cells. *Cell* **102**, 777-786
84. Lepper, C., Partridge, T. a., and Fan, C.-M. (2011) An absolute requirement for Pax7-positive satellite cells in acute injury-induced skeletal muscle regeneration. *Development (Cambridge, England)* **138**, 3639-3646
85. Sambasivan, R., Yao, R., Kissenpfennig, A., Van Wittenberghe, L., Paldi, A., Gayraud-Morel, B., Guenou, H., Malissen, B., Tajbakhsh, S., and Galy, A. (2011) Pax7-expressing satellite cells are indispensable for adult skeletal muscle regeneration. *Development (Cambridge, England)* **138**, 3647-3656
86. Murphy, M. M., Lawson, J. a., Mathew, S. J., Hutcheson, D. a., and Kardon, G. (2011) Satellite cells, connective tissue fibroblasts and their interactions are crucial for muscle regeneration. *Development (Cambridge, England)* **138**, 3625-3637

87. McCarthy, J. J., Mula, J., Miyazaki, M., Erfani, R., Garrison, K., Farooqui, A. B., Srikuea, R., Lawson, B. a., Grimes, B., Keller, C., Van Zant, G., Campbell, K. S., Esser, K. a., Dupont-Versteegden, E. E., and Peterson, C. a. (2011) Effective fiber hypertrophy in satellite cell-depleted skeletal muscle. *Development (Cambridge, England)* **138**, 3657-3666
88. Asakura, A., Komaki, M., and Rudnicki, M. (2001) Muscle satellite cells are multipotential stem cells that exhibit myogenic, osteogenic, and adipogenic differentiation. *Differentiation* **68**, 245-253
89. Kuang, S., Kuroda, K., Le Grand, F., and Rudnicki, M. A. (2007) Asymmetric self-renewal and commitment of satellite stem cells in muscle. *Cell* **129**, 999-1010
90. Montarras, D., L'Honoré, A., and Buckingham, M. (2013) Lying low but ready for action: the quiescent muscle satellite cell. *The FEBS journal* **280**, 4036-4050
91. Collins, C. A., Olsen, I., Zammit, P. S., Heslop, L., Petrie, A., Partridge, T. A., and Morgan, J. E. (2005) Stem cell function, self-renewal, and behavioral heterogeneity of cells from the adult muscle satellite cell niche. *Cell* **122**, 289-301
92. Sacco, A., Doyonnas, R., Kraft, P., Vitorovic, S., and Blau, H. M. (2008) Self-renewal and expansion of single transplanted muscle stem cells. *Nature* **456**, 502-506
93. Ohlstein, B., Kai, T., Decotto, E., and Spradling, A. (2004) The stem cell niche: theme and variations. *Curr Opin Cell Biol* **16**, 693-699
94. Burkin, D. J., and Kaufman, S. J. (1999) The alpha7beta1 integrin in muscle development and disease. *Cell Tissue Res* **296**, 183-190
95. Conboy, I. M., Conboy, M. J., Smythe, G. M., and Rando, T. a. (2003) Notch-mediated restoration of regenerative potential to aged muscle. *Science (New York, N.Y.)* **302**, 1575-1577
96. Conboy, I. M., and Rando, T. A. (2002) The regulation of Notch signaling controls satellite cell activation and cell fate determination in postnatal myogenesis. *Dev Cell* **3**, 397-409
97. Cornelison, D. D., and Wold, B. J. (1997) Single-cell analysis of regulatory gene expression in quiescent and activated mouse skeletal muscle satellite cells. *Dev Biol* **191**, 270-283
98. Kuang, S., Gillespie, M. a., and Rudnicki, M. a. (2008) Niche regulation of muscle satellite cell self-renewal and differentiation. *Cell stem cell* **2**, 22-31
99. Gopinath, S. D., and Rando, T. a. (2008) Stem cell review series: aging of the skeletal muscle stem cell niche. *Aging Cell* **7**, 590-598
100. Christov, C., Chre, F., Abou-khalil, R., Bassez, G., Bassaglia, Y., Shinin, V., Tajbakhsh, S., Gherardi, R. K., and Marne, P. X.-v. D. (2007) Muscle Satellite Cells and Endothelial Cells : Close Neighbors and Privileged Partners □. **18**, 1397-1409
101. Kelly, A. M. (1978) Perisynaptic satellite cells in the developing and mature rat soleus muscle. *Anat Rec* **190**, 891-903
102. Gibson, M. C., and Schultz, E. (1982) The distribution of satellite cells and their relationship to specific fiber types in soleus and extensor digitorum longus muscles. *Anat Rec* **202**, 329-337
103. Ryall, J. G. (2013) Metabolic reprogramming as a novel regulator of skeletal muscle development and regeneration. *FEBS J* **280**, 4004-4013

104. Shefer, G., Rauner, G., Yablonka-Reuveni, Z., and Benayahu, D. (2010) Reduced satellite cell numbers and myogenic capacity in aging can be alleviated by endurance exercise. *PLoS One* **5**, e13307
105. Bentzinger, C. F., von Maltzahn, J., and Rudnicki, M. A. (2010) Extrinsic regulation of satellite cell specification. *Stem Cell Res Ther* **1**, 27
106. Kadi, F., Charifi, N., Denis, C., Lexell, J., Andersen, J. L., Schjerling, P., Olsen, S., and Kjaer, M. (2005) The behaviour of satellite cells in response to exercise: what have we learned from human studies? *Pflugers Arch* **451**, 319-327
107. Kee, N., Sivalingam, S., Boonstra, R., and Wojtowicz, J. M. (2002) The utility of Ki-67 and BrdU as proliferative markers of adult neurogenesis. *J Neurosci Methods* **115**, 97-105
108. Snijders, T., Verdijk, L. B., Beelen, M., McKay, B. R., Parise, G., Kadi, F., and van Loon, L. J. (2012) A single bout of exercise activates skeletal muscle satellite cells during subsequent overnight recovery. *Exp Physiol* **97**, 762-773
109. Rodgers, J. T., King, K. Y., Brett, J. O., Cromie, M. J., Charville, G. W., Maguire, K. K., Brunson, C., Mastey, N., Liu, L., Tsai, C.-R., Goodell, M. a., and Rando, T. a. (2014) mTORC1 controls the adaptive transition of quiescent stem cells from G0 to GAlert. *Nature*
110. Wozniak, a. C., Pilipowicz, O., Yablonka-Reuveni, Z., Greenway, S., Craven, S., Scott, E., and Anderson, J. E. (2003) C-Met Expression and Mechanical Activation of Satellite Cells on Cultured Muscle Fibers. *Journal of Histochemistry & Cytochemistry* **51**, 1437-1445
111. Tatsumi, R., Liu, X., Pulido, A., Morales, M., Sakata, T., Dial, S., Hattori, A., Ikeuchi, Y., Allen, R. E., and Mo, M. (2006) Satellite cell activation in stretched skeletal muscle and the role of nitric oxide and hepatocyte growth factor. **0038**, 1487-1494
112. McCroskery, S., Thomas, M., Maxwell, L., Sharma, M., and Kambadur, R. (2003) Myostatin negatively regulates satellite cell activation and self-renewal. *J Cell Biol* **162**, 1135-1147
113. Wagner, K. R., Liu, X., Chang, X., and Allen, R. E. (2005) Muscle regeneration in the prolonged absence of myostatin. *Proc Natl Acad Sci U S A* **102**, 2519-2524
114. Jejurikar, S. S., and Kuzon, W. M., Jr. (2003) Satellite cell depletion in degenerative skeletal muscle. *Apoptosis* **8**, 573-578
115. Tajbakhsh, S., Rocancourt, D., Cossu, G., and Buckingham, M. (1997) Redefining the genetic hierarchies controlling skeletal myogenesis: Pax-3 and Myf-5 act upstream of MyoD. *Cell* **89**, 127-138
116. Morrison, S. J., and Kimble, J. (2006) Asymmetric and symmetric stem-cell divisions in development and cancer. *Nature* **441**, 1068-1074
117. Shea, K. L., Xiang, W., LaPorta, V. S., Licht, J. D., Keller, C., Basson, M. A., and Brack, A. S. (2010) Sprouty1 regulates reversible quiescence of a self-renewing adult muscle stem cell pool during regeneration. *Cell Stem Cell* **6**, 117-129
118. Zammit, P. S., Golding, J. P., Nagata, Y., Hudon, V., Partridge, T. a., and Beauchamp, J. R. (2004) Muscle satellite cells adopt divergent fates: a mechanism for self-renewal? *The Journal of cell biology* **166**, 347-357
119. Boldrin, L., Muntoni, F., and Morgan, J. E. (2010) Are human and mouse satellite cells really the same? *The journal of histochemistry and cytochemistry : official journal of the Histochemistry Society* **58**, 941-955

120. Sabourin, L. A., and Rudnicki, M. A. (2000) The molecular regulation of myogenesis. *Clin Genet* **57**, 16-25
121. Vignaud, A., Hourde, C., Butler-Browne, G., and Ferry, A. (2007) Differential recovery of neuromuscular function after nerve/muscle injury induced by crude venom from Notechis scutatus, cardiotoxin from Naja atra and bupivacaine treatments in mice. *Neurosci Res* **58**, 317-323
122. Gillies, A. R., and Lieber, R. L. (2011) Structure and function of the skeletal muscle extracellular matrix. *Muscle & nerve* **44**, 318-331
123. Serrano, A. L., Mann, C. J., and Vidal, B. (2011) *Cellular and Molecular Mechanisms Regulating Fibrosis in Skeletal Muscle Repair and Disease* Vol. 96
124. Jang, Y. C., Sinha, M., Cerletti, M., Dall'Osso, C., and Wagers, a. J. (2011) Skeletal Muscle Stem Cells: Effects of Aging and Metabolism on Muscle Regenerative Function. *Cold Spring Harbor Symposia on Quantitative Biology* **76**, 101-111
125. Davies, K. E., and Nowak, K. J. (2006) Molecular mechanisms of muscular dystrophies: old and new players. *Nat Rev Mol Cell Biol* **7**, 762-773
126. Barberi, L., Scicchitano, B. M., De Rossi, M., Bigot, A., Duguez, S., Wielgosik, A., Stewart, C., McPhee, J., Conte, M., Narici, M., Franceschi, C., Mouly, V., Butler-Browne, G., and Musarò, A. (2013) Age-dependent alteration in muscle regeneration: the critical role of tissue niche. *Biogerontology*
127. Chakkalakal, J. V., Jones, K. M., Basson, M. A., and Brack, A. S. (2012) The aged niche disrupts muscle stem cell quiescence. *Nature* **490**, 355-360
128. Bernet, J. D., Doles, J. D., Hall, J. K., Kelly Tanaka, K., Carter, T. a., and Olwin, B. B. (2014) p38 MAPK signaling underlies a cell-autonomous loss of stem cell self-renewal in skeletal muscle of aged mice. *Nature medicine* **20**, 265-271
129. Rossi, C. A., Pozzobon, M., and De Coppi, P. (2010) Advances in musculoskeletal tissue engineering: moving towards therapy. *Organogenesis* **6**, 167-172
130. Hamai, N., Nakamura, M., and Asano, A. (1997) Inhibition of mitochondrial protein synthesis impaired C2C12 myoblast differentiation. *Cell Struct Funct* **22**, 421-431
131. Rochard, P., Rodier, A., Casas, F., Cassar-Malek, I., Marchal-Victorion, S., Daury, L., Wrutniak, C., and Cabello, G. (2000) Mitochondrial activity is involved in the regulation of myoblast differentiation through myogenin expression and activity of myogenic factors. *J Biol Chem* **275**, 2733-2744
132. Wagatsuma, A., and Sakuma, K. (2013) Mitochondria as a potential regulator of myogenesis. *ScientificWorldJournal* **2013**, 593267
133. Labarge, S., McDonald, M., Smith-Powell, L., Auwerx, J., and Huss, J. M. (2013) Estrogen-related receptor-α (ERRα) deficiency in skeletal muscle impairs regeneration in response to injury. *FASEB journal : official publication of the Federation of American Societies for Experimental Biology*
134. Murray, J., Auwerx, J., and Huss, J. M. (2013) Impaired myogenesis in estrogen-related receptor γ (ERRγ)-deficient skeletal myocytes due to oxidative stress. *FASEB journal : official publication of the Federation of American Societies for Experimental Biology* **27**, 135-150
135. Murray, J., and Huss, J. M. (2011) Estrogen-related receptor alpha regulates skeletal myocyte differentiation via modulation of the ERK MAP kinase pathway. *Am J Physiol Cell Physiol* **301**, C630-645

136. Wang, Y., and Pessin, J. E. (2013) Mechanisms for fiber-type specificity of skeletal muscle atrophy. *Curr Opin Clin Nutr Metab Care* **16**, 243-250
137. Koning, M., Harmsen, M. C., van Luyn, M. J., and Werker, P. M. (2009) Current opportunities and challenges in skeletal muscle tissue engineering. *J Tissue Eng Regen Med* **3**, 407-415
138. Baar, K., Wende, A. R., Jones, T. E., Marison, M., Nolte, L. a., Chen, M., Kelly, D. P., and Holloszy, J. O. (2002) Adaptations of skeletal muscle to exercise: rapid increase in the transcriptional coactivator PGC-1. *FASEB journal : official publication of the Federation of American Societies for Experimental Biology* **16**, 1879-1886
139. Rowe, G. C., Safdar, A., and Arany, Z. (2014) Running forward: new frontiers in endurance exercise biology. *Circulation* **129**, 798-810
140. Hanai, J.-i., Cao, P., Tanksale, P., Imamura, S., Koshimizu, E., Zhao, J., Kishi, S., Yamashita, M., Phillips, P. S., Sukhatme, V. P., and Lecker, S. H. (2007) The muscle-specific ubiquitin ligase atrogin-1 / MAFbx mediates statin-induced muscle toxicity. **117**
141. Da Cruz, S., Parone, P. A., Lopes, V. S., Lillo, C., McAlonis-Downes, M., Lee, S. K., Vetto, A. P., Petrosyan, S., Marsala, M., Murphy, A. N., Williams, D. S., Spiegelman, B. M., and Cleveland, D. W. (2012) Elevated PGC-1alpha activity sustains mitochondrial biogenesis and muscle function without extending survival in a mouse model of inherited ALS. *Cell Metab* **15**, 778-786

4 Aims

Having in mind the beneficial effects of peroxisome proliferator-activated receptor γ coactivator 1α (PGC-1α) expression in skeletal muscle and its potential role in skeletal muscle regeneration and repair (see *PGC-1α in skeletal muscle regeneration and repair*), we wanted to elucidate several aspects of its function:

1. PGC-1α in skeletal muscle regeneration:
    - does PGC-1α have an effect on skeletal muscle regeneration
    - does boosting PGC-1α in differentiated myoblasts accelerate regenerative processes
    - does loss of PGC-1α in SCs affect proliferation and differentiation alike

2. PGC-1α in satellite cells:
    - does PGC-1α have a specific effect on SCs
    - what are the effects of overexpression or loss of PGC-1α in the SC niche and consequently the effects of myofiber metabolism on SC behavior
    - what are the effects of PGC-1α deletion in SCs and possible modifications of SC behavior

3. PGC-1α in skeletal muscle repair:
    - does PGC-1α modulate sarcolemma repair
    - what are the resealing properties of PGC-1α KO myoblasts
    - how can PGC-1α improve membrane stability and rupture patching

4. PGC-1α in regenerative medicine:
    - can PGC-1α improve muscle regeneration *in vivo* by improving environmental changes that otherwise limit tissue survival and function after transplantation

5 PGC-1α modulates inflammatory response and fibrotic tissue formation in skeletal muscle upon cardiotoxin injury (Project 1)

Authors: Ivana Dinulovic[1], Arnaud Ferry[2], Markus Beer[1], Christoph Handschin[1]

[1]Biozentrum, University of Basel, Klingelbergstrasse 50-70, 4056 Basel, Switzerland

[2] Thérapie des maladies du muscle strié INSERM U974 - CNRS UMR7215 - UPMC UM76 - Institut de Myologie/Adresse 1: 105 boulevard de l'Hôpital, Faculté de Médecine, 75634 Paris Cedex 13, France/Adresse 2: 47, bld de l'Hôpital, G.H. Pitié-Salpétrière, Bâtiment Babinski, bureau 98, 75651 Paris Cedex 13, France

Running title: PGC-1α in skeletal muscle regeneration

Key words: PGC-1α; muscle; regeneration; inflammation; fibrosis

Corresponding author: Christoph Handschin (e-mail: christoph.handschinATunibas.ch)

Author contributions: experiments designed by I.D. and C.H; experiments performed by I.D., A.F. (performed muscle contractility measurements) and M.B. (provided helped with RNA isolation, qPCR, cryosectioning and H&E image acquisition); experiments analyzed by I.D and C.H; manuscript written by I.D and C.H

5.1 Abstract

Skeletal muscle tissue possesses a great capacity for regeneration upon injury, and this mechanism partially depends on oxidative metabolism. PGC-1α is a main modulator of oxidative metabolism, but its role in skeletal muscle regeneration has not been addressed yet. Using mouse models for muscle-specific overexpression and knock-out of PGC-1α in combination with cardiotoxin (CTX) injury, we aimed to elucidate the role of this transcriptional coactivator throughout the process of regeneration. Although our results show successful recovery in both mouse models, we observed differences at the early stages of regeneration concerning inflammation and subsequent necrotic tissue clearance. Results obtained in transgenic animals indicate accelerated attraction and invasion of inflammatory cells measured by macrophage numbers and chemokine production, culminating in faster resolution of necrosis. Additionally, loss of PGC-1α resulted in increased fibrosis after multiple CTX injuries. Differential expression of myostatin (Mstn) and insulin-like growth factor 1 (IGF-1) in PGC-1α mouse models are a plausible cause for the aforementioned features of regeneration. These effects of PGC-1α modulation can become beneficial in the context of acute injury and explain some of the previously reported outcomes of PGC-1α overexpression in mouse dystrophy models.

5.2 Introduction

Skeletal muscle comprises 40% of human body weight, and is a very active metabolic tissue, important for posture, breathing and movement. It is distinguished by very high plasticity and a relatively low nuclear turnover rate (1), yet has a tremendous capacity for regeneration. Skeletal muscle regeneration is a highly organized and complex process that involves the coordinated activation of multiple cells types and factors (2). Cells indispensable for the formation of new muscle tissue are muscle stem cells, named satellite cells (3). Upon injury and exercise, these cells give rise to more muscle progenitors that eventually fuse together and form new myotubes or repair damaged ones. The whole process of regeneration, characterized by satellite cell activation, proliferation and differentiation, can be followed by the expression of the transcription factor Pax7 and myogenic regulatory factors (MRFs) (4). While upregulation of Pax7, Myf5 and MyoD marks the stage of muscle progenitor proliferation, myogenin (Myog) and MRF-4 mark the subsequent myoblast fusion and myotube maturation.

In parallel to the process of myogenesis, timely participation of other cell types is also necessary for successful regeneration to occur. Upon injury, muscle fibers undergo necrosis and attract inflammatory cells in order to eradicate cell debris and make room for newly formed muscle fibers (5, 6). A precisely ordered response to injury, in particular to macrophage attraction and clearance, is essential to successful regeneration as demonstrated in various mouse models. The first cells which respond to damage are muscle-resident mast cells and macrophages. By secreting tumor necrosis factor α (TNF-α) and interleukin 6 (IL-6), they attract neutrophils which invade the damaged area within hours (6, 7). Neutrophils continue secreting a myriad of chemokines: monocyte chemoattractant protein 1 (MCP-1) and macrophage inflammatory proteins (MIP-1α, MIP-1β), which in turn attract monocytes from the blood stream. Monocytes give rise to M1 macrophages, the function of which is to phagocyte necrotic tissue and form an environment that favors satellite cell activation and proliferation. Over a period of several days, M1 macrophages are replaced by M2 macrophages, whose role is to suppress the process of inflammation and produce extracellular matrix components that serve as a scaffold for the formation of new muscle tissue. The M2 type of macrophages is also essential for the switch from the proliferative to differentiative stage of regeneration. However, prolonged presence of M2 macrophages leads to uncontrolled activation and proliferation of fibroblasts and

overproduction of extracellular components resulting in fibrosis (8). The formation of excessive fibrous tissue prevents the full functional recovery of muscle tissue. Timely attraction of macrophages and the switch between subclasses, as well as eradication of these cells at the end of the regenerative process is a prerequisite for successful activation of muscle progenitor cells, as well as their proliferation and differentiation (9).

The transition from myoblast proliferation to differentiation is an energy demanding process and is accompanied by a switch from glycolysis to oxidative metabolism as the ATP producing pathway (10). The importance of the estrogen-related receptor α (ERRα) transcription factor in skeletal muscle regeneration and differentiation has been previously reported (11, 12). Given the significance of the interaction between peroxisome proliferator-activated receptor γ coactivator 1 α (PGC-1α) and ERRα for driving oxidative metabolism (13), we hypothesized that PGC-1α might have a role in the process of regeneration.

PGC-1α is a master regulator of mitochondrial biogenesis and oxidative metabolism (14, 15). Its overexpression in skeletal muscle leads to a shift from the glycolytic to oxidative phenotype (16), high capacity in endurance exercise (17) and lower systemic inflammation (18), while muscle specific knock-out induces the opposite effect (19, 20). In addition, PGC-1α overexpression protects muscles against atrophy (21), sarcopenia (22) and reduces the dystrophic phenotype in *mdx* mice (23-26), although the complete mechanisms behind these effects have not been determined. However, its role in skeletal muscle regeneration has not been investigated yet.

Considering the importance of oxidative metabolism for skeletal muscle regeneration and the protective role of PGC-1α in the context of dystrophic mice and exercise, we sought to address the question of the role of PGC-1α in skeletal muscle regeneration in response to severe cardiotoxin (CTX) injury using muscle specific overexpression and knock-out mouse models. Surprisingly, our results indicate no difference in terms of functional recovery at later stages of regeneration when the difference in PGC-1α levels between the mouse models is most pronounced. However, we detected differences in early stages of regeneration, where we noticed a correlation between necrotic area, macrophage numbers and PGC-1α levels in both of our mouse models. We show that PGC-1α levels in mice influence the velocity of response to damage by chemokine secretion and recruitment of inflammatory cells which leads to a faster clearance of necrotic tissue. In addition, we detected increased fibrosis in the knock-out mice

compared to the controls after multiple CTX injury. Therefore, PGC-1α expression affects not only initial recruitment of inflammatory cells, but also development of fibrosis. These effects of PGC-1α might prove advantageous as a therapy after acute muscle damage, and also explain some of the previously described consequences of PGC-1α overexpression in dystrophic mice.

5.3 Materials and Methods

Animals:

PGC-1α transgenic mice (mTG) express PGC-1α under the control of muscle creatine kinase (MCK) promoter and have been previously described (16). A muscle specific PGC-1α knock-out model (mKO) was generated by crossing a PGC-1α$^{flox/flox}$ line (27) with a Myf5-Cre line (The Jackson Laboratory, stock number 007845). The genotype of mice was determined by PCR from toe biopsies using specific primers (Table 1). All experimental procedures performed on mice were approved by the Swiss authorities. In this study, male 8-12 week old mice were used unless stated otherwise.

Cardiotoxin injury:

In anesthetized mice (O_2/sevoflurane, 3% sevoflurane) kept on a warm plate, lower limbs were shaved and cleaned using 70% ethanol. 30µl of control vehicle (phosphate buffered saline, PBS) or 30µl (3µg) of CTX (C9759 Sigma) was injected in the belly of the tibialis anterior (TA) using insulin syringes (U-100, 300µl, 29Gx1/2"). Mice were sacrificed at various time points and TA muscles collected, transversally cut into two pieces and frozen for histology or RNA isolation.

Histology:

Half of a TA muscle was placed in the OCT (Tissue-Tek, Sakura) in plastic molds and frozen in isopenthane precooled in liquid nitrogen. 8µm thick sections were cut with a cryostat (Leica CM1950) and stored at -20˚C. Hematoxylin and eosin (Sigma MHS32, HT110232) staining (H&E) and Masson's trichrome (Sigma HT15, HT1079, HT10132) staining were performed on dried sections fixed with paraformaldehyde (PFA) according to the manufacturer's instructions, and mounted with Eukitt mounting medium (O. Kindler). For nicotinamide adenine dinucleotide (NADH) staining, sections were incubated with NADH (Sigma, N-8129) and nitroblue (Sigma, N-5514) for 30 min at 37˚C. Immunostainings were performed on dried fixed sections or myotubes, blocked in 3% bovine serum albumin (BSA) in PBS, followed by primary antibody incubation (laminin ab11575 Abcam, DAPI 62248 Thermo Scientific, MF20 DSHB,

CD68 MCA1957GA Serotec). After washing with PBS, sections were incubated with secondary antibodies (goat-anti-mouse IgG2b Alexa488 A21141 Life Technologies, goat-anti-rabbit IgG Alexa488 A11008 Invitrogen, goat-anti-rat IgG Alexa488 A11006 Invitrogen, donkey-anti-rabbit IgG Alexa647 A31573 Life Technologies) then washed with PBS and mounted with Vectashield (H-1000 or H-1200 Vector).

Myoblast isolation:

A pure population of myoblasts was isolated using the single fiber technique explained elsewhere (28). In brief, muscle fibers were isolated from the extensor digitorum longus (EDL) muscle of 2-3 week old mice using collagenase A (Roche Diagnostics) and trituration by pipette, and incubated on matrigel (BD Biscience) coated dishes. Satellite cells emerging from the fibers were expanded using proliferation media (10% horse serum, 20% fetal bovine serum, 1% antibiotic mix, 1% chicken embryo extract, 2mM L-Glutamine, 5ng/ml basic fibroblast growth factor in HyClone DMEM media). High purity of the myoblast population was confirmed with desmin staining.

Myoblast differentiation:

Matrigel-coated plastic dishes were plated with the same number of myoblasts and differentiation was induced a day later (mKO) or after the myoblasts started fusing (mTG). A different approach was used due to the possibility of different kinetics of proliferation in the case of mKO, and induction of transgene at more mature stages of differentiation in the case of mTG myoblasts. Differentiation was induced by switching from high to low serum conditions (4% horse serum, 1% antibiotic mix, 1% chicken embryo extract in DMEM Glutamax). After two days of differentiation, RNA was extracted or the cells were fixed and stained.

Image acquisition and quantification:

Immunostained muscle sections and cells were acquired using a Zeiss LSM700 with the Zen 2010 software using a 25x objective with 0.5 zoom for sections or a 10x objective for myotubes. H&E and Masson's trichrome stainings were acquired using Olympus IX81 with a 4x objective. The entire area of the muscle sections was covered, and for myotubes 25 images were acquired. Quantification was performed on the complete area using the ImageJ software (section

area, necrotic area, intensity of NADH staining, area of macrophage staining, area of collagen staining), the Imaris software (nuclei counting in myotubes), or was done by hand (satellite cell and fusion index (FI) counting).

RNA extraction and relative quantitative PCR (qPCR):

Total RNA was extracted from half of a TA muscle or primary cells using TRI Reagent (Sigma) and/or lysing matrix tubes (MP Biomedicals) according to the manufacturer's instructions. After measuring RNA concentration on Nanodrop 1000 (Thermo Scientific), 1µg was treated with DNase I (Invitrogen) and used for cDNA synthesis using reverse transcriptase Superscript II (Invitrogen). Relative mRNA levels were measured by qPCR on a StepOne machine with SYBR green based detection, and normalized to TATA binding protein (TBP) expression using the ΔΔCt method. A list of primers is provided in Table 1.

Muscle contractility measurements *in situ*:

TA muscle regeneration was evaluated through measuring *in situ* isometric muscle contraction in response to nerve stimulation, as previously described (29). Mice were anesthetized using a pentobarbital solution (ip, 60 mg/kg) and supplemental doses were given as required, to maintain deep anesthesia during experiments. The paw was fixed with clamps to a platform and the knee was immobilized using stainless steel pins. The distal tendons of muscles were attached to an isometric transducer (Harvard Bioscience) using a silk ligature. The sciatic nerves were proximally crushed and distally stimulated by a bipolar silver electrode using supramaximal square wave pulses of 0.1ms duration. All data provided by the isometric transducer were recorded and analyzed on a computer, using the PowerLab software (4SP, AD Instruments). All isometric measurements were made at an initial length L0 (the length at which maximal tension was obtained during the tetanus). Responses to tetanic stimulation (pulse frequency from 6.25, 12.5, 25, 50, 100 and 143Hz) were successively recorded. Maximal tetanic force (P0) was determined. Muscle mass was measured to calculate specific force (P0 [g]/weight [g]). Finally, the fatigue resistance was assessed. The fatigue protocol consisted of one continuous contraction (50Hz for 45s). The time to reach 50% of the initial force was measured. After contractile measurements, mice were sacrificed with an overdose of anesthetic solution.

Statistical analysis

All data are presented as AV+/-SEM. CTX values are in most cases normalized to the PBS values of the corresponding genotype using unpaired comparison (e.g. each mTG CTX sample was normalized on average value of mTG PBS samples). Statistical analysis was performed using Student's t test for comparison of two groups (e.g. in most qPCR data those are two PBS- normalized CTX groups) and $p \leq 0.05$ was considered significant.

5.4 Figures

Target	Fwd primer (5'-3')	Rev primer (5'-3')
Arg-1	TGGCTTGCGAGACGTAGAC	GCTCAGGTGAATCGGCCTTTT
α-SMA	GTCCCAGACATCAGGGAGTAA	TCGGATACTTCAGCGTCAGGA
CD206	GTGGATTGTCTTGTGGAGCA	TTGTGGTGAGCTGAAAGGTG
CD68	CCAATTCAGGGTGGAAGAAA	CTCGGGCTCTGATGTAGGTC
Col1a1	GCTCCTCTTAGGGGCCACT	CCACGTCTCACCATTGGGG
Col3a1	CTGTAACATGGAAACTGGGGAAA	CCATAGCTGAACTGAAAACCACC
Col5a2	TTGGAAACCTTCTCCATGTCAGA	TCCCCAGTGGGTGTTATAGGA
Col6a1	CTGCTGCTACAAGCCTGCT	CCCCATAAGGTTTCAGCCTCA
Cox1	TGCTAGCCGCAGGCATTACT	GCGGGATCAAAGAAAGTTGTG
CycS	GCAAGCATAAGACTGGACCAAA	TTGTTGGCATCTGTGTAAGAGAATC
ERRα	GCAGGGCAGTGGGAAGCTA	CCTCTTGAAGAAGGCTTTGCA
F4/80	CTTTGGCTATGGGCTTCCAGTC	GCAAGGAGGACAGAGTTTATCGTG
Gabpa	AGCGCATCTCGTTGAAGAAG	TCCTGCTCTTTTCTGTAGCCT
HGF	ATGTGGGGGACCAAACTTCTG	GGATGGCGACATGAAGCAG
IGF-1	GCTATGGCTCCAGCATTCG	GCTCCGGAAGCAACACTCAT
IL-10	CTGGACAACATACTGCTAACCG	GGGCATCACTTCTACCAGGTAA
IL-1β	TGACGGACCCCAAAAGATGA	CTGCTGCGAGATTTGAAGCT
IL-1Ra	AAATCTGCTGGGGACCCTAC	TGAGCTGGTTGTTTCTCAGG
IL-4Rα	ACACTACAGGCTGATGTTCTTCG	TGGACCGGCCTATTCATTTCC
IL-6	CCTTCCTACCCCAATTTCCAA	TCCTTAGCCACTCCTTCTGTGACT
MCP-1	CCCAATGAGTAGGCTGGAGA	TCTGGACCCATTCCTTCTTG
MIP-1α	TTCTCTGTACCATGACACTCTGC	CGTGGAATCTTCCGGCTGTAG
MIP-1β	TTCCTGCTGTTTCTCTTACACCT	CTGTCTGCCTCTTTTGGTCAG
MIP-2	CTGCCAAGGGTTGACTTCAA	TTTTGACCGCCCTTGAGAGT
MMP-9	GCGTCGTGATCCCCACTTAC	CAGGCCGAATAGGAGCGTC
MRF-4	CGCGAAAGGAGGAGACTAAAGA	CCACAGTCCGACGCTTCAG
Mstn	GCTGGCCCAGTGGATCTAAA	CAGCCCCTCTTTTTCCACATT
MyoD1	GCCGGTGTGCATTCCAA	CACTCCGGAACCCCAACAG
Myog	GCAGCGCCATCCAGTACATT	ATCGCGCTCCTCCTGGTT
Pax7	AAAAAACCCTTTCCCTTCCTACA	AGCATGGGTAGATGGCACACT
PGC-1α ex2	TGATGTGAATGACTTGGATACAGACA	CGTCATTGTTGTACTGGTTGGATATG
PGC-1α ex3-5	AGCCGTGACCACTGACAACGAG	GCTGCATGGTTCTGAGTGCTAAG
PGC-1β	CCATGCTGTTGATGTTCCAC	GACGACTGACAGCACTTGGA
PRC	CACCCTGCCGGAGTGAAAT	CGCATTGACTGCTGCTTGTC
TBP	TGCTGTTGGTGATTGTTGGT	CTGGCTTGTGTGGGAAAGAT
Tfam	GGAATGTGGAGCGTGCTAAAA	TGCTGGAAAAACACTTCGGAATA
TGF-β1	GAAACGGAAGCGCATCGA	TGGCGAGCCTTAGTTTGGA
TNF-α	CACAAGATGCTGGGACAGTGA	TCCTTGATGGTGGTGCATGA
Cre (genotyping)	GCGGTCTGGCAGTAAAAACTATC	GTGAAACAGCATTGCTGTCACTT
LoxP (genotyping)	TCCAGTAGGCAGAGATTTATGAC	TGTCTGGTTTGACAATCTGCTAGGTC

Table 1. List of primers
All primers were used for qPCR measurements, except for Cre and LoxP primers which are used for genotyping mKO mice

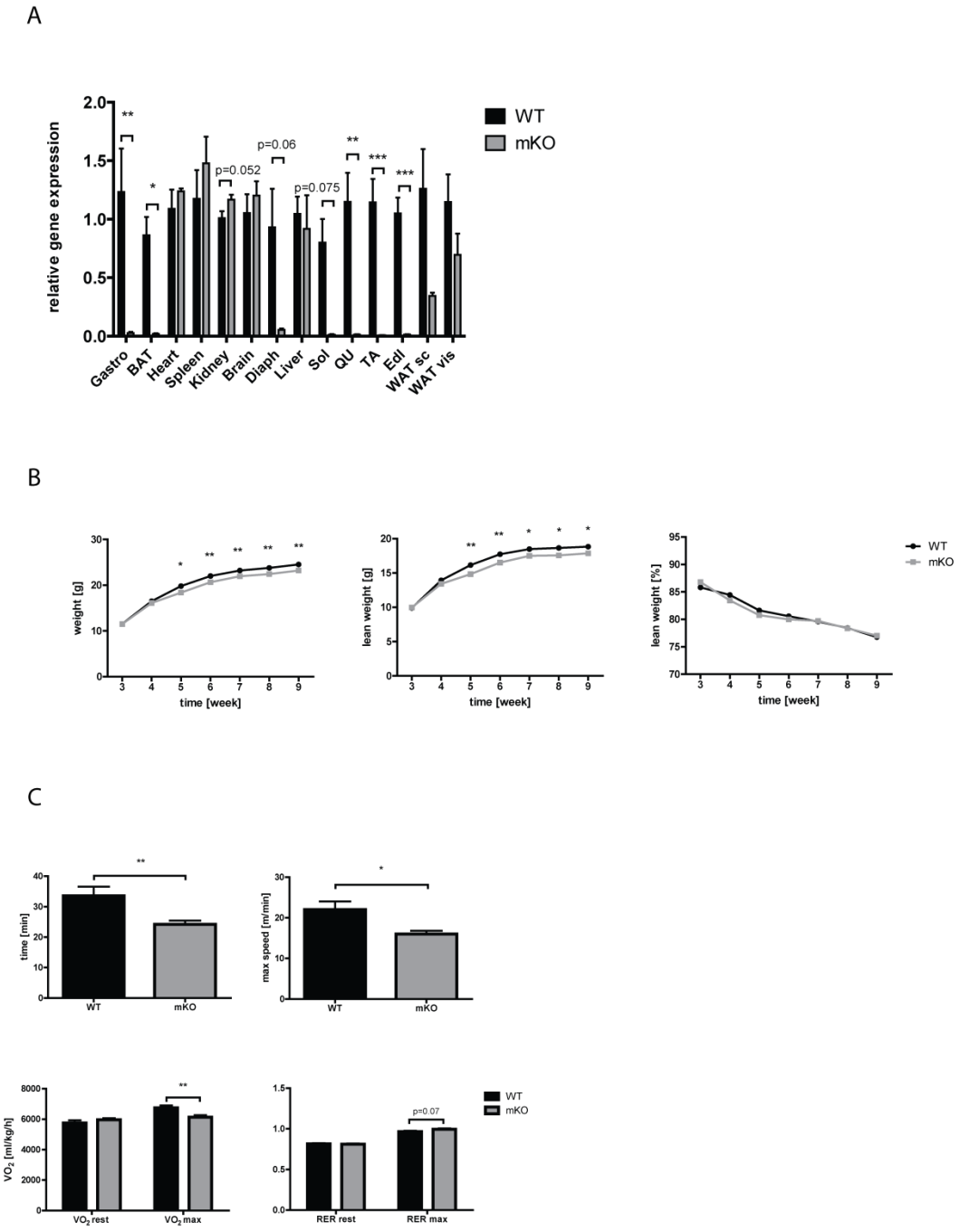

Supp Fig 1. Characterization of Myf5-mKO mice

A) Relative PGC1-α mRNA expression levels in various organs; mRNA levels in mKO mice were normalized to WT (control littermate) levels; n=6 per group; B) Body composition: weight and lean weight in mice from 3 to 9 weeks old; n=8-9 per group; C) Exercise capacity in mKO mice is reduced: time till exhaustion, maximal speed reached, VO_2 max and respiratory exchange ratio (RER) values before run and at the exhaustion; n=8-9 per group; only comparison between genotypes was made (t test); Values are plotted as AV+/-SEM; * p≤0.05, ** p≤0.01, *** p≤0.001; Abbreviations: Gastro (gastrocnemius), Sol (soleus), QU (quadriceps), Edl (extensor digitorum longus)

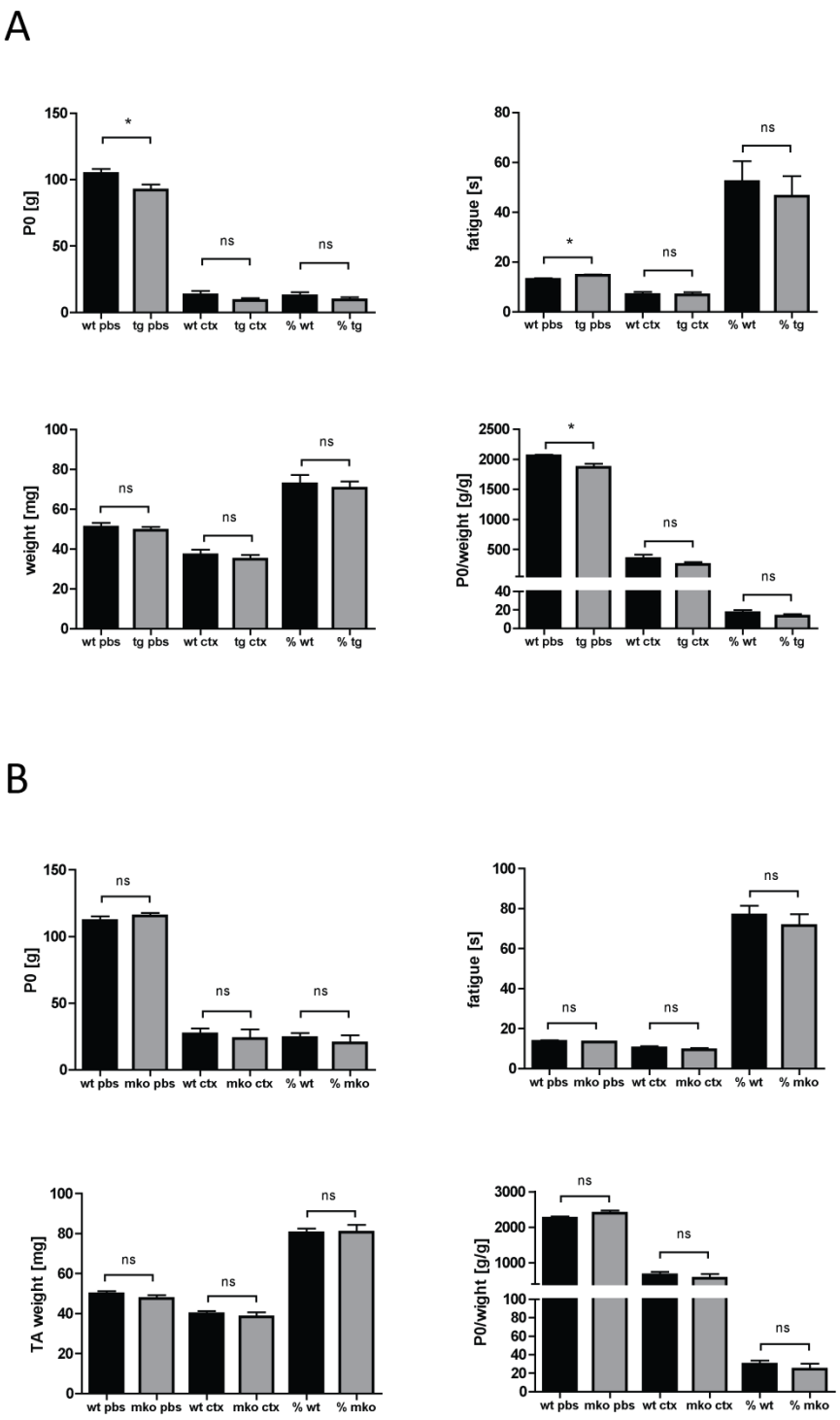

Fig 1. *In situ* TA contractility measurements 10 days after cardiotoxin injection in mTG and mKO mice
Maximal force (P0), fatigue, TA weight and specific force (P0/weight) in A) mTG and B) mKO mice; only comparison between genotypes was made (t test); Values are plotted as AV+/-SEM; n=7-11 per group; * $p \leq 0.05$, ** $p \leq 0.01$, *** $p \leq 0.001$

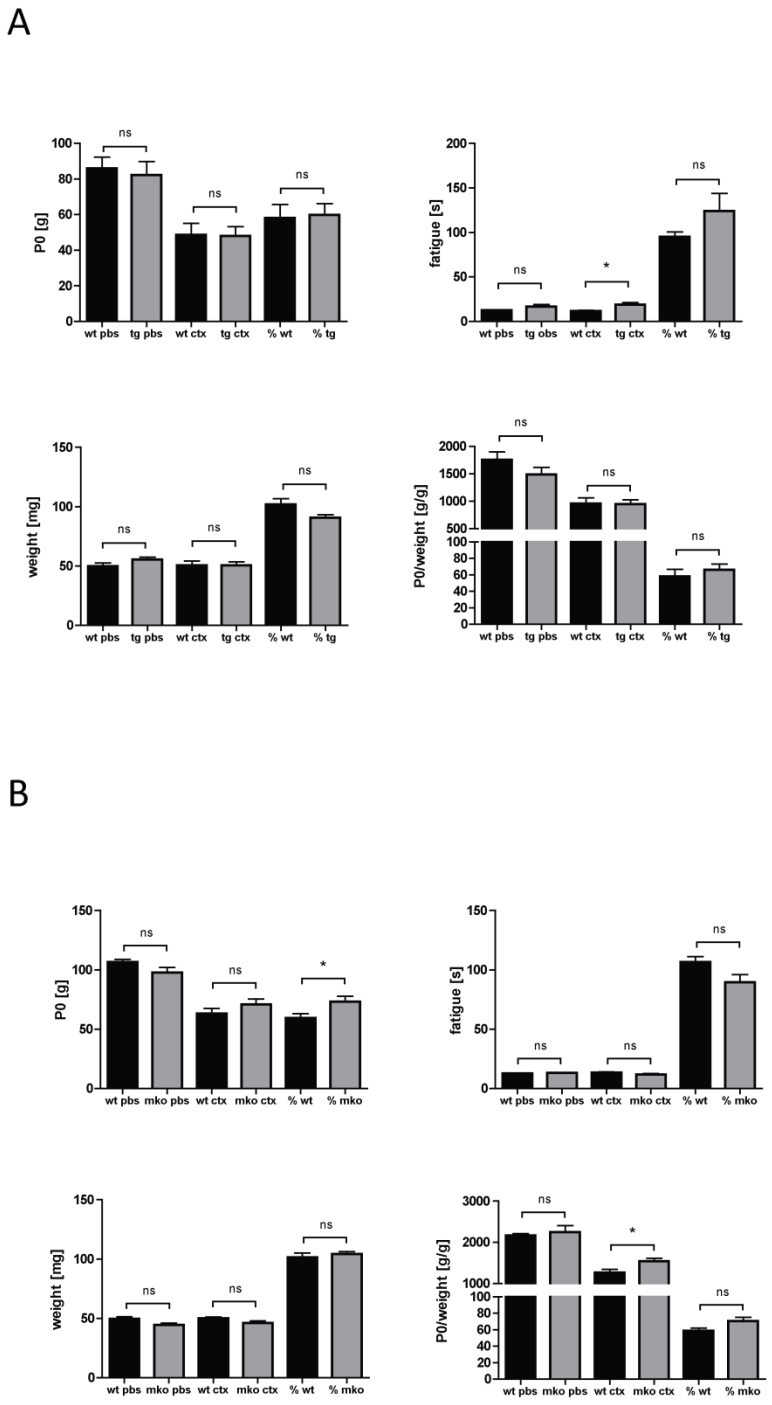

Supp Fig 2. *In situ* TA contractility measurements 16 days after cardiotoxin injections in mTG and mKO mice

Maximal force (P0), fatigue, TA weight and specific force (P0/weight) for A) mTG and B) mKO mice; only comparison between genotypes was made (t test); Values are plotted as AV+/-SEM; n=7-8 per group; * $p \leq 0.05$, ** $p \leq 0.01$, *** $p \leq 0.001$

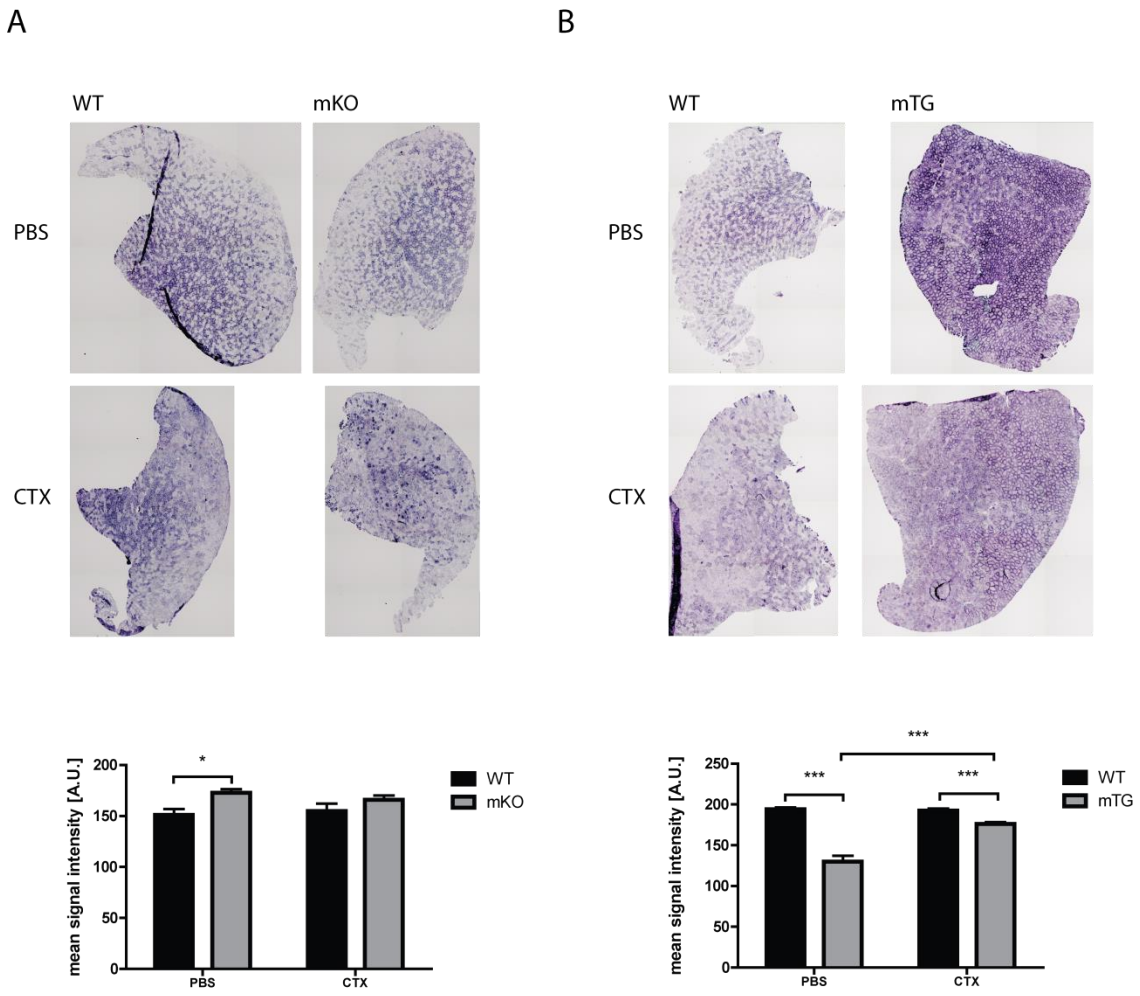

Supp Fig 3. NADH staining of TA 19 days after cardiotoxin injections
Representative images of NADH stained sections injected either with CTX or control (PBS injected) and signal intensity measurement in A) mKO and B) mTG mice. Note: lower values indicate darker staining (signal intensity 0-255, where 0 translated into no signal and 255 into fully saturated signal); comparison was made between genotypes and treatments (t test); Values are plotted as AV+/-SEM; n=5-10 per group; * $p \leq 0.05$, ** $p \leq 0.01$, *** $p \leq 0.001$

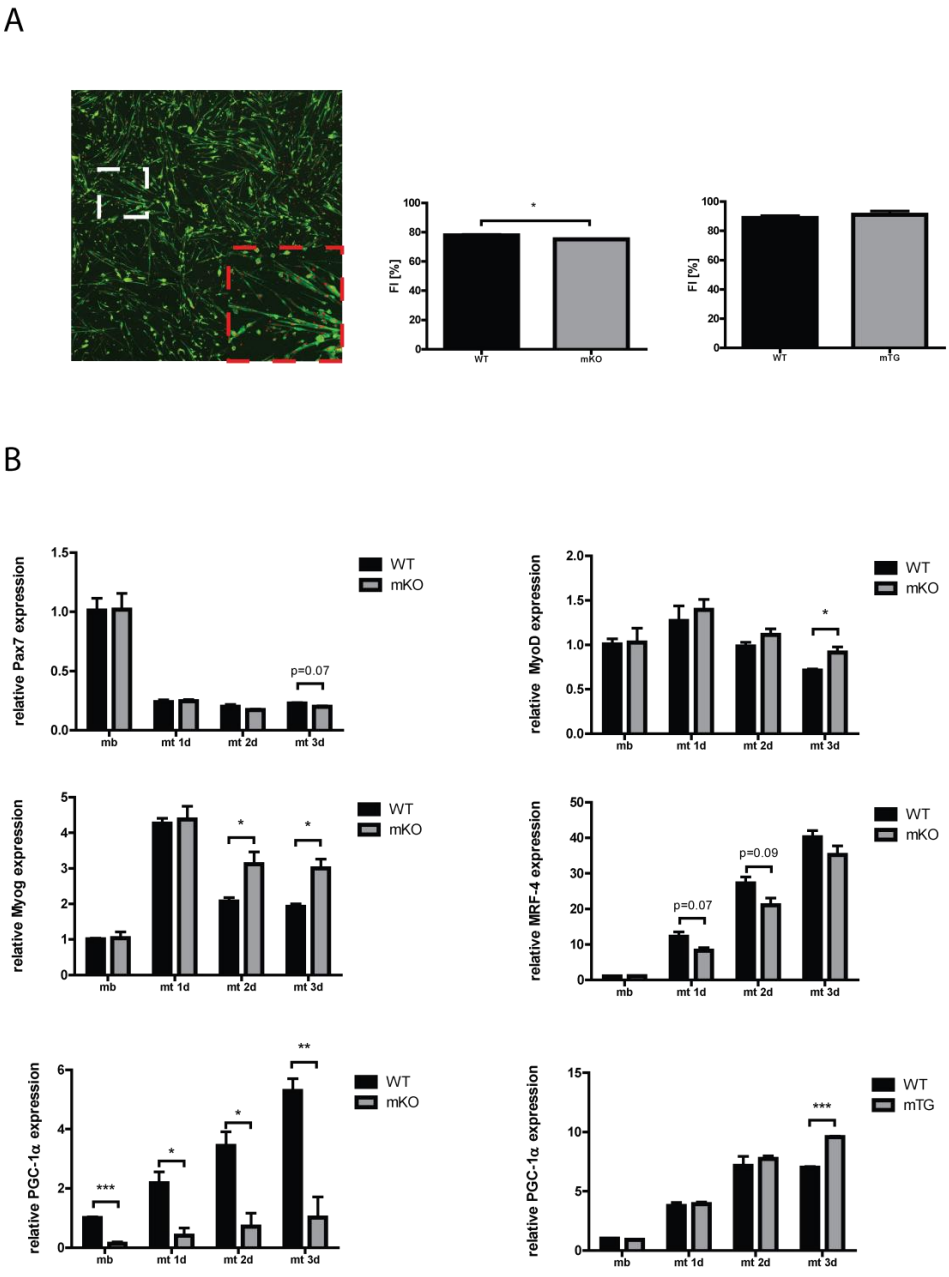

Supp Fig 4. *In vitro* myogenesis

A) Representative IHC image of differentiated myotubes 2 days after switching to low serum media (MF20: green; dapi/nuclei: blue) and fusion index (FI) for mKO and mTG mice at the same time point; quantification was done on area of 10.2 mm^2 per dish, 2 dishes per mouse and 3 mice per genotype; red quadrant represents enlarged area of white quadrant; B) Relative mRNA expression levels of Pax7 and MRFs at the proliferative state (MB, myoblast) and during differentiation (MT, myotubes at 1d, 2d and 3d of differentiation) in mKO. Same measurements were not performed for mTG due to the later expression from transgene (notice PGC-1α expression levels at 3d in mTG). Gene expression levels in myotubes were normalized to the myoblast levels of the corresponding genotype, except for PGC-1α expression levels, where WT PBS expression levels were used for normalization; only comparison between genotypes was made (t test); n=3 per group (in duplicate); Values are plotted as AV+/-SEM; * $p \leq 0.05$, ** $p \leq 0.01$, *** $p \leq 0.001$

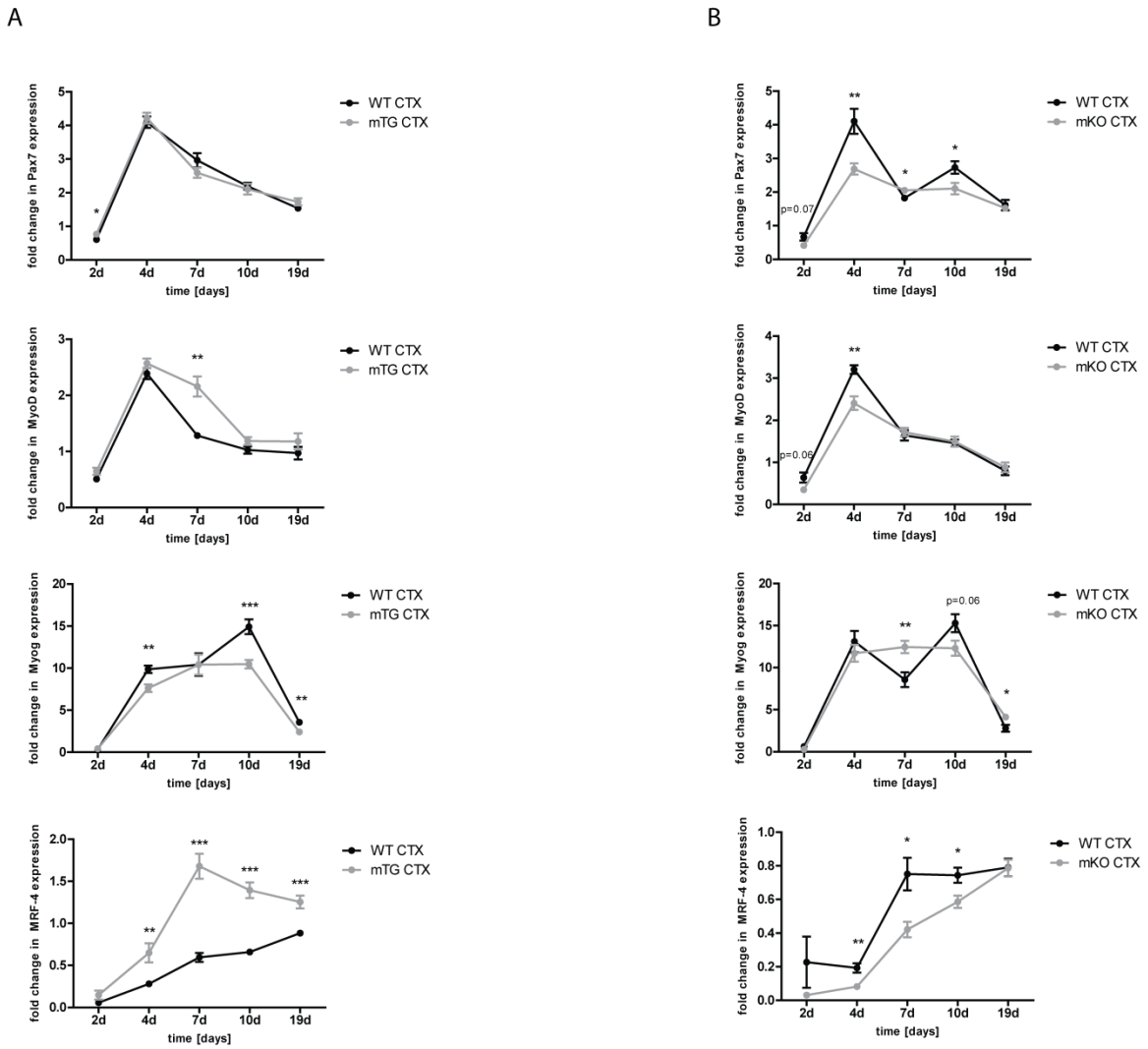

Fig 2. Kinetics of Pax7 and MRFs expression after cardiotoxin injury
Relative mRNA expression 4d, 7d, 10d and 19d post CTX injection in A) mTG and B) mKO mice; CTX expression levels were normalized to the PBS levels of the corresponding genotype; only comparison between genotypes was made (t test); Values are plotted as AV+/-SEM; n=4-12 per group (genotype and time point); * $p \leq 0.05$, ** $p \leq 0.01$, *** $p \leq 0.001$

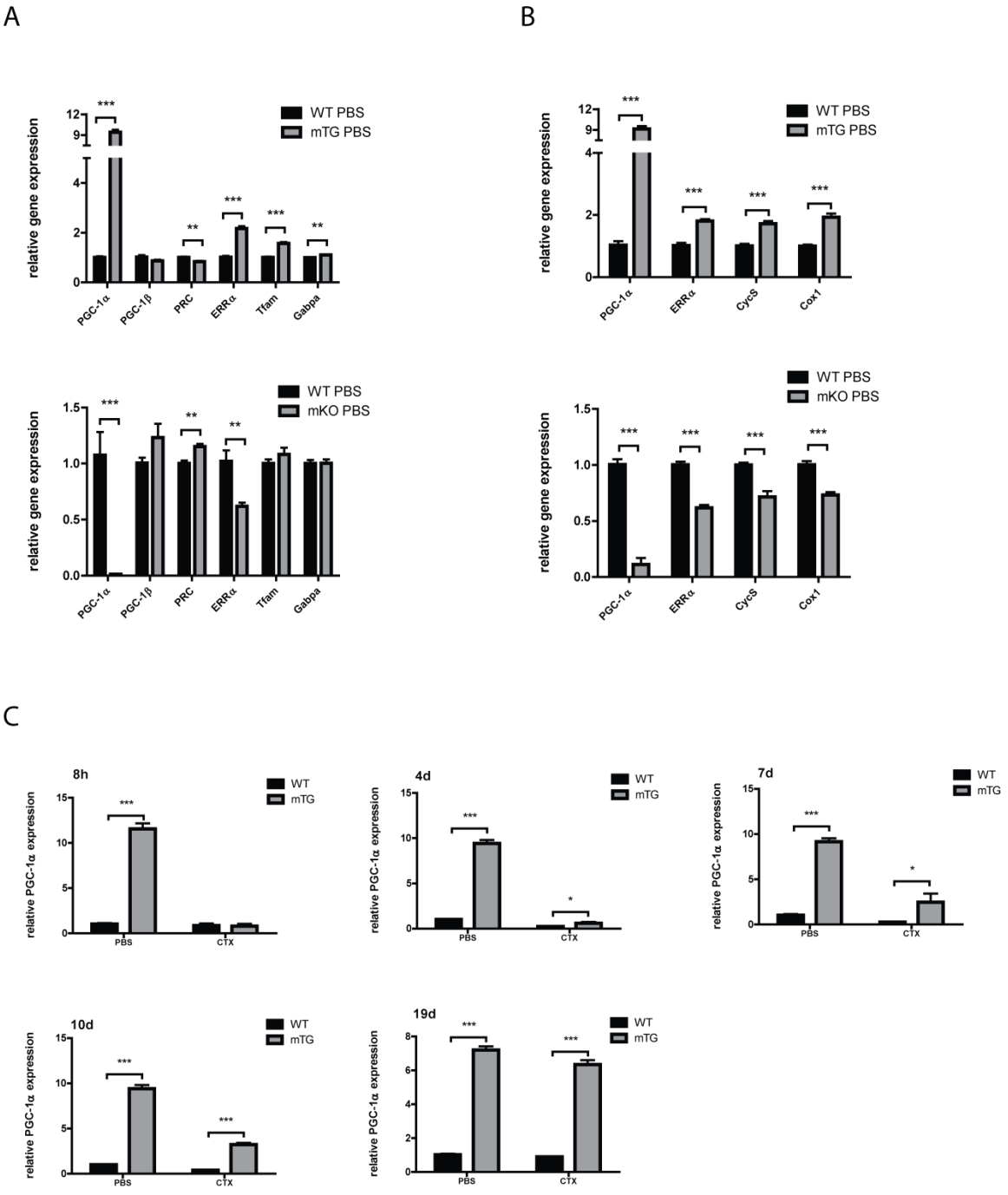

Supp Fig 5. Expression of metabolic genes at basal state and PGC-1α expression during regeneration
Relative mRNA levels of genes implicated in oxidative metabolism at A) 4d post CTX and B) 7d post CTX; C) Relative mRNA levels of PGC-1α at 8h, 4d, 7d and 10d post CTX. Normalization was based on WT PBS expression levels; only comparison between genotypes was made (t test); Values are plotted as AV+/-SEM; n=5-10 per group; * $p \leq 0.05$, ** $p \leq 0.01$, *** $p \leq 0.001$; Abbreviations: PRC (PGC-1-related coactivator), Tfam (mitochondrial transcription factor A), Gabpa (GA-binding protein alpha), CycS (cytochrome c, somatic), Cox1 (cytochrome oxidase subunit 1)

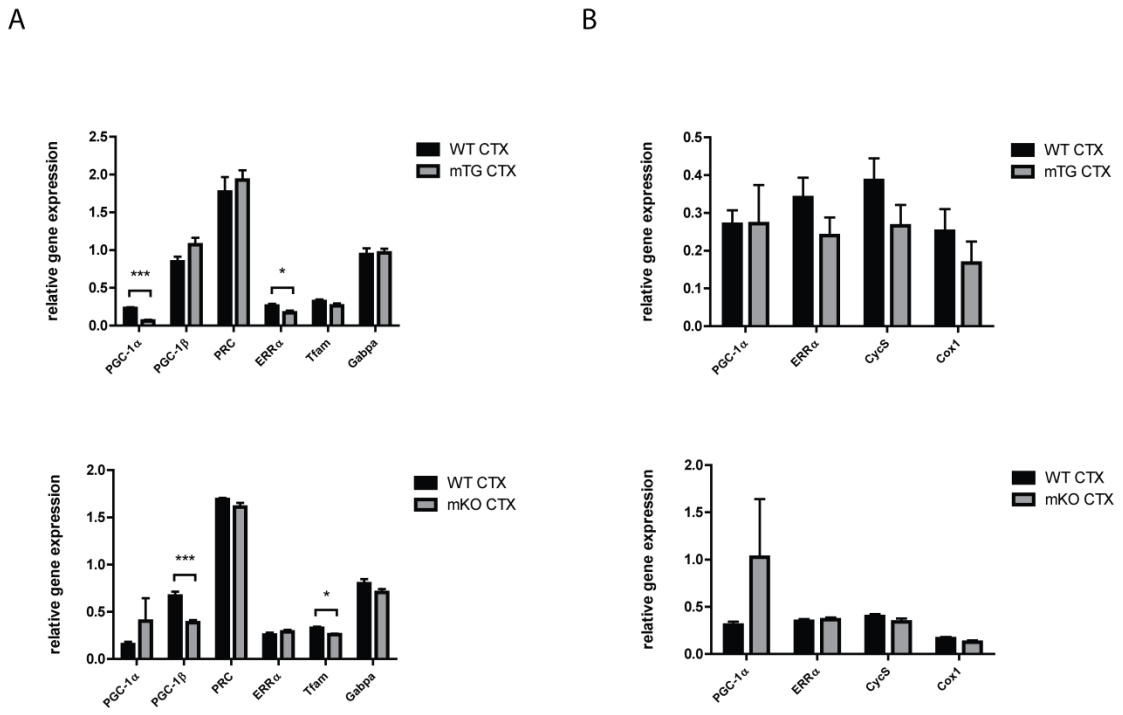

Fig 3. Expression of metabolic genes after cardiotoxin
Relative mRNA expression levels in mTG and mKO mice at A) 4d and B) 7d post CTX. CTX expression levels were normalized to the PBS levels of the corresponding genotype; only comparison between genotypes was made (t test); Values are plotted as AV+/-SEM; n=5-8 per group; * $p \leq 0.05$, ** $p \leq 0.01$, *** $p \leq 0.001$; Abbreviations: PRC (PGC-1-related coactivator), Tfam (mitochondrial transcription factor A), Gabpa (GA-binding protein alpha), CycS (cytochrome c, somatic), Cox1 (cytochrome oxidase subunit 1)

A

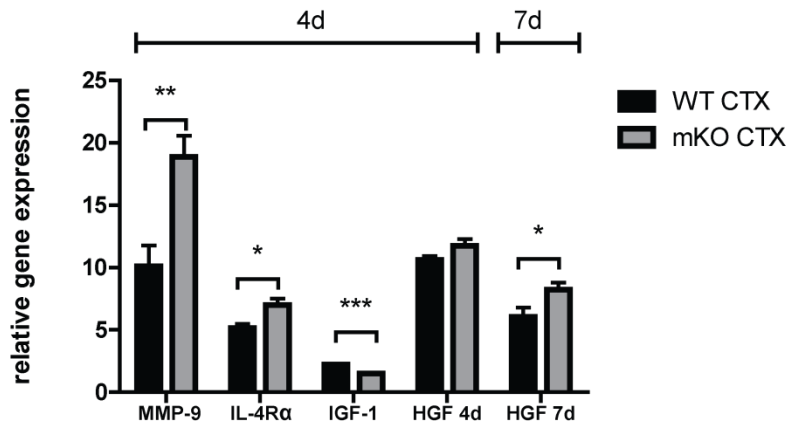

B

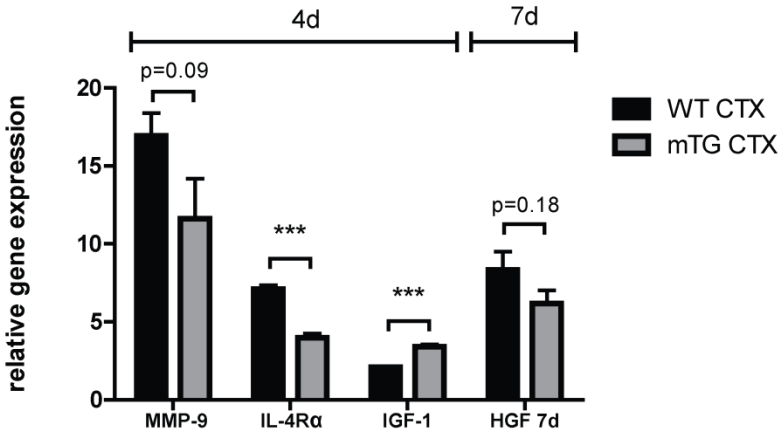

Supp Fig 6. Expression of genes participating in early stages of regeneration 4d and 7d after cardiotoxin injection

A) data for mKO and B) mTG mice. CTX expression levels were normalized to the PBS levels of the corresponding genotype; only comparison between genotypes was made (t test); Values are plotted as AV+/-SEM; n=5-8 per group; * $p \leq 0.05$, ** $p \leq 0.01$, *** $p \leq 0.001$

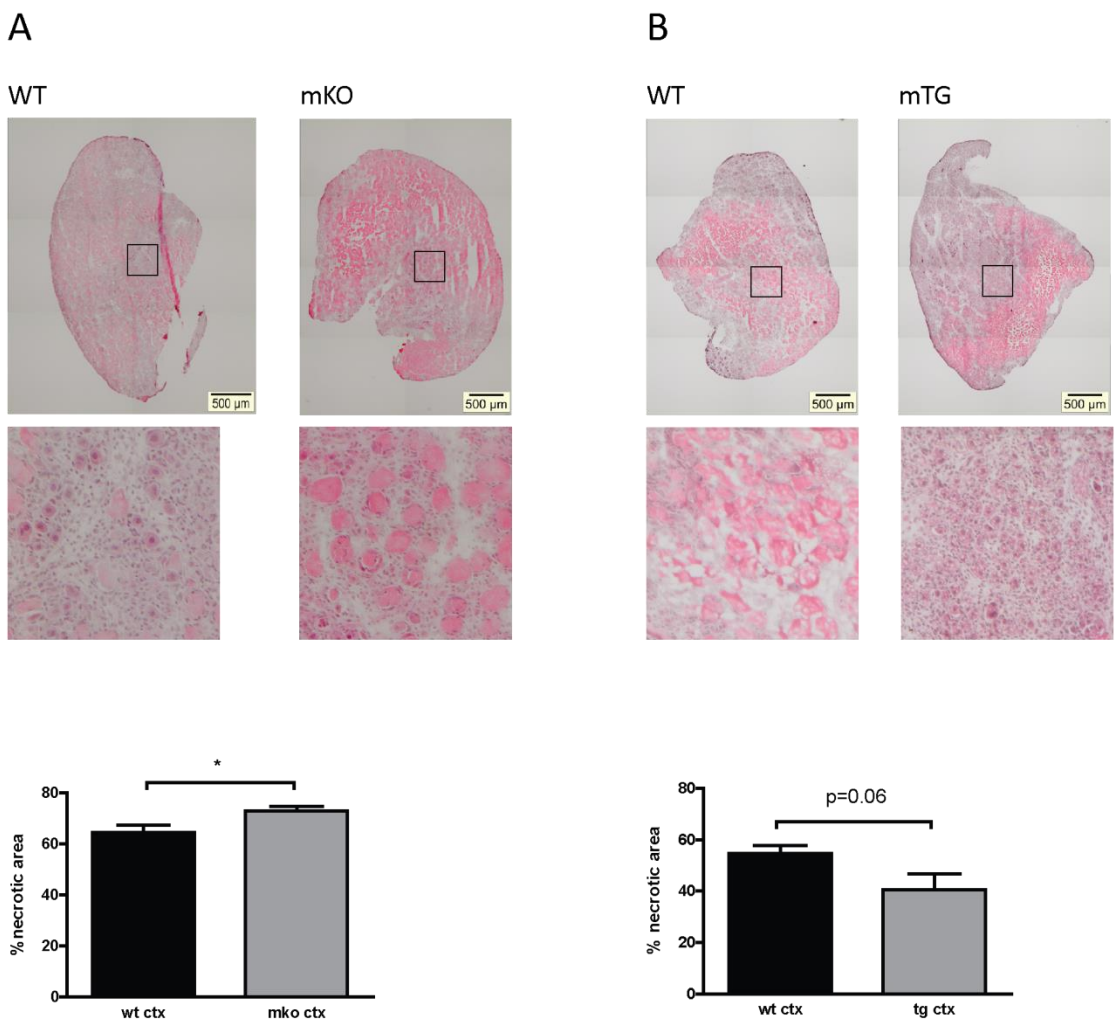

Fig 4. Necrosis at 4d post cardiotoxin
Representative H&E stained sections with enlarged areas showing necrotic and regenerating fibers and measurements of necrotic area normalized to the total section area for A) mKO and B) mTG mice; Values are plotted as AV+/-SEM; n=5-8 per group; * $p \leq 0.05$, ** $p \leq 0.01$, *** $p \leq 0.001$

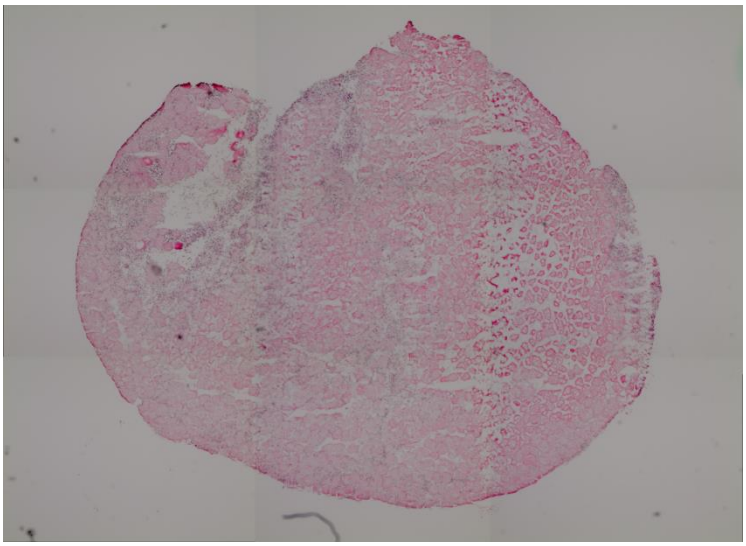

Supp Fig 7. H&E stained section 2d post cardiotoxin injury
Image shows complete muscle damage resulting in necrosis

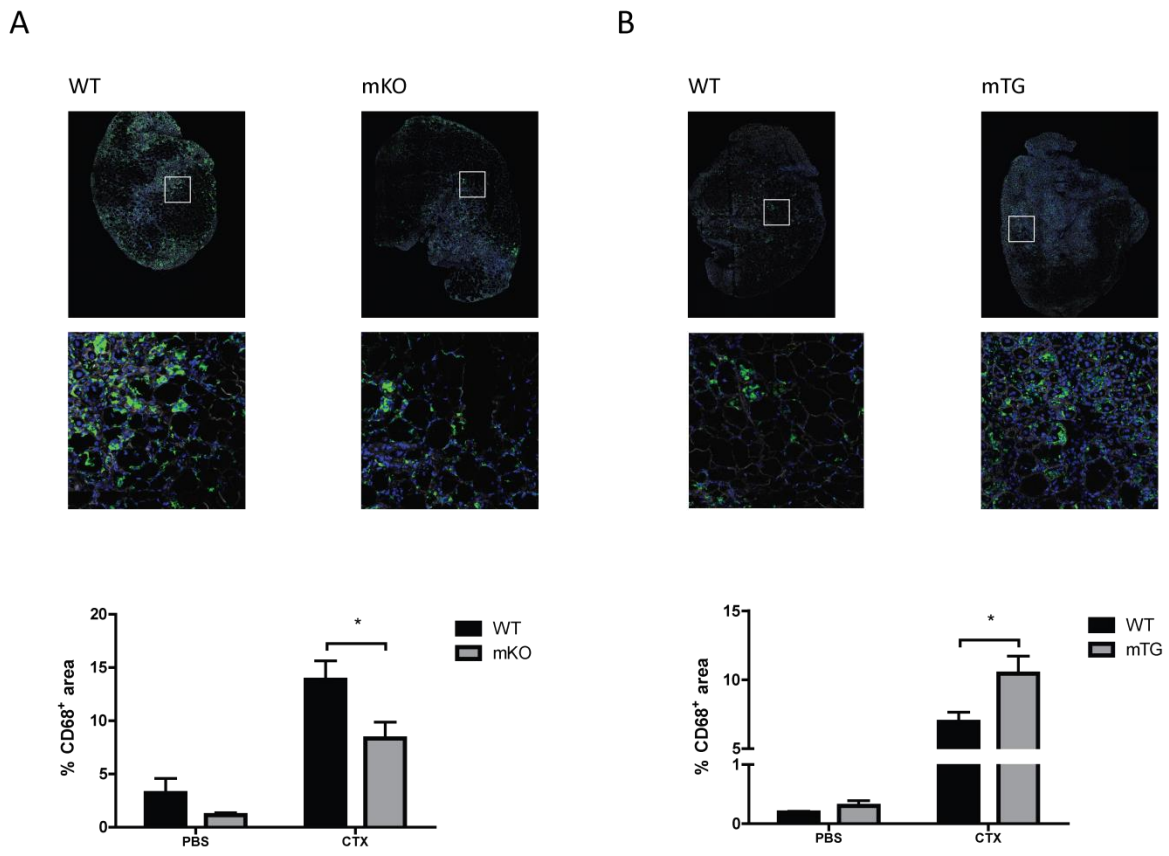

Fig 5. Macrophage staining and quantification 4d post cardiotoxin
Representative IHC images with enlarged areas showing accumulating macrophages (CD68: green; dapi/nuclei: blue; laminin: grey) and quantification results of $CD68^+$ area normalized to the total section area for A) mKO and B) mTG mice; only comparison between genotypes was made (t test); Values are plotted as AV+/-SEM; n=5-8 per group; * $p \leq 0.05$, ** $p \leq 0.01$, *** $p \leq 0.001$

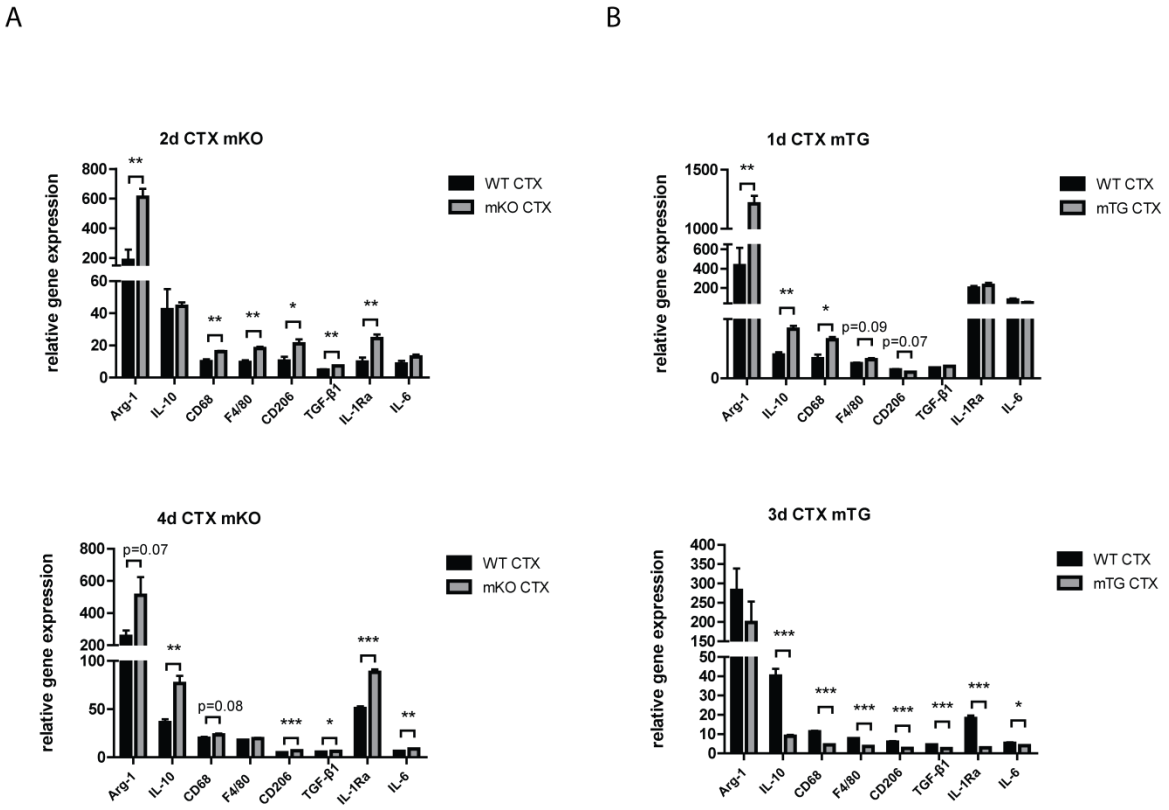

Supp Fig 8. Relative mRNA expression levels of M1 and M2 macrophage markers at two time points after cardiotoxin injection

A) mKO mice 2d and 4d after CTX; B) mTG mice 1d and 3d after CTX. CTX expression levels were normalized to the PBS levels of the corresponding genotype; only comparison between genotypes was made (t test); Values are plotted as AV+/-SEM; n=3-7 per group; * $p \leq 0.05$, ** $p \leq 0.01$, *** $p \leq 0.001$

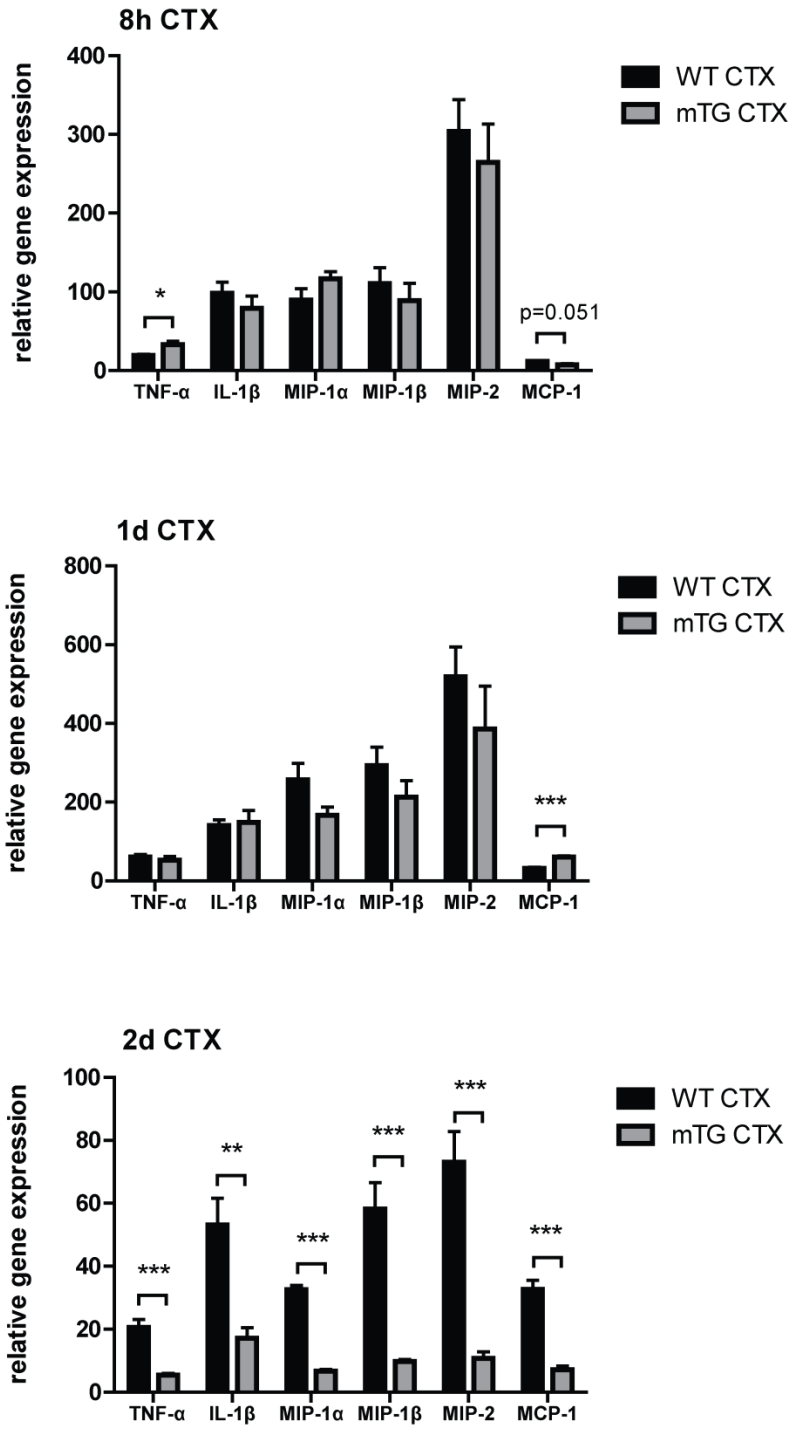

Fig 6. Chemokine and cytokine expression in mTG mice after cardiotoxin
A) 8h after CTX; B) 1d after CTX) and C) 2d after CTX. CTX expression levels were normalized to the PBS levels of the corresponding genotype; only comparison between genotypes was made (t test); Values are plotted as AV+/- SEM; n=4-6 per group; * $p \leq 0.05$, ** $p \leq 0.01$, *** $p \leq 0.001$

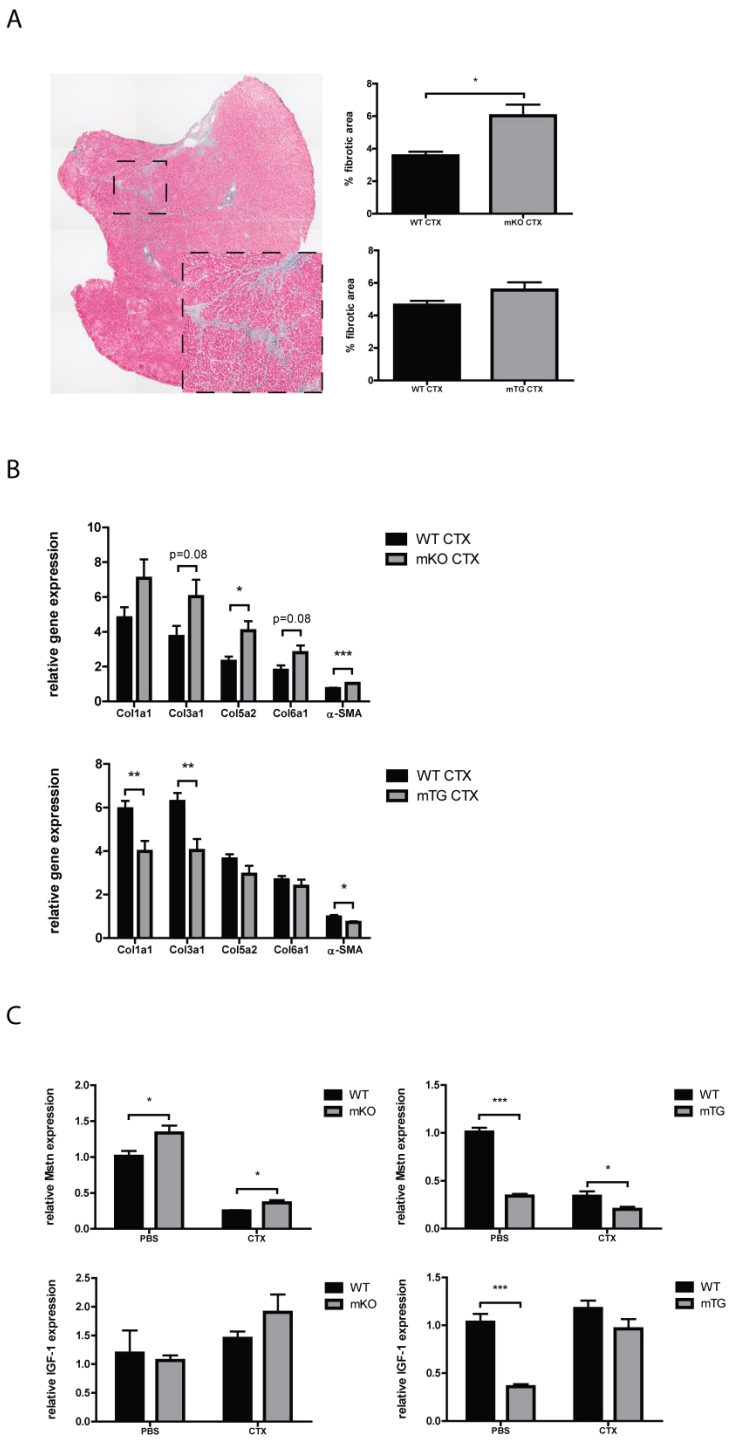

Fig 7. Fibrosis after multiple cardiotoxin injections

A) Representative Masson's Trichrome stained section with enlarged area and quantification of fibrotic area in mKO and mTG mice 3 weeks after the third CTX injection; B) Relative mRNA levels of profibrotic genes at the same time point in mKO and mTG mice; C) Relative mRNA levels of IGF-1 and Mstn 19d after single CTX injection in mKO and mTG mice. CTX expression levels were normalized to the PBS levels of the corresponding genotype; only comparison between genotypes was made (t test); Values are plotted as AV+/-SEM; n=4-10 per group; * $p \leq 0.05$, ** $p \leq 0.01$, *** $p \leq 0.001$; Abbreviations: Col (collagen)

5.5 Results

Myf5 Cre-PGC1α knock-out (mKO) and MCK-PGC-1α transgenic (mTG) mouse models

In order to study the role of PGC-1α in skeletal muscle regeneration, we generated muscle specific knock-out mice (mKO). PGC-1$\alpha^{loxP/loxP}$ homozygote mice with floxed PGC-1α exons 3-5 (30) were crossed with Myf5-Cre heterozygote mice (The Jackson Laboratory, 007845). The Myf5 promoter was chosen for achieving PGC-1α ablation at the muscle progenitor stage. Analysis of mKO mice confirmed reduction in PGC-1α transcript levels (Supp Fig 1). In addition to muscle tissue, Cre-driven ablation also affected brown adipose (BAT) and to a lower extent white adipose tissue (WAT) visceral (vis) and subcutaneous (sc) compartments, both of which share origins in $Myf5^{+}$ progenitors together with muscle cells (31, 32). Compared to Myog-Cre PGC-1α mice (19, 20), mKO mice have lower body weight due to reduced lean mass (Supp Fig 1). mKO are also characterized by diminished capacity for endurance exercise measured by time and maximal speed achieved during incremental uphill running to exhaustion in a closed treadmill. Additional measurements revealed decreased maximal oxygen consumption (VO_{2max}) confirming reduced endurance capacity (Supp Fig 1). Since mKO mice are not completely backcrossed to the C57BL/6 background while mTG are, we used separate littermate controls for both genotypes (wild type, WT).

Unaffected functional recovery of CTX injected TA in mTG and mKO mice

Given that PGC-1α is a very important driver of oxidative metabolism (33), and that skeletal muscle differentiation and regeneration are dependent on the transition from glycolytic to oxidative pathways for energy production (10, 34), we first aimed to see whether different levels of PGC-1α in the muscle would affect terminal regeneration in terms of functional recovery. In order to answer this question, we performed *in situ* contractility measurements on control (PBS injected) and injured (CTX injected) TA muscles of mKO and mTG animals. Measurements at 10 days (10d) time point (Fig 1A) confirmed previously published observation of decreased force and increased fatigue resistance in mTG mice prior to injury (35). The same measurements also revealed tendencies towards opposite phenotype in mKO (Fig 1B). There was no change in recovery of fatigue resistance (recovered 50-80%) or force (recovered 10-20%) 10

days after the injury in either genotype. Since the force at this time point recovered to only 20% of the initial levels (Fig 1), we decided to perform the measurements at a later time point after CTX. At 16d after CTX (Supp Fig 2), force recovery was ~60% of control values, and no difference between the genotypes and their controls was present. mKO mice had higher specific force after CTX compared to WT (Supp Fig 2B), however there was no difference in terms of percentage of recovery (CTX values normalized to PBS values of the corresponding genotype). Also, although values for fatigue resistance in mTG at 16d were higher compared to WT, recovery in WT was nearly complete (~90%) and hence is not indicative of regeneration, but rather the possibility of a fiber type switch in mTG (Supp Fig 2A). Supplementary measurements at 19d considering NADH staining (Supp Fig 3) confirmed successful regeneration in terms of oxidative capacity in both models, with control and mKO groups fully recovered, and mTG still reaching towards its intrinsically higher basal level.

MRF gene expression during differentiation in vitro indicates slower regeneration in mKO

In order to assess the role of PGC-1α levels on myogenesis separately from the complexity of regeneration *in vivo*, we tested the efficiency of myotube formation by myoblasts isolated from mTG and mKO EDL muscles (Supp Fig 4). We did not notice physiologically relevant differences in fusion index (FI) in either of our models 2 days after initiation of differentiation (2-4% difference, Supp Fig 4A), whereas mild overexpression of PGC-1α in mTG myoblasts was measured (Supp Fig 4B). However, we detected slight changes in MRF gene expression levels during myoblast fusion in mKO. More specifically, we measured retarded downregulation of MyoD in mKO at 3d after initiation of differentiation, in parallel with delayed downregulation of Myog at 2d and 3d after an initial burst in expression, as well as tendencies towards slower upregulation of MRF-4 most prominently present at 1d (Supp Fig 4B). Importantly, those differences were accompanied by increased PGC-1α expression throughout differentiation only in WT mice. The measurements of expression levels of MRFs were not performed in mTG due to mild overexpression achieved *in vitro* (Supp Fig 4B).

Gene expression *in vivo* confirms delayed regeneration in mKO and faster in mTG at early time points

Observed differences in *in vitro* myogenesis prompted us to check whether the same trend regarding the suppressed expression of MRF factors in mKO can be recapitulated *in vivo*. We measured expression of the aforementioned factors at different time points throughout the regeneration after the CTX injury, and observed modest, yet interesting differences from 4d to 10d after CTX (Fig 2). We observed a smaller fold induction of Pax7, MyoD and MRF-4 at 4d in mKO (Fig 2B). There was a smaller reduction of Pax7 at 2d and higher MyoD fold increase in expression at 7d in mTG (Fig 2A). In addition, a shift to lower Myog and higher MRF-4 fold increase was evident in mTG, whereas the opposite trend was detected in mKO (4d-10d). Expression levels of several genes relevant for mitochondrial biogenesis and oxidative metabolism at 4d (Fig 3A) and 7d (Fig 3B) post CTX revealed neither considerable impairment in regeneration in mKO nor an advantage in mTG mice, which was in line with the downregulated PGC-1α levels in mTG mice at those time points (Supp Fig 5C). Importantly, the same genes from Fig 3 were upregulated in mTG and downregulated in mKO mice in contralateral TAs (Fig 5A and 5B) at 4d and 7d post PBS injection, confirming correct genotypes of mice.

Since we did not detect a phenotype at later stages of regeneration by measuring recovery of muscle performance (Fig 1 and Supp Fig 2), we focused our attention on early stages of regeneration. Relative gene expression of several genes confirmed slower regenerative response in mKO mice at 4d and 7d post CTX (Supp Fig 6). In particular, we detected higher expression of interleukin 4 receptor alpha (IL-4Rα) in mKO and lower in mTG – a receptor essential for necrotic area clearance after CTX (36). During early phases post injury, matrix metalloproteinase (MMP) expression rapidly increases as well, contributing to extracellular matrix remodeling (37). However, sustained expression of MMPs is implicated in tissue destruction (38). We measured higher levels of MMP-9 in mKO and a tendency towards lower levels in mTG at 4d (Supp Fig 6). The same time point was characterized by high levels of hepatocyte growth factor (HGF), which is responsible, among other things, for satellite cell activation (39, 40). However, at 7d we detected slower downregulation of HGF in mKO (expression levels at 4d were unchanged) and the opposite trend in mTG (Supp Fig 6). Another growth factor essential for

myoblast proliferation and differentiation alike, and therefore for the entire process of regeneration, is insulin-like growth factor 1 (IGF-1) (41). Expression levels at 4d revealed higher induction in mTG and lower in mKO (Supp Fig 6). These observations might be related not only to intrinsic properties of myoblasts and myocytes due to differential PGC-1α expression, but also due to the complex interplay between various cell types that participate in the early phases of regeneration. In light of the latter, it is worth mentioning that production of growth factors such as HGF and IGF-1 in injured skeletal muscle is mediated primarily by macrophages.

mTG indicates accelerated clearance of necrosis, which coincides with faster accumulation of macrophages

One of the prominent populations of cells that invade damaged muscle tissue after injury is macrophages. Their role in early stages is to clear the cell debris accumulating due to necrosis of damaged muscle fibers (6). By measuring the area occupied by purple swollen fibers on H&E sections 4d after CTX, we detected larger necrotic area in mKO (Fig 4A) and tendency towards smaller necrotic area in mTG mice (Fig 4B) compared to WT controls. Given that the muscles are completely damaged by CTX injury, and that all fibers degenerate (Supp Fig 7), we can conclude that the differences in area are due to the velocity of clearance of necrosis. Since the removal of cell debris is a function of macrophages, we measured the area of the sections occupied by $CD68^+$ cells at the same time point after CTX (Fig 5). We observed that the staining for macrophages coincides with the regenerating area, and therefore detected reduced area occupied by $CD68^+$ cells in mKO sections (Fig 5A) and the opposite phenotype in mTG mice (Fig 5B).

Differences in cytokine expression at early time points suggest earlier recruitment of macrophages in mTG

The transition from M1 to M2 macrophages is described as a physiological process which unfolds during regeneration and is associated with the progression from myoblast proliferation towards their fusion (8). These populations of macrophages secrete distinct subsets of cytokines that prepare an environment suitable for myoblast expansion and myotube formation. We measured expression of several macrophage markers including the pan macrophage marker F4/80, the pro-inflammatory M1 markers CD68 and IL-6, as well as the anti-inflammatory M2

markers IL-10, transforming growth factor beta (TGF-β), arginase 1 (Arg-1), IL-1Ra and CD206 at two early time points after CTX injury, in order to assess the possibility of a macrophage subclass switch in either of the mouse models (Supp Fig 8). Our results demonstrate higher expression of several markers at 1d, followed by faster reduction at 3d in mTG mice (Supp Fig 8B). In mKO mice, we also noticed higher expression at 2d, with prolonged induction of macrophage markers at 4d compared to controls (Supp Fig 8A). In both genotypes, the kinetics seems not to be connected to a specific subclass of markers (M1 vs. M2), but rather to be independent of it. These results indicate that muscles with overexpressed PGC-1α can respond to injury in a swifter manner, which therefore leads to faster clearance of necrosis and early regeneration.

The first cells that respond to injury are resident macrophages and mast cells. In response to injury, they secrete TNF-α and IL-6 which attract neutrophils within hours (8, 42). Neutrophils will continue producing TNF-α, but also chemokines MCP-1, MIP-1α and MIP-1β in order to attract monocytes from the blood stream, which will give rise to macrophages once they enter the muscle tissue. To test the hypothesis of faster attraction of immune cells to injured areas in mTG animals, we measured chemokine and early cytokine expression at 8h, 1d and 2d after CTX (Fig 6). For all the genes tested, peak expression was detected at 1d in both mTG and WT. However, there was a difference in gene expression kinetics at these three time points between genotypes. In that sense, mTG showed faster induction in TNF-α at 8h followed by faster reduction at 2d CTX, and a higher peak of MCP-1 at 1d CTX. Importantly, a quicker drop in expression was measured for all the chemokines tested at 2d CTX in mTG (Fig 6). These data indicate that overexpressing PGC-1α in skeletal muscle primes the muscle for rapid reaction in case of injury by fast production of chemokines which will attract immune cells, clear the cellular debris and create appropriate conditions for myogenesis to take place. On the other hand, tardy recruitment of inflammatory cells after injury, an enduring presence of macrophages, or block in the shift from the M1 to M2 subclass all lead to unsuccessful or slower regeneration (43-45).

Multiple CTX injury leads to increased fibrosis in mKO mice

Prolonged occurrence of macrophages, especially M2 subtype, is connected to expansion of fibroblasts and excessive secretion of extracellular matrix (ECM) components (46). Although

these factors contribute to the regenerative process, their removal at later stages of regeneration is necessary in order to regain fully functional skeletal muscle tissue. Intrigued by the differences in macrophage recruitment seen at early stages of regeneration, and bearing in mind connection between inflammation and fibrosis, we decided to take a closer look at fibrotic tissue formation at later stages of regeneration.

This time, we took advantage of multiple CTX injuries as a model of chronic damage, in order to exacerbate preexisting conditions in muscle of our two mouse models. Three weeks after the last CTX injection, we did not observe statistically significant differences in the area of muscle sections occupied by fibrotic tissue in mTG, but mKO revealed increased accumulation of fibrosis compared to WT (Fig 7A). This was accompanied by increased expression of major collagens and alpha smooth muscle actin (α-SMA) in mKO and opposite profile in mTG (Fig 7B). Interestingly, although myostatin (Mstn) expression considerably drops with injury, mTG mice have lower and mKO higher levels of Mstn at 19d after single CTX injection (Fig 7C). In addition, IGF-1 levels are upregulated to the similar extent in mTG and mKO mice, despite the lower starting levels in mTG observed in PBS injected TAs (Fig 7C).

5.6 Discussion

The PGC-1α cofactor is a well-known master regulator of oxidative metabolism and mitochondrial biogenesis (33), yet its role in skeletal muscle regeneration has not been addressed. In this study, we show that modulating PGC-1α levels does not affect the outcome of regeneration and myogenesis despite the energy demanding nature of these processes (34, 47). Interestingly, however, it does influence response to injury by modifying chemokine expression in the muscle and macrophage attraction, and as a consequence alters the speed of necrotic area clearance.

Despite the undisturbed regeneration in mTG and mKO measured primarily by *in situ* contractility and confirmed by NADH staining at later stages after CTX, we decided to look closely at the kinetics of MRFs as indication of pace of regeneration. Mild differences in the expression of MRFs both *in vitro* and *in vivo* at different time points lend credence to the notion of faster regeneration in mTG and slower in mKO mice. A closer look at the expression of growth factors (HGF, IGF-1) and factors contributing to cell debris removal and remodeling of the extracellular matrix (IL-4Rα, MMP-9) not only confirms the difference in the pace of regeneration between the genotypes, but also suggests an effect by non-myogenic cells on observed differences. Namely, recent studies report the importance of IL-4Rα expression on fibro/adipogenic progenitors (FAPs) proliferation and contribution to necrosis clearance after injury (36) whereas MMP-9, although implicated in ECM remodeling upon injury (37), is connected to tissue damage and pathogenesis when present in high amounts (38). The latter factors were expressed at higher levels in mKO and lower in mTG at 4d CTX, further bolstering the aforementioned differences in the progression of regeneration, which is dependent on PGC-1α levels.

Early stages after injury are characterized by necrosis of the damaged muscle fibers, followed by inflammation and removal of necrotic tissue by macrophages and other cell types (48). We measured faster clearance of necrosis accompanied by larger area occupied by macrophages ($CD68^+$ cells) in mTG and the opposite phenotype in mKO at 4d CTX. In order to better assess the nature of the macrophages present at that time point, we measured expression of several receptors and cytokines in the muscle tissue. The importance of the switch from

classically-activated inflammatory (M1) to alternatively-activated and anti-inflammatory (M2) macrophages has been recently reported (45, 49). We did not observe prevalence of one over the other subclass between the two time points (1d and 3d for mTG; 2d and 4d for mKO) in our genetic models. Instead, we detected downregulation in all factors in mTG and sustained upregulation in mKO at the second time point (3d for mTG, 4d for mKO). These results suggest an intriguing possibility of faster attraction of immune cells upon injury given higher expression of PGC-1α. Interestingly, Rowe et al. recently demonstrated that PGC-1α induction in skeletal muscle of adult mice leads to macrophage infiltration and activation leading to MCP-1 production (50). Delayed infiltration or prolonged presence of immune cells has been associated with impaired regeneration (43, 44, 51). However, the importance of inflammation in the course of successful regeneration has been confirmed in multiple studies (52-56).

Since PGC-1α levels drop considerably already 8h after damage in mTG mice, we hypothesized that PGC-1α overexpression preconditions the muscle for swift response to injury, rather than inducing response upon injury. In order to take a closer look at this, we measured the expression of early chemokines at 1d and 2d after CTX. We detected a prominent drop in expression of MIP-1α, MIP-1β and TNF-α from 1d to 2d in control mice. However, this drop was even more prominent for mTG. More importantly, we observed higher expression of MCP-1 in mTG at 1d and lower at 2d compared to control mice. This indicates that mTG can respond faster to injury by increasing expression of important chemokines, whose function is to attract immune cells. Overexpression of TNF-α, which comprises the first response, probably comes from resident mast cells and macrophages whose contribution to regeneration is not fully understood (57, 58). TNF-α has been shown to attract neutrophils through MIP-2 induction (59). Neutrophils are the first immune cells that invade damaged muscle, appearing within hours. Massive production of chemokines such as MIP-1α, MIP-1β and MCP-1 by neutrophils and resident macrophages (42, 60, 61), serves as a signal to attract monocytes from the blood stream. Accumulating monocytes will differentiate into macrophages upon entering the tissue, and within a day, they will become the predominant inflammatory cells in the damaged tissue, replacing the neutrophils (58). Prolonged presence of neutrophils has turned out to be detrimental to the tissue, at least partly due to overproduction of the aforementioned chemokines (62-64). In that context, faster upregulation and especially downregulation of the critical chemokines in mTG might contribute to faster attraction of macrophages and faster regeneration, minimizing

the damaging effects of prolonged proinflammatory signaling. It is important to notice that the described inflammatory process is somewhat simplified, as cells other than neutrophils and macrophages can produce cytokines (e.g. eosinophils, mast cells, T cells). More importantly, muscle cells can modulate inflammatory response via interaction with inflammatory cells (5, 6). In addition, although the presence of macrophages has proven to be essential in different contexts of injury, there might be other cells that substantially contribute to phagocytosis of damaged tissue, like FAPs (36). Furthermore, the relevance of neutrophils in muscle regeneration is not definite (6).

Whereas timely clearance of proinflammatory phase is crucial for limiting the damaging effect to the host tissue, resolution of the second wave of macrophages, taking part in wound healing, is equally essential. Namely, sustained activity of M2 macrophages is connected to increased proliferation of fibroblasts and secretion of ECM components in the muscle tissue which results in fibrosis (46). Due to the link between inflammation and fibrosis, we aimed at assessing the fibrous tissue formation in the context of chronic injury. We observed increased fibrosis in mKO mice, with increased expression of collagens after multiple CTX injuries. Lower expression of collagens without the effect on fibrosis formation was seen in mTG mice in the same injury model. This coincided with the differential expression of IGF-1 in mTG and mKO after the injury. Interestingly, although Mstn is repressed during regeneration, we detected considerable differences in the expression at the basal level in our mouse models. Mstn is a member of TGF-β family, and known inducer of fibrosis (65). $Mstn^{-/-}$ mice are protected against fibrosis formation upon notexin injury, although Mstn is repressed during the regeneration in WT mice as well (66). At the same time, $Mstn^{-/-}$ mice exhibit faster recruitment of macrophages, comparable to mTG mice. Similar results regarding swift inflammation and reduced fibrosis are reported for IGF-1 transgenic mice (67). Therefore, IGF-1 overexpression, $Mstn^{-/-}$ and PGC-1α overexpression mice share similar regenerative phenotype, and consequently, increased IGF-1 expression in mTG mice after injury and decreased Mstn levels prior to injury can at least partially explain the differences that we observed.

The process of myoblast fusion is dependent on mitochondrial metabolism (68, 69). Due to that, the importance of several factors, drivers of oxidative metabolism, has been implicated and elucidated in the context of skeletal muscle differentiation and regeneration (11, 70-72). Of

special interest to this study is the role of the ERRα transcription factor, a distinctive binding partner of PGC-1α (73). Indeed, many of the effects of PGC-1α signaling, primarily regarding mitochondrial metabolism, are accomplished in partnership with ERRα (13, 74). Recent study demonstrated increased expression of both PGC-1α and ERRα during differentiation (11). In the same study, knock-out of ERRα negatively affected myogenesis *in vitro*, albeit unchanged expression of various metabolic and contractile proteins, the latter being explained by a compensatory increase in ERRγ and PGC-1α expression levels. Adenoviral ERRα induction on the other hand, led to improved myogenesis accompanied by increased PGC-1α levels as well. Our *in vitro* data investigating the effects of PGC-1α expression on myogenesis confirmed increased expression of this coactivator during differentiation. However, we did not observe pronounced alterations in myotube formation 2d post induction of differentiation, when the majority of nuclei were fused. It is important to note that at this time point we detected very mild PGC-1α expression from the transgene, and therefore the data are not indicative of PGC-1α overexpression in the context of myogenesis. Results from the mKO primary myoblasts on the other hand suggested a reduced pace of differentiation, but without a prominent effect on fusion index and formation of myotubes. It is conceivable that the modulation of PGC-1α *in vitro* might be evident with prolonged differentiation, as well as with more thorough examination of myotube formation, and future studies might look closer into these aspects.

The importance of ERRα for myogenesis has been recently investigated in the context of regeneration *in vivo* (12). Upon knock-out of ERRα, mice exhibited delayed regeneration characterized by perturbations in oxidative gene expression, but contrary to the *in vitro* study, ERRγ and PGC-1α expression levels were reduced throughout the process. However, increased PGC-1β and PRC levels at 3d post CTX in control mice, but not in KO, served as an explanation for the delayed regeneration seen in ERRα knock-out mice. In our study, we observed reduction in expression of the majority of oxidative genes tested upon CTX injection, with slow recovery towards basal levels during regeneration. An exception to this was PRC, which was upregulated in both mTG and mKO at 4d CTX. Interestingly, ERRα levels were reduced in both genotypes at the two time points tested, unlike previously published observations. These differences might come from slightly different kinetics of regeneration, induced by e.g. CTX potency (producer, concentration), keeping in mind that the expression levels of genes often drastically change within relatively small intervals of time during early stages of regeneration.

PGC-1α was previously linked with an anti-inflammatory state. In muscle specific PGC-1α knock-out mice, higher levels of systemic inflammation as well as inflammatory cytokine expression have been detected (20). In humans, type-2 diabetes has been correlated with lower PGC-1α levels and higher systemic levels of proinflammatory cytokines TNF-α and IL-6 (75). Recent *in vitro* work from our lab demonstrated anti-inflammatory effects of overexpressed PGC-1α via suppression of nuclear factor kappa B (NFκB) pathway (19, 76). Additionally, this study indicates a role of PGC-1α in modulating inflammation in the context of injury. In this regard, we propose that PGC-1α contributes to preparing the muscle for a prompt reply to injury by accelerating the process of cytokine secretion by resident cells, which in turn leads to faster attraction of macrophages, and clearance of damaged tissue. Based on the observation that PGC-1α expression drops as early as 8h after CTX in mTG, and that expression recovers slowly and reaches a considerable disproportion between the genotypes not earlier than 7d post CTX, we consider the direct effect of PGC-1α on modulation of gene expression upon injury less probable. However, in which way PGC-1α overexpression changes conditions in muscle, and whether it indirectly influences the resident inflammatory cell repertoire or through a direct influence modulates the secretome of muscle cells, awaits further investigation.

Interestingly, reduced macrophage accumulation associated with impaired regeneration was observed in ob/ob and db/db, but not high-fat diet (HFD) WT mice (all models of type-2 diabetes) (77), whereas another study reports impaired regeneration upon HFD due to reduced phosphatidylinositol (3,4,5)-trisphosphate (PIP3) levels partially through reduced activation of phosphatidylinositol-4,5-bisphosphate 3-kinase (PI3K) (78). One reason for the latter could be reduced IGF-1 levels. As mentioned earlier, mTG mice exhibit increased IGF-1 levels upon injury, the major producer of which are macrophages, whereas the opposite is observed in mKO. In addition, leptin treatment in leptin deficient ob/ob mice reverts the obesity and diabetes (79) and restores PGC-1α expression to the control level (80). Based on this, we could speculate that the reduced PGC-1α levels observed in type-2 diabetes can contribute to the impaired muscle regeneration phenotype seen in diabetic mice, and that increased PGC-1α levels could alleviate the pathology.

The effect of chemokine secretion ultimately resulting in necrosis clearance, which is dependent on PGC-1α, can be beneficial in diseases where delayed inflammation upon injury

leads or contributes to disease progression. One such example is dysferlinopathy, where not only membrane resealing, but also diminished neutrophil attraction to the site of injury followed by reduced secretion of chemokines contributes to dystrophy (81). The therapeutic potential of ectopic PGC-1α expression in the context of muscle diseases has been addressed in several studies – mitochondrial myopathy (82), statin-induced atrophy (83), and particularly Duchenne muscular dystrophy (DMD) (23-26). The beneficial consequences of PGC-1α overexpression in the DMD mouse model (*mdx*) go well beyond increased utrophin level, which was once seen as a primary effector. Intriguingly, while viral PGC-1α delivery in neonatal *mdx* mice leads to reduced central nucleation as an indicator of muscle degeneration/regeneration (24), the same treatment in 3-week old animals showed the same level of central nucleation with reduced markers of ongoing damage (25). The authors of the latter study interpret this observation as indicating the possibility of an additional valuable effect of PGC-1α modulation in the dystrophy model – improved regeneration. Our study supports this notion, and contributes to the list of the therapeutic effects of PGC-1α overexpression in the context of chronic injury.

5.7 References

1. Schmalbruch, H., and Hellhammer, U. (1977) The number of nuclei in adult rat muscles with special reference to satellite cells. *Anat Rec* **189**, 169-175
2. Ciciliot, S., and Schiaffino, S. (2010) Regeneration of Mammalian Skeletal Muscle: Basic Mechanisms and Clinical Implications. *Current Pharmaceutical Design* **16**, 906-914
3. Relaix, F., and Zammit, P. S. (2012) Satellite cells are essential for skeletal muscle regeneration: the cell on the edge returns centre stage. *Development (Cambridge, England)* **139**, 2845-2856
4. Sabourin, L. A., and Rudnicki, M. A. (2000) The molecular regulation of myogenesis. *Clin Genet* **57**, 16-25
5. Pillon, N. J., Bilan, P. J., Fink, L. N., and Klip, A. (2012) Crosstalk between skeletal muscle and immune cells: muscle-derived mediators and metabolic implications. *American journal of physiology. Endocrinology and metabolism*
6. Tidball, J. G. (2005) Inflammatory processes in muscle injury and repair. *Am J Physiol Regul Integr Comp Physiol* **288**, R345-353
7. Ceafalan, L. C., Popescu, B. O., and Hinescu, M. E. (2014) Cellular Players in Skeletal Muscle Regeneration. *BioMed research international* **2014**, 957014-957014
8. Kharraz, Y., Guerra, J., Mann, C. J., Serrano, A. L., and Munoz-Canoves, P. (2013) Macrophage plasticity and the role of inflammation in skeletal muscle repair. *Mediators Inflamm* **2013**, 491497
9. Mounier, R., Théret, M., Arnold, L., Cuvellier, S., Bultot, L., Göransson, O., Sanz, N., Ferry, A., Sakamoto, K., Foretz, M., Viollet, B., and Chazaud, B. (2013) AMPKα1 regulates macrophage skewing at the time of resolution of inflammation during skeletal muscle regeneration. *Cell metabolism* **18**, 251-264
10. Wagatsuma, A., and Sakuma, K. (2013) Mitochondria as a potential regulator of myogenesis. *ScientificWorldJournal* **2013**, 593267
11. Murray, J., and Huss, J. M. (2011) Estrogen-related receptor alpha regulates skeletal myocyte differentiation via modulation of the ERK MAP kinase pathway. *Am J Physiol Cell Physiol* **301**, C630-645
12. LaBarge, S., McDonald, M., Smith-Powell, L., Auwerx, J., and Huss, J. M. (2014) Estrogen-related receptor-alpha (ERRalpha) deficiency in skeletal muscle impairs regeneration in response to injury. *FASEB J* **28**, 1082-1097
13. Schreiber, S. N., Emter, R., Hock, M. B., Knutti, D., Cardenas, J., Podvinec, M., Oakeley, E. J., and Kralli, A. (2004) The estrogen-related receptor alpha (ERRalpha) functions in PPARgamma coactivator 1alpha (PGC-1alpha)-induced mitochondrial biogenesis. *Proc Natl Acad Sci U S A* **101**, 6472-6477
14. Puigserver, P., Wu, Z., Park, C. W., Graves, R., Wright, M., and Spiegelman, B. M. (1998) A cold-inducible coactivator of nuclear receptors linked to adaptive thermogenesis. *Cell* **92**, 829-839
15. Wu, Z., Puigserver, P., Andersson, U., Zhang, C., Adelmant, G., Mootha, V., Troy, A., Cinti, S., Lowell, B., Scarpulla, R. C., and Spiegelman, B. M. (1999) Mechanisms controlling mitochondrial biogenesis and respiration through the thermogenic coactivator PGC-1. *Cell* **98**, 115-124

16. Lin, J., Wu, H., Tarr, P. T., Zhang, C.-Y., Wu, Z., Boss, O., Michael, L. F., Puigserver, P., Isotani, E., Olson, E. N., Lowell, B. B., Bassel-Duby, R., and Spiegelman, B. M. (2002) Transcriptional co-activator PGC-1 alpha drives the formation of slow-twitch muscle fibres. *Nature* **418**, 797-801
17. Baar, K., Wende, A. R., Jones, T. E., Marison, M., Nolte, L. a., Chen, M., Kelly, D. P., and Holloszy, J. O. (2002) Adaptations of skeletal muscle to exercise: rapid increase in the transcriptional coactivator PGC-1. *FASEB journal : official publication of the Federation of American Societies for Experimental Biology* **16**, 1879-1886
18. Handschin, C., and Spiegelman, B. M. (2008) The role of exercise and PGC1alpha in inflammation and chronic disease. *Nature* **454**, 463-469
19. Handschin, C., Choi, C. S., Chin, S., Kim, S., Kawamori, D., Kurpad, A. J., Neubauer, N., Hu, J., Mootha, V. K., Kim, Y. B., Kulkarni, R. N., Shulman, G. I., and Spiegelman, B. M. (2007) Abnormal glucose homeostasis in skeletal muscle-specific PGC-1alpha knockout mice reveals skeletal muscle-pancreatic beta cell crosstalk. *J Clin Invest* **117**, 3463-3474
20. Handschin, C., Chin, S., Li, P., Liu, F., Maratos-Flier, E., Lebrasseur, N. K., Yan, Z., and Spiegelman, B. M. (2007) Skeletal muscle fiber-type switching, exercise intolerance, and myopathy in PGC-1alpha muscle-specific knock-out animals. *The Journal of biological chemistry* **282**, 30014-30021
21. Sandri, M., Lin, J., Handschin, C., Yang, W., Arany, Z. P., Lecker, S. H., Goldberg, A. L., and Spiegelman, B. M. (2006) PGC-1alpha protects skeletal muscle from atrophy by suppressing FoxO3 action and atrophy-specific gene transcription. *Proceedings of the National Academy of Sciences of the United States of America* **103**, 16260-16265
22. Wenz, T., Rossi, S. G., Rotundo, R. L., Spiegelman, B. M., and Moraes, C. T. (2009) Increased muscle PGC-1alpha expression protects from sarcopenia and metabolic disease during aging. *Proc Natl Acad Sci U S A* **106**, 20405-20410
23. Handschin, C., Kobayashi, Y. M., Chin, S., Seale, P., Campbell, K. P., and Spiegelman, B. M. (2007) PGC-1alpha regulates the neuromuscular junction program and ameliorates Duchenne muscular dystrophy. *Genes & development* **21**, 770-783
24. Selsby, J. T., Morine, K. J., Pendrak, K., Barton, E. R., and Sweeney, H. L. (2012) Rescue of dystrophic skeletal muscle by PGC-1α involves a fast to slow fiber type shift in the mdx mouse. *PloS one* **7**, e30063-e30063
25. Hollinger, K., Gardan-Salmon, D., Santana, C., Rice, D., Snella, E., and Selsby, J. T. (2013) Rescue of dystrophic skeletal muscle by PGC-1α involves restored expression of dystrophin-associated protein complex components and satellite cell signaling. *American journal of physiology. Regulatory, integrative and comparative physiology* **305**, R13-23
26. Chan, M. C., Rowe, G. C., Raghuram, S., Patten, I. S., Farrell, C., and Arany, Z. (2014) Post-natal induction of PGC-1alpha protects against severe muscle dystrophy independently of utrophin. *Skeletal Muscle* **4**, 2-2
27. Lin, J., Wu, P. H., Tarr, P. T., Lindenberg, K. S., St-Pierre, J., Zhang, C. Y., Mootha, V. K., Jager, S., Vianna, C. R., Reznick, R. M., Cui, L., Manieri, M., Donovan, M. X., Wu, Z., Cooper, M. P., Fan, M. C., Rohas, L. M., Zavacki, A. M., Cinti, S., Shulman, G. I., Lowell, B. B., Krainc, D., and Spiegelman, B. M. (2004) Defects in adaptive energy metabolism with CNS-linked hyperactivity in PGC-1alpha null mice. *Cell* **119**, 121-135
28. Rosenblatt, J. D., Lunt, A. I., Parry, D. J., and Partridge, T. A. (1995) Culturing satellite cells from living single muscle fiber explants. *In Vitro Cell Dev Biol Anim* **31**, 773-779

29. Vignaud, A., Cebrian, J., Martelly, I., Caruelle, J. P., and Ferry, A. (2005) Effect of anti-inflammatory and antioxidant drugs on the long-term repair of severely injured mouse skeletal muscle. *Exp Physiol* **90**, 487-495
30. Lin, J., Wu, P.-H., Tarr, P. T., Lindenberg, K. S., St-Pierre, J., Zhang, C.-Y., Mootha, V. K., Jäger, S., Vianna, C. R., Reznick, R. M., Cui, L., Manieri, M., Donovan, M. X., Wu, Z., Cooper, M. P., Fan, M. C., Rohas, L. M., Zavacki, A. M., Cinti, S., Shulman, G. I., Lowell, B. B., Krainc, D., and Spiegelman, B. M. (2004) Defects in adaptive energy metabolism with CNS-linked hyperactivity in PGC-1alpha null mice. *Cell* **119**, 121-135
31. Sanchez-Gurmaches, J., Hung, C.-M., Sparks, Cynthia A., Tang, Y., Li, H., and Guertin, David A. (2012) PTEN Loss in the Myf5 Lineage Redistributes Body Fat and Reveals Subsets of White Adipocytes that Arise from Myf5 Precursors. *Cell Metabolism* **16**, 348-362
32. Sanchez-Gurmaches, J., and Guertin, D. A. (2014) Adipocytes arise from multiple lineages that are heterogeneously and dynamically distributed. *Nat Commun* **5**, 4099
33. Puigserver, P. (2003) Peroxisome Proliferator-Activated Receptor-gamma Coactivator 1alpha (PGC-1alpha): Transcriptional Coactivator and Metabolic Regulator. *Endocrine Reviews* **24**, 78-90
34. Duguez, S., Feasson, L., Denis, C., and Freyssenet, D. (2002) Mitochondrial biogenesis during skeletal muscle regeneration. *Am J Physiol Endocrinol Metab* **282**, E802-809
35. Summermatter, S., Thurnheer, R., Santos, G., Mosca, B., Baum, O., Treves, S., Hoppeler, H., Zorzato, F., and Handschin, C. (2012) Remodeling of calcium handling in skeletal muscle through PGC-1α: impact on force, fatigability, and fiber type. *American journal of physiology. Cell physiology* **302**, C88-99
36. Heredia, J. E., Mukundan, L., Chen, F. M., Mueller, A. a., Deo, R. C., Locksley, R. M., Rando, T. a., and Chawla, A. (2013) Type 2 innate signals stimulate fibro/adipogenic progenitors to facilitate muscle regeneration. *Cell* **153**, 376-388
37. Kherif, S., Dehaupas, M., Lafuma, C., Fardeau, M., and Alameddine, H. S. (1998) Matrix metalloproteinases MMP-2 and MMP-9 in denervated muscle and injured nerve. *Neuropathol Appl Neurobiol* **24**, 309-319
38. Li, H., Mittal, A., Makonchuk, D. Y., Bhatnagar, S., and Kumar, A. (2009) Matrix metalloproteinase-9 inhibition ameliorates pathogenesis and improves skeletal muscle regeneration in muscular dystrophy. *Human molecular genetics* **18**, 2584-2598
39. Tatsumi, R., Anderson, J. E., Nevoret, C. J., Halevy, O., and Allen, R. E. (1998) HGF/SF is present in normal adult skeletal muscle and is capable of activating satellite cells. *Dev Biol* **194**, 114-128
40. Miller, K. J., Thaloor, D., Matteson, S., and Pavlath, G. K. (2000) Hepatocyte growth factor affects satellite cell activation and differentiation in regenerating skeletal muscle. *Am J Physiol Cell Physiol* **278**, C174-181
41. Mourkioti, F., and Rosenthal, N. (2005) IGF-1, inflammation and stem cells: interactions during muscle regeneration. *Trends in immunology* **26**, 535-542
42. Silva, M. T. (2010) When two is better than one: macrophages and neutrophils work in concert in innate immunity as complementary and cooperative partners of a myeloid phagocyte system. *J Leukoc Biol* **87**, 93-106
43. van der Poel, C., Gosselin, L. E., Schertzer, J. D., Ryall, J. G., Swiderski, K., Wondemaghen, M., and Lynch, G. S. (2011) Ageing prolongs inflammatory marker expression in regenerating rat skeletal muscles after injury. *J Inflamm (Lond)* **8**, 41

44. Senf, S. M., Howard, T. M., Ahn, B., Ferreira, L. F., and Judge, A. R. (2013) Loss of the inducible Hsp70 delays the inflammatory response to skeletal muscle injury and severely impairs muscle regeneration. *PLoS One* **8**, e62687
45. Wang, H., Melton, D. W., Porter, L., Sarwar, Z. U., McManus, L. M., and Shireman, P. K. (2014) Altered macrophage phenotype transition impairs skeletal muscle regeneration. *Am J Pathol* **184**, 1167-1184
46. Serrano, A. L., Mann, C. J., Vidal, B., Ardite, E., Perdiguero, E., and Munoz-Canoves, P. (2011) Cellular and molecular mechanisms regulating fibrosis in skeletal muscle repair and disease. *Curr Top Dev Biol* **96**, 167-201
47. Wagatsuma, A., Kotake, N., and Yamada, S. (2011) Muscle regeneration occurs to coincide with mitochondrial biogenesis. *Mol Cell Biochem* **349**, 139-147
48. Turner, N. J., and Badylak, S. F. (2012) Regeneration of skeletal muscle. *Cell and tissue research* **347**, 759-774
49. Deng, B., Wehling-Henricks, M., Villalta, S. A., Wang, Y., and Tidball, J. G. (2012) IL-10 triggers changes in macrophage phenotype that promote muscle growth and regeneration. *Journal of immunology (Baltimore, Md. : 1950)* **189**, 3669-3680
50. Rowe, G. C., Raghuram, S., Jang, C., Nagy, J. A., Patten, I. S., Goyal, A., Chan, M. C., Liu, L. X., Jiang, A., Spokes, K. C., Beeler, D., Dvorak, H., Aird, W. C., and Arany, Z. (2014) PGC-1alpha induces SPP1 to activate macrophages and orchestrate functional angiogenesis in skeletal muscle. *Circ Res* **115**, 504-517
51. Krause, M. P., Al-Sajee, D., D'Souza, D. M., Rebalka, I. A., Moradi, J., Riddell, M. C., and Hawke, T. J. (2013) Impaired macrophage and satellite cell infiltration occurs in a muscle-specific fashion following injury in diabetic skeletal muscle. *PLoS One* **8**, e70971
52. Lu, H., Huang, D., Ransohoff, R. M., and Zhou, L. (2011) Acute skeletal muscle injury: CCL2 expression by both monocytes and injured muscle is required for repair. *FASEB journal : official publication of the Federation of American Societies for Experimental Biology* **25**, 3344-3355
53. Segawa, M., Fukada, S., Yamamoto, Y., Yahagi, H., Kanematsu, M., Sato, M., Ito, T., Uezumi, A., Hayashi, S., Miyagoe-Suzuki, Y., Takeda, S., Tsujikawa, K., and Yamamoto, H. (2008) Suppression of macrophage functions impairs skeletal muscle regeneration with severe fibrosis. *Exp Cell Res* **314**, 3232-3244
54. Tidball, J. G., and Wehling-Henricks, M. (2007) Macrophages promote muscle membrane repair and muscle fibre growth and regeneration during modified muscle loading in mice in vivo. *J Physiol* **578**, 327-336
55. Warren, G. L., O'Farrell, L., Summan, M., Hulderman, T., Mishra, D., Luster, M. I., Kuziel, W. A., and Simeonova, P. P. (2004) Role of CC chemokines in skeletal muscle functional restoration after injury. *Am J Physiol Cell Physiol* **286**, C1031-1036
56. Shireman, P. K., Contreras-Shannon, V., Ochoa, O., Karia, B. P., Michalek, J. E., and McManus, L. M. (2007) MCP-1 deficiency causes altered inflammation with impaired skeletal muscle regeneration. *J Leukoc Biol* **81**, 775-785
57. Brigitte, M., Schilte, C., Plonquet, A., Baba-Amer, Y., Henri, A., Charlier, C., Tajbakhsh, S., Albert, M., Gherardi, R. K., and Chrétien, F. (2010) Muscle resident macrophages control the immune cell reaction in a mouse model of notexin-induced myoinjury. *Arthritis and rheumatism* **62**, 268-279

58. Radley, H. G., and Grounds, M. D. (2006) Cromolyn administration (to block mast cell degranulation) reduces necrosis of dystrophic muscle in mdx mice. *Neurobiol Dis* **23**, 387-397
59. Wang, Y., and Thorlacius, H. (2005) Mast cell-derived tumour necrosis factor-alpha mediates macrophage inflammatory protein-2-induced recruitment of neutrophils in mice. *British journal of pharmacology* **145**, 1062-1068
60. Chiba, K., Zhao, W., Chen, J., Wang, J., Cui, H. Y., Kawakami, H., Miseki, T., Satoshi, H., Tanaka, J., Asaka, M., and Kobayashi, M. (2004) Neutrophils secrete MIP-1 beta after adhesion to laminin contained in basement membrane of blood vessels. *Br J Haematol* **127**, 592-597
61. Kopydlowski, K. M., Salkowski, C. A., Cody, M. J., van Rooijen, N., Major, J., Hamilton, T. A., and Vogel, S. N. (1999) Regulation of macrophage chemokine expression by lipopolysaccharide in vitro and in vivo. *J Immunol* **163**, 1537-1544
62. Rigamonti, E., Touvier, T., Clementi, E., Manfredi, A. a., Brunelli, S., and Rovere-Querini, P. (2013) Requirement of inducible nitric oxide synthase for skeletal muscle regeneration after acute damage. *Journal of immunology (Baltimore, Md. : 1950)* **190**, 1767-1777
63. Dumont, N., Bouchard, P., and Frenette, J. (2008) Neutrophil-induced skeletal muscle damage: a calculated and controlled response following hindlimb unloading and reloading. *Am J Physiol Regul Integr Comp Physiol* **295**, R1831-1838
64. Pizza, F. X., McLoughlin, T. J., McGregor, S. J., Calomeni, E. P., and Gunning, W. T. (2001) Neutrophils injure cultured skeletal myotubes. *Am J Physiol Cell Physiol* **281**, C335-341
65. Li, Z. B., Kollias, H. D., and Wagner, K. R. (2008) Myostatin directly regulates skeletal muscle fibrosis. *The Journal of biological chemistry* **283**, 19371-19378
66. McCroskery, S., Thomas, M., Platt, L., Hennebry, A., Nishimura, T., McLeay, L., Sharma, M., and Kambadur, R. (2005) Improved muscle healing through enhanced regeneration and reduced fibrosis in myostatin-null mice. *Journal of cell science* **118**, 3531-3541
67. Pelosi, L., Giacinti, C., Nardis, C., Borsellino, G., Rizzuto, E., Nicoletti, C., Wannenes, F., Battistini, L., Rosenthal, N., Molinaro, M., and Musarò, A. (2007) Local expression of IGF-1 accelerates muscle regeneration by rapidly modulating inflammatory cytokines and chemokines. *FASEB journal : official publication of the Federation of American Societies for Experimental Biology* **21**, 1393-1402
68. Hamai, N., Nakamura, M., and Asano, A. (1997) Inhibition of mitochondrial protein synthesis impaired C2C12 myoblast differentiation. *Cell Struct Funct* **22**, 421-431
69. Rochard, P., Rodier, A., Casas, F., Cassar-Malek, I., Marchal-Victorion, S., Daury, L., Wrutniak, C., and Cabello, G. (2000) Mitochondrial activity is involved in the regulation of myoblast differentiation through myogenin expression and activity of myogenic factors. *J Biol Chem* **275**, 2733-2744
70. Murray, J., Auwerx, J., and Huss, J. M. (2013) Impaired myogenesis in estrogen-related receptor γ (ERRγ)-deficient skeletal myocytes due to oxidative stress. *FASEB journal : official publication of the Federation of American Societies for Experimental Biology* **27**, 135-150
71. Angione, A. R., Jiang, C., Pan, D., Wang, Y.-X., and Kuang, S. (2011) PPARδ regulates satellite cell proliferation and skeletal muscle regeneration. *Skeletal muscle* **1**, 33-33

72. Philp, A., Belew, M. Y., Evans, A., Pham, D., Sivia, I., Chen, A., Schenk, S., and Baar, K. (2011) The PGC-1α-related coactivator promotes mitochondrial and myogenic adaptations in C2C12 myotubes. *American journal of physiology. Regulatory, integrative and comparative physiology* **301**, R864-872
73. Huss, J. M., Kopp, R. P., and Kelly, D. P. (2002) Peroxisome proliferator-activated receptor coactivator-1alpha (PGC-1alpha) coactivates the cardiac-enriched nuclear receptors estrogen-related receptor-alpha and -gamma. Identification of novel leucine-rich interaction motif within PGC-1alpha. *J Biol Chem* **277**, 40265-40274
74. Mootha, V. K., Handschin, C., Arlow, D., Xie, X., St Pierre, J., Sihag, S., Yang, W., Altshuler, D., Puigserver, P., Patterson, N., Willy, P. J., Schulman, I. G., Heyman, R. A., Lander, E. S., and Spiegelman, B. M. (2004) Erralpha and Gabpa/b specify PGC-1alpha-dependent oxidative phosphorylation gene expression that is altered in diabetic muscle. *Proc Natl Acad Sci U S A* **101**, 6570-6575
75. Patti, M. E., Butte, A. J., Crunkhorn, S., Cusi, K., Berria, R., Kashyap, S., Miyazaki, Y., Kohane, I., Costello, M., Saccone, R., Landaker, E. J., Goldfine, A. B., Mun, E., DeFronzo, R., Finlayson, J., Kahn, C. R., and Mandarino, L. J. (2003) Coordinated reduction of genes of oxidative metabolism in humans with insulin resistance and diabetes: Potential role of PGC1 and NRF1. *Proc Natl Acad Sci U S A* **100**, 8466-8471
76. Eisele, P. S., Salatino, S., Sobek, J., Hottiger, M. O., and Handschin, C. (2013) The peroxisome proliferator-activated receptor γ coactivator 1α/β (PGC-1) coactivators repress the transcriptional activity of NF-κB in skeletal muscle cells. *The Journal of biological chemistry* **288**, 2246-2260
77. Nguyen, M. H., Cheng, M., and Koh, T. J. (2011) Impaired muscle regeneration in ob/ob and db/db mice. *ScientificWorldJournal* **11**, 1525-1535
78. Hu, Z., Wang, H., Lee, I. H., Modi, S., Wang, X., Du, J., and Mitch, W. E. (2010) PTEN inhibition improves muscle regeneration in mice fed a high-fat diet. *Diabetes* **59**, 1312-1320
79. Muzzin, P., Eisensmith, R. C., Copeland, K. C., and Woo, S. L. (1996) Correction of obesity and diabetes in genetically obese mice by leptin gene therapy. *Proc Natl Acad Sci U S A* **93**, 14804-14808
80. Sainz, N., Rodriguez, A., Catalan, V., Becerril, S., Ramirez, B., Gomez-Ambrosi, J., and Fruhbeck, G. (2009) Leptin administration favors muscle mass accretion by decreasing FoxO3a and increasing PGC-1alpha in ob/ob mice. *PLoS One* **4**, e6808
81. Chiu, Y. H., Hornsey, M. A., Klinge, L., Jorgensen, L. H., Laval, S. H., Charlton, R., Barresi, R., Straub, V., Lochmuller, H., and Bushby, K. (2009) Attenuated muscle regeneration is a key factor in dysferlin-deficient muscular dystrophy. *Hum Mol Genet* **18**, 1976-1989
82. Wenz, T., Diaz, F., Spiegelman, B. M., and Moraes, C. T. (2008) Activation of the PPAR/PGC-1alpha pathway prevents a bioenergetic deficit and effectively improves a mitochondrial myopathy phenotype. *Cell metabolism* **8**, 249-256
83. Hanai, J., Cao, P., Tanksale, P., Imamura, S., Koshimizu, E., Zhao, J., Kishi, S., Yamashita, M., Phillips, P. S., Sukhatme, V. P., and Lecker, S. H. (2007) The muscle-specific ubiquitin ligase atrogin-1/MAFbx mediates statin-induced muscle toxicity. *J Clin Invest* **117**, 3940-3951

6 PGC-1α impacts satellite cell number and proliferation through reduced expression of fibronectin (Project 2)

Authors: Ivana Dinulovic[1], Markus Beer[1], Christoph Handschin[1]

[1]Biozentrum, University of Basel, Klingelbergstrasse 50-70, 4056 Basel, Switzerland

Running title: PGC-1α influences satellite cells via niche modifications

Key words: PGC-1α, satellite cells; satellite cell niche; basal lamina

Corresponding author: Christoph Handschin (e-mail: christoph.handschinATunibas.ch)

Author contributions: experiments designed by I.D. and C.H; experiments performed by I.D. and M.B. (provided helped with RNA isolation and qPCR); experiments analyzed by I.D. and C.H.; manuscript written by I.D. and C.H.

6.1 Abstract

Satellite cells (SC) are quiescent adult muscle stem cells indispensable for skeletal muscle regeneration, however intrinsic and extrinsic factors influencing their number and activation remain incompletely understood. SCs are present in higher numbers in oxidative vs. glycolytic fibers and increase with exercise, concomitant with the induced expression of PGC-1α. As PGC-1α is a prominent driver of oxidative metabolism in skeletal muscle and mimics the trained phenotype including the oxidative fiber predominance, we were interested in exploring the potential effects of this coactivator on satellite cells.

By using a PGC-1α overexpression mouse model (MCK-mTG) and two knock-out models (Myf5-mKO and HSA-mKO) in combination with *in vivo* and *in vitro* approaches, we were able to reveal differences both in SC number and activation/proliferation following various stimuli. Increase in PGC-1α expression in fibers (MCK-mTG) surprisingly results in decreased SC numbers. However, SCs from these mice have a higher propensity for activation and proliferation. The opposite effect was not observed if PGC-1α was ablated from fibers alone (HSA-mKO), but when PGC-1α was missing both in SCs and fibers (Myf5-mKO), a reduction in SC activation and proliferation was detected without a difference in the resting number of SCs. These observations correlated with the differential expression of fibronectin between MCK-mTG and Myf5-mKO but not HSA-mKO, and its addition in culture media resulted in a reduction in SC activation and proliferation on isolated fibers.

Thus, the higher levels of PGC-1α in fibers lead to modifications in the basal lamina components of the SC niche, which affect the readiness of SCs to respond to injury. In addition, PGC-1α expression in SCs and muscle fibers is required for proper SC activation and proliferation. Therefore, by increasing PGC-1α levels, we can not only induce the trained phenotype and improve muscle function, but also enhance SC function.

6.2 Introduction

Satellite cells (SC) are adult muscle stem cells located at the periphery of the muscle fibers, between the sarcolemma and basal lamina (BL) (1), in the vicinity of blood vessels (2) and the neuro-muscular junction. This location within the muscle tissue exposes SCs to signals coming from within and outside of the fiber, and comprises the specific environment termed the SC niche. Although metabolically inactive and quiescent (G_0) in resting conditions, SCs quickly become activated in response to a stimulus such as injury or strenuous exercise (3). These stem cells are indispensable for skeletal muscle regeneration (4-7), even though many other cell progenitors (pericytes, mesoangioblasts, side population cells, $CD133^+$ progenitors) can take part in and contribute to the process (8). Despite being present in relatively small numbers (2-5% of total myonuclei), they are characterized by a vast proliferative and regenerative potential (3). However, chronic damage such as that seen in dystrophies as well as aging, leads to depletion of SC numbers, resulting in reduced regenerative capabilities (9, 10). Therefore, proper activation of SCs, as well as their return to quiescence, is essential to preserving their number and function.

Various markers which can contribute to rapid and easy detection of SCs have been discovered over the years, with Pax7 being the most widely used. Pax7 is a transcription factor specifically expressed only in the SC population in muscle tissue, present both in quiescent and activated satellite cells (11) . It has been shown that SCs in adult mice do not constitute a homogeneous population, and that approximately 90% of them express Myf5 at some point in their lifetime and are committed progenitors, whereas only around 10% are true stem cells (12). Upon activation, satellite cells increase in size, enter the cell cycle, and start expressing Myf5 and MyoD, becoming myoblasts. Although SC activation is poorly understood, hepatocyte growth factor (HGF) signaling through the c-Met receptor on SCs is considered the first step in this process (13). It has been shown for other stem cells that such an activation process is characterized by a switch from glycolysis to oxidative metabolism as the energy producing pathway (14). One part of the proliferating $Pax7^+/MyoD^+$ cells will continue on the differentiation path, and they will reduce Pax7 and increase myogenin expression, exit the cell cycle forming mononucleated postmitotic myocytes (15) and start fusing in order to form myotubes. Another part of the $Pax7^+/MyoD^+$ cells will, however, reduce MyoD expression and return to quiescence (16).

The simplicity of SC quiescence and the G_0 phase was recently questioned, when Rodgers et al. defined an alternative quiescent state, named G_{Alert} (17). They showed that even upon distant injury, SCs can respond by switching to an alerted state for a limited time through an increase in mammalian target of rapamycin complex 1 (mTORC1) signaling and increased mitochondrial biogenesis. Entering the cell cycle from G_{Alert} proved to be more efficacious than from G_0.

High expression of fibroblast growth factor 2 (FGF-2) by muscle fibers (18) and a reduction in sprouty 1 (Spry1) by SCs (19) are both connected to the inability of SCs to return to quiescence upon activation and subsequently to SC depletion, seen in old age. SCs from old animals were also characterized by reduced regenerative capabilities (20). Heterochronic parabiotic pairings in mice, however, showed that intrinsically, SCs from old and young mice are no different in their regenerative potential, but that it is rather the environment that leads to the aging effects seen in SCs (21).

One of the parameters that change with age regarding the SC niche is the BL. Accumulation of extracellular matrix (ECM) components leads to the thickening of the BL (22), and prevents SCs from sensing changes in the environment coming from outside the muscle fiber, and subsequently results in a reduced propensity to activate when needed. Whereas the ECM in skeletal muscle comprises mainly collagens type I and III, the main building blocks of the BL are laminins, collagen IV, perlecan, but also fibronectin (FN) and tenascin-C (TNC) (23, 24). ECM components are produced primarily by fibroblasts, and their overproduction leads to fibrosis (25). Although it was recently reported that local transient FN secretion by SCs is an important step in the cascade of SC activation and subsequent proliferation (26), excess FN in the BL was correlated with reduced ability of SCs to respond to injury (27). In addition, TNC was shown to prevent the interaction of FN with Syndecan-4 (Sdc4) (28) and in this way block the expansion of $Pax7^+/Myf5^-$ cells on fibers (26).

It has been noticed that SC numbers vary by muscle type, such that oxidative muscles contain more SCs per fiber than glycolytic ones (29). Also, exercise increases SC numbers in mice, rats and humans (30-32). Interestingly, oxidative muscles exhibit higher resistance to a variety of atrophic conditions compared to glycolytic muscles (33), including aging (34) and dystrophy (35). Peroxisome proliferator-activated receptor γ coactivator 1α (PGC-1α) is a major

driver of oxidative metabolism and mitochondrial biogenesis (36, 37), and is induced by exercise (38). It is expressed at higher levels in oxidative vs. glycolytic fibers (39), and it protects oxidative fibers against fasting and denervation induced atrophy (40). Skeletal muscle overexpression of PGC-1α leads to a fiber type switch towards oxidative muscles and mimics a trained phenotype (39), but also improves pathologies in dystrophic mouse models (41-44). Therefore, we hypothesized that PGC-1α overexpression (MCK-mTG) in muscle fibers might induce an increase in SC numbers in the same manner as it mirrors other features of oxidative fibers. At the same time, we were wondering about the differences between the lack of PGC-1α in fibers (HSA-mKO) and in SCs as well (Myf5-mKO), especially in regard to the possible switch from glycolytic to oxidative metabolism by activating SCs (17, 45).

To our surprise, we detected a reduction in SC numbers in our transgenic model in various muscles, along with a reduction in expression of several myogenic regulatory factors (MRFs). In both knock-out models, SC numbers were unchanged. Interestingly, we noticed that the pace of SC activation correlated with PGC-1α expression levels in MCK-mTG and Myf5-mKO mice in several paradigms (downhill running (DHR), phosphate buffered saline (PBS) injected muscles) which resulted in faster proliferation upon cardiotoxin injury (CTX) as well as *in vitro* ($Pax7^{+}/MyoD^{-}$, $Pax7^{+}/MyoD^{+}$, $Pax7^{-}/MyoD^{+}$ cells on isolated fibers). However, PGC-1α expressed by SCs but not by fibers (HSA-mKO), did not affect the proliferation rate. Additionally, we showed that the differences in SC proliferation were at least partially due to differential expression of BL component FN. Deciphering the intrinsic and especially extrinsic factors that influence SC activation and quiescence is essential for keeping these cells in culture and expanding prior to using them in stem-cell based therapies. Here we add one piece to the puzzle by classifying PGC-1α as both a direct and indirect contributor to SC behavior. We show that PGC-1α in SCs is necessary for timely activation upon stimulus, and that overexpression of PGC-1α in fibers is enough to modulate the SC niche and indirectly increase SC readiness to engage in activation.

6.3 Materials and Methods

Animals:

In this study we used three mouse models: muscle specific PGC-1α transgenic model (mTG) which expresses PGC-1α under the control of muscle creatine kinase (MCK) promoter (39) and two muscle specific PGC-1α knock-out models, in which PGC-1α exons 3-5 are knocked-out under Myf5-driven Cre (Myf5-mKO) (characterized in Project 1) or human α-skeletal actin (HSA)-driven Cre (HSA-mKO) (46). Male mice, 8-16 weeks old, were used and wild type (WT) littermates served as controls. All animal experimental procedures performed in this study were approved by the Swiss authorities.

Cardiotoxin injury:

Mice were anasthesized using O_2/sevoflurane gas mixture (3% sevoflurane). Lower part of hind limbs was shaved, and belly region of tibialis anterior (TA) muscle injected with control vehicle (30µl PBS) or cardiotoxin **(**30µl containing 3µg of CTX, C9759 Sigma) using insulin syringes (U-100, 300ul, 29Gx1/2"). Mice were sacrificed and muscles collected at various time points. In the repeated injury model, CTX was injected three times with a three week interval between injections. Three weeks after the last injection, the mice were sacrificed and TAs collected. TAs were transversally cut into two pieces and frozen for histology or RNA isolation.

Downhill running:

Mice were put in open treadmill (Exer Treadmill Columbus Instruments) at - 10˚ and let run with alternating speed: 5min at 7m/min followed by 5min at 12m/min, for the 60 min duration period. 3h after running, mice were sacrificed and quadriceps (QU) muscles collected.

Immunohistochemistry (IHC):

TA, extensor digitorum longus (EDL), soleus (SOL), and QU muscles were immediately after isolation covered by OCT (Tissue-Tek, Sakura) and frozen in isopenthane precooled in liquid nitrogen. Frozen muscles were cut at 8µm thick sections using cryostat (Leica CM1950)

and kept at -20˚C until staining. Sections were dried at room temperature (RT), then fixed with 4% paraformaldehyde (PFA), premeabilized in methanol and antigen retrieved in citrate buffer using microwave. After blocking (1h at RT) and overnight (o/n) incubation at 4˚C with primary antibodies, sections were washed with PBS, incubated with secondary antibodies for 1.5h at RT, then washed again and mounted with Vectashield with DAPI. Blocking was performed using 1:100 diluted mouse IgG Fab fragment 015-000-007 Jackson Immunosearch in 3% bovine serum albumin (BSA) in PBS. Antigen retrieval was not used for myoblast staining. Primary antibodies are: Pax7 DSHB, Ki67 TEC-3 Dako, laminin ab11575 Abcam, desmin ab15200; secondary antibodies are: biotin goat-anti-mouse IgG Fcγ1 115-065-205 Jackson Immunosearch, streptavidin Alexa568 S11226 Invitrogen, goat-anti-rat IgG Alexa488 A11006 Invitrogen, donkey-anti-rabbit IgG Alexa647 A31573 Life Technologies, goat-anti-rabbit Alexa488 A11008 Invitrogen, goat-anti-rabbit IgG Cy3 111-165-045 Jackson Immunoresearch.

Fiber isolation, culture and Immunocytochemistry:

Muscle fibers were isolated from EDL muscle of 12-16 week old animals, described in details elsewhere (47). Briefly, isolated muscles were digested in 2mg/ml Collagenase A (Roche Diagnostics) solution (DMEM, 2mM L-Gln, 1% antibiotic cocktail) for 1.5h, and fibers further separated using glass Pasteur pipettes. Single fibers were either fixed immediately (T0) in 10% PFA or after 3 day incubation (T3) in culture media (DMEM, 2mM L-Glutamine, 10% fetal bovine serum, 0.5% chicken embryo extract, 1% antibiotic cocktail). For treatments, 100µg/ml human plasma FN (Merck Millipore, FC010) or 5µg/ml human TNC (Merck Millipore, CC065) was added to the media. Fixed fibers were permeabilized in 0.5% Triton X-100 in PBS, blocked in 20% horse serum in PBS 30min at RT and incubated with primary antibodies (Pax7 DSHB, MyoD C-20 sc-304, DAPI) o/n at 4˚C. After washing with PBS, fibers were incubated with secondary antibodies (goat-anti-mouse IgG1 Alexa568 A21124 Invitrogen, goat-anti-rabbit Alexa488 A11008 Invitrogen) for 1.5h at RT, washed with PBS and mounted on glass slides with Vectashield.

Myoblast isolation, culture and Immunocytochemistry (IHC):

Myoblast were isolated from EDL of 2-3 week-old male mice using single fiber technique (48); EDL fibers were separated using collagenase A (Roche Diagnostics) and

incubated in plastic dishes coated with matrigel (BD Biscience). After a couple of days, proliferating myoblasts coming from fibers were propagated further in culture media (HyClone DMEM, 10% horse serum, 20% fetal bovine serum, 1% chicken embryo extract, 2mM L-Glutamine, 5ng/ml basic fibroblast growth factor, 1% antibiotic cocktail) and used for assessing myoblast proliferation rate. For that purpose, same number of cells were plated on plastic dishes in low concentration and fixed in 4% PFA after different incubation periods (e.g. 2d and 4d post plating). Cells were permeabilized in 0.5% Triton X-100 in PBS, blocked in 3% BSA in PBS and incubated o/n at 4˚C with primary antibody (desmin ab15200) in 3% BSA in PBS. After washing in PBS, cells were incubated 1h at RT with secondary antibody (goat-anti-rabbit IgG Cy3 111-165-045 Jackson Immunoresearch), washed with PBS and mounted using Vectashield with DAPI.

Image acquisition and quantification:

Images covering the whole area of muscle transversal sections were captured using Zeiss LSM700 microscope with the Zen 2010 software using a 25x objective with 0.5 zoom. Satellite cell number ($Pax7^+/DAPI^+$) was expressed per area unit for all muscles. Area was measured using ImageJ software. SCs/myoblasts were quantified by hand on Leica DM5000B microscope. For that, approximately 60 fibers/mouse for T0 or approximately 20 fibers/mouse for T3 were used, and cell numbers expressed per fiber. Proliferating myoblasts (single cells) were quantified prior fixation on 10 random fields on Leica DMI4000B microscope using 10x objective or after staining ($desmin^+/DAPI^+$) on 100 fields on Zeiss LSM700 microscope using 10x objective. Myoblast quantification was done by hand or using the Imaris software.

RNA extraction and relative quantitative PCR (qPCR):

RNA was isolated from muscles using lysing matrix tubes (MP Biomedicals) and TRI Reagent (Sigma) according to the manufacturer's instructions, and concentration was measured on Nanodrop 1000 (Thermo Scientific). 1μg of RNA was digested with DNase I (Invitrogen), after which cDNA synthesis was performed using reverse transcriptase Superscript II (Invitrogen). qPCR measurements were done on a StepOne machine with SYBR green based detection, and used for assessing relative gene expression levels. TATA binding protein (TBP)

served as a housekeeping gene and normalizations were calculated with ΔΔCt method. A list of qPCR primers is in Table 1.

Statistical analysis

Data are expressed as AV+/-SEM. Statistical analysis was based on Student's t test and used for comparison of two genotypes under same conditions (e.g. mTG vs. WT). $p \leq 0.05$ was considered significant.

6.4 Figures

Target	Fwd primer (5' - 3')	Rev primer (5' - 3')
Agrn	GCG GTA CTT GAA AGG CAA AGA	CTC CAA AGC CAC CAA TTA CCA
Bmp1	ACC CTC CAA GAC AGC ACT G	GGC TAC GGT ACA GGT CCA T
c-Met	CCC CAA CTT CAC GGC AGA AA	GTA GTT TGT GGC TCC GAG ATA AA
Col1a1	GCT CCT CTT AGG GGC CAC T	CCA CGT CTC ACC ATT GGG G
Col3a1	CTG TAA CAT GGA AAC TGG GGA AA	CCA TAG CTG AAC TGA AAA CCA CC
Col4a1	TCC GGG AGA GAT TGG TTT CC	CTG GCC TAT AAG CCC TGG T
Col4a2	AGT GCT ACC CGG AGA AAG GAG	CCC TGT AGT CCT GGG AAT CC
Col5a2	TTG GAA ACC TTC TCC ATG TCA GA	TCC CCA GTG GGT GTT ATA GGA
Col6a1	CTG CTG CTA CAA GCC TGC T	CCC CAT AAG GTT TCA GCC TCA
FGF-2	GCG ACC CAC ACG TCA AAC TA	TCC CTT GAT AGA CAC AAC TCC TC
Fn1	ATG TGG ACC CCT CCT GAT AGT	GCC CAG TGA TTT CAG CAA AGG
HGF	ATG TGG GGG ACC AAA CTT CTG	GGA TGG CGA CAT GAA GCA G
Hspg2	TTC CAG ATG GTC TAT TTC CGG G	CTT GGC ACT TGC ATC CTC C
Lama2	TCC CAA GCG CAT CAA CAG AG	CAG TAC ATC TCG GGT CCT TTT TC
Lamb1	AGA CTT TGG GGG TTC ATG TCA	ATC GTC CCG TCT CCT TGT CA
Lamc1	CTG TGA GAA CAC GTA CTC AAA GG	AGG GTT GAA AAG GCC ACG TT
MRF-4	CGC GAA AGG AGG AGA CTA AAG A	CCA CAG TCC GAC GCT TCA G
Mstn	GCT GGC CCA GTG GAT CTA AA	CAG CCC CTC TTT TTC CAC ATT
Myf5	CAT GTG GGC CTG CAA AGC	TGC GCC GAT CCA TGG TA
MyoD1	GCC GGT GTG CAT TCC AA	CAC TCC GGA ACC CCA ACA G
Myog	GCA GCG CCA TCC AGT ACA TT	ATC GCG CTC CTC CTG GTT
Nid1	CCC AGC TTC GGC TCA GTA G	AAC GGG GAT AAG TCT TCT CGA T
Nid2	CTC TTT CCT TAC GGG GAG TCG	GGC ATC GTA GAA ACG CAG G
Pax7	AAA AAA CCC TTT CCC TTC CTA CA	AGC ATG GGT AGA TGG CAC ACT
Pcolce	GCC AGA CCC CCA ACT ACA C	CCG TAA TTG TCC AGA TGC ACT T
PGC-1a ex2	TGA TGT GAA TGA CTT GGA TAC AGA CA	CGT CAT TGT TGT ACT GGT TGG ATA TG
PGC-1a ex3-5	AGC CGT GAC CAC TGA CAA CGA G	GCT GCA TGG TTC TGA GTG CTA AG
Spry 1	ATG GAT TCC CCA AGT CAG CAT	CCT GTC ATA GTC TAA CCT CTG CC
TBP	TGC TGT TGG TGA TTG TTG GT	CTG GCT TGT GTG GGA AAG AT
Tnc	TTT GCC CTC ACT CCC GAA G	AGG GTC ATG TTT AGC CCA CTC

Table 1. qPCR primer list

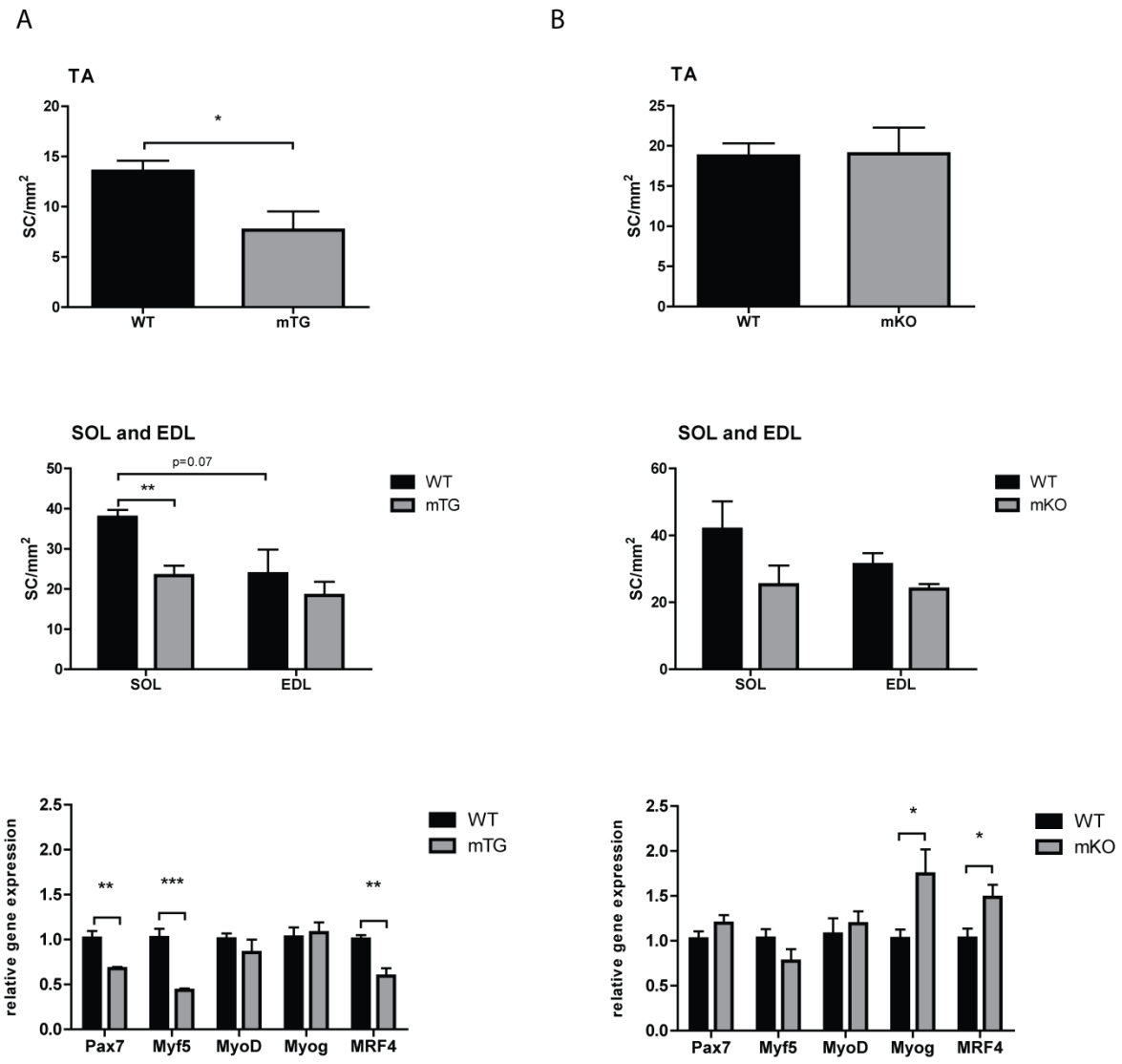

Fig 1. SC numbers and MRFs expression in MCK-mTG and Myf5-mKO mice
SC numbers per area in TA, SOL and EDL muscles and relative mRNA levels of Pax7 and MRFs in TA of A) mTG mice and B) Myf5-mKO mice compared to controls (WT); mRNA levels in mTG and Myf5-mKO were normalized to littermate control levels; Values are plotted as AV+/-SEM; n=4 per group for SC quantification and n=6 per group for mRNA measurements; * $p \leq 0.05$, ** $p \leq 0.01$, *** $p \leq 0.001$

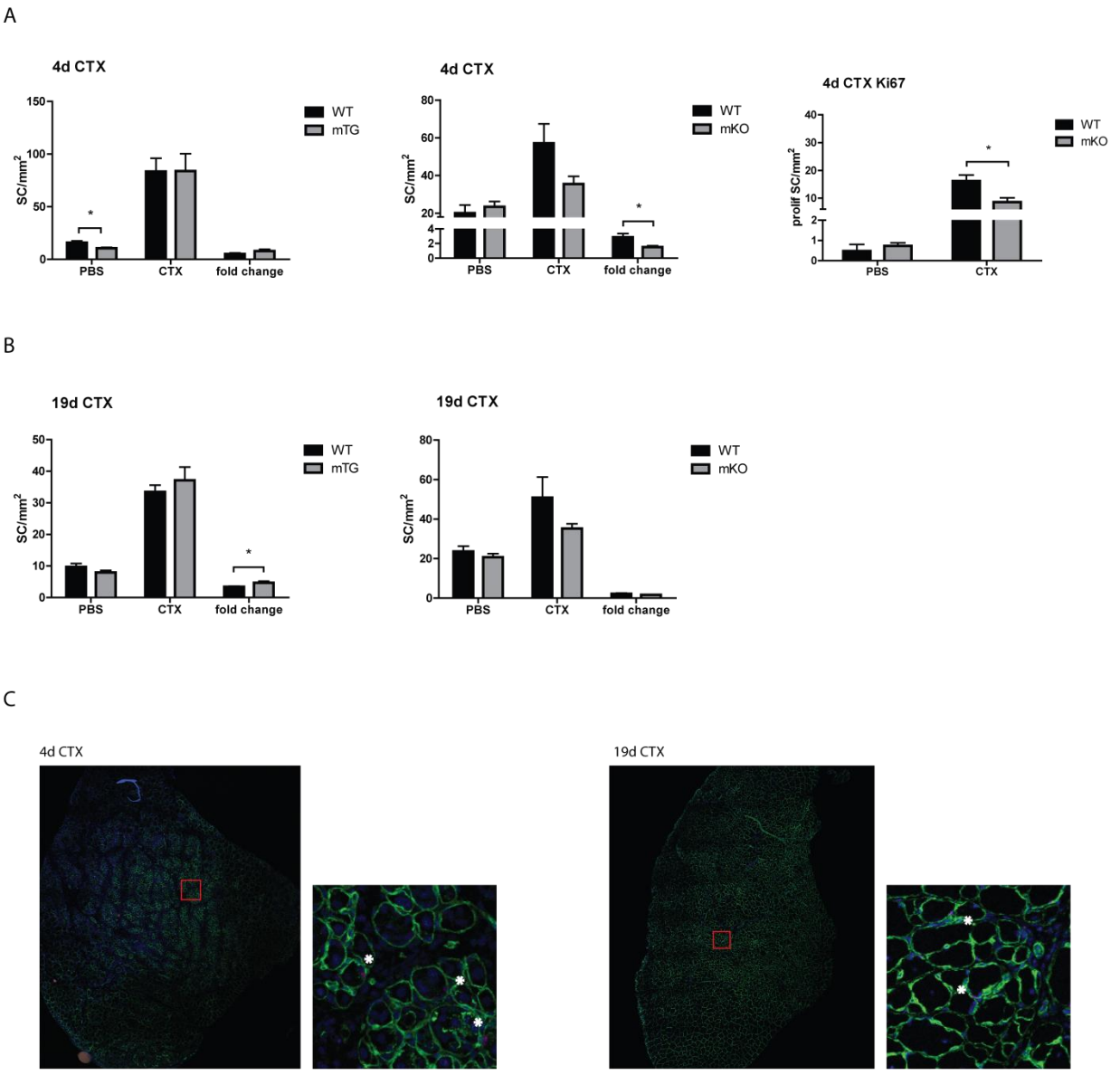

Fig 2. SC numbers in mTG and Myf5-mKO TAs after cardiotoxin injections
A) SC numbers per area 4d post CTX in mTG and Myf5-mKO and proliferating SCs per area ($Pax7^{+}/Ki67^{+}$) in Myf5-mKO; B) 19d post CTX; C) Representative IHC images (laminin: green, dapi/nuclei: blue; Pax7: red) of SCs 4d and 19d after CTX. Red quadrants from sections are enlarged and SCs marked with white stars; Values are plotted as AV+/-SEM; n=5-10 per group per time point; * $p \leq 0.05$, ** $p \leq 0.01$, *** $p \leq 0.001$

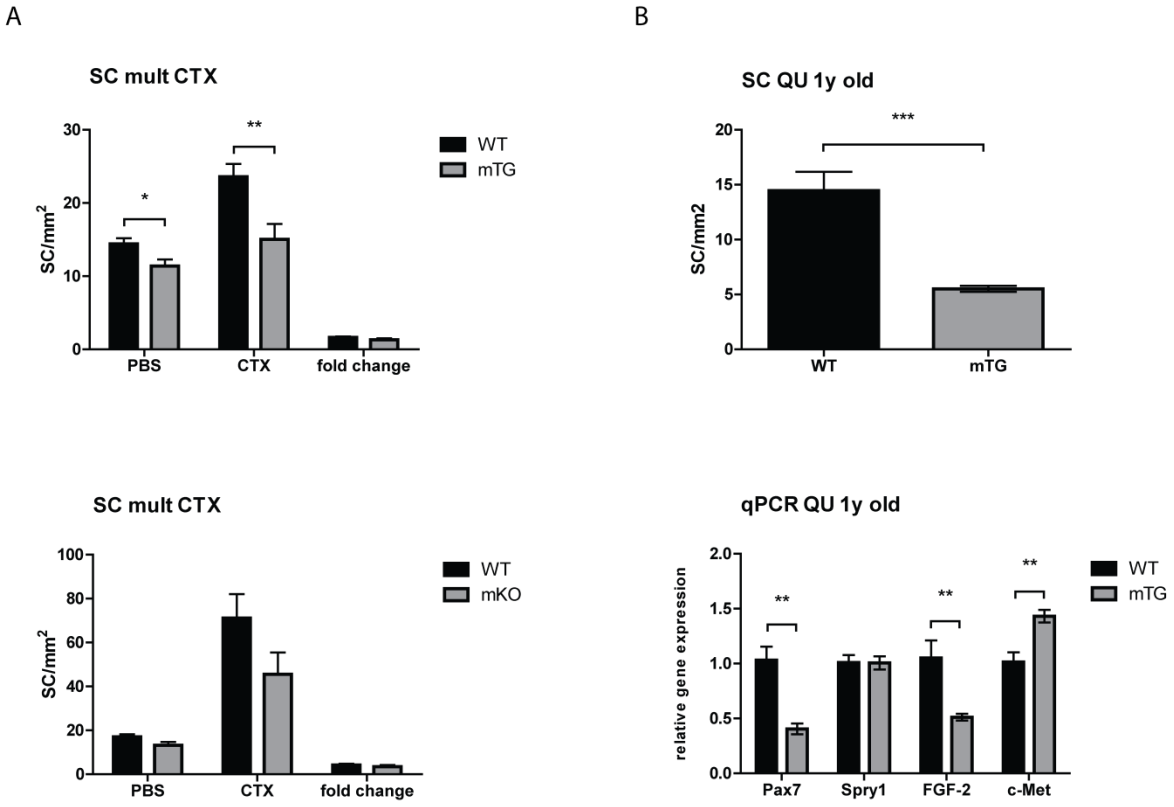

Supp Fig 1. SC numbers and relative gene expression after multiple cardiotoxin injuries and in one-year old mTG mice

A) SC numbers in mTG and Myf5-mKO mice 3 weeks after triple CTX injections (each injection was separated by 3-week period); B) SC numbers and relative gene expression in one-year old mTG mice. mRNA levels in mTG were normalized to WT levels; Values are plotted as AV+/-SEM; n= 5-8 per group; * $p \leq 0.05$, ** $p \leq 0.01$, *** $p \leq 0.001$

A

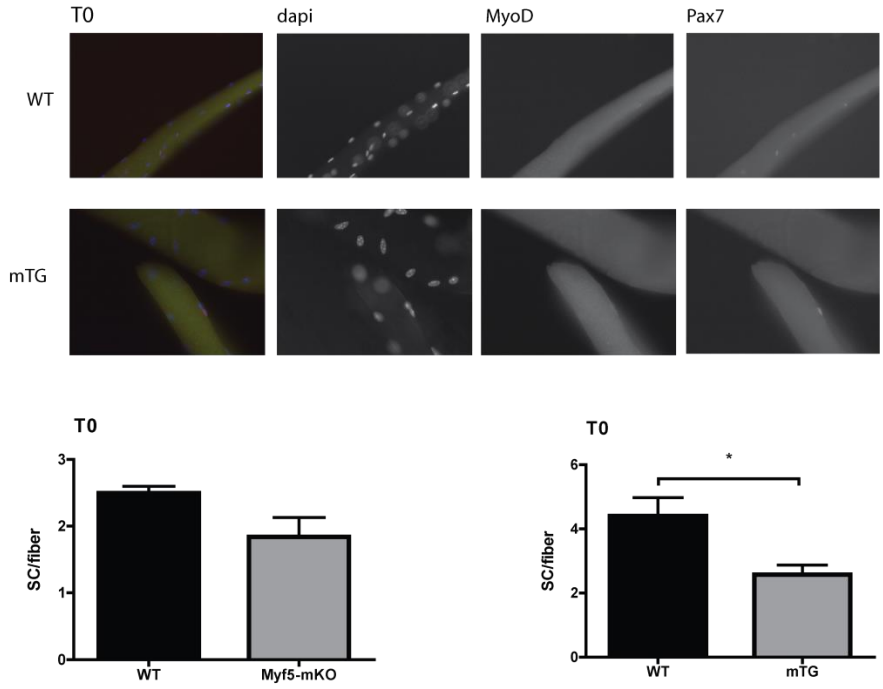
T0
dapi
MyoD
Pax7
WT
mTG
T0
SC/fiber
3
2
1
0
WT
Myf5-mKO
T0
*
SC/fiber
6
4
2
0
WT
mTG

B

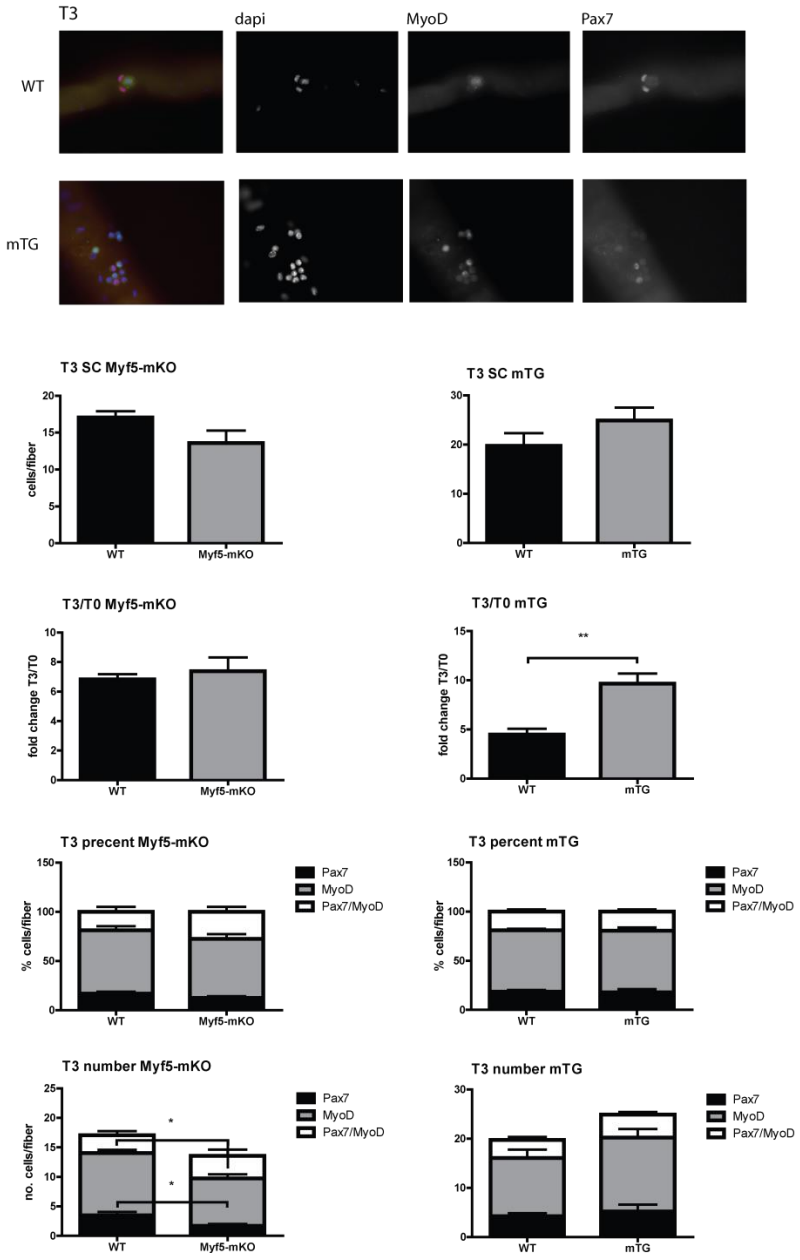

Fig 3. SC numbers and proliferation in culture on fibers in mTG and Myf5-mKO mice
A) Representative IHC images (dapi/nuclei-blue; MyoD-green; Pax7-red) of SCs on freshly isolated fibers (T0) and SC quantification per fiber in mTG and Myf5-mKO mice. Approximately 60 fibers per mouse were used and 5 mice per group; B) Representative IHC images (dapi/nuclei: blue; MyoD: green; Pax7: red) of SC progeny on fibers kept for 3d in culture media (T3) and quantification results. Total proliferative output of SCs and separate quantification of $Pax7^{+}/MyoD^{-}$, $Pax7^{+}/MyoD^{+}$, and $Pax7^{-}/MyoD^{+}$ cells per fiber. Approximately 20 fibers per mouse and 5 mice per group were used; Values are plotted as AV+/-SEM; * $p \leq 0.05$, ** $p \leq 0.01$, *** $p \leq 0.001$

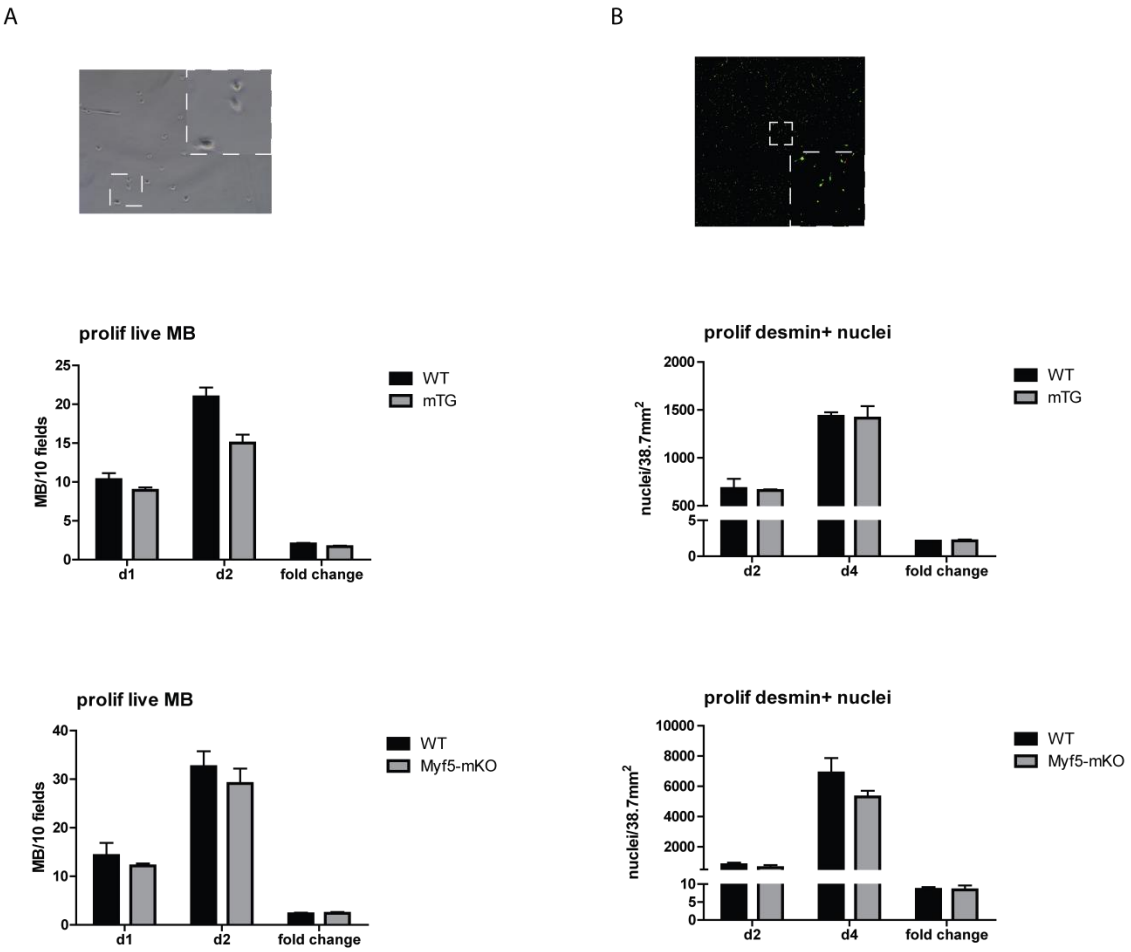

Supp Fig 2. Myoblast proliferation outside SC niche

A) Live myoblast quantification 1 and 2 days after plating equal number of myoblasts (MB), and fold change in numbers between these two days. Cells were quantified on 10 fields per dish, 2 dishes per mouse and 3 mice per genotype. Representative bright field image with enlarged white quadrant is included; B) Desmin positive cell quantification 2 and 4 days after plating equal number of myoblasts and fold change between these two days. Cells were quantified on area of 38.7 mm2 per dish, 2 dishes per mouse and 3 mice per genotype. Representative IHC image (dapi/nuclei: red; desmin: green) with enlarged white quadrant is included; Values are plotted as AV+/-SEM

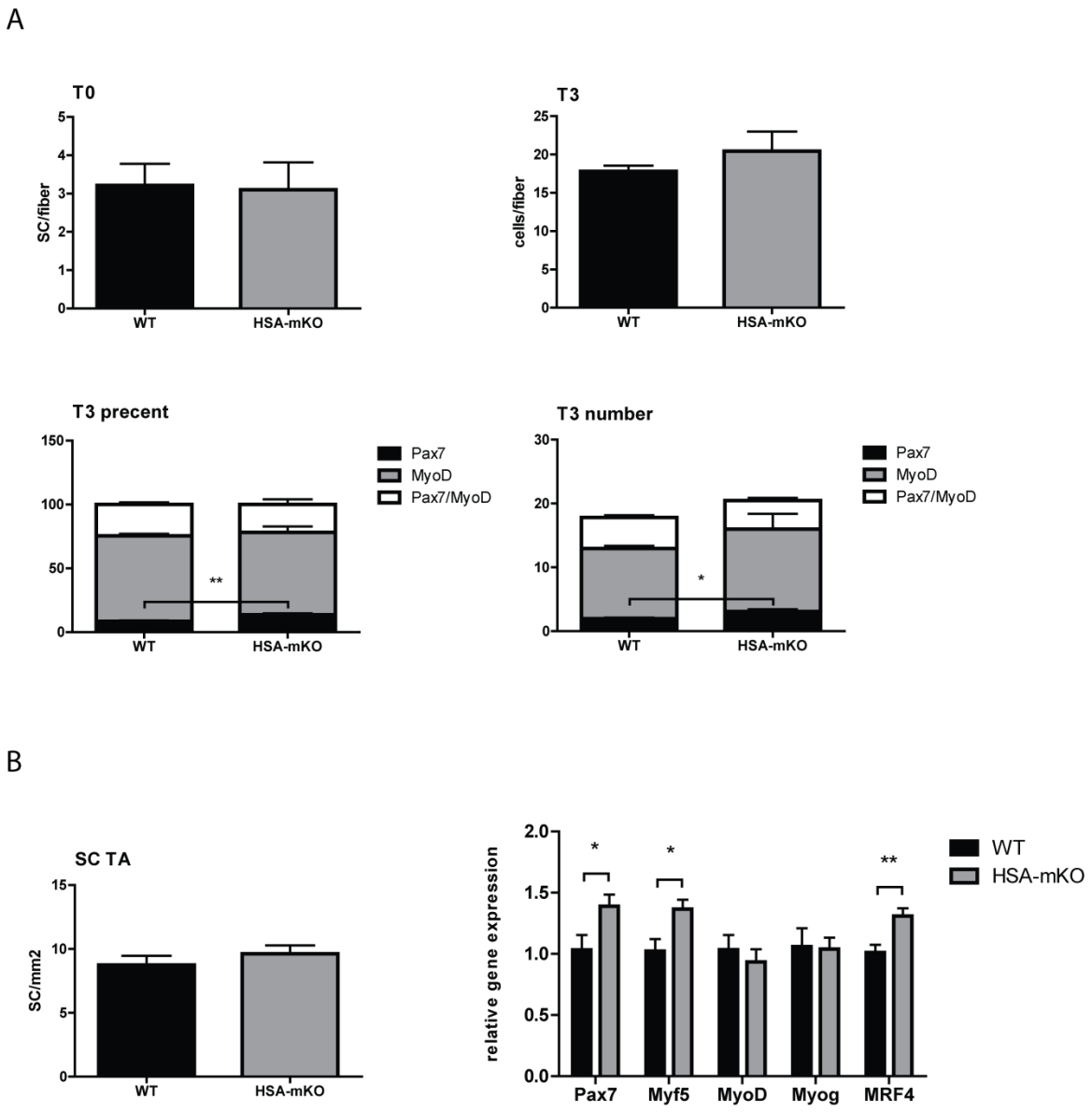

Fig 4. SC numbers and MRFs expression in HSA-mKO mice

A) SC numbers on freshly isolated fibers and quantification of SC proliferative output after 3d in culture media (T3), including separate quantification of $Pax7^{+}/MyoD^{-}$, $Pax7^{+}/MyoD^{+}$, and $Pax7^{-}/MyoD^{+}$ cells per fiber. Approximately 60 fibers per mouse and 5 mice per group for T0 and 20 fibers per mouse and 5 mice per group for T3 were used; B) SC number per area and relative mRNA levels of Pax7 and MRFs in TA muscle. mRNA levels in HSA-mKO mice were normalized to WT (control littermate) levels; Values are plotted as AV+/-SEM; n=5-6 per group; * $p \leq 0.05$, ** $p \leq 0.01$, *** $p \leq 0.001$

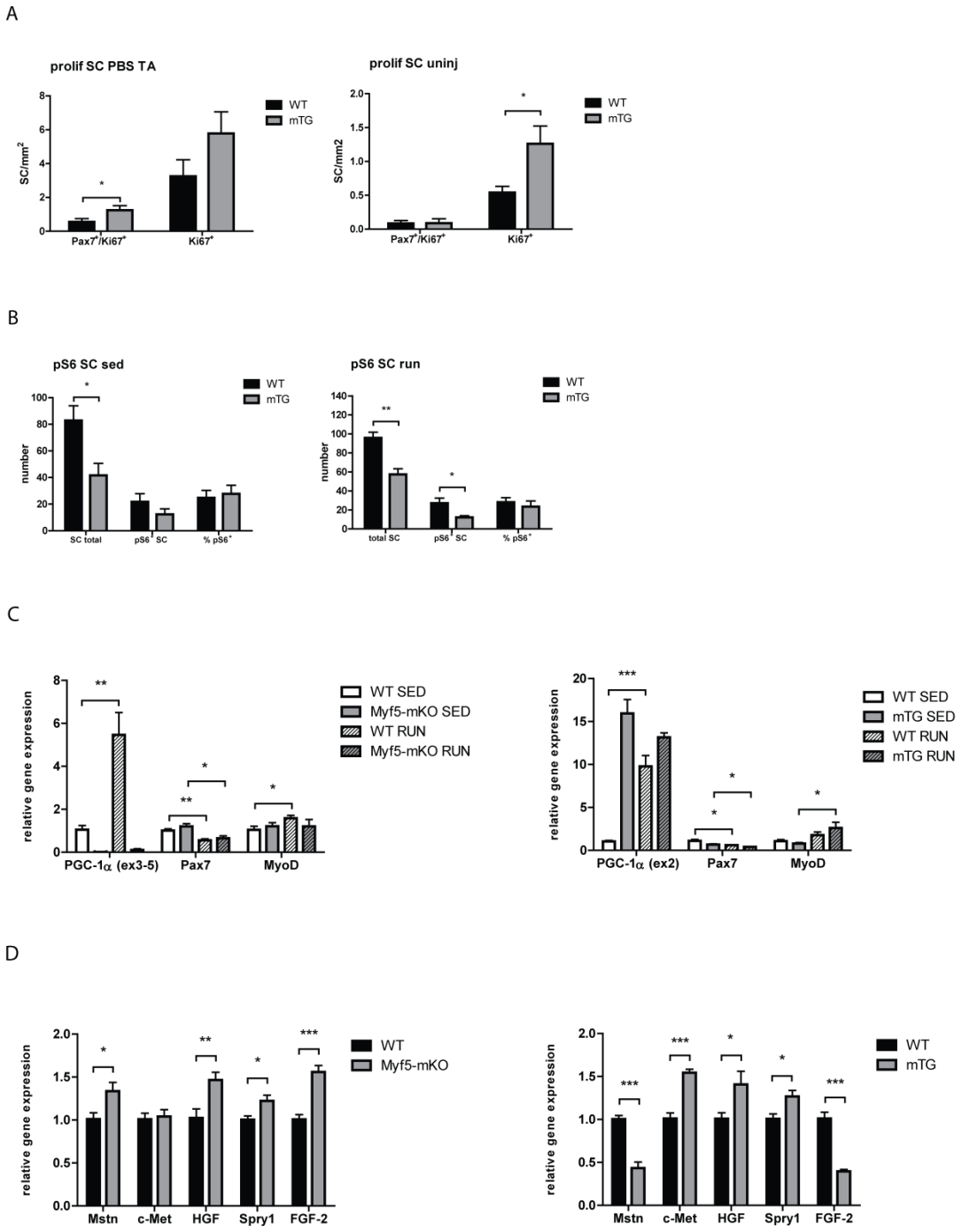

Fig 5. SC activation in MCK-mTG and Myf5-mKO mice

A) Proliferating SC numbers ($Pax7^+/Ki67^+$) per area in uninjected and PBS injected TAs of mTG mice; n=7-8 per group; B) $pS6^+$ SCs (SCs in alerted quiescent state) before and 2d after DHR running in QUs of mTG mice; n=5-6 per group C) Relative mRNA levels of PGC-1α, Pax7 and MyoD 3h after DHR in QUs of Myf5-mKO and mTG mice. mRNA levels were normalized to WT SED levels; n=4-7 per group; D) Relative mRNA levels in the basal state in TAs of Myf5-mKO and mTG mice; n=5-6 per group. mRNA levels in mTG and Myf5-mKO were normalized to WT levels; Values are plotted as AV+/-SEM; * $p \leq 0.05$, ** $p \leq 0.01$, *** $p \leq 0.001$

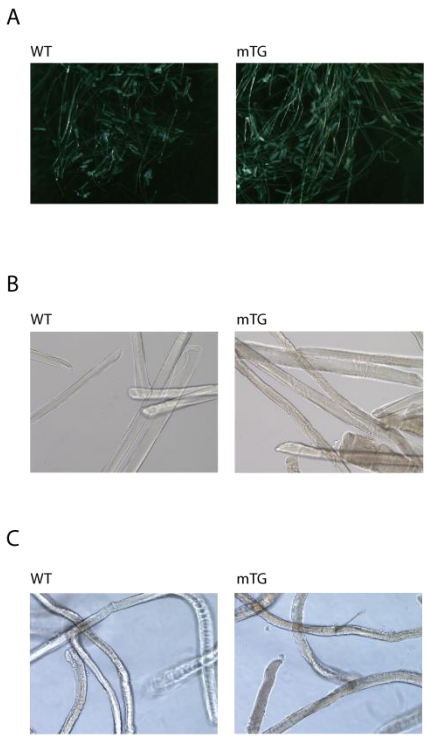
A
WT
mTG
B
WT
mTG
C
WT
mTG

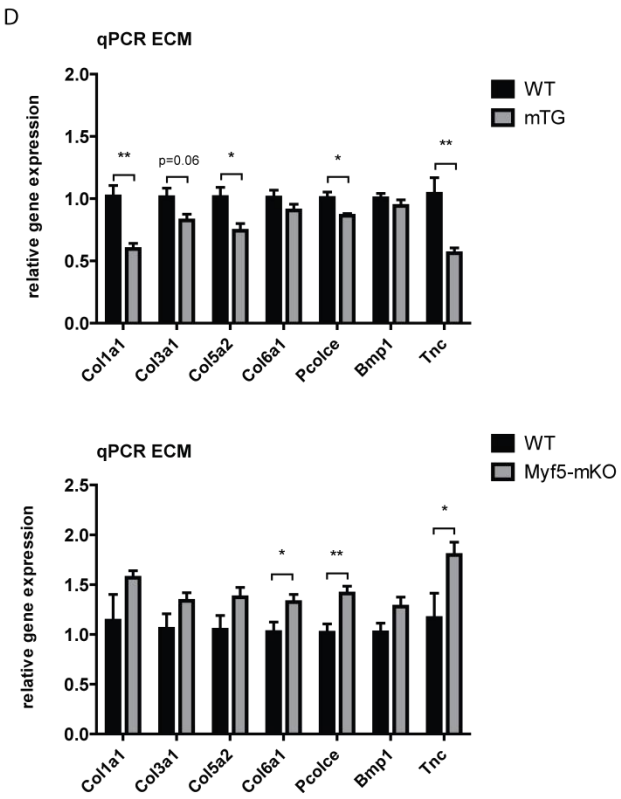
D
qPCR ECM
relative gene expression
2.0
1.5
1.0
0.5
0.0
WT
mTG
**
p=0.06
*
*
**
Col1a1
Col3a1
Col5a2
Col6a1
Pcolce
Bmp1
Tnc

qPCR ECM
relative gene expression
2.5
2.0
1.5
1.0
0.5
0.0
WT
Myf5-mKO
*
**
*
Col1a1
Col3a1
Col5a2
Col6a1
Pcolce
Bmp1
Tnc

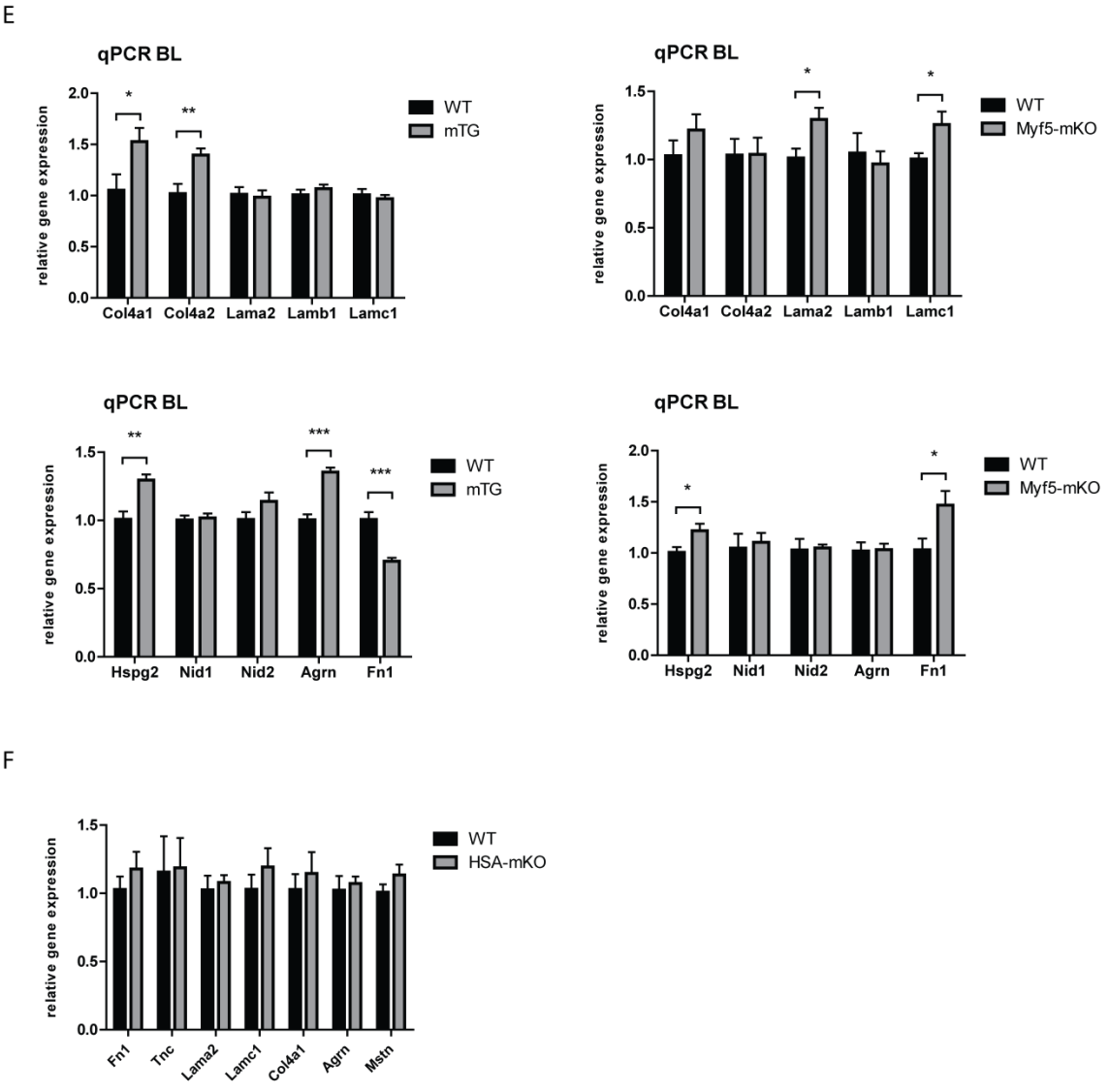

Fig 6. Extracellular matrix and basal lamina gene expression in mTG, Myf5-mKO and HSA-mKO mice
A) and B) Representative images of freshly isolated fibers from mTG and WT mice; C) images of WT and mTG fibers after 3d in culture media, prior to fixation. WT fibers look translucent and silky while mTG fibers appear matte and with cracks on the surface; D) Relative mRNA levels of ECM components in mTG and Myf5-mKO mice; E) Relative mRNA levels of basal lamina (BL) components in mTG and Myf5-mKO mice; F) Relative gene expression in HSA-mKO mice; mRNA levels in mTG, Myf5-mKO and HSA-mKO mice were normalized to WT (control littermate) levels; Values are plotted as AV+/-SEM; n=6 per group; * $p \leq 0.05$, ** $p \leq 0.01$, *** $p \leq 0.001$

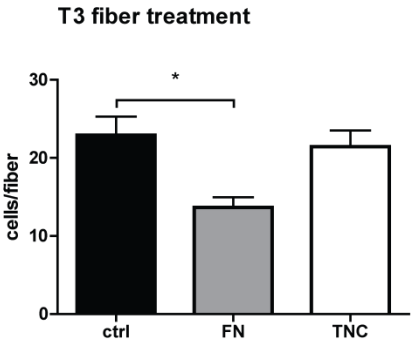

Fig 7. Fiber treatment with fibronectin and tenascin-C in culture
WT fibers were isolated and incubated for 3d in culture media supplemented with 100µg/ml FN or 5µg/ml TNC. Total proliferative output ($Pax7^{+}/MyoD^{-}$, $Pax7^{+}/MyoD^{+}$, and $Pax7^{-}/MyoD^{+}$ cells) of SCs was quantified and expressed per fiber. Approximately 20 fibers per mouse and 4 mice per group were used; Values are plotted as AV+/-SEM; * $p \leq 0.05$, ** $p \leq 0.01$, *** $p \leq 0.001$

6.5 Results

PGC-1α overexpression in fibers results in reduced SC numbers in muscles

MCK-mTG mice have muscles with a higher percentage of oxidative fibers at the expense of glycolytic ones (39). Their muscles are also rich in blood vessels and have greater endurance than their WT littermates. On the other hand, muscle specific knock-out mice exhibit the opposite phenotype (49). The change in the fiber type is followed by a change in metabolism, and the effect of PGC-1α in muscle on whole body metabolism has been extensively studied (50). Another important difference between fiber types is their resistance to atrophy, dystrophy and sarcopenia, and the role of PGC-1α on these aspects has been investigated as well (40, 42, 51). However, the connection between PGC-1α levels and SC numbers has not been addressed yet. Keeping in mind that oxidative fibers contain more SCs than glycolytic fibers (29), we expected to detect higher number of SCs in MCK-mTG mice.

For this reason, we first checked the expression of Pax7 and MRFs in the basal state of MCK-mTG and Myf5-mKO TA muscles (Fig 1A and 1B). Interestingly, we detected a decrease in several MRFs and Pax7 in MCK-mTG mice and an increase in Myf5-mKO. Next, we determined the SC numbers ($Pax7^{+}$/$DAPI^{+}$) in cross-sections of TAs, and detected lower numbers in MCK-mTG and no change in Myf5-mKO mice (Fig 1). The same change considering SC numbers was observed for MCK-mTG SOL. Importantly, we confirmed that in WT mice, oxidative muscles such as SOL tend to have more SCs than highly glycolytic muscles such as EDL (Fig 1A).

PGC-1α levels modulate SC proliferation after CTX injury

SCs are muscle stem cells that are activated upon injury, when they enter the cell cycle and proliferate in order to regenerate damaged muscle (3). Decrease in SC numbers is a hallmark of chronic diseases such as Duchenne muscular dystrophy (DMD), but is also seen during aging (9, 10). This reduction is associated with SC senescence, inability to return to quiescence after the proliferative phase, and as a consequence - impaired regeneration (18, 52). In order to see how lower numbers of SCs in MCK-mTG affect their ability to cope with acute injury, we quantified SCs in TA cross-sections 4 days and 19 days after CTX both in MCK-mTG and

Myf5-mKO TAs (Fig 2). To our surprise, we spotted a reduction in proliferative capacity in Myf5-mKO mice at 4d post CTX, accompanied with reduced numbers of proliferating SCs, whereas in MCK-mTG we measured mild tendency towards higher proliferative output (Fig 2A). At 19d time point, we observed significant difference in SC proliferation in MCK-mTG and tendencies of lower values for Myf5-mKO (Fig 2B).

To test whether lower numbers of SCs in MCK-mTG would impair regeneration in chronic injury, we performed a multiple CTX injury experiment and quantified SC numbers on TA cross-sections 3 weeks after the last CTX injection (Supp Fig 1A). We could not detect a difference in the fold change of SC numbers in either of the two genotypes, suggesting that PGC-1α does not affect SC return to quiescence. In addition, gene expression relevant for SC behavior and SC numbers seemed unaltered with aging in MCK-mTG mice (Supp Fig 1B).

Immediate niche, not PGC-1α dependent inflammatory conditions upon injury alone, influences SC behavior

One reason for the observed differences in MCK-mTG and Myf5-mKO mice after CTX injury could be modulation of inflammatory response and necrotic area clearance (see *Project 1*). Skeletal muscle regeneration is a very complex process, in which both muscle and non-muscle cells simultaneously participate in order to clear away the damaged tissue and form new muscle tissue (53, 54). In order to assess the SCs' proliferative potential depending on PGC-1α expression, we took the *ex vivo* approach by isolating single muscle fibers and keeping them in culture for several days. Comparison of SC numbers and their progeny at T0 (on freshly isolated fibers) and at T3 (after 3 days in culture) let us evaluate the SCs' proliferative capacity while in the immediate niche of their muscle fiber (Fig 3). Firstly, we confirmed that MCK-mTG have lower numbers of SCs ($Pax7^+/DAPI^+$) per fiber, whereas SC numbers were unchanged for Myf5-mKO (Fig 3A). Next, we quantified quiescent SCs ($Pax7^+/MyoD^-/DAPI^+$), committed progenitors ($Pax7^+/MyoD^+/DAPI^+$) and myoblasts ($Pax7^-/MyoD^+/DAPI^+$) per fiber at T3. In line with the *in vivo* observations, we detected higher relative proliferative output (T3/T0) in MCK-mTG fibers (Fig 3B). In Myf5-mKO fibers, on the other hand, relative proliferative output was unchanged, yet there were lower numbers of quiescent SCs and myoblasts, indicating slower progression in differentiation (Fig 3B). These results indicate that the differences seen in SC

numbers after CTX injury are not only due to changes in the inflammatory stages of regeneration (see *Project 1*). Therefore, fiber properties, either in the form of secreted factors or proteins present in the sarcolemma and BL, are enough to evoke this phenotype, at least for MCK-mTG mice.

In order to test if the observed differences in Myf5-mKO mice are due to fiber properties and not SCs alone, we isolated primary myoblasts from the two PGC-1α knock-out mouse models and tested their proliferative rate using immunocytochemistry (Supp Fig 2). The high purity of the primary population was verified by desmin staining. qPCR data confirmed PGC-1α ablation in Myf5-mKO myoblasts and unchanged PGC-1α expression in MCK-mTG myoblasts (see Supp Fig 4B in *Project 1*). Myoblast proliferation was assessed by comparing cell numbers between two incubation periods, in order to minimize the influence of variations in the numbers of cells plated. Quantification was performed on live cells (Supp Fig 2A), as well as fixed and stained myoblasts (Supp Fig 2B). We did not observe differences in the proliferation rates of either MCK-mTG or Myf5-mKO myoblasts (Supp Fig 2).

Loss of PGC-1α both in SCs and fibers and not fibers alone, leads to reduced SC proliferation rate

Thus far, we were able to see that overexpression of PGC-1α in fibers (MCK-mTG) has an effect on SC numbers and their proliferation, probably due to modified properties of the immediate niche. However, the differences observed in proliferation rate in Myf5-mKO mice were harder to interpret since in these mice PGC-1α was ablated from the SC stage. In isolated myoblasts of Myf5-mKO mice, we did not detect reduced proliferation rates (Supp Fig 2), suggesting that the effects observed in fibers (Fig 3B) and muscles *in vivo* (Fig 2A) are probably not cell intrinsic. In order to better assess the input from fibers, we used the HSA-mKO mouse model in which PGC-1α is exclusively deleted in fibers.

Although qPCR data for Pax7 and MRFs in TA of HSA-mKO indicated the possibility of an opposite SC phenotype compared to MCK-mTG mice, we measured no difference in SC numbers on TA cross-sections (Fig 4B). These results were substantiated by quantifications performed on freshly isolated fibers (Fig 4A). In addition, there were no differences in proliferative output measured by numbers of SCs and their progeny on fibers at T3 (Fig 4A).

Collectively, the data suggest that PGC-1α overexpression in fibers is enough to modify the niche and influence SC activation/proliferation, whereas deleting PGC-1α from fibers does not change the SC behavior. PGC-1α deletion in SCs and fibers together, seems necessary for reduction in SC proliferation.

PGC-1α levels in fibers and SCs modulate SC activation upon injury

Described modifications in SC proliferation in MCK-mTG and Myf5-mKO mice could be due to a faster activation of SCs and entering the cell cycle from quiescence. Recently, Rodgers et al. described an alternative state of quiescence in SCs, termed G_{Alert}, which enable cells to faster respond to injury (17).

We investigated the activation status of SCs in our mouse models in several experiments. In PBS injected muscles, we detected higher numbers of proliferating SCs ($Pax7^+/Ki67^+/DAPI^+$) in MCK-mTG outside of the injured part of a muscle (Fig 5A). This was not the case with a completely uninjured muscle (Fig 5A). In addition, QU muscles of Myf5-mKO mice 3h after DHR showed lack of upregulation of MyoD compared to WT controls, whereas Pax7 expression was reduced in both genotypes (Fig 5C). Similar experiment with MCK-mTG mice also resulted in a decrease in Pax7 expression, while an increase in MyoD expression was significant in MCK-mTG group and only tendency was observed in WT controls (Fig 5C). These results indicate faster activation of SCs in MCK-mTG and slower in Myf5-mKO upon a stimulus.

In order to better define the observed differences and assesse them through newly defined G_{Alert} state, we quantified $Pax7^+/pS6^+/DAPI^+$ cells on QU of sedentary (uninjured) and running MCK-mTG mice (Fig 5B). Our results did not indicate increased SC alertness in either of the experimental groups. SC numbers were just slightly increased upon running in both genotypes.

Myostatin (Mstn) is a known inhibitor of SC activation and proliferation (55). Therefore, it is worth mentioning that we measured decreased expression of Mstn and increased expression of HGF and c-Met in MCK-mTG TAs, which can contribute to the observed differences in SC activation (Fig 5D). Opposite expression profile regarding Mstn was detected in Myf5-mKO TAs (Fig 5D).

Fibronectin is at least partially responsible for the proliferative rate of SCs seen in PGC-1α mouse models

Due to the observed difference in fiber translucence when viewed under the light microscope (Fig 6A, 6B and 6C), we decided to look closer into the ECM components which surround isolated fibers (Fig 6D). Thickening of BL, which happens in aging, leads to the reduced responsiveness of SCs (22). For that reason, we looked at gene expression of collagens and glycoproteins, especially the ones which comprise the closest layer of the ECM (Fig 6E). We noticed that the variety of collagens are downregulated in MCK-mTG and exhibit tendencies towards higher expression in Myf5-mKO (Fig 6D), but more importantly, we detected the opposite expression patterns in two components of BL – FN and TNC (Fig 6E and 6D). Interestingly, the same difference was not observed in HSA-mKO TAs (Fig 6F), which also did not exhibit the phenotype connected to SC proliferation (Fig 4A).

We decided to focus our attention on FN and TNC for several reasons: increased expression of FN is present in fibrotic conditions (25), and is additionally associated to the similar SC phenotype that we observed in Myf5-mKO mice (27); TNC on the other hand blocks the interaction between FN, secreted by SCs upon activation, and Sdc4 (28), intercepting in that way Wnt7a signaling and SC proliferation (26). To test whether these components can block the SC proliferation on fibers *in vitro*, we incubated WT fibers for 3 days in culture media with addition of FN or TNC. Approximately 40% reduction in proliferation output was detected in FN treated fibers, whereas TNC did not induce changes (Fig 7).

6.6 Discussion

PGC-1α is a coactivator which induces mitochondrial biogenesis (36, 37), drives the switch from glycolytic to oxidative fibers (39), increases with exercise (38) and is also responsible for some of the positive effects of exercise. Despite the reported effects of exercise (30-32) and oxidative fibers (29) on SC numbers, the impact of PGC-1α on SC biology has not been investigated. In this study, we primarily consider the effects PGC-1α might have on the SC niche, and therefore the indirect effects of fiber properties on SC behavior. The role the metabolic status of a fiber can have on SCs is expected to be great, but in which way it could affect SC activation is not known (45). This is especially interesting having in mind recent advances in understanding the importance of metabolic reprogramming in stem cell biology. In cancer and stem cells, glycolysis and fatty acid oxidation (FAO) are characteristic of dormant cells, aerobic glycolysis with the active pentose-phosphate pathway is representative of the proliferative state, and mitochondrial oxidative phosphorylation (OXPHOS) is distinctive of differentiation (14). In muscle stem cells, there is a paucity of data in this regard, and generally, while glycolysis is linked to SC quiescence, increase in mitochondrial metabolism favors proliferation and differentiation (45).

Unexpectedly, we show here that MCK-mTG muscles have lower SC numbers compared to WT littermates. This is the first example that we are aware of, where PGC-1α overexpression in muscle does not reflect the oxidative muscle characteristics. Although SC presence is an imperative of successful regeneration, lower SC numbers do not necessarily imply reduced regenerative capability. Namely, although decline in SC numbers reported in aging served as an explanation for impaired regeneration in these conditions, SC regenerative potential and role of extrinsic factors in this context are increasingly seen as a causation of pathology (56). Actually, both decreased and increased numbers in aging (22) and DMD (9, 57) have been reported. This could be due to technical reasons (methods used), but also due to variations in age or stage of disease tested. One could imagine that in the case of constant low damage, SCs will become activated and proliferate to a certain extent, increasing in numbers. However, under chronic conditions, this will eventually lead to SC exhaustion and therefore lower SC numbers.

Nevertheless, the lower SC numbers we detected in MCK-mTG mice did not lead to impaired regeneration (see *Project 1*) and were not linked to SC depletion. On the contrary, SCs from MCK-mTG mice exhibited higher proliferation potential both *in vitro* and *in vivo*. *In vivo* results, obtained after CTX injury, could be partially due to systemic effect and therefore not directly the consequence of SCs and/or their immediate niche. Indeed, we detected increased attraction of macrophages and necrotic area clearance in mTG mice after CTX injury (see *Project 1*). These effects can provide an environment which favors SC proliferation and myogenesis (58). In order to minimize the contributing factors of other cells in muscle tissue, we looked at SC proliferation potential on isolated fibers. The SC niche *in vivo* comprises of effectors emerging from the muscle fiber and surrounding ECM, but also factors coming from blood vessels, macrophages and other locally present cells (59). On isolated fibers, the focus is on the immediate niche, consisting mostly of factors emanating from muscle fibers and the surrounding BL.

As with the results obtained *in vivo*, we observed increased SC proliferation in MCK-mTG on isolated fibers. qPCR results on TA muscles indicated reduced expression of various EMC and BL components in MCK-mTG mice. BL thickening is associated with aging and is related to lower SC activation and diminished regenerative ability (22). Indeed, heterochronic parabiotic experiments infer that SCs from old and young mice do not involve intrinsic differences, but that rather differential environmental cues evoke this effect (21). Nevertheless, the impact of cell intrinsic aspects of SC aging such as elevated p38α/β mitogen-activated protein kinase (MAPK) activity and increase in senescence marker p16, should not be underestimated (52, 54).

Specifically, we detected reduced expression of FN and TNC in MCK-mTG muscles. The importance of FN in SC activation was recently demonstrated. Bentzinger et al. showed that SCs increase the expression and locally secrete FN upon activation (26). FN interacts with Sdc4, potentiating in that way Wnt7a signaling through frizzled-7 (Fzd7)/Sdc4, and favoring symmetric division of stem SCs (60). However, chronically elevated levels of FN are a hallmark of fibrosis and BL thickening (22, 25, 61, 62). In addition, Ross et al. reported increased basal expression of FN in like-acetylglucosaminyltransferase myodystrophy ($LARGE^{myd}$) mice, which correlated with increased SC numbers and reduced proliferative potential on fibers *ex vivo* (27).

This phenotype is the opposite of what we detected in MCK-mTG mice. On the other hand, accumulation of TNC, an extracellular glycoprotein highly expressed in development, regeneration and cancer, is also linked to fibrosis (63, 64). Importantly, TNC was shown to obstruct the aforementioned interaction of FN with Sdc4 and therefore block stem SC proliferation (26, 28). Hence, the decreases in FN and TNC seen in MCK-mTG could have provided an explanation for the increased SC proliferative potential detected on fibers.

Additionally, we were interested in the effects PGC-1α ablation in SCs and/or fibers might have on SCs. The opposite proliferative potential of SCs on fibers and *in vivo*, compared to MCK-mTG mice, was observed in Myf5-mKO. Interestingly, reversed ECM expression patterns, particularly regarding FN and TNC were detected as well. Indeed, we were able to show that WT fibers treated with FN *in vitro* had reduced SC proliferation. Absence of effects in TNC treated fibers could be due to the concentration used. In order to distinguish whether the observed effects are due to PGC-1α loss in fibers or SCs, we performed the same measurements with HSA-mKO mice. Surprisingly, loss of PGC-1α in fibers did not affect SC behavior, or notably, BL composition. We conclude that increased PGC-1α expression in fibers leads to lower expression of ECM components, in particular FN, which in turn affect SC activation and proliferation. Loss of PGC-1α both in SCs and fibers is needed in order to trigger opposite response from the one observed in MCK-mTG mice.

The alterations in proliferation output detected both *in vivo* and *in vitro* in MCK-mTG and Myf5-mKO mice could be due to faster activation of SCs with overexpression of PGC-1α in their niche. To test for this, we quantified proliferating SCs in uninjured and PBS injected MCK-mTG TAs. Although activated SCs were very rare in uninjured TAs, there were higher numbers of activated SCs 4 days after PBS injection ($Pax7^{+}/Ki67^{+}/DAPI^{+}$) in MCK-mTG compared to WT. In addition, 3 hours after DHR, QUs of Myf5-mKO had unchanged expression of MyoD whereas controls showed increased expression. Importantly, DHR was accompanied by an increase in PGC-1α expression only in WT controls. According to the same parameters, DHR experiment in MCK-mTG mice demonstrated tendencies of faster activation of SCs in MCK-mTG mice compared to controls. Altogether, these results suggest faster activation of SCs in MCK-mTG and slower in Myf5-mKO mice.

In addition to that, we detected higher expression levels of both HGF and c-Met in TAs of MCK-mTG. c-Met is a receptor tyrosine kinase, present primarily on quiescent and activated SCs, and HGF is a growth factor that can be found inactive and bound to the ECM of the muscle (3). Upon contraction, Ca^{2+} signaling increases nitrogen monoxide (NO) free radical levels which activate matrix metalloproteinases and therefore cause HGF detachment and activation. HGF then binds to the c-Met receptor on SCs and leads to SC activation and proliferation. This cascade is considered the initial pathway in SC activation (65, 66). Therefore, increased expression of HGF and c-Met could predispose SCs in MCK-mTG muscles to faster activation upon stimulus. In Myf5-mKO muscles, we detected unchanged c-Met levels and increased HGF, which could have a compensatory role.

Another interesting observation is related to the expression levels of Mstn. Mstn is considerably downregulated in MCK-mTG in the basal state, but is increased in Myf5-mKO. It is a member of transforming growth factor beta (TGF-β) family, an important regulator of fibrosis (67) and muscle mass (68). In addition, several studies reported that Mstn reduces SC and myoblast proliferation (55, 69-71). Although initial studies connected this effect with muscle hypertrophy and improved regeneration in $Mstn^{-/-}$ mice (69, 71, 72), the contribution of SCs to increased muscle mass upon blocking Mstn was recently challenged (73-75). Nevertheless, Mstn seems to be expressed by quiescent SCs (55), but more importantly, exogenous Mstn can block SC activation and proliferation *in vitro* (71). Therefore, even if the expression levels detected in our mouse models primarily represent differences in fibers and not SCs, Mstn from fibers can still modulate SC behavior upon stimulus by blocking SC activation.

Up until recently, SC quiescence was very poorly understood. We are now aware of an alternate quiescent state named G_{Alert} (17). SCs can transition from the G_0 to the G_{Alert} state due to distal injury. SCs in the G_{Alert} state are not activated as they do not express Ki67 or MyoD. However, these cells can rapidly start proliferating upon injury compared to SCs in the G_0 state and therefore provide a regenerative advantage. Interestingly, this alertness is dependent on mitochondrial activity and mTORC1 signaling. Given that PGC-1α is a key regulator of mitochondrial metabolism, we were interested in investigating the SC quiescence status in MCK-mTG mice. Quantification of $pS6^+$ SCs ($Pax7^+/DAPi^+$) on QU sections of sedentary and running MCK-mTG mice showed no difference between genotypes nor treatments (sedentary and

running), indicating that the observed differences in SC proliferative output and activation in MCK-mTG mice are not due to increased SC alertness.

Based on our results, we can conclude that PGC-1α overexpression in the niche induces reduction of FN and Mstn, as well as increase in c-Met and HGF, which enables faster SC activation and proliferation, without influencing their quiescence. Knowledge of the effects of PGC-1α overexpression in SC niche could be advantageous in stem-cell based transplantations, where knowing the modulators of SC proliferation and self-renewal is of paramount importance for successful therapeutic solutions.

6.7 References

1. Mauro, a. (1961) Satellite cell of skeletal muscle fibers. *The Journal of biophysical and biochemical cytology* **9**, 493-495
2. Christov, C., Chretien, F., Abou-Khalil, R., Bassez, G., Vallet, G., Authier, F. J., Bassaglia, Y., Shinin, V., Tajbakhsh, S., Chazaud, B., and Gherardi, R. K. (2007) Muscle satellite cells and endothelial cells: close neighbors and privileged partners. *Mol Biol Cell* **18**, 1397-1409
3. Yin, H., Price, F., and Rudnicki, M. a. (2013) Satellite cells and the muscle stem cell niche. *Physiological reviews* **93**, 23-67
4. Lepper, C., Partridge, T. a., and Fan, C.-M. (2011) An absolute requirement for Pax7-positive satellite cells in acute injury-induced skeletal muscle regeneration. *Development (Cambridge, England)* **138**, 3639-3646
5. Sambasivan, R., Yao, R., Kissenpfennig, A., Van Wittenberghe, L., Paldi, A., Gayraud-Morel, B., Guenou, H., Malissen, B., Tajbakhsh, S., and Galy, A. (2011) Pax7-expressing satellite cells are indispensable for adult skeletal muscle regeneration. *Development (Cambridge, England)* **138**, 3647-3656
6. Murphy, M. M., Lawson, J. a., Mathew, S. J., Hutcheson, D. a., and Kardon, G. (2011) Satellite cells, connective tissue fibroblasts and their interactions are crucial for muscle regeneration. *Development (Cambridge, England)* **138**, 3625-3637
7. McCarthy, J. J., Mula, J., Miyazaki, M., Erfani, R., Garrison, K., Farooqui, A. B., Srikuea, R., Lawson, B. a., Grimes, B., Keller, C., Van Zant, G., Campbell, K. S., Esser, K. a., Dupont-Versteegden, E. E., and Peterson, C. a. (2011) Effective fiber hypertrophy in satellite cell-depleted skeletal muscle. *Development (Cambridge, England)* **138**, 3657-3666
8. Otto, A., Collins-Hooper, H., and Patel, K. (2009) The origin, molecular regulation and therapeutic potential of myogenic stem cell populations. *J Anat* **215**, 477-497
9. Jejurikar, S. S., and Kuzon, W. M., Jr. (2003) Satellite cell depletion in degenerative skeletal muscle. *Apoptosis* **8**, 573-578
10. Shefer, G., Van de Mark, D. P., Richardson, J. B., and Yablonka-Reuveni, Z. (2006) Satellite-cell pool size does matter: defining the myogenic potency of aging skeletal muscle. *Dev Biol* **294**, 50-66
11. Seale, P., Sabourin, L. a., Girgis-Gabardo, a., Mansouri, a., Gruss, P., and Rudnicki, M. a. (2000) Pax7 is required for the specification of myogenic satellite cells. *Cell* **102**, 777-786
12. Kuang, S., Kuroda, K., Le Grand, F., and Rudnicki, M. A. (2007) Asymmetric self-renewal and commitment of satellite stem cells in muscle. *Cell* **129**, 999-1010
13. Wozniak, a. C., Pilipowicz, O., Yablonka-Reuveni, Z., Greenway, S., Craven, S., Scott, E., and Anderson, J. E. (2003) C-Met Expression and Mechanical Activation of Satellite Cells on Cultured Muscle Fibers. *Journal of Histochemistry & Cytochemistry* **51**, 1437-1445
14. Ito, K., and Suda, T. (2014) Metabolic requirements for the maintenance of self-renewing stem cells. *Nature Reviews Molecular Cell Biology* **15**, 243-256
15. Knight, J. D., and Kothary, R. (2011) The myogenic kinome: protein kinases critical to mammalian skeletal myogenesis. *Skeletal Muscle* **1**, 29-29

16. Wang, Y. X., and Rudnicki, M. a. (2012) Satellite cells, the engines of muscle repair. *Nature reviews. Molecular cell biology* **13**, 127-133
17. Rodgers, J. T., King, K. Y., Brett, J. O., Cromie, M. J., Charville, G. W., Maguire, K. K., Brunson, C., Mastey, N., Liu, L., Tsai, C. R., Goodell, M. A., and Rando, T. A. (2014) mTORC1 controls the adaptive transition of quiescent stem cells from G0 to G(Alert). *Nature* **510**, 393-396
18. Chakkalakal, J. V., Jones, K. M., Basson, M. A., and Brack, A. S. (2012) The aged niche disrupts muscle stem cell quiescence. *Nature* **490**, 355-360
19. Shea, K. L., Xiang, W., LaPorta, V. S., Licht, J. D., Keller, C., Basson, M. A., and Brack, A. S. (2010) Sprouty1 regulates reversible quiescence of a self-renewing adult muscle stem cell pool during regeneration. *Cell Stem Cell* **6**, 117-129
20. Jang, Y. C., Sinha, M., Cerletti, M., Dall'Osso, C., and Wagers, a. J. (2011) Skeletal Muscle Stem Cells: Effects of Aging and Metabolism on Muscle Regenerative Function. *Cold Spring Harbor Symposia on Quantitative Biology* **76**, 101-111
21. Conboy, I. M., Conboy, M. J., Wagers, A. J., Girma, E. R., Weissman, I. L., and Rando, T. a. (2005) Rejuvenation of aged progenitor cells by exposure to a young systemic environment. *Nature* **433**, 760-764
22. Gopinath, S. D., and Rando, T. a. (2008) Stem cell review series: aging of the skeletal muscle stem cell niche. *Aging Cell* **7**, 590-598
23. Sanes, J. R. (2003) The basement membrane/basal lamina of skeletal muscle. *The Journal of biological chemistry* **278**, 12601-12604
24. Gillies, A. R., and Lieber, R. L. (2011) Structure and function of the skeletal muscle extracellular matrix. *Muscle & nerve* **44**, 318-331
25. Serrano, A. L., Mann, C. J., Vidal, B., Ardite, E., Perdiguero, E., and Munoz-Canoves, P. (2011) Cellular and molecular mechanisms regulating fibrosis in skeletal muscle repair and disease. *Curr Top Dev Biol* **96**, 167-201
26. Bentzinger, C. F., Wang, Y. X., von Maltzahn, J., Soleimani, V. D., Yin, H., and Rudnicki, M. a. (2013) Fibronectin regulates Wnt7a signaling and satellite cell expansion. *Cell Stem Cell* **12**, 75-87
27. Ross, J., Benn, A., Jonuschies, J., Boldrin, L., Muntoni, F., Hewitt, J. E., Brown, S. C., and Morgan, J. E. (2012) Defects in glycosylation impair satellite stem cell function and niche composition in the muscles of the dystrophic Large(myd) mouse. *Stem cells (Dayton, Ohio)* **30**, 2330-2341
28. Huang, W., Chiquet-Ehrismann, R., Moyano, J. V., Garcia-Pardo, A., and Orend, G. (2001) Interference of tenascin-C with syndecan-4 binding to fibronectin blocks cell adhesion and stimulates tumor cell proliferation. *Cancer Res* **61**, 8586-8594
29. Gibson, M. C., and Schultz, E. (1982) The distribution of satellite cells and their relationship to specific fiber types in soleus and extensor digitorum longus muscles. *Anat Rec* **202**, 329-337
30. Parise, G., McKinnell, I. W., and Rudnicki, M. a. (2008) Muscle satellite cell and atypical myogenic progenitor response following exercise. *Muscle & Nerve* **37**, 611-619
31. Shefer, G., Rauner, G., Yablonka-Reuveni, Z., and Benayahu, D. (2010) Reduced satellite cell numbers and myogenic capacity in aging can be alleviated by endurance exercise. *PLoS One* **5**, e13307

32. Dreyer, H. C., Blanco, C. E., Sattler, F. R., Schroeder, E. T., and Wiswell, R. a. (2006) Satellite cell numbers in young and older men 24 hours after eccentric exercise. *Muscle & nerve* **33**, 242-253
33. Wang, Y., and Pessin, J. E. (2013) Mechanisms for fiber-type specificity of skeletal muscle atrophy. *Curr Opin Clin Nutr Metab Care* **16**, 243-250
34. Lexell, J. (1995) Human aging, muscle mass, and fiber type composition. *J Gerontol A Biol Sci Med Sci* **50 Spec No**, 11-16
35. Webster, C., Silberstein, L., Hays, A. P., and Blau, H. M. (1988) Fast muscle fibers are preferentially affected in Duchenne muscular dystrophy. *Cell* **52**, 503-513
36. Puigserver, P., Wu, Z., Park, C. W., Graves, R., Wright, M., and Spiegelman, B. M. (1998) A cold-inducible coactivator of nuclear receptors linked to adaptive thermogenesis. *Cell* **92**, 829-839
37. Wu, Z., Puigserver, P., Andersson, U., Zhang, C., Adelmant, G., Mootha, V., Troy, A., Cinti, S., Lowell, B., Scarpulla, R. C., and Spiegelman, B. M. (1999) Mechanisms controlling mitochondrial biogenesis and respiration through the thermogenic coactivator PGC-1. *Cell* **98**, 115-124
38. Baar, K., Wende, A. R., Jones, T. E., Marison, M., Nolte, L. a., Chen, M., Kelly, D. P., and Holloszy, J. O. (2002) Adaptations of skeletal muscle to exercise: rapid increase in the transcriptional coactivator PGC-1. *FASEB journal : official publication of the Federation of American Societies for Experimental Biology* **16**, 1879-1886
39. Lin, J., Wu, H., Tarr, P. T., Zhang, C.-Y., Wu, Z., Boss, O., Michael, L. F., Puigserver, P., Isotani, E., Olson, E. N., Lowell, B. B., Bassel-Duby, R., and Spiegelman, B. M. (2002) Transcriptional co-activator PGC-1 alpha drives the formation of slow-twitch muscle fibres. *Nature* **418**, 797-801
40. Sandri, M., Lin, J., Handschin, C., Yang, W., Arany, Z. P., Lecker, S. H., Goldberg, A. L., and Spiegelman, B. M. (2006) PGC-1alpha protects skeletal muscle from atrophy by suppressing FoxO3 action and atrophy-specific gene transcription. *Proceedings of the National Academy of Sciences of the United States of America* **103**, 16260-16265
41. Handschin, C., Kobayashi, Y. M., Chin, S., Seale, P., Campbell, K. P., and Spiegelman, B. M. (2007) PGC-1alpha regulates the neuromuscular junction program and ameliorates Duchenne muscular dystrophy. *Genes & development* **21**, 770-783
42. Selsby, J. T., Morine, K. J., Pendrak, K., Barton, E. R., and Sweeney, H. L. (2012) Rescue of dystrophic skeletal muscle by PGC-1α involves a fast to slow fiber type shift in the mdx mouse. *PloS one* **7**, e30063-e30063
43. Hollinger, K., Gardan-Salmon, D., Santana, C., Rice, D., Snella, E., and Selsby, J. T. (2013) Rescue of dystrophic skeletal muscle by PGC-1α involves restored expression of dystrophin-associated protein complex components and satellite cell signaling. *American journal of physiology. Regulatory, integrative and comparative physiology* **305**, R13-23
44. Chan, M. C., Rowe, G. C., Raghuram, S., Patten, I. S., Farrell, C., and Arany, Z. (2014) Post-natal induction of PGC-1alpha protects against severe muscle dystrophy independently of utrophin. *Skeletal Muscle* **4**, 2-2
45. Ryall, J. G. (2013) Metabolic reprogramming as a novel regulator of skeletal muscle development and regeneration. *FEBS J* **280**, 4004-4013
46. Perez-Schindler, J., Summermatter, S., Santos, G., Zorzato, F., and Handschin, C. (2013) The transcriptional coactivator PGC-1alpha is dispensable for chronic overload-induced

skeletal muscle hypertrophy and metabolic remodeling. *Proc Natl Acad Sci U S A* **110**, 20314-20319

47. Pasut, A., Jones, A. E., and Rudnicki, M. a. (2013) Isolation and culture of individual myofibers and their satellite cells from adult skeletal muscle. *Journal of visualized experiments : JoVE*, e50074-e50074
48. Rosenblatt, J. D., Lunt, A. I., Parry, D. J., and Partridge, T. A. (1995) Culturing satellite cells from living single muscle fiber explants. *In Vitro Cell Dev Biol Anim* **31**, 773-779
49. Handschin, C., Chin, S., Li, P., Liu, F., Maratos-Flier, E., Lebrasseur, N. K., Yan, Z., and Spiegelman, B. M. (2007) Skeletal muscle fiber-type switching, exercise intolerance, and myopathy in PGC-1alpha muscle-specific knock-out animals. *The Journal of biological chemistry* **282**, 30014-30021
50. Chan, M. C., and Arany, Z. (2014) The Many roles of PGC-1α in Muscle – Recent Developments. *Metabolism*, 1-11
51. Wenz, T., Rossi, S. G., Rotundo, R. L., Spiegelman, B. M., and Moraes, C. T. (2009) Increased muscle PGC-1alpha expression protects from sarcopenia and metabolic disease during aging. *Proc Natl Acad Sci U S A* **106**, 20405-20410
52. Cosgrove, B. D., Gilbert, P. M., Porpiglia, E., Mourkioti, F., Lee, S. P., Corbel, S. Y., Llewellyn, M. E., Delp, S. L., and Blau, H. M. (2014) Rejuvenation of the muscle stem cell population restores strength to injured aged muscles. *Nature Medicine* **20**, 255-264
53. Chargé, S. B. P., and Rudnicki, M. a. (2004) Cellular and molecular regulation of muscle regeneration. *Physiological reviews* **84**, 209-238
54. Sousa-Victor, P., Gutarra, S., Garcia-Prat, L., Rodriguez-Ubreva, J., Ortet, L., Ruiz-Bonilla, V., Jardi, M., Ballestar, E., Gonzalez, S., Serrano, A. L., Perdiguero, E., and Munoz-Canoves, P. (2014) Geriatric muscle stem cells switch reversible quiescence into senescence. *Nature* **506**, 316-321
55. McCroskery, S., Thomas, M., Maxwell, L., Sharma, M., and Kambadur, R. (2003) Myostatin negatively regulates satellite cell activation and self-renewal. *J Cell Biol* **162**, 1135-1147
56. Hikida, R. S. (2011) Aging changes in satellite cells and their functions. *Current aging science* **4**, 279-297
57. Kottlors, M., and Kirschner, J. (2010) Elevated satellite cell number in Duchenne muscular dystrophy. *Cell Tissue Res* **340**, 541-548
58. Turner, N. J., and Badylak, S. F. (2012) Regeneration of skeletal muscle. *Cell and tissue research* **347**, 759-774
59. Hawke, T. J., and Garry, D. J. (2001) Myogenic satellite cells: physiology to molecular biology. *J Appl Physiol (1985)* **91**, 534-551
60. Le Grand, F., Jones, A. E., Seale, V., Scime, A., and Rudnicki, M. A. (2009) Wnt7a activates the planar cell polarity pathway to drive the symmetric expansion of satellite stem cells. *Cell Stem Cell* **4**, 535-547
61. To, W. S., and Midwood, K. S. (2011) Plasma and cellular fibronectin: distinct and independent functions during tissue repair. *Fibrogenesis & tissue repair* **4**, 21-21
62. Mann, C. J., Perdiguero, E., Kharraz, Y., Aguilar, S., Pessina, P., Serrano, A. L., and Muñoz-Cánoves, P. (2011) Aberrant repair and fibrosis development in skeletal muscle. *Skeletal Muscle* **1**, 21-21
63. Chiquet-Ehrismann, R., and Chiquet, M. (2003) Tenascins: regulation and putative functions during pathological stress. *The Journal of pathology* **200**, 488-499

64. Ringelmann, B., Roder, C., Hallmann, R., Maley, M., Davies, M., Grounds, M., and Sorokin, L. (1999) Expression of laminin alpha1, alpha2, alpha4, and alpha5 chains, fibronectin, and tenascin-C in skeletal muscle of dystrophic 129ReJ dy/dy mice. *Exp Cell Res* **246**, 165-182
65. Allen, R. E., Sheehan, S. M., Taylor, R. G., Kendall, T. L., and Rice, G. M. (1995) Hepatocyte growth factor activates quiescent skeletal muscle satellite cells in vitro. *J Cell Physiol* **165**, 307-312
66. Tatsumi, R., Anderson, J. E., Nevoret, C. J., Halevy, O., and Allen, R. E. (1998) HGF/SF is present in normal adult skeletal muscle and is capable of activating satellite cells. *Dev Biol* **194**, 114-128
67. Li, Z. B., Kollias, H. D., and Wagner, K. R. (2008) Myostatin directly regulates skeletal muscle fibrosis. *The Journal of biological chemistry* **283**, 19371-19378
68. McPherron, A. C., Lawler, A. M., and Lee, S. J. (1997) Regulation of skeletal muscle mass in mice by a new TGF-beta superfamily member. *Nature* **387**, 83-90
69. Thomas, M., Langley, B., Berry, C., Sharma, M., Kirk, S., Bass, J., and Kambadur, R. (2000) Myostatin, a negative regulator of muscle growth, functions by inhibiting myoblast proliferation. *J Biol Chem* **275**, 40235-40243
70. Taylor, W. E., Bhasin, S., Artaza, J., Byhower, F., Azam, M., Willard, D. H., Jr., Kull, F. C., Jr., and Gonzalez-Cadavid, N. (2001) Myostatin inhibits cell proliferation and protein synthesis in C2C12 muscle cells. *Am J Physiol Endocrinol Metab* **280**, E221-228
71. Wagner, K. R., Liu, X., Chang, X., and Allen, R. E. (2005) Muscle regeneration in the prolonged absence of myostatin. *Proc Natl Acad Sci U S A* **102**, 2519-2524
72. McCroskery, S., Thomas, M., Platt, L., Hennebry, A., Nishimura, T., McLeay, L., Sharma, M., and Kambadur, R. (2005) Improved muscle healing through enhanced regeneration and reduced fibrosis in myostatin-null mice. *Journal of cell science* **118**, 3531-3541
73. Lee, S. J., Huynh, T. V., Lee, Y. S., Sebald, S. M., Wilcox-Adelman, S. A., Iwamori, N., Lepper, C., Matzuk, M. M., and Fan, C. M. (2012) Role of satellite cells versus myofibers in muscle hypertrophy induced by inhibition of the myostatin/activin signaling pathway. *Proc Natl Acad Sci U S A* **109**, E2353-2360
74. Wang, Q., and McPherron, A. C. (2012) Myostatin inhibition induces muscle fibre hypertrophy prior to satellite cell activation. *J Physiol* **590**, 2151-2165
75. Amthor, H., Otto, A., Vulin, A., Rochat, A., Dumonceaux, J., Garcia, L., Mouisel, E., Hourde, C., Macharia, R., Friedrichs, M., Relaix, F., Zammit, P. S., Matsakas, A., Patel, K., and Partridge, T. (2009) Muscle hypertrophy driven by myostatin blockade does not require stem/precursor-cell activity. *Proc Natl Acad Sci U S A* **106**, 7479-7484

7 PGC-1α can contribute to alleviating dystrophic phenotypes by increasing sarcolemma stability and improving membrane resealing (Project 3)

Authors: Ivana Dinulovic[1], Bilal Azakir[2], Christoph Handschin[1]

[1]Biozentrum, University of Basel, Klingelbergstrasse 50-70, 4056 Basel, Switzerland

[2]Neuromuscular Research Group, Departments of Neurology and Biomedicine, University Hospital and University of Basel, 4031 Basel, Switzerland

Running title: The role of PGC-1α in skeletal muscle membrane resealing

Key words: PGC-1α; membrane resealing; membrane stability

Corresponding author: Christoph Handschin (e-mail: christoph.handschinATunibas.ch)

Author contributions: experiments designed by I.D. and C.H; experiments performed by I.D. and B.A. (performed laser injuries); experiments analyzed by I.D and C.H; manuscript written by I.D and C.H

7.1 Abstract

Improper membrane resealing and compromised membrane stability are central to many muscular dystrophies. PGC-1α is the main driver of oxidative metabolism and provides beneficial effect in several dystrophic models with not fully elucidated mechanisms. However, its contribution to membrane resealing has not been investigated yet. Here we show that knock-down of PGC-1α in C2C12 myoblasts results in reduced resealing capacity after the laser injuries. We were able to identify several genes with the potential role in sarcolemma repair, which expression depended on the PGC-1α levels in cells and mice, with synaptotagmin VII (Syt7) being the most prominent one. Syt7 expression was massively induced *in vitro* after viral overexpression of PGC-1α, and its protein levels were increased in PGC-1α overexpressing transgenic mice. In addition, we show that eccentric exercise does not cause explicit damage to the sarcolemma of PGC-1α mKO mice, but fails to induce Integrin 7α (Itga7) expression, which stabilizes sarcolemma and makes it resistant to future injuries. Collectively, our results demonstrate that PGC-1α can positively affect membrane resealing process through upregulation of Syt7, and membrane stability through increased Itga7 levels upon exercise. These results provide further explanation to the beneficial effects of PGC-1α in muscular dystrophies.

7.2 Introduction

The repair of damaged cell membranes is an evolutionarily preserved process which represents an important strategy in the survival of many cell types. In mammalian organisms, it is of particular importance for damage-prone tissues, such as secreting epithelial cells of the mammary gland and mechanically active skeletal and cardiac muscle tissue (1). By counteracting the alternative fate, cell death, resealing reduces energy expenditure and prevents loss of irreplaceable cells types such as cardiomyocytes.

It was suggested that membranes can self-reseal in cases of minor injuries, closing the rupture by tending to the favorable low energy state (2), whereas tears bigger than 1μm require extracellular Ca^{2+} (1) in order to trigger membrane patch formation out of vesicles which will eventually close the opening in the membrane in a manner similar to exocytosis (3-6). In that respect, patching relies on intracellular sources of membranes, the origin of which remains undetermined but can include lysosomal (7), enlargeosomal (8) and other compartments. Recent research, however, suggests that apart from patching relaying on exocytosis (9), endocytosis (10) and membrane shedding (11) are alternative mechanisms observed in membrane resealing. Type and size of injury are probably determinants of which mechanism will take place (11). In addition to extracellular Ca^{2+}, intracellular Ca^{2+} seem to be necessary for the membrane repair as well (12).

Similarly, knowledge of the proteins necessary for successful resealing is still expanding and the majority of the work has been done on sea-urchin eggs and fibroblasts, and has not been confirmed for muscle cells. Although the rupture closing process is shared between different organisms, the discovery of muscle specific proteins implicated in resealing would not be surprising having in mind the importance of such a process for a tissue subject to contraction-induced damage. In general, proteins essential for vesicle fusion, transport, exocytosis, as well as Ca^{2+} sensors, have tended to attract most research attention. In that respect, soluble N-ethylmaleimide-sensitive factor attachment protein (SNAP) receptor (SNARE) proteins (synaptobrevins, SNAPs and syntaxins) (13), synaptotagmins (14), kinesins, myosins (13, 15), and cytoskeletal proteins (16), have proven to be important in the different cell types examined. In skeletal muscle, however, the situation is far less clear.

Inability to repair damage to the sarcolemma results in myofiber necrosis. This triggers the sequence of events known as regeneration, which rely on the participation of muscle stem cells to produce new muscle fibers. Constant tears in the muscle membrane induced by repetitive contractions will eventually result in a dystrophic phenotype characterized by inflammation, the presence of regenerating fibers and fibrosis. To date, the role of dysferlin (Dysf) (17), mitsugumin 53 (MG53) (9), annexin A6 (anxa6) (18) as well as intracellular Ca^{2+} channel mucolipin-1 (MCOLN1) (12) in resealing of skeletal muscle cells has been confirmed. Dysf is a structural protein localized in the sarcolemma and intracellular membrane compartments. Mutations in Dysf lead to limb-girdle muscular dystrophy type 2B (LGMD 2B) or Miyoshi myopathy. Upon injury, non-functional protein in mice leads to accumulation of vesicles below the sarcolemma, blocking the Ca^{2+} dependent fusion step and membrane repair (17). MG53, on the other hand, seems to function upstream of Dysf, leading to vesicle nucleation and transport to the injury site. This process has been shown to be dependent on changes in the oxidative state when the integrity of the muscle membrane is compromised (9). Beside these proteins, relevance has also been attributed to synaptogamin VII (Syt7) and annexin A1 (anxa1), whose importance in resealing has been confirmed in fibroblasts (14) and HeLa cells, respectively (19). Syt7 is a ubiquitously present Ca^{2+} sensor (20) similar to Dysf, while anxa1 is one of the binding partners of Dysf (21). In addition, it is important to note that mouse knock-out models for Dysf, MG53, MCOLN1 and Syt7 (22) exhibit myopathy phenotypes.

Peroxisome proliferator-activated receptor γ coactivator 1α (PGC-1α) is a master regulator of oxidative metabolism in various tissues, with additional tissue-specific functions (23). It induces mitochondrial biogenesis and respiration, concomitant with a reduction in reactive oxygen species (ROS) production (24). In skeletal muscle, PGC-1α overexpression leads to a fiber type switch favoring slow-twitch, oxidative fibers (25) as well as increased angiogenesis (26), resulting in a trained muscle phenotype. Although the majority of research has focused on the role of this coactivator in metabolism and its implications in type 2 diabetes, some has investigated the effects of PGC-1α in muscle dystrophies.

PGC-1α muscle specific knock-out mice were reported to exhibit a mild dystrophic phenotype, with increased inflammation and membrane permeability upon exercise (27). In addition, several studies focused on PGC-1α overexpression in *mdx* mice, a model of Duchenne

muscular dystrophy (DMD), and reported alleviation in dystrophy (28-31). *Mdx* mice are naturally occurring mice (32) with a mutation in dystrophin, a structural protein connecting the cytoskeleton with the extracellular matrix (ECM). Although the initial explanation for the muscle function improvement seen upon PGC-1α overexpression in *mdx* mice was increased expression of utrophin and remodeling of the neuromuscular junction, the net effect soon turned out to be far more complex. For example, we recently demonstrated that induced PGC-1α levels can improve initial phases of skeletal muscle regeneration, including macrophage attraction and necrotic tissue removal (see *Project 1*), and this effect can also contribute to the improvement of the dystrophy phenotype of *mdx*-PGC-1α mTG mice. In addition, positive effects on the dystrophic phenotype were also achieved when PGC-1α was induced in dystrophin-utrophin double knock-out mice, as well as with the induction of PGC-1β which does not affect the expression of neuromuscular junction (NMJ) genes (31). However, the possible role PGC-1α might have on membrane permeability has not been further explored.

Other forms of muscular dystrophies are also linked to the leaky membrane phenotype, dysferlinopathies being one of them. Dysf$^{-/-}$ mice do not exhibit reduced membrane stability as seen in *mdx* mice, but rather demonstrate an inability to repair membrane ruptures formed upon damage (17). However, increased membrane permeability is a hallmark of both dystrophies.

In addition to the previously published observations, we propose that PGC-1α can alleviate dystrophic phenotypes also by improving membrane resealing and stability. We demonstrate that knock-down (KD) of PGC-1α in C2C12 myoblasts results in impaired membrane resealing after laser injury. This is probably due to the differential expression of several genes that can contribute to the resealing process, the most prominent one being Syt7. Viral overexpression (OE) of PGC-1α in C2C12 myoblasts and myotubes massively induces Syt7 expression. In addition, Syt7 protein levels are increased in PGC-1α overexpressing mice. Previously published ChIP-Seq data revealed binding of PGC-1α to the Syt7 promoter, indicating a direct effect of this coactivator on the expression of Syt7 (33). In addition, this study indicates that eccentric exercise has little effect on Myf5-PGC-1α mKO mice compared to wild type (WT) control, proposing overall undisturbed membrane stability in the absence of PGC-1α. However, PGC-1α was necessary for the induction of Integrin 7α (Itga7) expression upon exercise, indicating a contribution to the protective state of the sarcolemma in cases of

subsequent damaging contractions. Collectively, our results suggest a direct effect of PGC-1α on membrane resealing, with potential therapeutic applications in the other forms of muscle dystrophies apart from DMD, one being dysferlinopathy.

7.3 Materials and methods

C2C12 cells and transduction

C2C12 myoblasts (MBs) were propagated in the growth media (DMEM, 10% fetal bovine serum (FBS), 1% antibiotic cocktail) in plastic dishes up until 80% confluency. For myotube (MT) formation, cells were allowed to proliferate until reaching confluency, after which differentiation was stimulated by changing the media to the differentiation media (DMEM, 2% horse serum (HS), 1% antibiotic cocktail) for 4 days.

For the overexpression experiments, adenoviruses expressing only GFP (Ad-GFP, control virus) or GFP and PGC-1α (Ad-GFP-PGC-1α virus) were added to cells in culture. For achieving downregulation, adenoviruses expressing GFP and scrambled siRNA (Ad-GFP-scrambled, control virus) or GFP and siRNA against PGC-1α (Ad-GFP-siPGC-1α virus) were used. MBs were transduced with the respective viruses for 2 days without reaching confluency, whereas MTs were transduced for 2 days, starting after 4 days of differentiation. Prior to collection, cells were washed twice with PBS, and then suspended in Trizol for RNA extraction or sucrose buffer for protein isolation.

Animals

Mice overexpressing PGC-1α (mTG) under the control of muscle creatine kinase (MCK) promoter have been described elsewhere (25). Myf5-Cre mouse line (The Jackson Laboratory, stock number 007845) or HSA-Cre mouse line were crossed with a PGC-1$\alpha^{flox/flox}$ mice in order to generate muscle specific PGC-1α knock-out models (mKO). All procedures involving mice were approved by the Swiss authorities. 8-12 week old male mice were used in this study.

RNA isolation, cDNA synthesis and qPCR

Total RNA was isolated from C2C12 MBs/MTs or tibialis anterior (TA)/gastrocnemius (Gastro) muscle using TRI Reagent (Sigma) and/or lysing matrix tubes (MP Biomedicals) following manufacturer's instructions. RNA concentration was measured with Nanodrop 1000 (Thermo Scientific), and 1μg of RNA was treated with DNase I (Invitrogen) and employed for cDNA synthesis using RT Superscript II (Invitrogen). Relative gene expressions were estimated

using the ΔΔCt method: qPCR reactions ran on a StepOne machine with SYBR green based detection, and TATA binding protein (TBP) expression was used for normalizations. A list of qPCR primers is provided in Table 1.

Protein isolation and Western Blotting (WB)

Total protein content was extracted from cells in culture or previously mechanically crushed TA/Gastro muscles using a sucrose buffer (50mM TrisHCl pH7.5, 1mM EDTA, 1mM EGTA, 1mM Na_3VO_4, 50mM NaF, 5mM $Na_4P_2O_7x10H_2O$, 250mM sucrose, 1mM DTT, 0.25% Nonident 40 supplemented with a protease inhibitor cocktail from Roche and a phosphatase inhibitor cocktail 2 from Sigma-Aldrich) and polytron homogenizer. Protein concentration was determined according to the Bradford method. Proteins were separated by sodium dodecyl sulfate polyacrylamide gel electrophoresis (SDS-PAGE) prior to electrotransfer on a polyvinylidene difluoride (PVDF) membrane. After blocking in 5% non-fat milk, the membranes were incubated with a primary antibody: α-tubulin (2125S, Cell Signaling), Dysf (VP-D503, Vector Laboratories), Syt7 (105173, Synaptic Systems), KifC3 (10125-2-AP, ProteinTech) or PGC-1α (AB3242, Millipore) overnight at 4˚C. The membranes were then washed and incubated with an HRP-conjugated secondary antibody for 1h at room temperature (RT). After washing, the membranes were incubated briefly with the ECL Substrate (Pierce) and the signal was detected on an X-ray film. The intensity of the protein bands of interest was quantified using the ImageJ software. α-tubulin was used as a loading control.

Laser injuries

For the laser injuries, C2C12 myoblasts were grown on poly-D lysine coated glass-bottom Nunc Lab-Tek chamber slides (VWR 734-2058) and transduced with Ad-GFP-siPGC-1α or control Ad-GFP-scramble virus 2 days prior to injuries. Ahead of the experiment, growth media was exchanged with 10mM HEPES buffer pH7.2 containing 1mM Ca^{2+} and 2.5μM FM 1-43 dye (Invitrogen T35356). The laser injuries were performed on a LSM510 microscope using a 40X objective, 1AU pinhole, maximal power of 405nm, 458nm, 488 nm lasers, and 4000 iterations on an area of 8.4μm x 8.4μm. As resealing incompetent and competent controls, untransduced C2C12 myoblasts in 10mM HEPES buffer pH7.2 containing 1mM EGTA and 1mM Ca^{2+} respectively, were used. Images were acquired every 4s for 4min after injury. One

image was obtained prior to injury as well. Calculations based on the FM 1-43 dye intensity changes in the injured and uninjured regions were performed using the Zen2009 software.

Downhill running (DHR) and Evans Blue dye (EBD) injections in mice

For the 3 hour (h) time point, mice were acclimatized to the open treadmill (Exer Treadmill Columbus Instruments) shortly before the run. Animals received intraperitoneal injection of Evans Blue solution (10x weight [g] in [µl] of 1% w/v solution of EBD in PBS) 16h prior to running. Mice ran for 1h on the open treadmill at -10˚ downhill at a speed alternating every 5min (7m/min and 12m/min). 3h after the run, mice were sacrificed, and muscles and blood were collected.

For the 7 day (d) time point, mice were not injected with EBD. They were acclimatized to the treadmill 15min for two days prior to the run. The running protocol was the same as for the 3h time point, and was executed for two consecutive days in order to boost the damaging effect of lengthening contractions. Blood was withdrawn from the tail vein prior to running, as well as right after the first and second day of running. 7d after the second run, mice were sacrificed and muscles and blood were collected.

For both experiments, TA, quadriceps (QU) and soleus (SOL) muscles were dissected and frozen either directly in N_2 (l) for the RNA isolation, or in isopenthane precooled in N_2 (l) for the histology.

Lactate dehydrogenase (LDH), creatine kinase (CK) and EBD level measurements

Plasma was isolated using Lithium heparin coated tubes (Microvette, Sarstedt) and used for measuring the enzymatic activity of LDH and CK based on spectrophotometric assays (Cobas c111, Roche).

Evans Blue staining was observed on the cross-sections of TA, QU and SOL muscles of animals subject to running, as well as sedentary ones. Muscles were cut on 8µm thick sections using a cryostat (Leica CM1950). Images were acquired using a Leica DM5000B microscope and a 20x objective. Quantification of the signal intensity coming from EBD was performed on

10 images from random parts of each QU section using ImageJ software. In addition, the presence of EB positive fibers was evaluated on TA, QU and SOL muscles.

Statistical Analysis

The experimental groups were compared using the Student's t-test, and $p \leq 0.05$ was considered significant.

7.4 Figures

Target	Fwd primer (5'-3')	Rev primer (5'-3')
Anxa1	TCA GAA TTA CGG AAA GTA CAG TCA ACA	TCA ATG TCA CCC TTC AGT TCC A
CycS	GCA AGC ATA AGA CTG GAC CAA A	TTG TTG GCA TCT GTG TAA GAG AAT C
Dysf	CAT GCC CCC GAG ACA ATT C	GCC AAA TGC TCG GAC GAT AT
ERRα	GCA GGG CAG TGG GAA GCT A	CCT CTT GAA GAA GGC TTT GCA
Glut4	GAT GAG AAA CGG AAG TTG GAG AGA	GCA CCA CTG CGA TGA TCA GA
Itga7	CTG CTG TGG AAG CTG GGA TTC	CTC CTC CTT GAA CTG CTG TCG
KifC3	AGG CAT GCT GTC GGA ACT G	GCC AGC CGG TCC GTT T
MG53	GGC CGC AGG CTC TAA GC	CGC CAA ACC CTC CAC AAG
PGC-1α ex2	TGATGTGAATGACTTGGATACAGACA	CGTCATTGTTGTACTGGTTGGATATG
PGC-1α ex3-5	AGCCGTGACCACTGACAACGAG	GCTGCATGGTTCTGAGTGCTAAG
Rab27b	CAT GAA GAG AAT GGA AAA GTG TGT AGA	CAT CCA GCT TTC CAG AAT TTC CT
Rab3a	TCC TCT TCC GCT ACG CAG AT	ATG CCA ACG GTG CTG ACA
Sytl2	GAG CGA TGA CAG AGA AAC AGA C	AAG ATT GGT TAA TGA GCT GGG G
Syt7	CCA GAC GCC ACA CGA TGA G	ACG AGG TCC GAG ACA GAG GAA
TBP	TGCTGTTGGTGATTGTTGGT	CTGGCTTGTGTGGGAAAGAT
Vamp1	TGA ATG TGG ACA AGG TCT TGG A	GCG TCA GCC CGG TCA TC

Table 1. List of qPCR primers

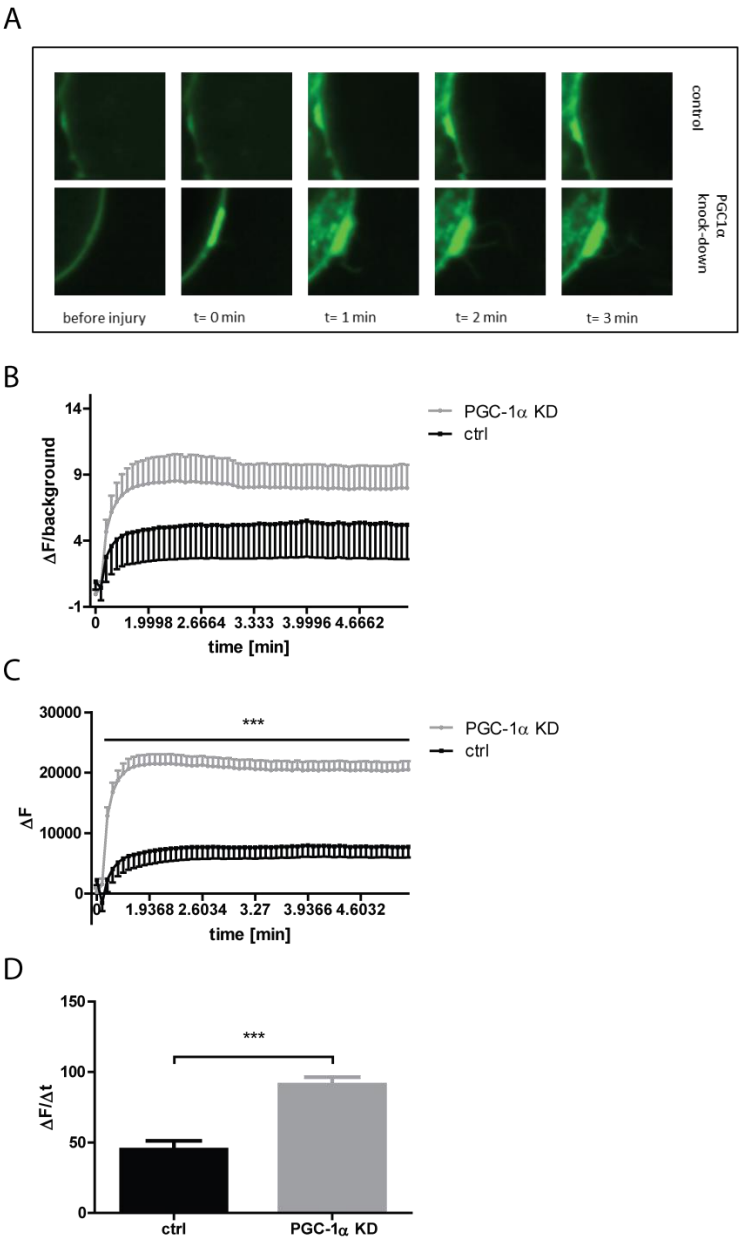

Fig 1. Impaired membrane resealing after knock-down (KD) of PGC-1α
A) representative images from the live cell imaging; C2C12 MBs transduced with Ad-GFP-scrambled (control) do not accumulate excessive FM 1-43 dye in the membranes due to successful resealing; C2C12 transduced with Ad-GFP-siPGC-1α (PGC-1α KD) cannot reseal and gather increasing quantity of dye over time B) ΔF normalized additionally to the GFP fluorescence before laser injury and plotted over time C) Intensity of the fluorescent signal normalized to the uninjured part of the membrane (ΔF) over time D) ΔF between the two time points (ΔΔF); Values are plotted as AV+/-SEM; n=13 (control cells), n=28 (PGC-1α KD cells); * p≤0.05, ** p≤0.01, *** p≤0.001

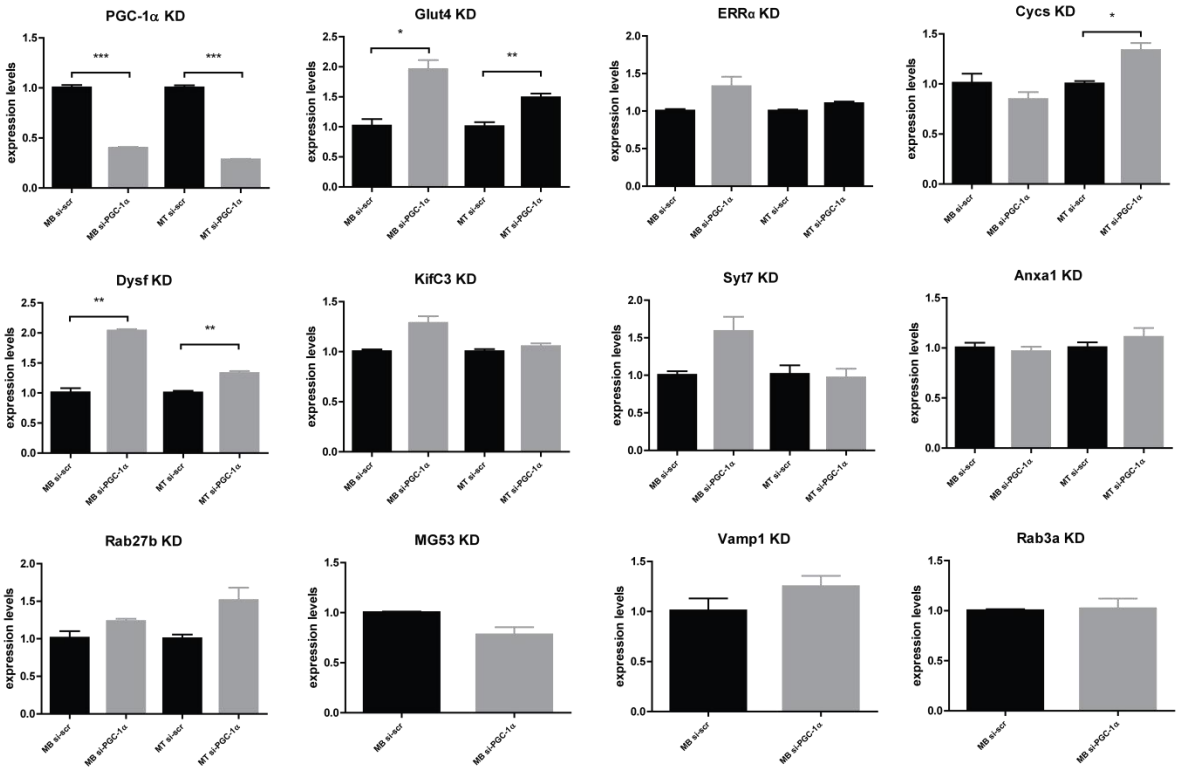

Fig 2. Relative mRNA expression levels upon KD of PGC-1α in C2C12 MBs and MTs
Expression levels in MBs and MTs transduced with Ad-GFP-siPGC-1α are compared to the MBs and MTs transduced with Ad-GFP-scrambled respectively. TBP was used for the normalization of the data; Values are plotted as AV+/-SEM; n=1-3 per group

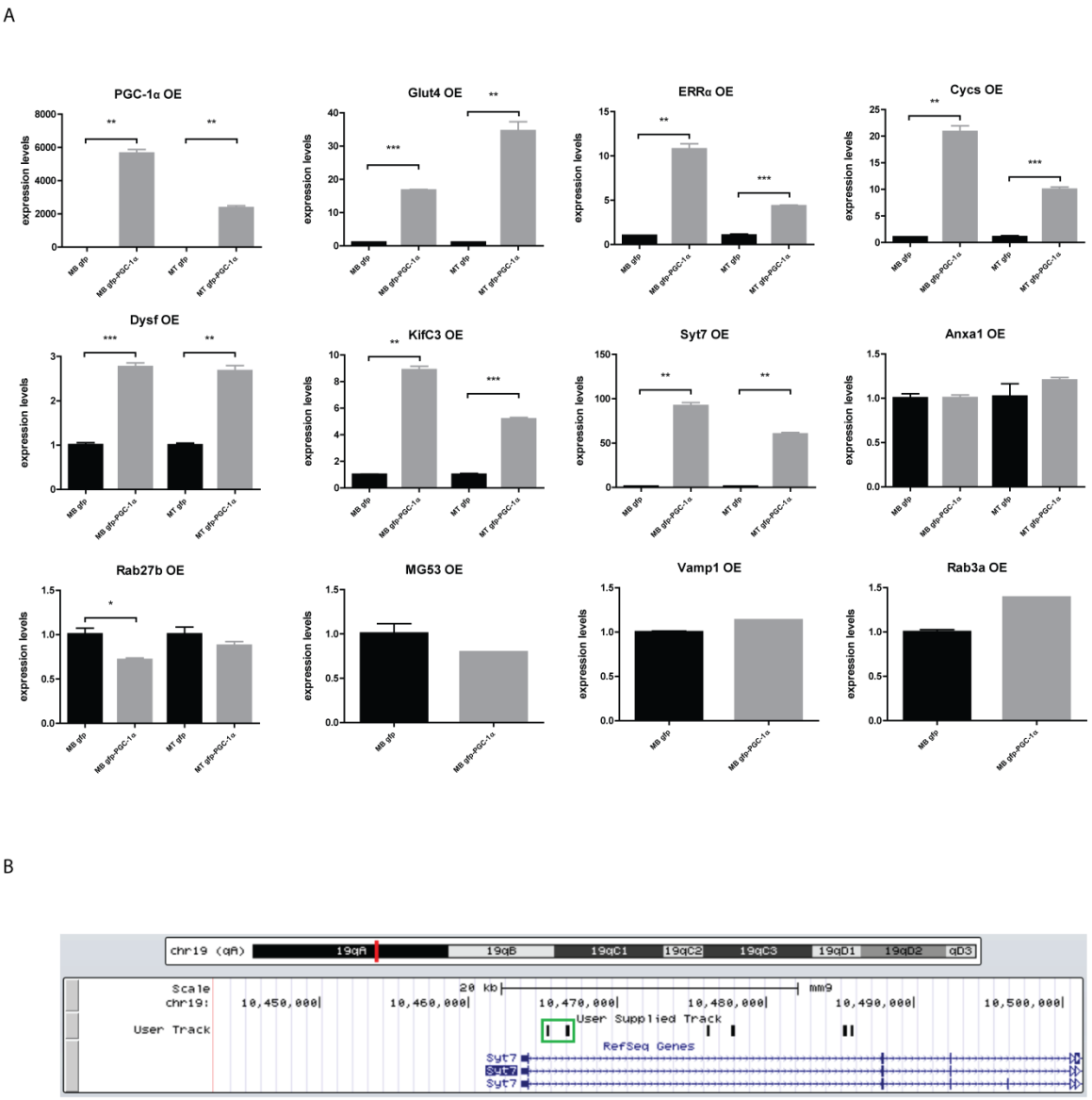

Fig 3. Relative mRNA expression levels upon overexpression (OE) of PGC-1α in C2C12 MBs and MTs, and PGC-1α ChIP-Seq peaks around Syt7 promoter

A) Expression levels in MBs and MTs transduced with Ad-GFP-PGC-1α are compared to the MBs and MTs transduced with Ad-GFP respectively. TBP expression levels were used for the normalization of the data; Values are plotted as AV+/-SEM; n=1-3 per group; B) PGC-1α ChIP-Seq peaks (in green box) located within ±10kb region around transcription start site (TSS) in Syt7

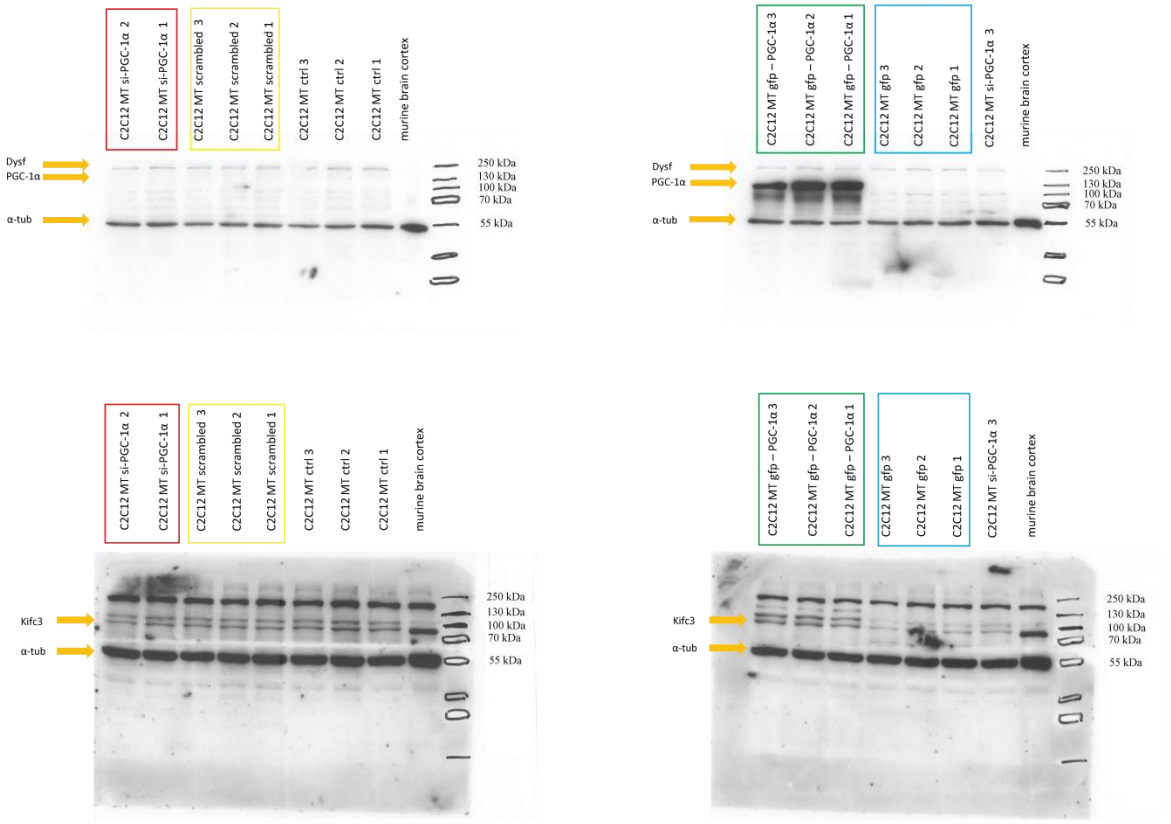

Fig 4. WB on C2C12 MTs with KD or OE of PGC-1α
Band intensity for any of the proteins tested is not changed upon KD of PGC-1α (Ad-GFP-siPGC-1α in red box vs. Ad-GFP-scrambled in yellow box) including PGC-1α itself which levels were below detection limit; Upon OE of PGC-1α (Ad-GFP-PGC-1α in green box vs. Ad-GFP in blue box), Dysf levels stayed unchanged, whereas PGC-1α and KifC3 levels were increased; α-tubulin served as a loading control

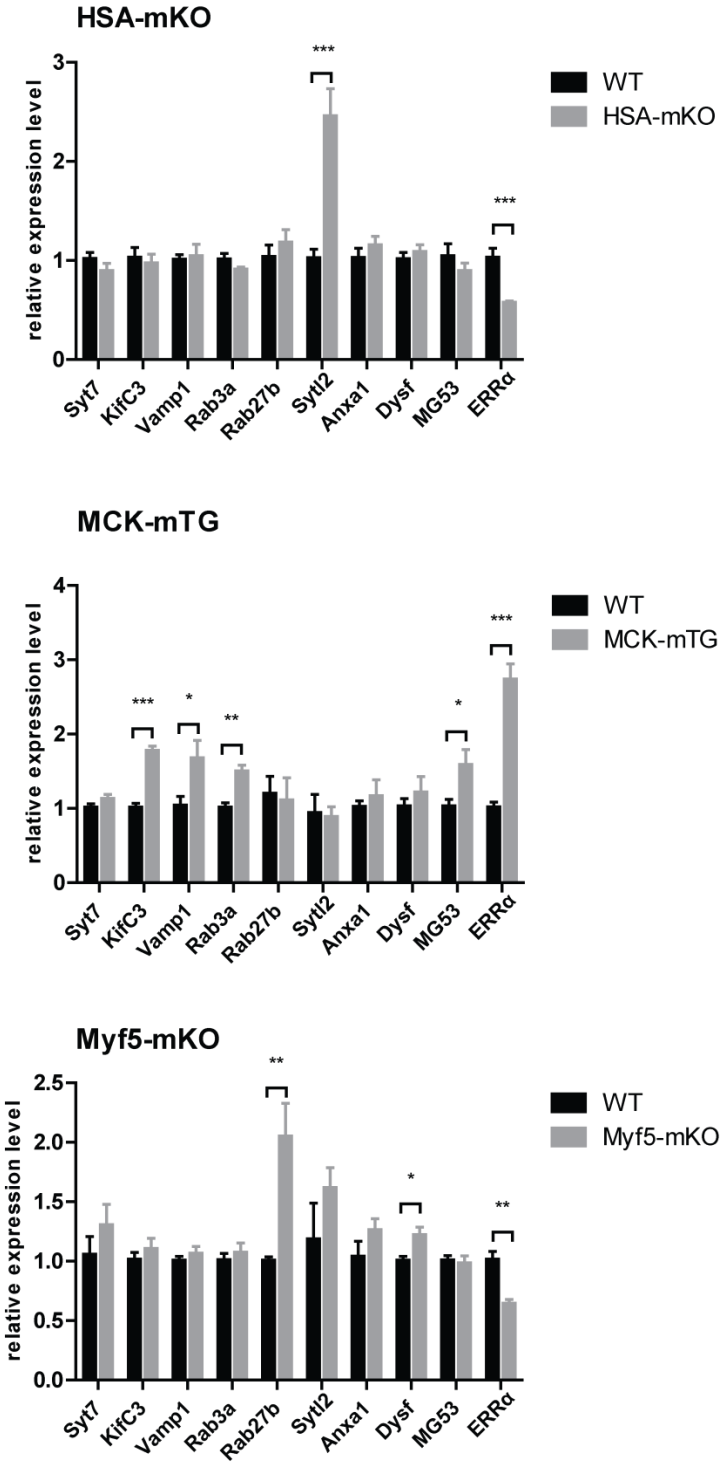

Fig 5. Relative mRNA expression levels in TA muscles of MCK-mTG, Myf5-mKO and HSA-mKO mice: Expression levels were compared to control littermate mice (WT). TBP expression levels were used for the normalization of the data; Values are plotted as AV+/-SEM; n=6 per group

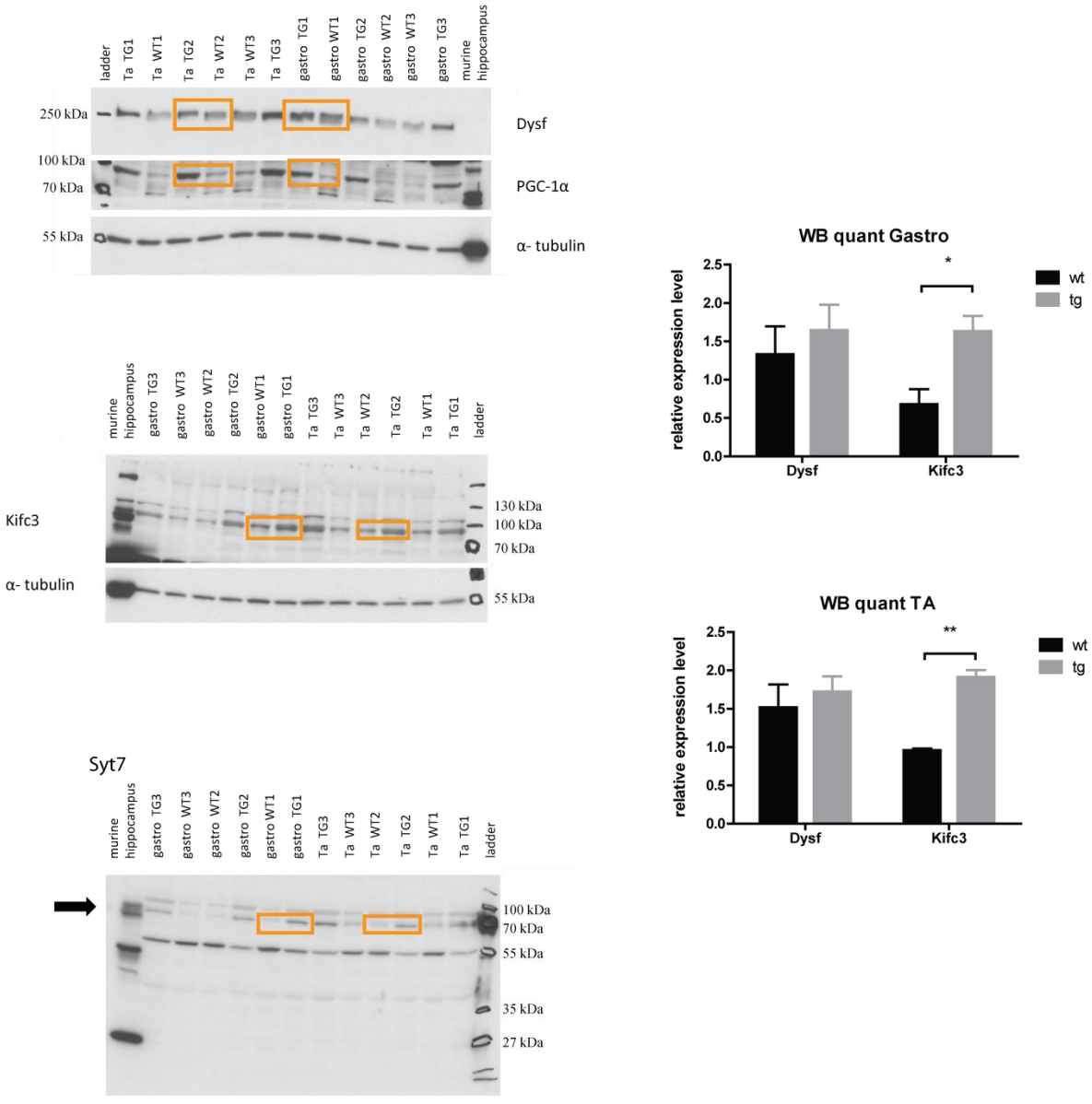

Fig 6. WB on TA and Gastro muscles of MCK-mTG mice:
Increase in Syt7 levels at band at ~70kDa (arrow) and PGC-1α levels at band ~90kDa in MCK-mTG are obvious and therefore not quantified. Levels of Dysf and Kifc3 were quantified using ImageJ software and presented as AV+/-SEM; representative bands for WT and TG for two muscles are marked in orange for all proteins; n=3 per group; * p≤0.05, ** p≤0.01, *** p≤0.001

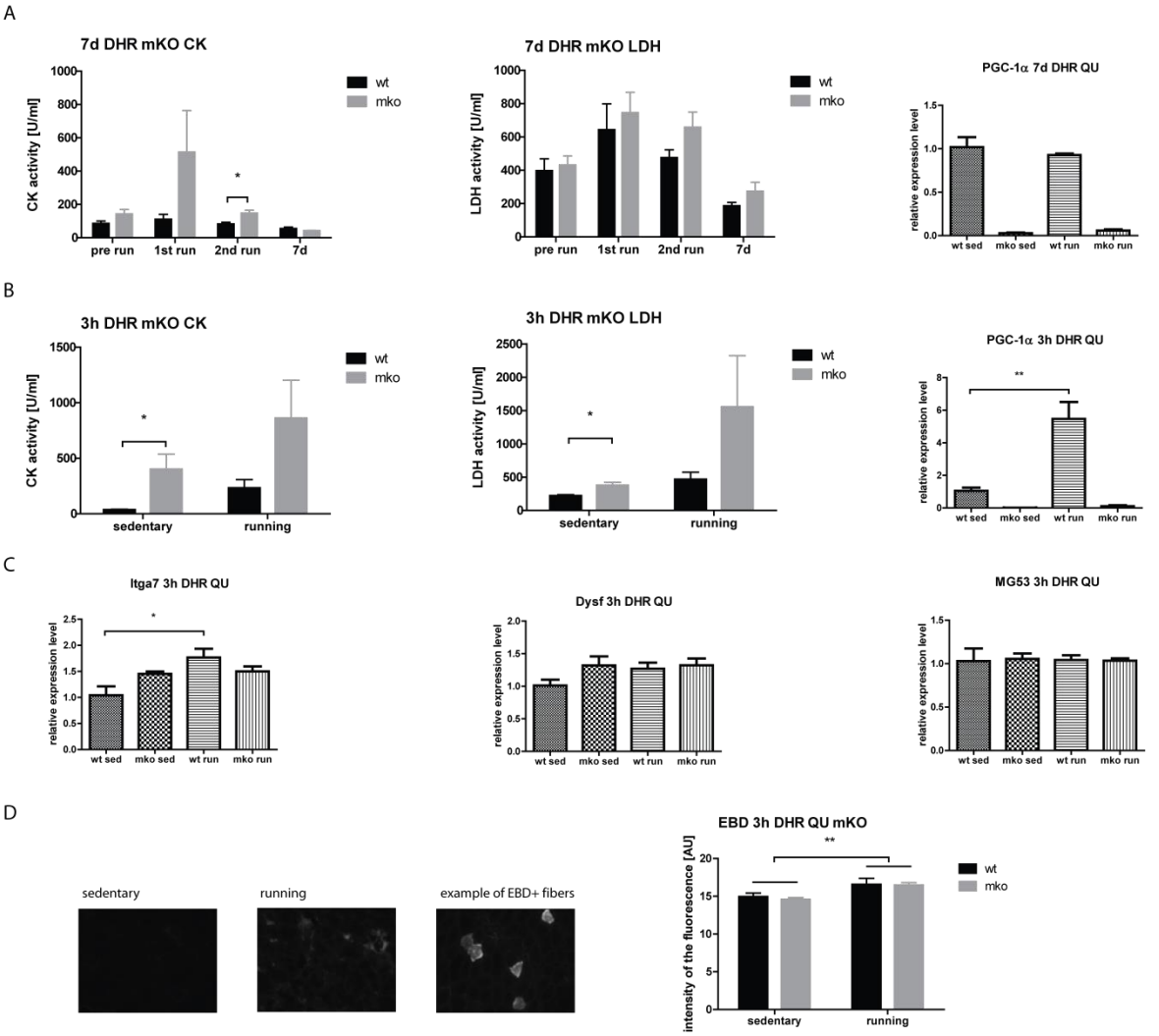

Fig 7. Injury after DHR in Myf5-mKO mice:
A) CK and LDH levels were measured before running, right after the first and second run, as well as 7 days after the second run. Relative mRNA level of PGC-1α 7 days after the exercise compared to sedentary WT littermates; B) CK and LDH enzymatic activity, and relative mRNA level of PGC-1α, in sedentary animals and 3h after the DHR; C) Relative mRNA expression levels 3h after the exercise compared to sedentary WT littermates; D) EBD fluorescence intensity in QU muscles of sedentary and running animals including representative images. Values are ploted as AV+/-SEM; n=4-6 per group. For the CK and LDH activity, as well as for EBD intensity, we were interested in the difference between genotypes and not the effect of exercise on the genotype. For the gene expression measurements however, we were interested in the effect of exercise, not the difference between genotypes.

7.5 Results

PGC-1α is necessary for proper resealing in myoblasts

Membrane resealing is an essential process in contractile tissues, where it repairs cells otherwise destined for necrosis (34). Proof for this can be found in dystrophies that develop over time in cases of diminished ability to reseal the sarcolemma, as seen in patients and mouse models with mutations in genes such as Dysf (17) or Syt7 (22). In order to explore the effects of PGC-1α in membrane resealing, we used C2C12 myoblasts transduced with viruses expressing scrambled siRNA (control) or siRNA against PGC-1α (PGC-1α KD). Successfully transduced myoblasts (GFP expressing) were subject to laser injury on a defined part of the membrane, and the effect of the resealing was observed over time by measuring the fluorescence intensity of FM 1-43 dye (Fig 1). Although the experiment was hindered by the overlapping emission spectra of GFP and FM 1-43 dye, bleaching of the GFP signal at the time of the injury made it possible to differentiate between the GFP and FM 1-43 fluorescence. Assessing the changes in fluorescence intensity between two time points in the course of resealing permitted the detection of a marked difference between control and PGC-1α KD myoblasts (Fig 1D). These results indicate that lack of PGC-1α reduces the ability of myoblasts to close the rupture in their membranes.

Syt7 represents the most promising target gene implicated in resealing and regulated by PGC-1α

Our approach to finding possible genes responsible for the effect seen in resealing was to compare existing microarray data on C2C12 myotubes transduced with Ad-GFP-PGC-1α and the literature on membrane resealing and exocytosis (33). In this way, selected potentially interesting genes that we wanted to test further. Based on this approach, we could speculate that knocking-down PGC-1α might induce the opposite effect of the one observed in the microarray data of PGC-1α overexpression, and therefore lower the levels of certain proteins necessary for closing membrane ruptures. First, we decided to check the expression of the shortlisted genes on PGC-1α KD myoblasts and myotubes (Fig 2). Although the laser injury experiment was performed only on myoblasts due to technical limitations (e.g. difficulty to differentiate cells on glass), the expression measurements were done in myotubes as well in order to increase the experimental

window when knocking-down PGC-1α, given the higher expression of PGC-1α in myotubes compared to myoblasts (35). To our surprise, there was no decrease in the expression of any of the tested genes, and some even underwent a slight increase with KD of PGC-1α (Fig 2). However, KD of 60%-70% was not enough to lower the expression of glucose transporter type 4 (Glut4), estrogen-related receptor α (ERRα) and cytochrome c (CycS) (Fig 2) – known downstream target genes of PGC-1α (23). Therefore, we found this system to be suboptimal for testing the outcome of PGC-1α KD on changes in gene expression.

Next, we wanted to test the effect of PGC-1α overexpression (OE) in myoblasts and myotubes, and verify the increased expression of at least the genes found in the microarray data (Fig 3). Some genes, such as synaptobrevin 1 (Vamp1) and Ras-associated protein Rab-3A (Rab3a), did not corroborate our microarray data and demonstrate an increase in expression. However, the most promising finding was the induction of kinesin family member C3 (KifC3) and Syt7 in PGC-1α OE myoblasts and myotubes (Fig 3A). The latter was in line with the ChIP-Seq PGC-1α peaks found in the Syt7 promoter region (Fig 3B). Importantly, massive overexpression of PGC-1α also led to a rise in the expression of the abovementioned downstream target genes (Fig 3A).

To test this further, we checked the expression of several genes on the protein level as well, first using C2C12 myotubes with KD and OE of PGC-1α (Fig 4). Western Blot data revealed no changes in PGC-1α levels after KD, as well as no changes in Dysf and KifC3 levels, in line with the qPCR results (Fig 4). On the other hand, OE of PGC-1α led to considerable upregulation of PGC-1α on the protein level, followed by unchanged expression of Dysf and increased levels of KifC3, again confirming the qPCR data (Fig 4).

Next, we decided to move to an *in vivo* system, and measure the mRNA expression of the aforementioned genes in our mouse models (Fig 5). For this, we used TA muscles of transgenic mice which overexpress PGC-1α in the myotube stage (MCK-mTG) and two knock-out lines which lack PGC-1α from the myoblast or myotube stage (Myf5-mKO and HSA-mKO). ERRα was used as a control gene in these measurements, in order to confirm the effect of PGC-1α overexpression or knock-out (Fig 5). We observed upregulation of KifC3 in MCK-mTG, albeit no downregulation in either of the KO mouse models (Fig 5). Additionally, we were able to detect a small increase in Vamp1, Rab3a and MG53 in MCK-mTG mice, which were *in vitro*

tested only in the myoblast stage. Synaptotagmin-like 2 (Sytl2) and Ras-related protein Rab-27B (Rab27b) were increased in HSA-mKO and Myf5-mKO mice respectively (Fig 5). They belong to the protein families implicated in vesicle trafficking and therefore could play a role in resealing (36). Dysf was also expressed at higher levels in Myf5-mKO and this could represent a compensatory effect for impaired resealing (Fig 5). Interestingly, we did not observe a difference in the expression of Syt7 in any of the mice tested (Fig 5). This was not in line with our findings *in vitro*, where we saw massive upregulation of this gene with PGC-1α OE (Fig 3).

In order to approach this question from a different angle, we performed western blot on TA and Gastro muscles from MCK-mTG mice (Fig 6). We confirmed no difference in Dysf expression, as well as upregulation of KifC3 in mTG mice. In addition, we observed the presence of several isoforms of Syt7. Interestingly, the isoforms at ~70kDa and ~55kDa displayed opposite expression patterns within each genotype, as well as between the genotypes (Fig 6). In addition, we detected different Syt7 isoforms between hypocampus and muscle tissues. However, since the main Syt7 isoform was shown to be Syt7α (37) running above 66kDa in muscle tissue (22), we focused our attention on this band (marked with an arrow in Fig 6) in order to assess the difference in expression levels between the genotypes. Indeed, we could clearly observe an increase in the expression of the main Syt7 isoform in mTG compared to WT muscles (Fig 6).

Eccentric exercise does not cause overt damage to PGC-1α KO mice, indicating uncompromised sarcolemma integrity

Previous studies demonstrated reduced exercise capacity accompanied by increased damage to muscle fibers in PGC-1α mKO mice (27). This phenotype resembles the dystrophic phenotype observed in *mdx* mice, albeit in a much milder form. In order to test for the same effect in our Myf5-mKO mice, we first subjected the mice to one bout of downhill running and evaluated the muscle damage by measuring the enzymatic activity of LDH and CK in the plasma of the mice 3h after the run (Fig 7B). In addition, we assessed membrane permeability by looking at the Evans Blue dye (EBD) accumulation in the muscle fibers due to eccentric exercise (Fig 7D). By measuring the levels of CK and LDH as well as EBD fluorescence 3h post exercise, we were able to detect only tendencies towards higher damage in the mKO mice (Fig 7B and

7D). EBD positive fibers were rare and scattered between the genotypes regardless of exercise status (sedentary vs. running), and therefore were not quantified. Damage levels tended to be higher in the basal state in mKO mice, without exercise, although this was dependent on the variability within the group of animals of the same genotype (Fig 7B). Hence, we did not notice the increased damage at the basal level when we performed an additional experiment with two bouts of running on two consecutive days and measured CK and LDH activity at several time points in the course of the experiment (Fig 7A). However, in this experimental setup, we observed increased CK activity in mKO mice after the second bout of DHR.

PGC-1α levels are known to increase with exercise (38, 39). We measured the difference in PGC-1α mRNA expression levels prior to and after DHR, and detected an increase in the WT running group 3h after the exercise (Fig 7B). The same increase was not detected in the mKO group. This boost in expression returned to the control levels 7 days after the run (Fig 7A). In order to examine a potential correlation between the increase in PGC-1α and membrane stability and resealing, we measured expression of genes important for sarcolemma resealing – Dysf and MG53. Their expression stayed unchanged in both genotypes 3h after exercise (Fig 7C). Additionally, we measured the expression of Itga7, a protein know to be regulated by exercise and important for membrane stability and muscle protection against injury (40, 41). We were able to detect an increase in Itga7 expression 3h after DHR in the WT running mice (Fig 7C), which was in line with a previously published study (41). However, Itga7 levels were unchanged in the mKO running mice (Fig 7C). These data suggest that PGC-1α expression in mice is necessary to induce a rise in Itga7 levels upon exercise, which is known to provide protection to the muscle membrane.

7.6 Discussion

Membrane stability and resealing are important determinants in skeletal muscle homeostasis. Mutations in several genes have been shown to compromise sarcolemma integrity and therefore result in repeated degeneration/regeneration cycles, leading eventually to dystrophic conditions (42). It has been repeatedly demonstrated that PGC-1α relieves dystrophy in *mdx* mice (28-31), with several possible lines of explanations for the mechanism – from increased utrophin levels to increase in regenerative capacity. However, thus far, the role PGC-1α might play directly in membrane resealing and stability has not been closely examined.

Here we show that PGC-1α is necessary for sarcolemma resealing after laser injury in C2C12 myoblasts. Although no reduction in genes implicated in resealing was observed with the KD of PGC-1α, higher Syt7 and KifC3 expression was detected in response to PGC-1α overexpression. In addition, KifC3 levels were increased in muscles of MCK-mTG mice on both transcript and protein levels. KifC3 belongs to the kinesin family of proteins, whose function is to transport cargo along the microtubules primarily in the anterograde manner (43). The importance of kinesins in membrane resealing has been demonstrated in sea-urchin eggs and fibroblasts (13, 15). However, the role of these molecular motors, and especially KifC3, in sarcolemma resealing has not been proven. Therefore, we can merely speculate that increased expression of this transporter might be beneficial in terms of membrane repair in skeletal muscle, although KifC3 was shown to be involved in retrograde transport in kidney cells (44).

The more interesting finding concerns Syt7, a ubiquitously expressed Ca^{2+} sensing protein implicated in lysosomal exocytosis (45). Its relevance in fibroblast resealing and myositis in mice have been previously shown (22). Interestingly, increased Syt7 expression was detected in C2C12 cells with OE of PGC-1α, but not in mTG mice. One possible explanation for this might come from the differential expression of various isoforms. Syt7 has several isoforms, whose presence and expression varies between tissues (37). These isoforms can also be variably expressed between cells in culture and adult muscle. Therefore, in case we indeed have differential and opposite expression of several isoforms, the net effect can still be no change in the total mRNA levels. Importantly, the Syt7 specific primers we used in this study recognize all three isoforms of Syt7, detecting the total expression levels of the gene transcripts.

Hence, we decided to assess the Syt7 expression at the protein level and evaluate the possible presence of different isoforms. We observed multiple bands in murine hypocampus sample and muscle samples that differed between the two tissues. Previous research on Syt7 isoforms revealed the Syt7α isoform as the main one (37). This isoform runs at a size higher than 66kDa in the muscle samples (22). With this in mind, we can observe an increased quantity of Syt7 in mTG mice compared to WT controls (band at ~70kDa). It is interesting to mention that the several bands in our blots, possibly representing several isoforms of Syt7, are regulated in the opposite direction between genotypes, probably leading to unchanged protein levels overall. This is consistent with our qPCR data, where we detected unchanged transcript levels for all Syt7 isoforms combined. Additionally, ChIP-Seq data demonstrated PGC-1α binding to the Syt7 promoter, suggesting direct regulation in expression of Syt7 by PGC-1α (33).

In order to examine the effect of membrane resealing *in vivo*, we performed a DHR experiment on the Myf5-mKO mice. Previous work on PGC-1α mKO mice suggests presence of a mild myopathy phenotype, accompanied by a lower tolerance to contraction-induced damage (27). Our data confirm these observations, as a modest increase in CK is observed in the plasma of mKO mice compared to WT after DHR.

However, it is worth mentioning that DHR and laser injures evaluate different parameters of the sarcolemma homeostasis. While both lead to a leaky membrane, essentially different processes might lie at their core (46). This is perhaps best demonstrated by comparing the response of *mdx* and Dysf$^{-/-}$ mice to laser injuries and DHR. Both mouse models exhibit dystrophy, which is associated with increased membrane permeability. However, while fibers from Dysf$^{-/-}$ mice are not able to repair membrane ruptures after laser injuries, fibers from *mdx* mice are (17). On the other hand, *mdx* mice sustain profound damage to their muscle fibers after DHR, while Dysf$^{-/-}$ mice respond to it in a rather mild manner, similarly to PGC-1α mKO mice (17). Therefore, the concepts of membrane stability, which is reduced in *mdx* mice, and membrane repair, which is compromised in Dysf$^{-/-}$, should be differentiated.

Some research proposes that the increased leakiness of the sarcolemma observed in the *mdx* model after exercise could be due to higher Ca^{2+} entry into the fibers through stretch-activated channels, which then boosts ROS production leading to membrane lipid peroxidation (46). Essentially, this suggests that membrane tears are not responsible for the injury observed

after the DHR, and therefore do not lead to severe damage in the mouse models for impaired membrane resealing. This would in turn indicate, based on our results, that PGC-1α might be indeed directly involved in the membrane repair process.

Contrary to that, the beneficial effects observed with PGC-1α overexpression in *mdx* mice might be due to multiple factors as previously suggested, one of them possibly being decrease in ROS production which would reduce membrane permeability. In addition, our results indicate that increase in Itga7 after exercise is dependent on PGC-1α expression. Itga7 is a structural glycoprotein which connects the ECM with the cytoskeleton through laminin-actin linkage (47). Since Itga7 expression protects muscle from damage by stabilizing the sarcolemma (40), and lack of it induces injury after the DHR (41), we can speculate that the alleviation in the dystrophic phenotype seen in *mdx*-PGC-1α mTG mice can be also due to increase in Itga7 expression. Interestingly, we observed a slight increase both in Dysf and Itga7 expression at the basal level in Myf5-mKO mice. This could be a compensatory mechanism, similar to what has been recently observed for Dysf in DMD (48) and for other proteins implicated in membrane resealing in muscular dystrophy patients (49).

Therefore, future work should try to further delineate the role of PGC-1α in membrane stability and repair, and confirm its effect in resealing by determining if increasing the expression of PGC-1α in Dysf$^{-/-}$ mice can rescue the overall phenotype, especially in terms of membrane repair after laser injury. Nevertheless, our results support the therapeutic potential of PGC-1α in muscle dystrophies.

7.7 References

1. McNeil, P. L., and Kirchhausen, T. (2005) An emergency response team for membrane repair. *Nat Rev Mol Cell Biol* **6**, 499-505
2. Parsegian, V. A., Rand, R. P., and Gingell, D. (1984) Lessons for the study of membrane fusion from membrane interactions in phospholipid systems. *Ciba Found Symp* **103**, 9-27
3. Miyake, K., and McNeil, P. L. (1995) Vesicle accumulation and exocytosis at sites of plasma membrane disruption. *J Cell Biol* **131**, 1737-1745
4. McNeil, P. L., Vogel, S. S., Miyake, K., and Terasaki, M. (2000) Patching plasma membrane disruptions with cytoplasmic membrane. *J Cell Sci* **113 (Pt 11)**, 1891-1902
5. McNeil, P. L., and Baker, M. M. (2001) Cell surface events during resealing visualized by scanning-electron microscopy. *Cell Tissue Res* **304**, 141-146
6. Bi, G. Q., Alderton, J. M., and Steinhardt, R. A. (1995) Calcium-regulated exocytosis is required for cell membrane resealing. *J Cell Biol* **131**, 1747-1758
7. Andrews, N. W. (1995) Lysosome recruitment during host cell invasion by Trypanosoma cruzi. *Trends Cell Biol* **5**, 133-137
8. Cerny, J., Feng, Y., Yu, A., Miyake, K., Borgonovo, B., Klumperman, J., Meldolesi, J., McNeil, P. L., and Kirchhausen, T. (2004) The small chemical vacuolin-1 inhibits Ca(2+)-dependent lysosomal exocytosis but not cell resealing. *EMBO Rep* **5**, 883-888
9. Cai, C., Masumiya, H., Weisleder, N., Matsuda, N., Nishi, M., Hwang, M., Ko, J.-K., Lin, P., Thornton, A., Zhao, X., Pan, Z., Komazaki, S., Brotto, M., Takeshima, H., and Ma, J. (2009) MG53 nucleates assembly of cell membrane repair machinery. *Nature cell biology* **11**, 56-64
10. Idone, V., Tam, C., Goss, J. W., Toomre, D., Pypaert, M., and Andrews, N. W. (2008) Repair of injured plasma membrane by rapid Ca2+-dependent endocytosis. *J Cell Biol* **180**, 905-914
11. Jimenez, A. J., Maiuri, P., Lafaurie-Janvore, J., Divoux, S., Piel, M., and Perez, F. (2014) ESCRT Machinery Is Required for Plasma Membrane Repair. *Science (New York, N.Y.)*
12. Cheng, X., Zhang, X., Gao, Q., Ali Samie, M., Azar, M., Tsang, W. L., Dong, L., Sahoo, N., Li, X., Zhuo, Y., Garrity, A. G., Wang, X., Ferrer, M., Dowling, J., Xu, L., Han, R., and Xu, H. (2014) The intracellular Ca channel MCOLN1 is required for sarcolemma repair to prevent muscular dystrophy. *Nat Med*
13. Steinhardt, R. a., Bi, G., and Alderton, J. M. (1994) Cell membrane resealing by a vesicular mechanism similar to neurotransmitter release. *Science (New York, N.Y.)* **263**, 390-393
14. Reddy, A., Caler, E. V., and Andrews, N. W. (2001) Plasma membrane repair is mediated by Ca(2+)-regulated exocytosis of lysosomes. *Cell* **106**, 157-169
15. Bi, G. Q., Morris, R. L., Liao, G., Alderton, J. M., Scholey, J. M., and Steinhardt, R. a. (1997) Kinesin- and myosin-driven steps of vesicle recruitment for Ca2+-regulated exocytosis. *The Journal of cell biology* **138**, 999-1008
16. Mandato, C. A., and Bement, W. M. (2001) Contraction and polymerization cooperate to assemble and close actomyosin rings around Xenopus oocyte wounds. *J Cell Biol* **154**, 785-797

17. Bansal, D., Miyake, K., Vogel, S. S., Groh, S., Chen, C. C., Williamson, R., McNeil, P. L., and Campbell, K. P. (2003) Defective membrane repair in dysferlin-deficient muscular dystrophy. *Nature* **423**, 168-172
18. Swaggart, K. a., Demonbreun, A. R., Vo, A. H., Swanson, K. E., Kim, E. Y., Fahrenbach, J. P., Holley-Cuthrell, J., Eskin, A., Chen, Z., Squire, K., Heydemann, A., Palmer, A. a., Nelson, S. F., and McNally, E. M. (2014) Annexin A6 modifies muscular dystrophy by mediating sarcolemmal repair. *Proceedings of the National Academy of Sciences of the United States of America*, 1-6
19. McNeil, A. K., Rescher, U., Gerke, V., and McNeil, P. L. (2006) Requirement for annexin A1 in plasma membrane repair. *J Biol Chem* **281**, 35202-35207
20. Ullrich, B., and Sudhof, T. C. (1995) Differential distributions of novel synaptotagmins: comparison to synapsins. *Neuropharmacology* **34**, 1371-1377
21. Lennon, N. J., Kho, A., Bacskai, B. J., Perlmutter, S. L., Hyman, B. T., and Brown, R. H., Jr. (2003) Dysferlin interacts with annexins A1 and A2 and mediates sarcolemmal wound-healing. *J Biol Chem* **278**, 50466-50473
22. Chakrabarti, S., Kobayashi, K. S., Flavell, R. a., Marks, C. B., Miyake, K., Liston, D. R., Fowler, K. T., Gorelick, F. S., and Andrews, N. W. (2003) Impaired membrane resealing and autoimmune myositis in synaptotagmin VII-deficient mice. *The Journal of cell biology* **162**, 543-549
23. Lin, J., Handschin, C., and Spiegelman, B. M. (2005) Metabolic control through the PGC-1 family of transcription coactivators. *Cell metabolism* **1**, 361-370
24. St-Pierre, J., Drori, S., Uldry, M., Silvaggi, J. M., Rhee, J., Jager, S., Handschin, C., Zheng, K., Lin, J., Yang, W., Simon, D. K., Bachoo, R., and Spiegelman, B. M. (2006) Suppression of reactive oxygen species and neurodegeneration by the PGC-1 transcriptional coactivators. *Cell* **127**, 397-408
25. Lin, J., Wu, H., Tarr, P. T., Zhang, C.-Y., Wu, Z., Boss, O., Michael, L. F., Puigserver, P., Isotani, E., Olson, E. N., Lowell, B. B., Bassel-Duby, R., and Spiegelman, B. M. (2002) Transcriptional co-activator PGC-1 alpha drives the formation of slow-twitch muscle fibres. *Nature* **418**, 797-801
26. Arany, Z., Foo, S.-Y., Ma, Y., Ruas, J. L., Bommi-Reddy, A., Girnun, G., Cooper, M., Laznik, D., Chinsomboon, J., Rangwala, S. M., Baek, K. H., Rosenzweig, A., and Spiegelman, B. M. (2008) HIF-independent regulation of VEGF and angiogenesis by the transcriptional coactivator PGC-1alpha. *Nature* **451**, 1008-1012
27. Handschin, C., Chin, S., Li, P., Liu, F., Maratos-Flier, E., Lebrasseur, N. K., Yan, Z., and Spiegelman, B. M. (2007) Skeletal muscle fiber-type switching, exercise intolerance, and myopathy in PGC-1alpha muscle-specific knock-out animals. *The Journal of biological chemistry* **282**, 30014-30021
28. Handschin, C., Kobayashi, Y. M., Chin, S., Seale, P., Campbell, K. P., and Spiegelman, B. M. (2007) PGC-1alpha regulates the neuromuscular junction program and ameliorates Duchenne muscular dystrophy. *Genes & development* **21**, 770-783
29. Selsby, J. T., Morine, K. J., Pendrak, K., Barton, E. R., and Sweeney, H. L. (2012) Rescue of dystrophic skeletal muscle by PGC-1α involves a fast to slow fiber type shift in the mdx mouse. *PloS one* **7**, e30063-e30063
30. Hollinger, K., Gardan-Salmon, D., Santana, C., Rice, D., Snella, E., and Selsby, J. T. (2013) Rescue of dystrophic skeletal muscle by PGC-1α involves restored expression of

dystrophin-associated protein complex components and satellite cell signaling. *American journal of physiology. Regulatory, integrative and comparative physiology* **305**, R13-23
31. Chan, M. C., Rowe, G. C., Raghuram, S., Patten, I. S., Farrell, C., and Arany, Z. (2014) Post-natal induction of PGC-1alpha protects against severe muscle dystrophy independently of utrophin. *Skeletal Muscle* **4**, 2-2
32. Bulfield, G., Siller, W. G., Wight, P. A., and Moore, K. J. (1984) X chromosome-linked muscular dystrophy (mdx) in the mouse. *Proc Natl Acad Sci U S A* **81**, 1189-1192
33. Baresic, M., Salatino, S., Kupr, B., van Nimwegen, E., and Handschin, C. (2014) Transcriptional network analysis in muscle reveals AP-1 as a partner of PGC-1alpha in the regulation of the hypoxic gene program. *Mol Cell Biol* **34**, 2996-3012
34. McNeil, P. L., and Khakee, R. (1992) Disruptions of muscle fiber plasma membranes. Role in exercise-induced damage. *Am J Pathol* **140**, 1097-1109
35. Murray, J., and Huss, J. M. (2011) Estrogen-related receptor ␣ regulates skeletal myocyte differentiation via modulation of the ERK MAP kinase pathway. **2**, 630-645
36. Kesari, A., Fukuda, M., Knoblach, S., Bashir, R., Nader, G. a., Rao, D., Nagaraju, K., and Hoffman, E. P. (2008) Dysferlin deficiency shows compensatory induction of Rab27A/Slp2a that may contribute to inflammatory onset. *The American journal of pathology* **173**, 1476-1487
37. Fukuda, M., Ogata, Y., Saegusa, C., Kanno, E., and Mikoshiba, K. (2002) Alternative splicing isoforms of synaptotagmin VII in the mouse, rat and human. *The Biochemical journal* **365**, 173-180
38. Baar, K., Wende, A. R., Jones, T. E., Marison, M., Nolte, L. a., Chen, M., Kelly, D. P., and Holloszy, J. O. (2002) Adaptations of skeletal muscle to exercise: rapid increase in the transcriptional coactivator PGC-1. *FASEB journal : official publication of the Federation of American Societies for Experimental Biology* **16**, 1879-1886
39. Akimoto, T., Pohnert, S. C., Li, P., Zhang, M., Gumbs, C., Rosenberg, P. B., Williams, R. S., and Yan, Z. (2005) Exercise stimulates Pgc-1alpha transcription in skeletal muscle through activation of the p38 MAPK pathway. *J Biol Chem* **280**, 19587-19593
40. Boppart, M. D., Burkin, D. J., and Kaufman, S. J. (2006) Alpha7beta1-integrin regulates mechanotransduction and prevents skeletal muscle injury. *Am J Physiol Cell Physiol* **290**, C1660-1665
41. Boppart, M. D., Volker, S. E., Alexander, N., Burkin, D. J., and Kaufman, S. J. (2008) Exercise promotes alpha7 integrin gene transcription and protection of skeletal muscle. *Am J Physiol Regul Integr Comp Physiol* **295**, R1623-1630
42. Davies, K. E., and Nowak, K. J. (2006) Molecular mechanisms of muscular dystrophies: old and new players. *Nat Rev Mol Cell Biol* **7**, 762-773
43. Hirokawa, N., and Takemura, R. (2004) Kinesin superfamily proteins and their various functions and dynamics. *Experimental cell research* **301**, 50-59
44. Noda, Y., Okada, Y., Saito, N., Setou, M., Xu, Y., Zhang, Z., and Hirokawa, N. (2001) KIFC3, a microtubule minus end-directed motor for the apical transport of annexin XIIIb-associated Triton-insoluble membranes. *The Journal of cell biology* **155**, 77-88
45. Martinez, I., Chakrabarti, S., Hellevik, T., Morehead, J., Fowler, K., and Andrews, N. W. (2000) Synaptotagmin VII regulates Ca(2+)-dependent exocytosis of lysosomes in fibroblasts. *J Cell Biol* **148**, 1141-1149

46. Allen, D. G., and Whitehead, N. P. (2011) Duchenne muscular dystrophy - What causes the increased membrane permeability in skeletal muscle? *The international journal of biochemistry & cell biology* **43**, 290-294
47. Song, W. K., Wang, W., Foster, R. F., Bielser, D. A., and Kaufman, S. J. (1992) H36-alpha 7 is a novel integrin alpha chain that is developmentally regulated during skeletal myogenesis. *J Cell Biol* **117**, 643-657
48. Vontzalidis, A., Terzis, G., and Manta, P. (2014) Increased dysferlin expression in Duchenne muscular dystrophy. *Anal Quant Cytopathol Histpathol* **36**, 15-22
49. Waddell, L. B., Lemckert, F. a., Zheng, X. F., Tran, J., Evesson, F. J., Hawkes, J. M., Lek, A., Street, N. E., Lin, P., Clarke, N. F., Landstrom, A. P., Ackerman, M. J., Weisleder, N., Ma, J., North, K. N., and Cooper, S. T. (2011) Dysferlin, Annexin A1, and Mitsugumin 53 Are Upregulated in Muscular Dystrophy and Localize to Longitudinal Tubules of the T-System With Stretch. *Journal of neuropathology and experimental neurology* **70**, 302-313

8 Sinergia Project: Improving human muscle engineering by PGC-1α expression and molecular imaging using positron emission tomography (PET) (Project 4)

Main contributors: Ivana Dinulovic, Thomas Betzel, Deana Haralampieva, Simone Amatamey, Daniel Eberli, Christoph Handschin

*This is a collaborative interdisciplinary project between three Swiss institutions, supported by an SNSF grant.

Contribution of participating laboratories:

Christoph Handschin, Daniel Eberli and Simon Amatamey designed and supervised the study.

Laboratory of Prof. Christoph Handschin (Biozentrum, University of Basel):

Ivana Dinulovic performed experiments concerning the cloning strategy, virus generation, functionality, toxicity and production. Optimizations related to the titer determination of viruses, high titer batch production and cellular transduction were an integral part of her work. Markus Beer provided assistance with the final steps of virus production.

Laboratory of Dr. Daniel Eberli (University Hospital Zurich, University of Zurich):

Experiments concerning muscle regeneration *in vivo* were performed by Deana Haralampieva and Souzan Salemi, and are not presented here due to the preliminary status of the data.

Laboratory of Prof. Simon Ametamey (ETH Zurich):

PET experiments *in vitro* and *in vivo*, as well as CT, biodistribution and autoradiography measurements were performed by Thomas Betzel, Stefanie Kramer and Claudia Keller, and are partially presented in this chapter as a proof of functionality of the mutated hD2R virus.

8.1 Introduction

Skeletal muscle is an organ crucial for locomotion, breathing and metabolism, and is therefore indispensable for healthy life of an individual. Although this tissue possesses a remarkable capacity for self-repair and is relatively stable, with a low turn-over rate of nuclei, limitations to successful regeneration are many (1). In that regard, muscle pathologies as well as aging and injuries affecting a large volume of muscle, prevent restoration of highly functional muscle tissue in humans (2).

The field of regenerative medicine has been aiming to improve skeletal muscle restoration by transplanting cells, implanting biomaterials, or a combination of both (3). Although basic research has revealed that many cell types including perycites, hematopoetic stem cells, mesoangioblasts, to name only a few, can actively participate in skeletal muscle regeneration (4), major attention in clinics has been devoted to skeletal muscle specific progenitors – satellite cells (5) . And rightfully so, since recent findings have confirmed the essential role of these cells in successful regeneration in mice after injury compared with other contributing cell populations (6-9).

One of the major persisting limitations in the treatment of large muscle beds, such as in muscle dystrophies, is the systemic delivery of treatment. Intramuscular injections of myoblasts are necessary since injected cells cannot cross the endothelium and home in on muscles (5). In addition, multiple injections in the same muscle are often required due to the limited migration of injected cells (10). This problem currently restricts the transplantation approaches to the treatment of small muscles, such as sphincter muscles in the urethra and esophagus, whose impairment leads to incontinence and reflux, respectively.

However, many other obstacles exist within the field of cell transplantation, one of them being the low survival rate of injected cells caused by reduced innervation and vascularization of the newly formed tissue (11). A dense vascular network is essential, as oxygen and nutrient delivery as well as toxic metabolic byproduct removal, limits cell survival. Even though previous attempts implicating vascular endothelial growth factor (VEGF) have managed to alleviate this problem to some extent (12), the hurdle, especially regarding innervation, remains. Adequate innervation of skeletal muscle tissue ensures tissue maturation and function and prevents muscle

atrophy (13, 14). However, although motor unit formation has been demonstrated in cases of myoblast injection, synchronous contractions of nascent muscle tissue upon nerve stimulation have not been verified (15).

It is important to note that small muscle injuries, such as sphincter injuries, occur mainly in the elderly. For example, urinary incontinence develops as a result of surgical injury secondary to prostate surgery in men (15), but age-related factors also contribute to the condition since the ability of skeletal muscle to regenerate diminishes with age (16). Therefore, ageing additionally impedes muscle tissue formation and functionality upon transplantation treatments.

Peroxisome proliferator-activated receptor γ coactivator 1 α (PGC-1α) is a transcriptional coactivator and regulator of oxidative metabolism (17). It has been demonstrated that PGC-1α leads to VEGF expression favoring angiogenesis (18), and in addition controls the expression of neuromuscular junction (NMJ) genes (19). PGC-1α overexpression improves the phenotype not only in the mouse model for Duchenne muscular dystrophy (DMD) (19-22), but also in mitochondrial myopathy (23) and statin-induced muscle damage (24). In addition, PGC-1α protects muscle against denervation-induced atrophy (25). Muscle specific PGC-1α transgenic mice possess increased exercise endurance, which is related to a fiber-type switch from the glycolytic to the oxidative phenotype (26), while muscle specific knock-out mice exhibit mirrored characteristics (27). Importantly, PGC-1α also reduces sarcopenia (28), and is therefore a promising factor that alleviates aging-related conditions.

As these changes brought about by PGC-1α would be highly beneficial in reducing the aforementioned transplantation impediments, we sought to induce PGC-1α overexpression in skeletal muscle precursor cells prior to transplantation into injured muscle tissue and assess the outcomes on muscle tissue formation *in vivo*. For this purpose, we chose to use adenoviruses as delivery vectors. We wanted to assess PGC-1α driven benefits not only *in vitro* and *ex vivo* relying on histology, contractility and gene expression measurements, but also to follow tissue formation *in vivo* using a non-invasive technique – positron emission tomography (PET).

PET is a highly sensitive technique used to monitor spatio-temporal and quantitative aspects of reporter gene expression in live animals and humans (29). It is based on the detection of gamma rays coming from positron-emitting radionuclides incorporated into biological

molecules (30). PET is mainly employed in oncology in combination with glucose analog 2-deoxy-2-[^{18}F]-fluoro-D-glucose (FDG) as a tracer, although applications in neurology and cardiology are emerging (31-33). FDG enables tracking cells with high glucose consumption, such as proliferating cancer cells, although it can also be used for monitoring contracting muscle cells. This functional imaging is often combined with X-ray computed tomography (CT) for precise assessment of anatomical location (34).

An evaluation of the results obtained from *in vitro* studies, *in vivo* measurements and *ex vivo* experiments would provide us with a clear picture of the hypothesized advantages of PGC-1α induction on muscle regeneration and therefore potential applications in human subjects.

8.2 Overview of study design

In this study, human muscle precursor cells (hMPCs, here used interchangeably with myoblasts) isolated from *rectus abdominis* muscle biopsies from healthy human subjects, were used for cell transplantations. Myoblasts were transduced with adenoviruses harboring sequences of human dopamine type 2 receptor (hD2R; used for PET purposes), human (h) PGC-1α or hVEGF prior to their injection *in vivo*. The expression of these genes of interest (GOI) is under the control of cytomegalovirus (CMV) promoter. As a control, previously generated adenovirus expressing green fluorescent protein (GFP) was used. In order to minimize the effect of immune rejection in mice, nude mice were used for subcutaneous and intramuscular post-crush injury injections (Figure 1).

In vitro techniques were employed to generate the aforementioned adenoviruses, optimize transduction settings and evaluate their toxicity. Additional experiments should complement *in vivo* and *ex vivo* results, and take a closer look at myotube formation and maturation, as well as NMJ formation.

For *in vivo* assessment, we were primarily interested in repetitive observations of injected cells in order to monitor their survival and migration. For this application, we decided to use D2R as a reporter (35) in combination with [^{18}F]-Fallypride as a tracer. D2R is predominantly expressed in striatum (36) but only at a very low level in the muscle, ensuring that only injected muscle cells previously transduced with adenovirus containing D2R would be detected. Furthermore, PET enables us to assess additional aspects of engineered tissue *in vivo*, using a set of established tracers. In that respect, we plan to use fluoroiminidasole ([^{18}F]-FMISO) for measuring tissue hypoxia, [^{64}Cu]-NODAGA-RGD for assessing tissue vascularization and the aforementioned FDG for glucose consumption measurements. All these tracers in combination with D2R transduced injected cells will assure thorough evaluation of the survival, growth and functionality of the nascent tissue.

Importantly, the engineered muscle tissue will be eventually isolated at different time points after cell transplantation, and evaluated *ex vivo*. Experiments concerning contractility properties, myotube and NMJ formation, vascularization, and gene expression will provide data complementing the *in vitro* and *in vivo* results well.

We hypothesized that myoblast gene therapy by adenoviral delivery of PGC-1α prior to cell transplantation would improve the resistance, survival and growth of the formed tissue by increasing its vascularity, endurance and innervation. In addition, we were interested in determining if VEGF expression in combination with PGC-1α would provide additional benefit in terms of tissue survival. After the design and production of the desired viral vectors, followed by initial tests *in vitro*, experiments are planned to be executed in two animal models – subcutaneous injections for assessment of tissue formation, growth, survival and vascularization, and intramuscular injection after crush injury for examining the participation of the transplanted cells in skeletal muscle regeneration.

These experiments are intended to serve as a proof-of-concept study for evaluating the benefits of PGC-1α overexpression in muscle cells, and future approaches in human patients for the treatment of small muscles injuries (Figure 1).

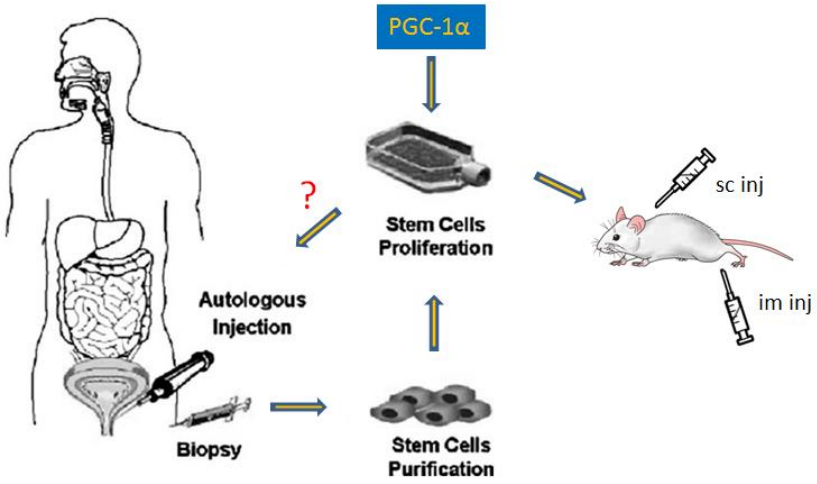

Figure 1 Schematic representation of study design and potential application in humans
Sc inj (subcutaneous injection), im inj (intramuscular injection); adapted from Smaldone and Chancellor, World J Urol, 2008, wecort.com and clipartist.info

8.3 Plasmid design

Our objective was to test the potential beneficial outcomes of PGC-1α and VEGF overexpression in myoblasts prior to injection *in vivo*, for which we intended to generate two separate adenoviruses. In addition, it was essential to track injected cells *in vivo* and to estimate their contribution to the formation of new muscle with and without PGC-1α or VEGF overexpression. For this purpose, we planned to generate an additional adenovirus, expressing D2R, as a PET reporter gene. The expression of each gene was designed to be under the control of a CMV promoter in order to assure robust expression of the transgene (Figure 2).

Each vector was designed to contain a different fluorophore, expressed under a separate CMV promoter. For achieving this, we decided to use GFP together with PGC-1α, red fluorescent protein (RFP) with D2R and yellow fluorescent protein (YFP) with VEGF. The expression of these fluorescent proteins should coincide with the expression of the transgene, and therefore enable easier detection of transduced cells both on muscle sections after transplantation, but also prior to transplantation for assessing the cell transduction efficiency. Importantly, given appropriate filters, it is possible to differentiate between all three fluorescent proteins when expressed in the same cell.

In addition, each vector is designed to have specific tags for easier detection and/or distinguishing of the transgene from the endogenous protein. In that respect, the PGC-1α construct includes an HA tag on its N-terminus, the D2R sequence has 6xHis and V5 tags on its C-terminus, while VEGF contains Myc and DDK (same sequence as FLAG) on the C-terminus (Figure 2).

As a control, we aimed to use adenovirus expressing only GFP under a CMV promoter, and this virus had already been generated and regularly used in our laboratory.

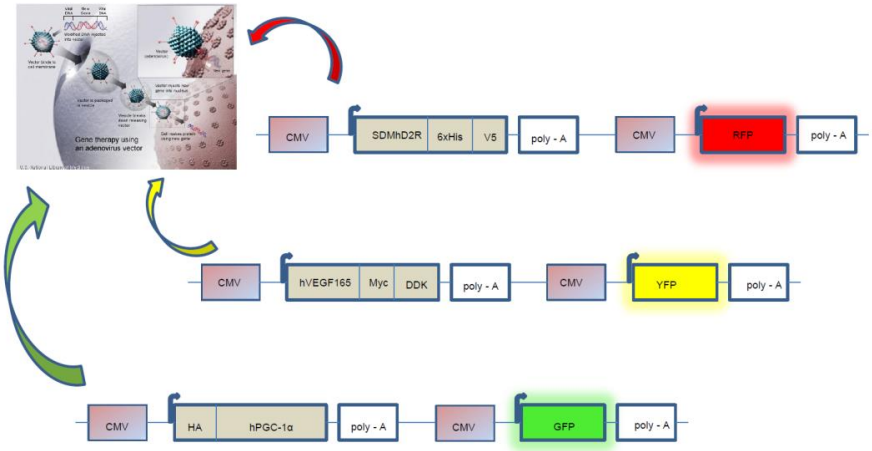

Figure 2 Constructs of final plasmids used for adenoviral generation
Adapted from www.genetherapynet.com

8.3.1 Cloning of pAdTrack-CMV-hPGC-1α

A construct containing human PGC-1α with C-terminal Myc and His tags in a pcDNA4 backbone was ordered from Addgene. To change the tags, we subcloned the hPGC-1α sequence into a pcDNA 3.1 vector using the Directional TOPO Expressional Kit (Invitrogen) according to the manufacturer's instructions. This subcloning technique is based on a PCR reaction using specific primers and Pfu ULTRA high-fidelity polymerase (Agilent). A separate PCR reaction using primers designed to cover the insertion sites confirmed successful insertion of required sequence (Figure 3).

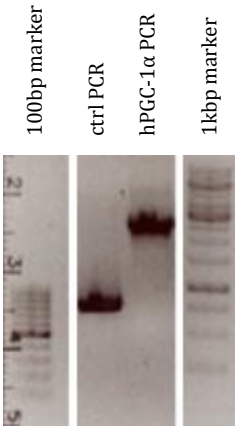

Figure 3 PCR reactions loaded onto gel

Chemically competent XL-10 Gold bacteria (Stratagene) were transformed and grown overnight on LB plates with ampicillin (Amp), after which several colonies were selected. PCR on the selected colonies enabled us to confirm the correct orientation and size of the insert (Figure 4).

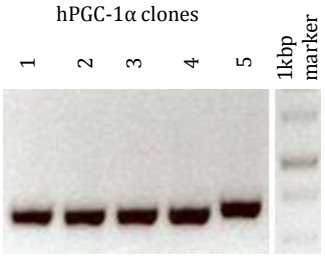

Figure 4 Colony PCR for hPGC-1α
All tested colonies resulted in insertion of PCR product, but only colony No. 5 contained HA tag, as revealed upon sequencing

Several colonies were chosen for further expansion in Luria-Bertani broth (LB) with Amp for purposes of sequencing and glycerol stock preparation. Thorough sequencing identified clones with correct insertion, including the desired tag. However, we were also able to detect three point mutations in the hPGC-1α sequence, two of which were silent and therefore did not require further attention. Due to a G to A switch, the third mutation resulted in Gly in position 482 being exchanged with Ser (G482S). Since this mutation was previously associated with incidence of type 2 diabetes (37), we decided to correct it using site-directed mutagenesis (SDM). SDM was carried out according to the protocol adapted from the Stratagene Quick Change Site-Directed Mutagenesis Kit, and is based on the PCR reaction using Pfu ULTRA high-fidelity polymerase (Agilent). Mutagenic primers were designed using the Quick Change Primer Design application (Agilent). The PCR product was confirmed on a gel (Figure 5), and the rest was used for transforming bacteria and subsequent sequencing of the plasmid, which confirmed successful mutagenesis.

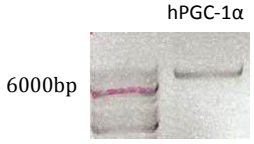

Figure 5 SDM PCR for hPGC-1α

Finally, we were ready to subclone the hPGC-1α with the N-terminal HA tag into a pAd-Track-CMV vector. For that, we decided to use sticky end ligation, and therefore digest both the pcDNA3.1 vector containing the hPGC-1α and pAd-Track CMV vector with KpnI and XhoI restriction enzymes according to the manufacturer's instructions (NEB). After phosphatase treatment of the pAd-Track-CMV vector and subsequent heat inactivation, the digested bands were gel purified (Figure 6).

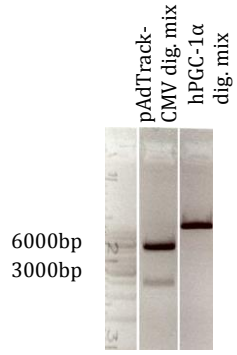

Figure 6 Double digest mixes loaded onto gel

The bands of interest were extracted using the QIAquick Gel Extraction Kit (Qiagen) and their concentration was measured on Nanodrop. Ligation of the purified bands was performed using Quick T4 ligase (NEB) and an insert:vector ratio of 3:1, after which the bacteria were transfected with the ligation reaction and plated on kanamycin (Kan) containing Luria-Bertani Agar (LA) plates. The following morning, there was only one colony present on the plate. After expansion in liquid media containing Kan and plasmid isolation, sequencing results confirmed correct ligation (Figure 7).

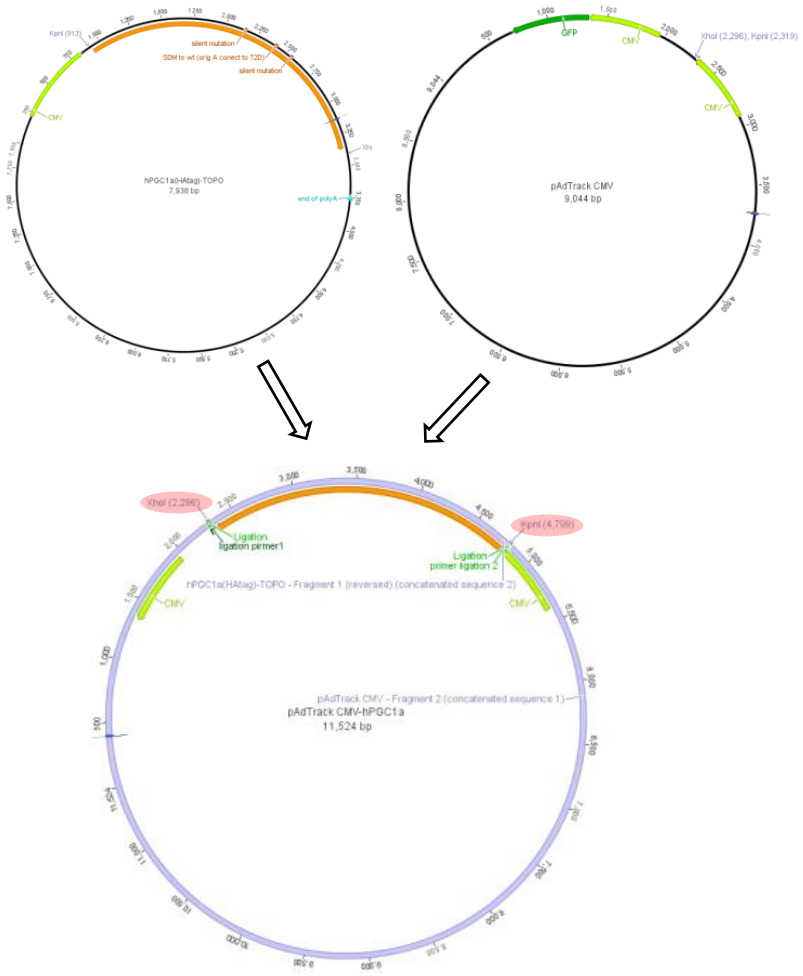

Figure 7 Schema for hPGC-1α cloning into pAd-Track-CMV vector

8.3.2 Cloning of pShuttle-CMV-mRFP-hD2R

A IRAUp969E0451D vector containing hD2R was ordered from ImaGenes, whereas a pcDNA3 plasmid containing monomer (m) RFP was obtained from Addgene. We first subcloned the sequence of interest into the pcDNA 3.1 TOPO expressional vector (Invitrogen) according to the manufacturer's instructions, in order to simplify the next cloning steps and to add 6xHis and V5 tags on the C-terminus of the hD2R. This subcloning step is PCR-based, and requires Pfu ULTRA high-fidelity polymerase (Agilent) and the design of specific primers (Figure 8).

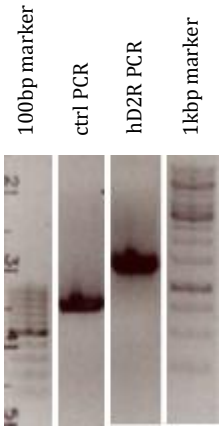

Figure 8 PCR reactions loaded onto gel
Markers and ctrl PRC are same as in Figure 3

An additional PCR reaction using primers overlapping the insertion sites on the plasmid isolated from the transfected bacteria confirmed successful subcloning (Figure 9).

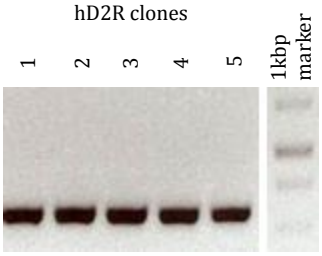

Figure 9 Colony PCR for hD2R
Marker lane is same as in Figure 4

Next, we wanted to ensure that the ligand binding by the hD2R would not initiate a signal transduction pathway in the cells that would be transduced with it. For that reason we performed SDM in order to mutate Phe into Ala in position 411 (F411A) (Figure 10). This mutation is known to block the inhibition of adenylyl cyclase thorough D2R, without compromising ligand binging to the receptor (38). The approach for SDM was similar to the one described above for the hPGC-1α sequence. Of the utmost importance for successful SDM is that the mutagenic primers are polyacrylamide gel electrophoresis (PAGE) purified, and not only desalted.

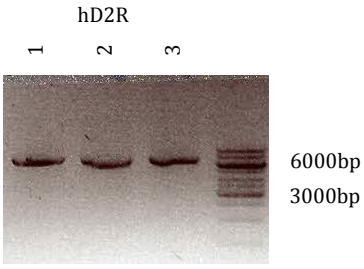

Figure 10 SDM PCR for hD2R

After bacterial transfection and propagation, the isolated plasmids were used to confirm accomplishment of the desired mutation.

Regarding the mRFP contatining vector, we first checked for the presence of the correct sequence and existence of restriction endonuclease sites. In the process of generating new adenoviruses, it is necessary to perform the digestion step prior to the formation of the recombinant adenovirus plasmid in AdEasier cells, using either PmeI or EcoRI restriction enzymes. For that reason, we had to make sure that the desired sequences do not contain cutting sites for both of the enzymes. As this was the case for the mRFP sequence, an SDM reaction was necessary to mutate the EcoRI site.

Finally, we were ready to combine the hD2R and mRFP sequences into the backbone of the pShuttle-CMV vector. Since the first trial using a specifically designed linker to combine the purified digested sequences into a single vector failed, we decided to use sticky end ligation. The easiest cloning approach required introducing a DraIII cutting site into the mRFP containing vector. To achieve this, we once again used SDM.

After the successful mutation was obtained, we preformed double digests following the suggestions for the optimal activity of the endonucleases used (NEB) for the three vectors: the pcDNA3.1 TOPO – hD2R was digested using KpnI and DraIII, pcDNA3 – mRFP was digested with XbaI and DraII, while pShuttle-CMV was digested with KpnI and XbaI. After phosphatase treatment of the digested pShuttle-CMV vector and subsequent heat inactivation of all three digests, the digestion mixes were gel purified.

The bands of interest were cut and DNA fragments isolated using the QIAquick Gel Extraction Kit (Qiagen), while DNA concentration was measured using Nanodrop. Ligation was performed using Quick NEB ligase and an insert:insert:vector ratio of 3:3:1. The bacteria were transfected with the ligation soup and the colonies were screened for the presence of the correct plasmids using colony PCR (Figure 11).

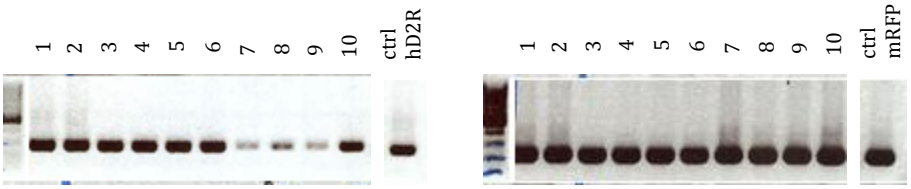

Figure 11 Colony PCR for ligation of hD2R and mRFP

From the propagated colonies, the plasmids were isolated and tested again for the presence of the desired sequences using PCR, and then sent for complete sequencing (Figure 12).

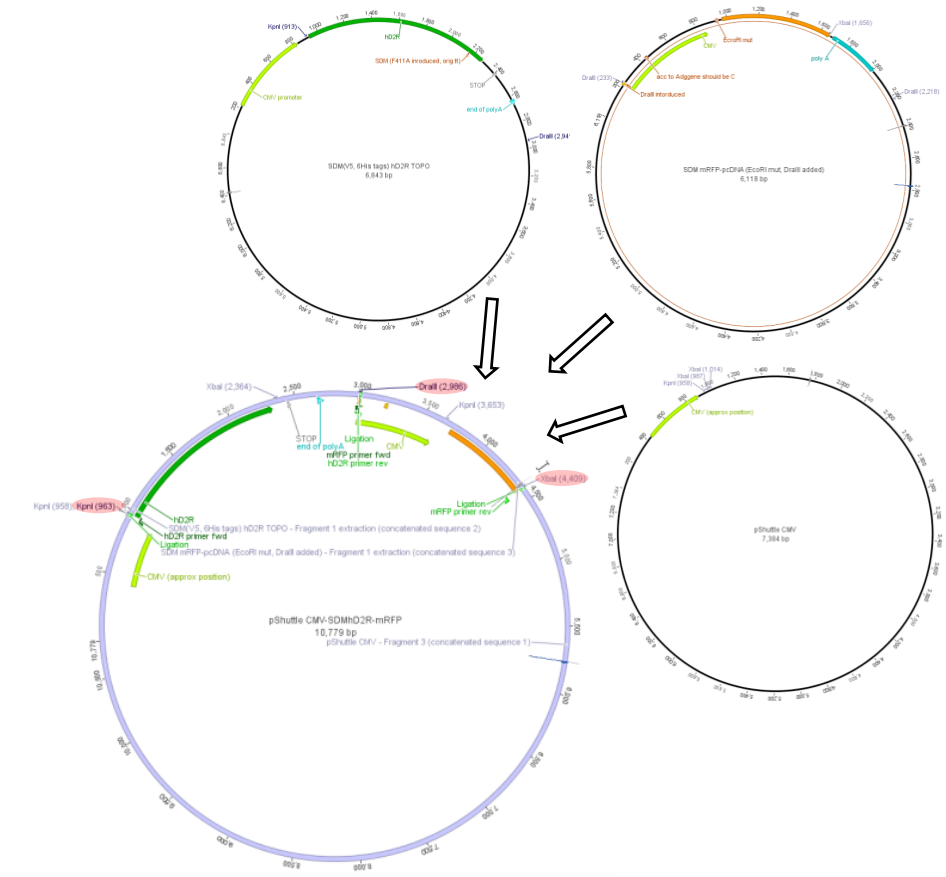

Figure 12 Schema for hD2R and mRFP cloning into pShuttle-CMV vector

8.3.3 Cloning of pShuttle-CMV-YFP-hVEGF

A pCMV6-Entry plasmid with human VEGF165 (transcript variant 4) already containing C-terminal Myc and DDK (FLAG) tags was ordered from Origene. A YFP-pcDNA3 plasmid was ordered from Addgene. After initial sequencing of both plasmids, a strategy for subcloning the genes of interest into the pShuttle-CMV vector was defined based on the existing restriction endonuclease sites. Again, we aimed for the sticky end ligation of the sequences into the final plasmid.

First, for the purpose of generating viral particles containing YFP, we had to mutate the existing EcoRI restriction site in the YFP sequence for the same reasons previously explained for the mRFP vector. Next, we created a NruI restriction site in the VEGF165 vector via SDM, in order to apply the sticky end approach for ligation. After we confirmed the desired changes in the sequences, we continued with double digests of the three vectors: the pShutlle-CMV vector was digested with KpnI and XbaI, the mRFP containing plasmid was digested with XbaI and NruI, while the VEGF expressing vector was incubated with KpnI and NruI. All the digests were carried out according to NEB's suggestions. After phosphatase treatment and heat inactivation of the pShuttle-CMV vector, the desired DNA sequences were obtained after the gel separation step (Figure 13).

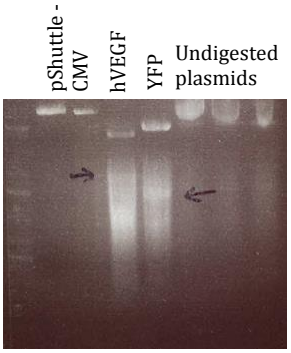

Figure 13 Double digest mixes loaded onto gel
Smear is due to DNA carrier digested by NruI

The bands of interest were extracted and three-part ligation was performed using NEB Quick ligase with an insert:insert:vector ratio of 3:3:1. The bacteria were transformed using the

ligation mix and the next day, several clones were checked for the presence of the correct plasmid using colony PCR (Figure 14).

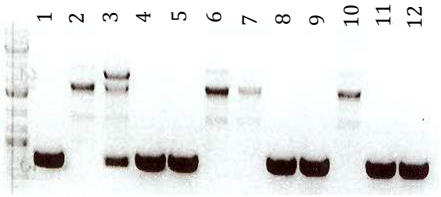

Figure 14 Colony PCR for checking presence of YFP sequence
Colony 9 was later confirmed to have adequate sequence

Several clones were sent for sequencing and one containing the appropriate ligation product was found (Figure 15).

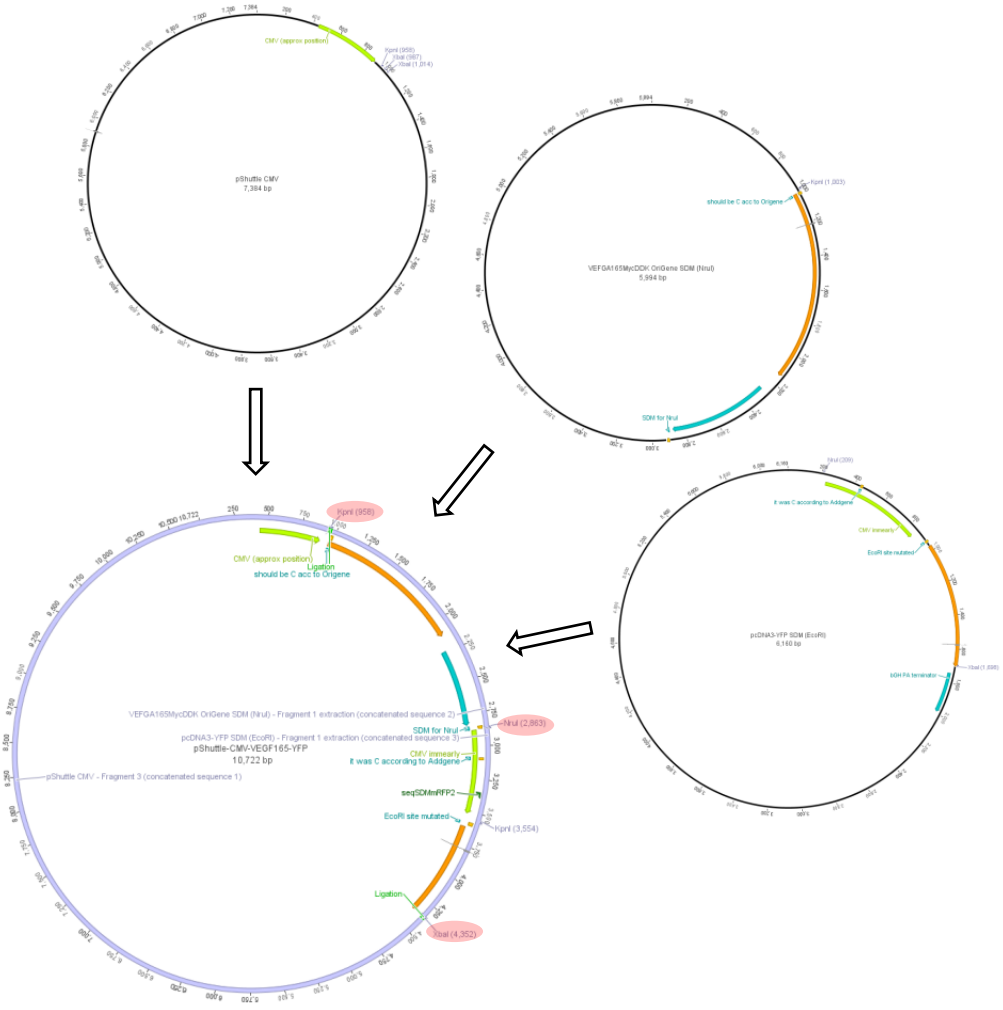

Figure 15 Schema for hVEGF and YFP cloning into pShuttle-CMV vector

8.3.4 Testing plasmid functionality

Prior to generating viruses, it is important to check the functionality of all plasmids. For that purpose, we transfected AD293 cells using Lipofectamine 2000 (Invitrogen). Detection of GFP/RFP/YFP positive cells by microscopy confirmed a high rate of transfection. Two days later, the cells were collected in Trizol for RNA isolation, or in a sucrose buffer for protein isolation. Quantitative PCR (qPCR) and Western Blotting (WB) were used for assessing gene expression from the plasmids. A list of human specific qPCR primers is provided in Table 1. Out of the three PGC-1α antibodies tested, only one (4C.13, Millipore) gave an additional band for PGC-1α in the case of positively transduced cells (Figure 16B). For D2R detection, none of the three D2R antibodies tested resulted in specific detection. However, we were able to detect a massive upregulation of the GOIs in all three vectors (Figure 16A and 16C) and therefore continued with viral generation.

A

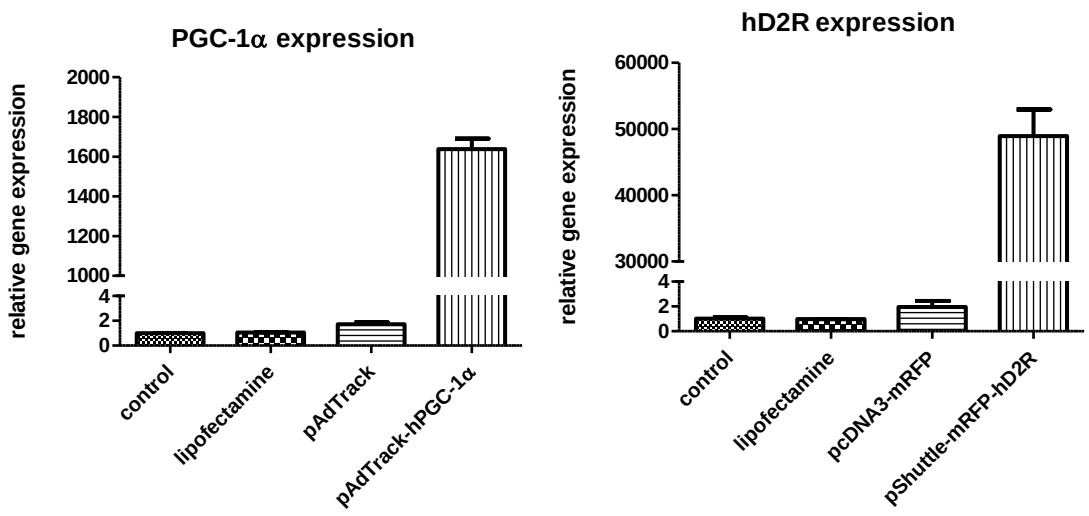

B

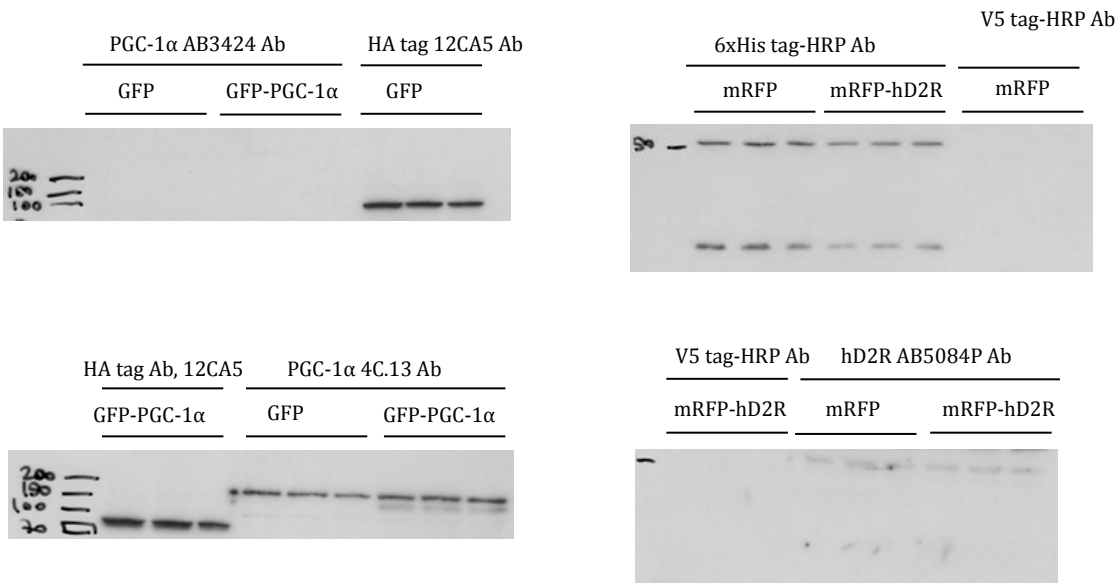

C

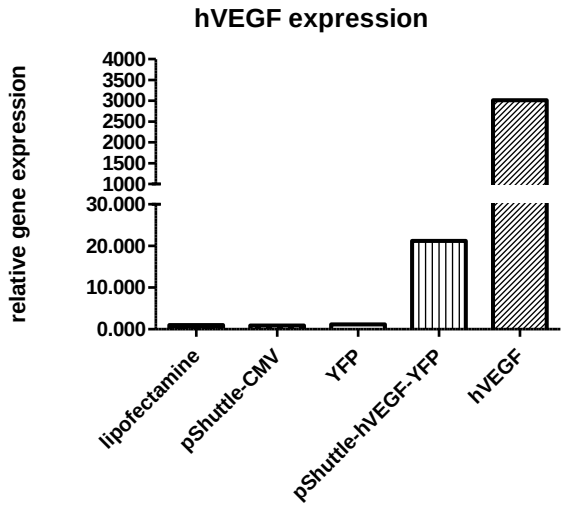

Figure 16 Functional plasmids according to GOI expression (qPCR) after transfection into AD293 cells
(A and C) qPCR of GOIs, (B) WB for GOIs

#Note: For qPCR and WB protocols, see section Materials and Methods in *Project 3*

8.4 Virus generation and amplification

All viruses were generated according to a previously established and published protocol (39). Here, the procedure is briefly explained and summarized in Figure 17.

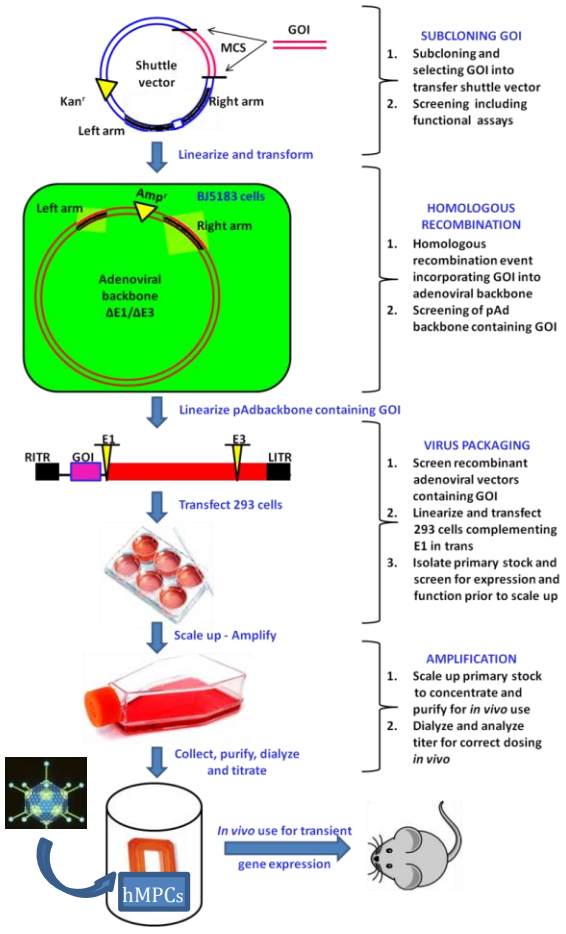

Figure 17 Steps in virus generation, amplification, titration and usage
Adapted from nl.wikipedia.org and www.labome.com

In brief, the final plasmids containing GOIs in the backbone of one of the shuttle vectors (pAdTrack-CMV or pShuttle-CMV) were digested with EcoRI or PmeI and electroporated into recombination-competent AdEasier cells. The next day, very small colonies were selected, the plasmids isolated and correct recombination checked with PacI digestion (Figure 18). Digestion of correctly recombined plasmids should give one band above 20kDa and one band at 3kDa or 4.5kDa after separation on the gel. LacZ plasmids served as controls for bacterial recombination.

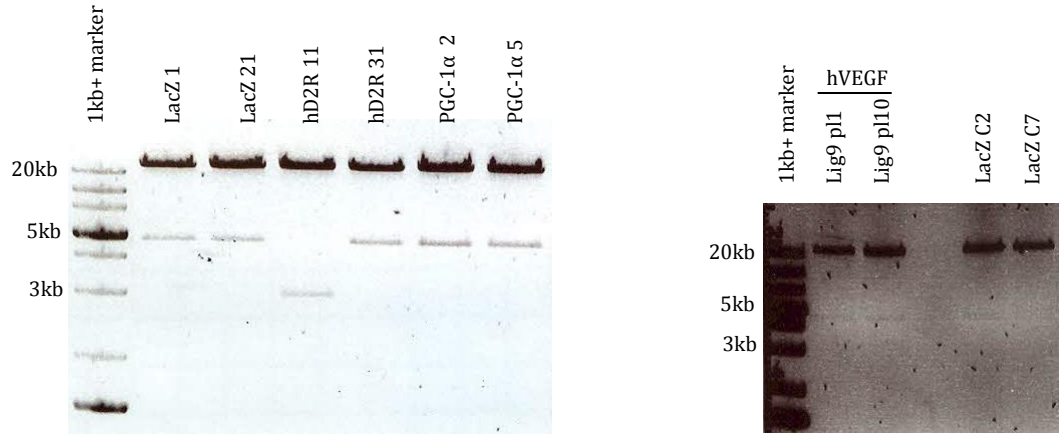

Figure 18 Correct recombination of plasmids with GOIs in AdEasier cells

The correct plasmids were linearized with PacI and AD293 cells transfected using Lipofectamine 2000 (Invitrogen). AD293 are packaging cells which express the E1 region of the viral genome and therefore enable viral particle formation. Generation of the first viral particles takes 2-3 weeks and can be monitored through appearance of fluorescent plaques. However, in order to achieve a high titer, one needs to perform several rounds of virus amplification. Each phase consists of infecting packaging-competent cells, incubation until the appearance of a prominent cytopathic effect and cell detachment, cell collection and opening using a freeze-thaw approach in order to liberate the viral particles. It is important to note that before embarking on extensive amplification, one needs to check the functionality of the viral particles using an approach analogous to the one previously described for the final plasmids containing the GOIs.

Cell transplantation experiments in mice require large numbers of cells and therefore large batches of viruses. Due to inaccuracy in the titer determination procedure, we decided to perform a single amplification producing sufficient quantities of viruses for all the experiments to come, instead of producing small batches as needed. For this, we used many large plating surface area dishes, and the obtained viruses were used for titer determination and tests *in vitro* and *in vivo*.

8.4.1 Optimization of titer determination and testing virus functionality

Titer was determined using a protocol adapted from the AdEasy Viral Titer Kit (Agilent). The method was tested using AD293 cells, COS-7 and primary hMPCs. Application of the simplified method for titer determination, which does not require staining, was possible do to the expression of fluorescent proteins by our viruses. In short, the cells were plated, transduced and the fluorescent positive cells were quantified using a fluorescent microscope and their number compared to the total number of cells per field.

As expected, titers were dependent on the cell line, as shown in the example below (Figure 19). In addition, this method turned out to be suboptimal for large cells because of the low number of cells that can fit into one field of view, resulting in imprecise quantification and therefore unreliable results. For that reason, hMPCs could not be used for titer assessment with this approach, and we decided to determine the titer with AD293 cells, as was suggested in the protocol.

VIRUS	TITER IN AD293		VIRUS	TITER IN hMPCs
AdTrack	1.05*10^11 IFU/ml		AdTrack	1.04*10^8 IFU/ml
AdTrack-hPGC1-α 2	1.11*10^11 IFU/ml		AdTrack-hPGC1-α 2	1.07*10^8 IFU/ml
AdTrack-hPGC1-α 5	8.25*10^10 IFU/ml		AdTrack-hPGC1-α 5	5.49*10^7 IFU/ml
pShuttle-mRFP-hD2R 11	2.84*10^10 IFU/ml		pShuttle-mRFP-hD2R 11	1.29*10^7 IFU/ml
pShuttle-mRFP-hD2R 31	3.96*10^9 IFU/ml		pShuttle-mRFP-hD2R 31	5.76*10^6 IFU/ml

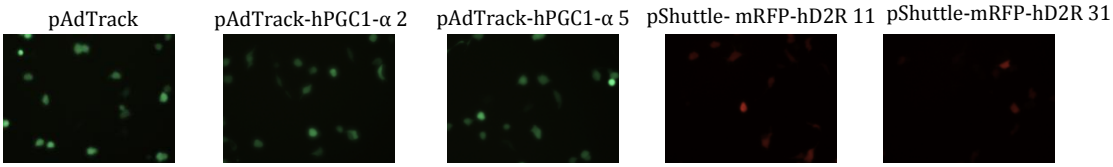

Figure 19 Example of titer determination of same batches of viruses using AD293 cells or hMPCs and picture of transduced AD293 cells expressing GFP or RFP

It was therefore decided that the multiplicity of infection (MOI – the ratio of the number of viral particles to cells) for transducing hMPCs would be calculated based on the AD293 titer. We tested virus functionality in hMPCs, at two different MOIs (Figure 20) using two clones for both viruses.

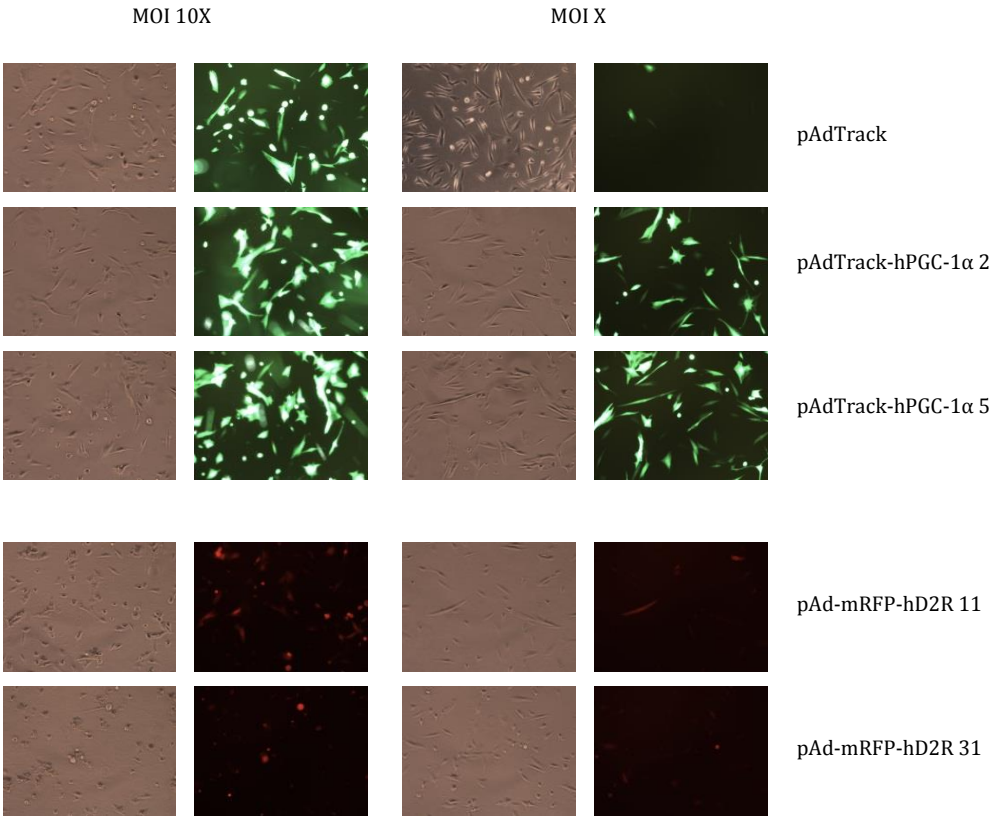

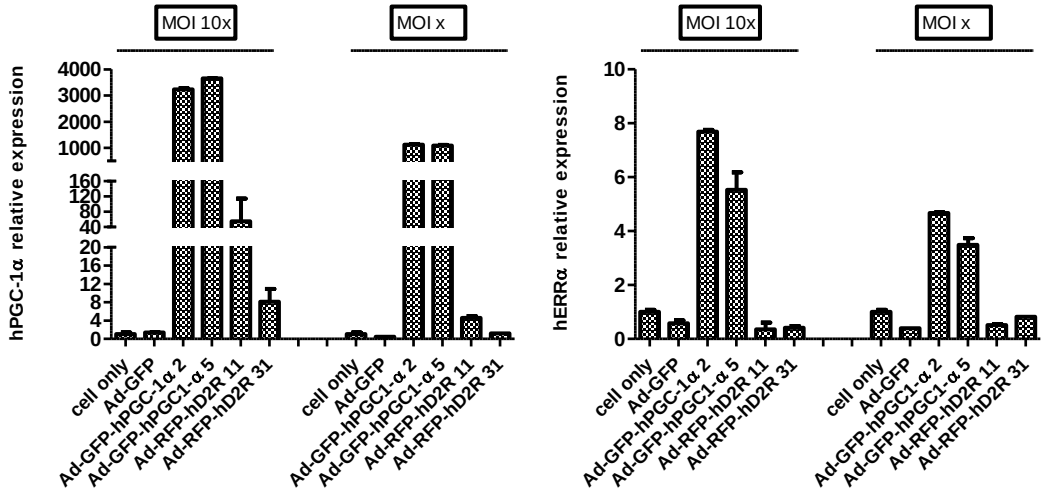
MOI 10x
MOI x
hPGC-1α relative expression
4000
3000
2000
1000
160
120
80
40
20
16
12
8
4
0
cell only
Ad-GFP
Ad-GFP-hPGC-1α 2
Ad-GFP-hPGC1-α 5
Ad-RFP-hD2R 11
Ad-RFP-hD2R 31
hERRα relative expression
10
8
6
4
2
0

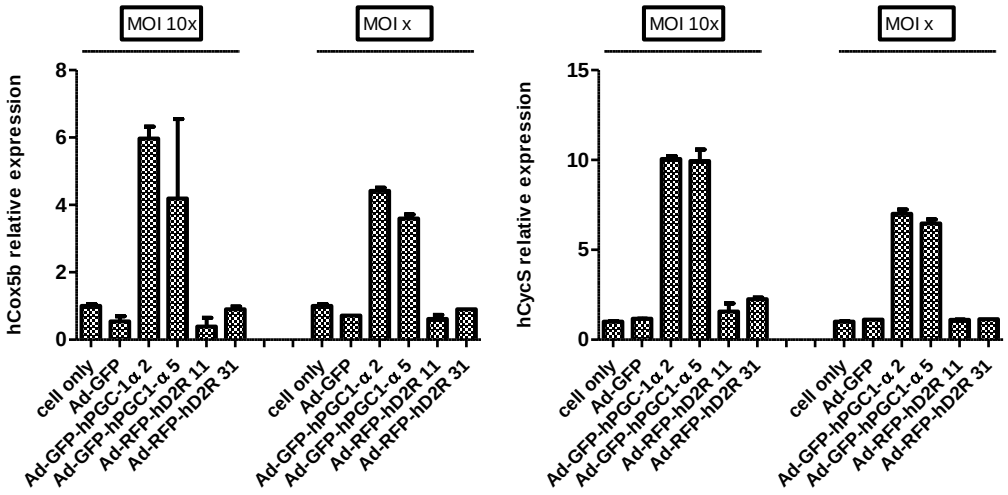
MOI 10x
MOI x
hCox5b relative expression
8
6
4
2
0
hCycS relative expression
15
10
5
0
cell only
Ad-GFP
Ad-GFP-hPGC-1α 2
Ad-GFP-hPGC1-α 5
Ad-RFP-hD2R 11
Ad-RFP-hD2R 31

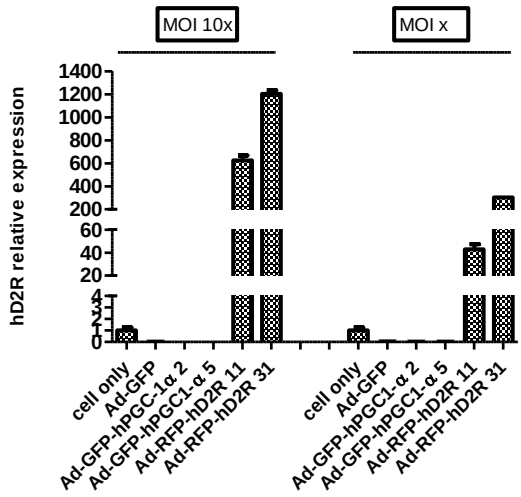

Figure 20 Cell transduction and virus functionality at two different MOIs
Testing two clones for each virus (hPGC-1α 2 and 5; hD2R 11 and 31)

#Note: For qPCR protocol, see section Materials and Methods in *Project 3*

As we can see in Figure 20, the viruses are well-designed based on their transduction capability (GFP/RFP) and qPCR expression of the GOIs (hPGC-1α/hD2R) in hMPCs. In addition, there is a dose dependence in expression based on the transduction efficiency (the percentage of cells transduced). The lower MOI tested resulted in healthier cells (based on morphology), yet resulted in only modestly lower levels of gene expression. Importantly, expression of PGC-1α-regulated genes increased in cells transduced with the hPGC-1α virus, which confirmed the presence of functional viral particles (a list of human specific qPCR primers is provided in Table 1).

However, for the hD2R virus, a different approach was required. Since we generated a virus containing mutated hD2R, unable to activate the signal transduction pathway (38), the best way to test its functionality was to check for its ligand binding properties. We decided to evaluate the hD2R virus with PET, using [^{18}F]-Fallypride as a ligand. These experiments were performed by members of Prof. Amatamey's lab. First, they tested the virus on transduced hMPCs *in vitro*, using cells transfected with a wild-type D2R plasmid (kindly provided by Prof.

Kovoor) as a control. Indeed, they were able to detect significant activity in transfected cells compared to untransfected ones (Figure 21).

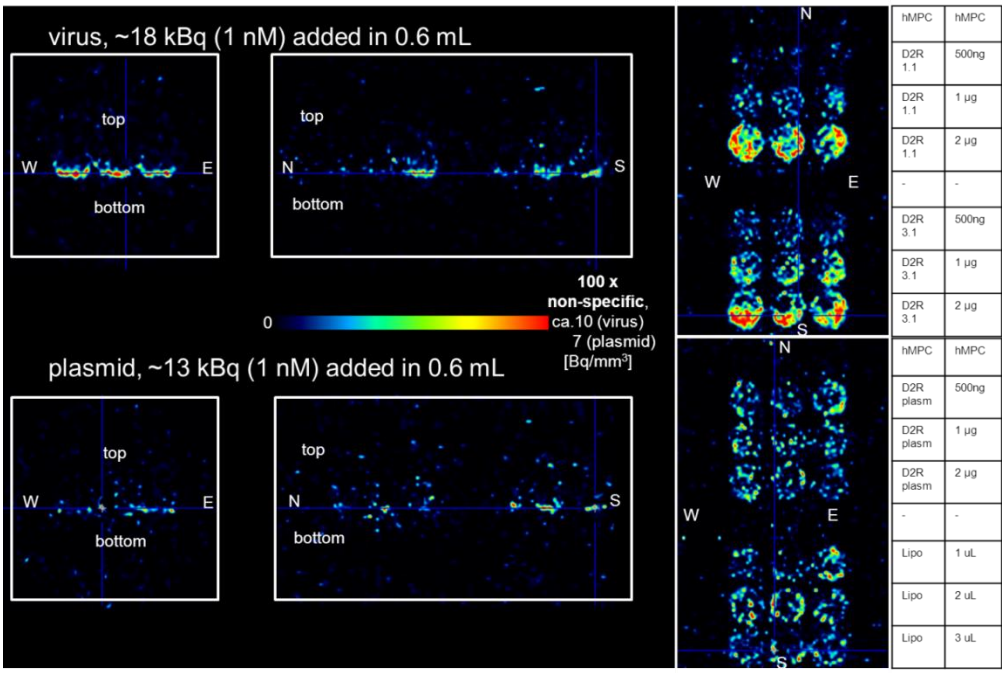

Figure 21 Upper panel: [^{18}F]-Fallypride (ligand) binding to hMPCs transduced with increasing amounts of hD2R viruses
Upper panel: two viral clones (D2R 11 and D2R 31); untransduced cells served as a negative control. Lower panel: [^{18}F]-Fallypride binding in hMPCs transfected with increasing amount of D2R plasmid (positive control) using Lipofectamine (Lipo). Stronger signal can be observed in transduced vs. transfected cells, which is probably due to differences in vectors, i.e virus vs. plasmid.

Next, we decided to check the performance of the virus in an *in vivo* setting. In this way, we could test for the feasibility of cell tracking *in vivo*. For this experiment, ~25% transduced hMPCs were injected subcutaneously in the dorsal region of mice, and 2-4 weeks later the signal was measured by PET (Figure 22A and 22B).

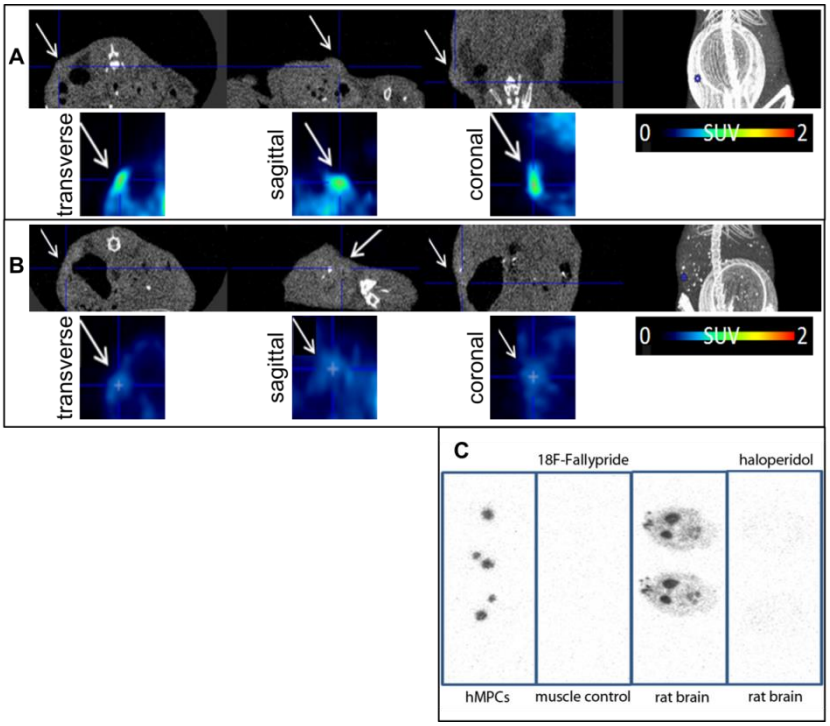

Figure 22 CT-PET experiment *in vivo*
30 million Ad-RFP-hD2R transduced hMPCs (~25% RFP^+) were injected subcutaneously into nude mice. Signal was measured using [^{18}F]-Fallypride injected via tail vein (A) 2 weeks later and (B) 4 weeks later; (C) Autoradiography confirmed presence of transduced cells. Native muscle tissue served as negative, and brain tissue as positive control. Haloperidol is D2R blocking agent and therefore demonstates [^{18}F]-Fallypride binding specificity.

A specific signal was difficult to detect due to high signal spillage from internal organs. In addition, a decrease in signal was observed with time (from 2 to 4 weeks post-transplantation). The presence of transduced cells was also confirmed *post mortem* by autoradiography on cryosections of engineered tissues (Figure 22C). Therefore, injection of ~7.5 million RFP^+ hMPCs (~25% of the 30 million injected hMPCs) was enough to detect the signal *in vivo*.

8.4.2 Determination of virus titer and optimal MOI

After viral functionality was validated, viruses were produced in high amounts in the way previously described (see *Virus generation and amplification*). Based on the functionality results, we decided to continue with only one clone of each of the viruses generated. The titers of the final viral batches were determined in AD293 cells (Figure 23). We were able to produce ~10ml of high titer batches of all the viruses.

Viral titers determined in AD293 according to the Agilent protocol

AdTrack		pAdTrack-hPGC-1α 2		pShuttle-mRFP-hD2R 31	
dil 10^-7		dil 10^-7		dil 10^-7	dil 10^-6
25		34		7	10
27		25		8	12
19		32		9	12
26		33		3	8
19		47		1	18
33		29		1	18
34		33		1	7
30		32		7	14
24		30		11	19
12		29		4	15
32		22		8	15
30		22		2	16
25		21		4	12
38		10		6	26
37		19		3	11
33		28		7	20
23		30		8	15
25		35		3	10
29		27		4	15
27		34		11	10
32		24		5	9
24		37		6	14
27		24		1	15
25		34		5	18
19		40		5	25
15		37		8	17
24		42		5	11
21		36		2	19
13		32		3	18
24		26		6	16
				6	
av	25.73		30.13	5.16	14.83
titer [IFU/ml]	**1.38*10^12**		**1.61*10^12**	2.76*10^11	7.95*10^10
				av	**1.78*10^11**

objective 20x
24-well plates
10 different fields (per 2 well - duplicates)
eyepiece 10x/22

observed field=22mm/(10x1)=2.2mm
area of the field=0.055cm*0.055cm*3.1415 = 9.5*10^-3 cm2
area of a well=0.9cm*o.9cm*3.1415=2.5446cm2
total number of fields=2.5446/9.5*10^-3 = 267.85

titer=(average number of transduced cells) * 267.85 / (V(ml) of added virus * dilution factor)
titer=(average number of transduced cells) * 267.85 / (V(ml) of added virus * dilution factor)

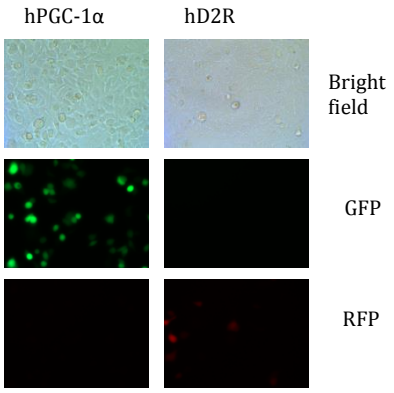

Figure 23 Viral titer determination of final batches including images of AD293 cells transduced with either hPGC-1α (green) or hD2R (red) virus

Optimal MOIs, based on the titers determined in AD293 cells, were tested for hMPCs. For the hD2R virus, an MOI of 100 gave ~25% transduced cells, whereas for the AdTrack and hPGC-1α viruses, an MOI of 1000 resulted in 100% transduction efficiency. We followed fluorescent protein expression for several days after cell transduction using different MOIs for the hPGC-1α virus (Figure 24).

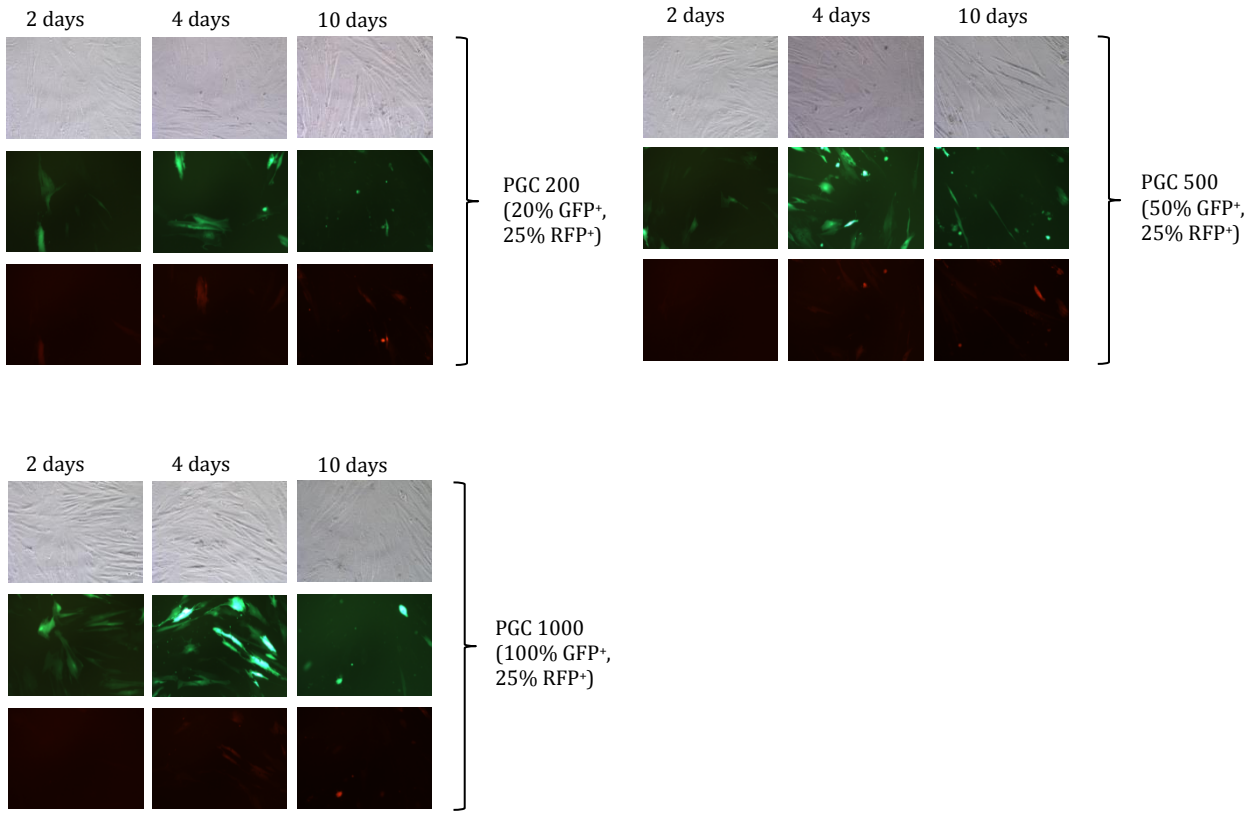

Figure 24 Bright field and fluorescent images of hMPCs transduced with hPGC-1α and hD2R viruses over period of 8 days
Three different MOIs for hPGC-1α virus were tested in combination with MOI of 100 for hD2R

We were able to notice that the maximum fluorescent intensity was achieved at the 4-day time point, whereas at later time points fluorescence was diminished due to cell death of transduced cells. This could be due to the high MOI, as the effect tended to be alleviated with lower MOIs, or due to the CMV promoter which drives a massive expression from the viral genome, possibly negatively impacting endogenous transcriptional processes and therefore the cell's own needs.

8.4.3 Kinetics of gene expression and virus toxicity

For the experiments *in vivo*, we were interested in transducing cells with multiple viruses at the same time without overwhelming the transcriptional apparatus of the cells. PET experiments with the hD2R virus demonstrated that the transduction rate of ~25% of injected cells is enough to track hMPCs *in vivo*. However, the minimal dose of the hPGC-1α virus that could still have an impact on mitochondrial gene expression and desired phenotypic changes was not known. For that reason, we decided to test several MOIs for hPGC-1α, in combination with 25% transduction for the hD2R virus and using 100% transduction for the GFP virus (AdTrack) as a control *in vitro*.

Although as previously mentioned, we observed the death of transduced cells over time *in vitro*, we did not detect an increase in creatine kinase (CK) levels in the media (Figure 25A). In addition, no difference was observed with increasing MOI for the hPGC-1α virus. Increased CK levels would indicate damaged cell membranes due to the toxic effect of the viruses. In fact, at 2 days after transduction, we measured a decrease in CK levels in the hPGC-1α transduced cells, which could indicate that increased hPGC-1α provides additional protection to the cell membrane. However, as the results were normalized to the total CK levels in cells, the difference in % CK between the AdTrack (GFP) and hPGC-1α transduced cells is partially due to the increase in total CK in the hPGC-1α transduced cells, at least for the highest MOI tested (Figure 25B). Given that the CK levels are low in myoblasts and increase with myotube formation, this result could indicate that viral overexpression of hPGC-1α drives higher CK expression possibly due to faster differentiation. In addition, no difference in % CK was detected 6 days after cell transduction.

A

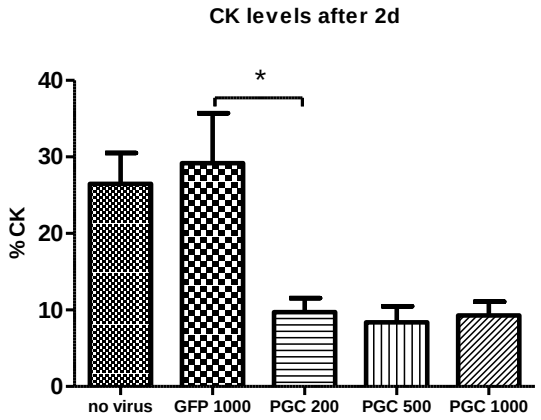

- **no viruses** = no viruses added
- **PGC 200** = PGC MOI 200 (20% GFP+) and D2R MOI 100 (25% RFP+)
- **PGC 500** = PGC MOI 500 (50% GFP+) and D2R MOI 100 (25% RFP+)
- **PGC 1000** = PGC MOI 1000 (100% GFP+) and D2R MOI 100 (25% RFP+)
- **GFP 1000** = GFP MOI 1000 (100% GFP+) and D2R MOI 100 (25% RFP+)

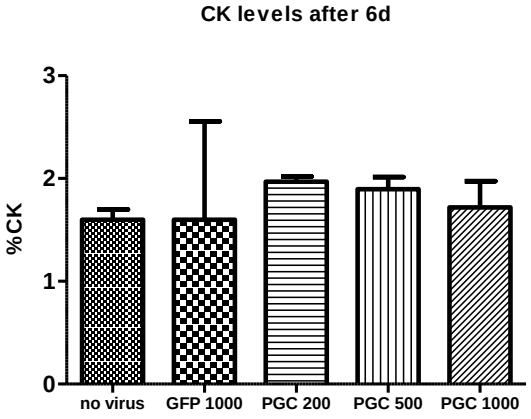

B

CK levels after 2 days

total CK	patient 1	patient 2	patient 3	t test
no virus	10.95	23.50	19.00	
GFP 1000	11.90	24.20	20.45	
PGC 1000	41.80	33.40	37.40	0.01
PGC 500	19.80	29.20	25.50	
PGC 200	14.30	23.35	24.45	

CK levels after 6 days

total CK	patient 1	patient 2
no virus	179.95	814.30
GFP 1000	105.15	798.90
PGC 1000	195.10	731.65
PGC 500	156.25	730.60
PGC 200	154.30	634.95

Figure 25 Creatine kinase activity of untransduced and transduced hMPCs at two different time points
(A) CK activity in media as a percentage to total CK in cells; (B) total CK levels in cells

Next, we measured gene expression in hMPCs at 2 and 6 days post-transduction, compared to the untransduced controls (a list of human specific qPCR primers is provided in Table 1). At the 2-day time point, we measured a massive overexpression of hD2R and hPGC-1α in transduced cells. There was a dose-dependent response in hPGC-1α expression with increasing MOI (Figure 26A). Interestingly, we detected a tendency towards lower hD2R expression in hPGC-1α and hD2R transduced cells compared to AdTrack (GFP) and hD2R transduced cells (Figure 26B). This could be due to competition between transgenes, although the effect was not significant. Importantly, hPGC-1α overexpression led to an increase in the expression of downstream target genes (Figure 26C) in a dose-dependent manner.

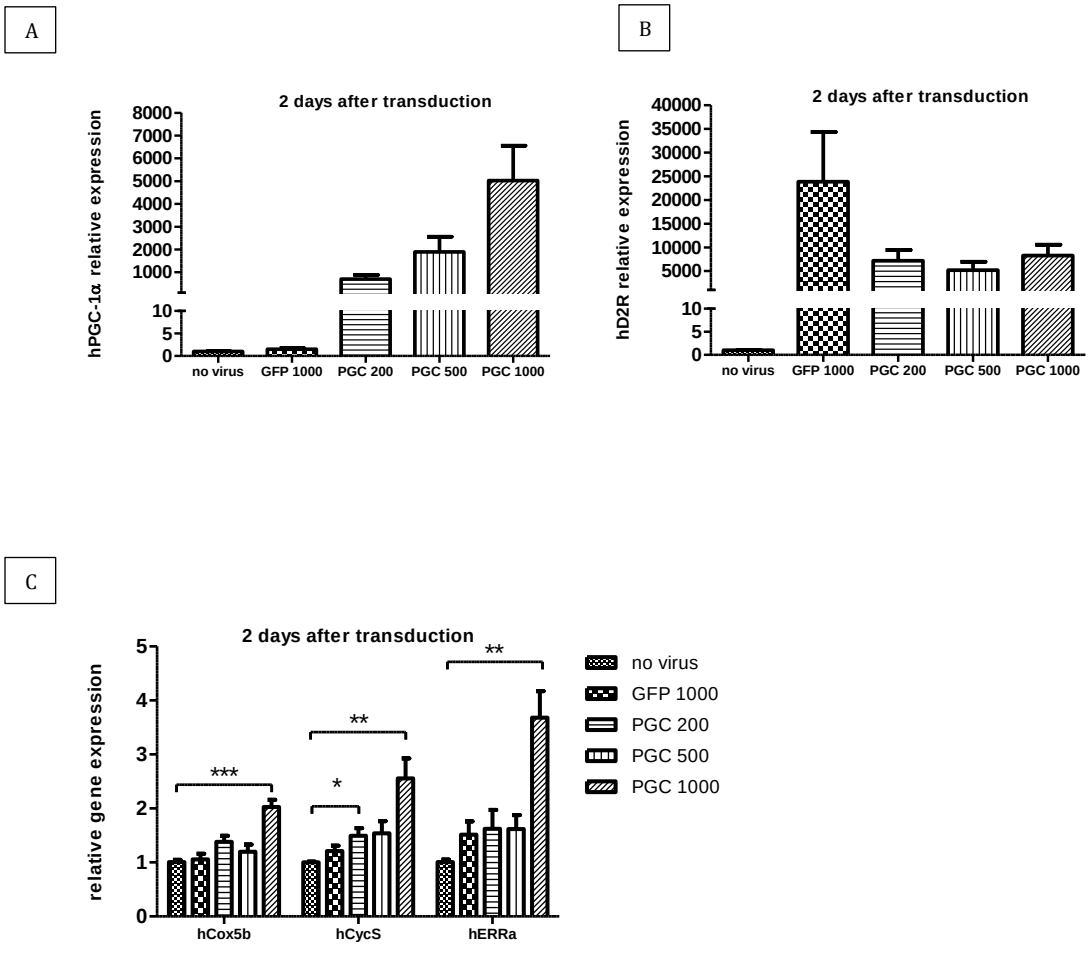

D

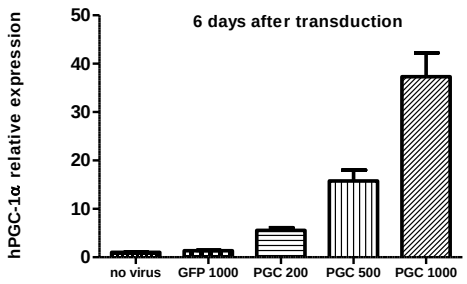

E

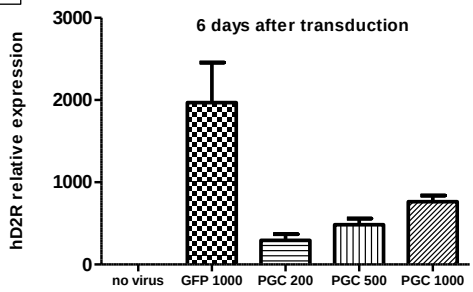

F

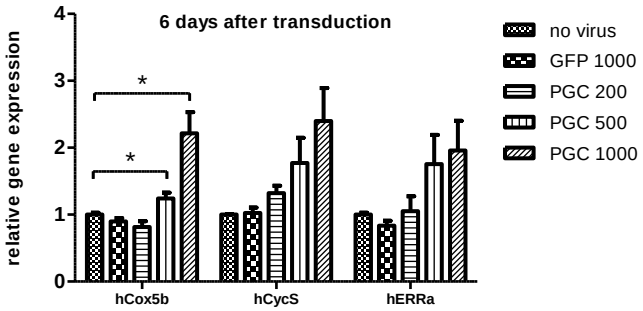

- **no viruses** = no viruses added
- **PGC 200** = PGC MOI 200 (20% GFP+) and D2R MOI 100 (25% RFP+)
- **PGC 500** = PGC MOI 500 (50% GFP+) and D2R MOI 100 (25% RFP+)
- **PGC 1000** = PGC MOI 1000 (100% GFP+) and D2R MOI 100 (25% RFP+)
- **GFP 1000** = GFP MOI 1000 (100% GFP+) and D2R MOI 100 (25% RFP+)

Figure 26 GOI gene expression and hPGC-1*α* target gene expression in hMPCs 2 days and 6 days after transduction

#Note: For qPCR protocol, see section Materials and Methods in *Project 3*

Target	Fwd primer (5'-3')	Rev primer (5'-3')
hCox5b	ATG GCT TCA AGG TTA CTT CGC	CCC TTT GGG GCC AGT ACA TT
hCycS	CTT TGG GCG GAA GAC AGG TC	TTA TTG GCG GCT GTG TAA GAG
hD2R	CCC CGC CAA ACC AGA GAA G	TTT TGC CAT TGG GCA TGG TCT
hERRα	AGG GTT CCT CGG AGA CAG AG	TCA CAG GAT GCC ACA CCA TAG
hPGC-1α	TCT GAG TCT GTA TGG AGT GAC AT	CCA AGT CGT TCA CAT CTA GTT CA
hTBP	CCC GAA ACG CCG AAT ATA ATC C	AAT CAG TGC CGT GGT TCG TG
hVEGF	GGA GGA GGG CAG AAT CAT CA	ACC AGG GTC TCG ATT GGA TG

Table 1 List of qPCR primers

At the 6-day time point, although analogous data were obtained regarding hD2R and hPGC-1α expression as well as expression of hPGC-1α regulated genes, lower levels were observed for all the genes measured (Figure 26D, 26E and 26F). This is consistent with our previous observation (see *Determination of virus titer and optimal MOI*) of cell death of transduced cells *in vitro*. However, at least based on the hPGC-1α target gene expression at 6 days, this increase in hPGC-1α was enough to account for the effect, as similar induction of cytochrome C oxidase subunit 5b (Cox5b), cytochrome c (CycS) and estrogen-related receptor α (ERRα) is detected in PGC-1α transgenic mice (previous observations).

8.5 Current state of research

The results obtained *in vitro* confirm the validity and usability of the generated viruses. They also indicate the possibility of at least several-week long transgene expression in hMPCs. However, the results *in vitro* cannot predict cell behavior or survival *in vivo*. Since we expect swift cell differentiation *in vivo* upon transplantation, it is possible that the transgene will be rapidly diluted in existing myotubes and therefore the effect on cell death might be negligible. The first *in vivo* experiments using the hPGC-1α expressing virus will shed light on these questions.

However, if the CMV promoter turns out to be suboptimal and responsible for cell toxicity *in vivo*, one could test other promoters which could be more useful for these purposes. In that regard, hPGC-1α can be driven from the muscle creatine kinase (MCK) promoter, and therefore expressed in the postmytotic stage of muscle cells. This should provide a physiologically closer model, driving hPGC-1α expression at the differentiated stage and at lower levels compared to the CMV promoter. Alternatively, one could aim at using inducible promoters for timely-defined and controlled expression from the transgene.

To date, we have been able to generate the viral vectors, test their functionality and toxicity *in vitro*, find optimal transduction settings, and produce batches of high titers required for cell transplantation applications. In addition, the PET results confirmed the possibility of spatio-temporal tracing of injected cells using the hD2R virus. Optimizations of [^{18}F]-Fallypride tracer synthesis and the timeline of signal detection have been achieved. Conditions related to cell transplantation and *ex vivo* assessment of regeneration have also been defined. Therefore, final *in vivo* results with the hPGC-1α expressing virus are expected in the near future.

In this study, adenoviruses were chosen as delivery vehicles, due to their high transduction efficiency, capacity to generate high titer batches and inability to integrate into the genome (40). However, they induce a considerable immune response and as such are a suboptimal choice for skeletal muscle gene therapy in the clinic (41). Therefore, if treatments concerning PGC-1α overexpression prove beneficial in terms of muscle regeneration, prior to application in humans, alternative delivery options for hPGC-1α would need to be selected.

8.6 References

1. Ciciliot, S., and Schiaffino, S. (2010) Regeneration of Mammalian Skeletal Muscle: Basic Mechanisms and Clinical Implications. *Current Pharmaceutical Design* **16**, 906-914
2. Turner, N. J., and Badylak, S. F. (2012) Regeneration of skeletal muscle. *Cell and tissue research* **347**, 759-774
3. Rossi, C. A., Pozzobon, M., and De Coppi, P. (2010) Advances in musculoskeletal tissue engineering: moving towards therapy. *Organogenesis* **6**, 167-172
4. Péault, B., Rudnicki, M., Torrente, Y., Cossu, G., Tremblay, J. P., Partridge, T., Gussoni, E., Kunkel, L. M., and Huard, J. (2007) Stem and progenitor cells in skeletal muscle development, maintenance, and therapy. *Molecular therapy : the journal of the American Society of Gene Therapy* **15**, 867-877
5. Tedesco, F. S., Dellavalle, A., Diaz-Manera, J., Messina, G., and Cossu, G. (2010) Repairing skeletal muscle: regenerative potential of skeletal muscle stem cells. *J Clin Invest* **120**, 11-19
6. Lepper, C., Partridge, T. a., and Fan, C.-M. (2011) An absolute requirement for Pax7-positive satellite cells in acute injury-induced skeletal muscle regeneration. *Development (Cambridge, England)* **138**, 3639-3646
7. Sambasivan, R., Yao, R., Kissenpfennig, A., Van Wittenberghe, L., Paldi, A., Gayraud-Morel, B., Guenou, H., Malissen, B., Tajbakhsh, S., and Galy, A. (2011) Pax7-expressing satellite cells are indispensable for adult skeletal muscle regeneration. *Development (Cambridge, England)* **138**, 3647-3656
8. Murphy, M. M., Lawson, J. a., Mathew, S. J., Hutcheson, D. a., and Kardon, G. (2011) Satellite cells, connective tissue fibroblasts and their interactions are crucial for muscle regeneration. *Development (Cambridge, England)* **138**, 3625-3637
9. McCarthy, J. J., Mula, J., Miyazaki, M., Erfani, R., Garrison, K., Farooqui, A. B., Srikuea, R., Lawson, B. a., Grimes, B., Keller, C., Van Zant, G., Campbell, K. S., Esser, K. a., Dupont-Versteegden, E. E., and Peterson, C. a. (2011) Effective fiber hypertrophy in satellite cell-depleted skeletal muscle. *Development (Cambridge, England)* **138**, 3657-3666
10. Price, F. D., Kuroda, K., and Rudnicki, M. A. (2007) Stem cell based therapies to treat muscular dystrophy. *Biochim Biophys Acta* **1772**, 272-283
11. Koning, M., Harmsen, M. C., van Luyn, M. J., and Werker, P. M. (2009) Current opportunities and challenges in skeletal muscle tissue engineering. *J Tissue Eng Regen Med* **3**, 407-415
12. Delo, D. M., Eberli, D., Williams, J. K., Andersson, K.-E., Atala, A., and Soker, S. (2008) Angiogenic gene modification of skeletal muscle cells to compensate for ageing-induced decline in bioengineered functional muscle tissue. *BJU international* **102**, 878-884
13. Fu, S. Y., and Gordon, T. (1995) Contributing factors to poor functional recovery after delayed nerve repair: prolonged denervation. *J Neurosci* **15**, 3886-3895
14. Niederle, B., and Mayr, R. (1978) Course of denervation atrophy in type I and type II fibres of rat extensor digitorum longus muscle. *Anat Embryol (Berl)* **153**, 9-21

15. Yiou, R., Yoo, J. J., and Atala, A. (2003) Restoration of functional motor units in a rat model of sphincter injury by muscle precursor cell autografts. *Transplantation* **76**, 1053-1060
16. Carosio, S., Berardinelli, M. G., Aucello, M., and Musaro, A. (2011) Impact of ageing on muscle cell regeneration. *Ageing Res Rev* **10**, 35-42
17. Handschin, C., and Spiegelman, B. M. (2006) Peroxisome proliferator-activated receptor gamma coactivator 1 coactivators, energy homeostasis, and metabolism. *Endocrine reviews* **27**, 728-735
18. Arany, Z., Foo, S.-Y., Ma, Y., Ruas, J. L., Bommi-Reddy, A., Girnun, G., Cooper, M., Laznik, D., Chinsomboon, J., Rangwala, S. M., Baek, K. H., Rosenzweig, A., and Spiegelman, B. M. (2008) HIF-independent regulation of VEGF and angiogenesis by the transcriptional coactivator PGC-1alpha. *Nature* **451**, 1008-1012
19. Handschin, C., Kobayashi, Y. M., Chin, S., Seale, P., Campbell, K. P., and Spiegelman, B. M. (2007) PGC-1alpha regulates the neuromuscular junction program and ameliorates Duchenne muscular dystrophy. *Genes & development* **21**, 770-783
20. Selsby, J. T., Morine, K. J., Pendrak, K., Barton, E. R., and Sweeney, H. L. (2012) Rescue of dystrophic skeletal muscle by PGC-1α involves a fast to slow fiber type shift in the mdx mouse. *PloS one* **7**, e30063-e30063
21. Hollinger, K., Gardan-Salmon, D., Santana, C., Rice, D., Snella, E., and Selsby, J. T. (2013) Rescue of dystrophic skeletal muscle by PGC-1α involves restored expression of dystrophin-associated protein complex components and satellite cell signaling. *American journal of physiology. Regulatory, integrative and comparative physiology* **305**, R13-23
22. Chan, M. C., Rowe, G. C., Raghuram, S., Patten, I. S., Farrell, C., and Arany, Z. (2014) Post-natal induction of PGC-1alpha protects against severe muscle dystrophy independently of utrophin. *Skeletal Muscle* **4**, 2-2
23. Wenz, T., Diaz, F., Spiegelman, B. M., and Moraes, C. T. (2008) Activation of the PPAR/PGC-1alpha pathway prevents a bioenergetic deficit and effectively improves a mitochondrial myopathy phenotype. *Cell metabolism* **8**, 249-256
24. Hanai, J.-i., Cao, P., Tanksale, P., Imamura, S., Koshimizu, E., Zhao, J., Kishi, S., Yamashita, M., Phillips, P. S., Sukhatme, V. P., and Lecker, S. H. (2007) The muscle-specific ubiquitin ligase atrogin-1 / MAFbx mediates statin-induced muscle toxicity. **117**
25. Sandri, M., Lin, J., Handschin, C., Yang, W., Arany, Z. P., Lecker, S. H., Goldberg, A. L., and Spiegelman, B. M. (2006) PGC-1alpha protects skeletal muscle from atrophy by suppressing FoxO3 action and atrophy-specific gene transcription. *Proceedings of the National Academy of Sciences of the United States of America* **103**, 16260-16265
26. Lin, J., Wu, H., Tarr, P. T., Zhang, C.-Y., Wu, Z., Boss, O., Michael, L. F., Puigserver, P., Isotani, E., Olson, E. N., Lowell, B. B., Bassel-Duby, R., and Spiegelman, B. M. (2002) Transcriptional co-activator PGC-1 alpha drives the formation of slow-twitch muscle fibres. *Nature* **418**, 797-801
27. Handschin, C., Chin, S., Li, P., Liu, F., Maratos-Flier, E., Lebrasseur, N. K., Yan, Z., and Spiegelman, B. M. (2007) Skeletal muscle fiber-type switching, exercise intolerance, and myopathy in PGC-1alpha muscle-specific knock-out animals. *The Journal of biological chemistry* **282**, 30014-30021
28. Wenz, T., Rossi, S. G., Rotundo, R. L., Spiegelman, B. M., and Moraes, C. T. (2009) Increased muscle PGC-1 ⎵ expression protects from sarcopenia and metabolic disease during aging. *PNAS* **106**, 20405-20410

29. Herschman, H. R. (2004) Noninvasive imaging of reporter gene expression in living subjects. *Adv Cancer Res* **92**, 29-80
30. Gambhir, S. S. (2002) Molecular imaging of cancer with positron emission tomography. *Nat Rev Cancer* **2**, 683-693
31. Facey, K., Bradbury, I., Laking, G., and Payne, E. (2007) Overview of the clinical effectiveness of positron emission tomography imaging in selected cancers. *Health Technol Assess* **11**, iii-iv, xi-267
32. Tulving, E., Kapur, S., Craik, F. I., Moscovitch, M., and Houle, S. (1994) Hemispheric encoding/retrieval asymmetry in episodic memory: positron emission tomography findings. *Proc Natl Acad Sci U S A* **91**, 2016-2020
33. Tillisch, J., Brunken, R., Marshall, R., Schwaiger, M., Mandelkern, M., Phelps, M., and Schelbert, H. (1986) Reversibility of cardiac wall-motion abnormalities predicted by positron tomography. *N Engl J Med* **314**, 884-888
34. Lardinois, D., Weder, W., Hany, T. F., Kamel, E. M., Korom, S., Seifert, B., von Schulthess, G. K., and Steinert, H. C. (2003) Staging of non-small-cell lung cancer with integrated positron-emission tomography and computed tomography. *N Engl J Med* **348**, 2500-2507
35. MacLaren, D. C., Gambhir, S. S., Satyamurthy, N., Barrio, J. R., Sharfstein, S., Toyokuni, T., Wu, L., Berk, A. J., Cherry, S. R., Phelps, M. E., and Herschman, H. R. (1999) Repetitive, non-invasive imaging of the dopamine D2 receptor as a reporter gene in living animals. *Gene Ther* **6**, 785-791
36. Missale, C., Nash, S. R., Robinson, S. W., Jaber, M., and Caron, M. G. (1998) Dopamine receptors: from structure to function. *Physiol Rev* **78**, 189-225
37. Ek, J., Andersen, G., Urhammer, S. A., Gaede, P. H., Drivsholm, T., Borch-Johnsen, K., Hansen, T., and Pedersen, O. (2001) Mutation analysis of peroxisome proliferator-activated receptor-gamma coactivator-1 (PGC-1) and relationships of identified amino acid polymorphisms to Type II diabetes mellitus. *Diabetologia* **44**, 2220-2226
38. Cho, W., Taylor, L. P., Mansour, A., and Akil, H. (1995) Hydrophobic residues of the D2 dopamine receptor are important for binding and signal transduction. *J Neurochem* **65**, 2105-2115
39. Luo, J., Deng, Z.-L., Luo, X., Tang, N., Song, W.-X., Chen, J., Sharff, K. a., Luu, H. H., Haydon, R. C., Kinzler, K. W., Vogelstein, B., and He, T.-C. (2007) A protocol for rapid generation of recombinant adenoviruses using the AdEasy system. *Nature protocols* **2**, 1236-1247
40. Quantin, B., Perricaudet, L. D., Tajbakhsh, S., and Mandel, J. L. (1992) Adenovirus as an expression vector in muscle cells in vivo. *Proc Natl Acad Sci U S A* **89**, 2581-2584
41. Jooss, K., and Chirmule, N. (2003) Immunity to adenovirus and adeno-associated viral vectors: implications for gene therapy. *Gene Ther* **10**, 955-963

9 Discussion and outlook

Our aim was to explore the role of peroxisome proliferator-activated receptor γ coactivator 1α (PGC-1α) in skeletal muscle regeneration and repair from several angles and using various approaches – *in vitro*, *in vivo*, e*x vivo* and *in situ* in combination with cardiotoxin, eccentric exercise, laser injuries and overexpression in cells prior to their transplantation into injured muscle. We hypothesized that PGC-1α would improve regeneration as its expression rises with differentiation of myoblasts into myotubes (1), alleviates some dystrophic and atrophy phenotypes (2-6), reduces inflammation (7-9) and reactive oxygen species (ROS) levels (10), is responsible for the oxidative endured muscle phenotype (11), leads to increased oxidative metabolism (12-14), improves vascularization (15), modulates neuromuscular junction (NMJ) (2) and preserves muscle integrity compromised by aging (16). Indeed, we were able to reveal several important parameters of regeneration that are influenced by PGC-1α levels in muscle.

Namely, we detected an initially faster regenerative response in PGC-1α transgenic mice upon cardiotoxin (CTX) injury, through prompter modulation of chemokine expression resulting in faster accumulation of macrophages and clearance of necrotic tissue. This response was dependent on PGC-1α, since muscle-specific transgenic and knock-out mice exhibited opposite phenotypes. We proposed that plausible drivers of these effects are insulin-like growth factor 1 (IGF-1) and myostatin (Mstn), whose expression levels seem to be dependent on PGC-1α. IGF-1 transgenic and $Mstn^{-/-}$ mice were reported to have an analogous phenotype to the one we observed in PGC-1α transgenic mice (17, 18).

We speculated that the prompter response to injury observed in PGC-1α transgenic mice might be due to the specific inflammatory cell milieu that exists in the muscle prior to injury. In that respect, it would be interesting to explore in detail the muscle mast cell and macrophage phenotype in PGC-1α transgenic and knock-out animals. These are the first cells that respond to injury (19, 20), and therefore might modulate the subsequent inflammatory stages, such as neutrophil and monocyte attraction.

Skeletal muscle regeneration *in vivo* can be followed using several injury models: intramuscular toxin injections, mechanical infliction of a wound, and eccentric contractions (21).

Although very harsh and physiologically distant, cardiotoxin injection is one of the most widely applied injury models. Toxin injection model is prevalent in the literature probably due to the ease of accomplishing injury and reproducibility, offering a large body of literature for comparison. Therefore, we decided to study the role of PGC-1α in skeletal muscle regeneration using cardiotoxin injection model.

However, we also experimented with crush injury (mechanical model) and downhill running (eccentric contraction model) in search of a less damaging and physiologically closer injury model. We hypothesized that the less damage might let the differences between genotypes become more pronounced. Crush injuries were performed on the belly region of the TA muscle, and only part of the muscle was affected (Figure 1), in contrast to the cardiotoxin injection, which damaged the whole muscle.

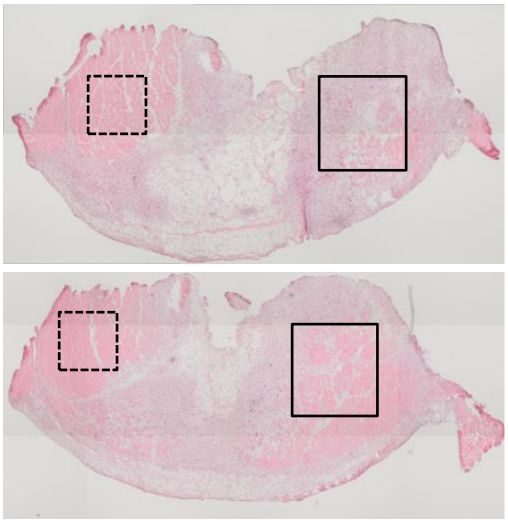

[#]Figure 1 Hematoxylin and eosin (H&E) staining on crushed tibialis anterior muscle (TA) section illustrating non-homogeneity of the damage
Dashed black box – undamaged fibers. Sections of the same muscle separated by several hundreds of μm apart additionally illustrate longitudinal non-homogeneity of the damage: black box – necrotic/regenerating area. Notice that the black box on one section contains only necrotic fibers, while on other necrotic parts are reduced.

[#]Note: for protocol, see Histology in Materials and Methods section of *Project 1*

We assumed that this type of injury might therefore have less damaging effect, and result mainly in regeneration of the damaged fibers rather than complete fiber necrosis and formation of new fibers as in the case of cardiotoxin. Nevertheless, crushing led to severe damage evaluated by contractility measurements at 10 days post injury (Figure 2). Results were similar to the ones obtained for cardiotoxin injection at the same time point after the infliction of a wound.

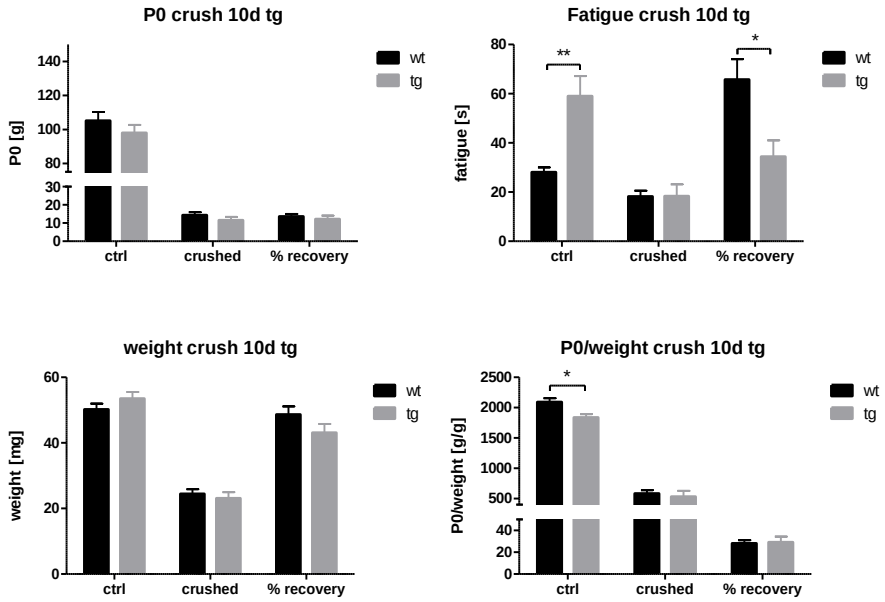

#Figure 2 Muscle contractility measurements on injured and uninjured TA muscles 10 days after the crush of muscle creatine kinase muscle-specific PGC-1α transgenic (MCK-mTG) mice
Values for crushed muscles are normalized to the values of uncrushed ones and plotted as % of recovery. (A) Maximal force measurement; (B) Fatigue resistance measurement (repetitive measurements), (C) weight of TA muscles; (D) Specific force calculation

[#]Note: for protocol, see Muscle contractility measurements *in situ* in Materials and Methods section of *Project 1*; here, fatigue protocol consisted of 50 repeated contractions (100Hz for 500ms, evoked once every 2 seconds). The time to reach 70% of the initial force was measured.

Furthermore, data obtained from crush injuries were difficult to analyze due to heterogeneous destruction of the muscle tissue, which complicated quantification and normalization (Figure 3). Since our results did not indicate considerably lower impact of crush injury compared to cardiotoxin, we decided not to focus on this injury model.

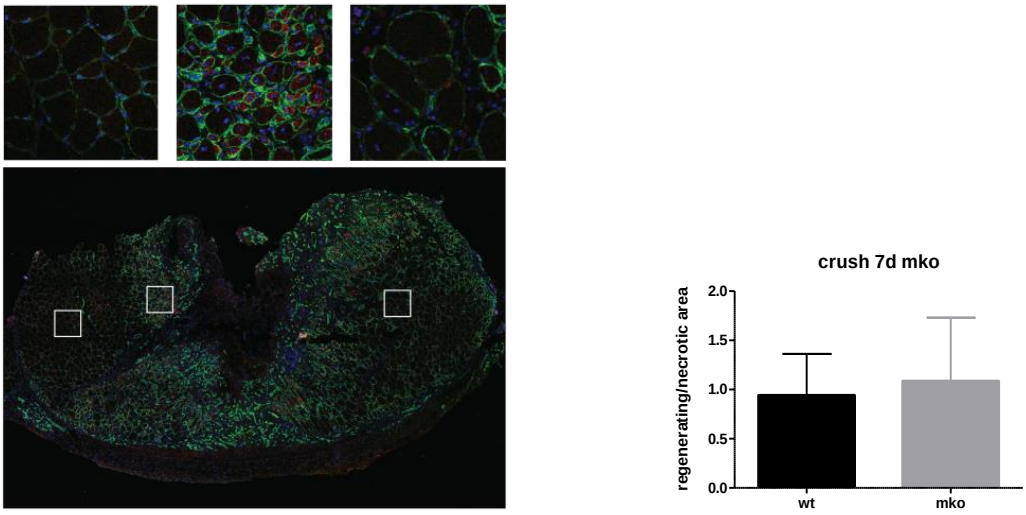

#Figure 3 Immunohistochemistry (IHC) and quantification of regenerative area on same muscle sample as in Figure 1
(A) laminin-green, dapi-blue, embryonic myosin heavy chain (eMyHC)-red. Undamaged, regenerating and necrotic parts of tissue section are in white boxes and magnified above. (B) Quantification results of regeneration based on eMyHC staining 7 days after the crush injury in TA of myogenic factor 5 muscle-specific knock-out (Myf5- mKO) mice

#Note: for protocol, see Histology in Materials and Methods section of *Project 1* (primary antibody against eMyHC: F1.652 DSHB; secondary antibody: goat-anti-mouse IgG1 Alexa568 A21124 Invitrogen)

Likewise, we also tested downhill running as a strenuous exercise model, which through eccentric contractions inflicts damage to the muscle (22). After extensive optimization of the running protocol, time points analyzed and choice of affected muscles, we were not able to achieve measurable injury relevant to the process of regeneration. More specifically, we could not detect necrosis and regeneration of fibers on the histological level. Consequently, this injury model was also excluded from the study.

However, there are other means of inducing injury in muscle tissue based on lengthening contractions, and in a more pronounced and controllable way compared to forced eccentric exercise. The exercise based, and therefore physiologically relevant model, employs *in situ* contractions of the muscle of choice in anesthetized mice (23). It would be important to complement the data that we obtained with this model of injury before excluding the contribution of PGC-1α in the regeneration outcome in terms of pace of reaching full recovery. In our

experiments, cardiotoxin induced complete necrosis of myotubes and PGC-1α levels dropped drastically in both transgenic and wild-type mice. We demonstrated that PGC-1α expression slowly increased and reached basal levels regardless of the transgene's presence. Therefore, if we make use of an injury method that will preserve the existing difference in PGC-1α levels between genotypes by not inducing thorough destruction of myotubes, which is something that is observed in most human muscle injuries, we might expect to see more relevant alterations in the recovery process.

Regarding *in vitro* experiments, it would be useful to expand the current data by closely analyzing differentiation of transgenic vs. wild-type myoblasts, especially after prolonged differentiation, which should result in pronounced differences in PGC-1α expression compared to our results. Alternatively, one can induce PGC-1α expression virally in the myoblast stage at the initiation of differentiation, and determine if PGC-1α controls the differentiation process. Based on the *in vitro* data from the toxicity studies of the viruses we generated (increased creatine kinase expression after 2 days of transduction with PGC multiplicity of infection (MOI) 1000 compared to GFP MOI 1000), it is possible to expect an increase in differentiation with higher levels of PGC-1α (24).

In addition to affecting regeneration, PGC-1α seems to make a direct contribution to sarcolemma resealing capabilities as well. We demonstrated a reduced propensity for resealing in C2C12 myoblasts upon knock-down (KD) of PGC-1α. This was accompanied by differential expression of several important genes, the most promising being synaptotagmin VII (Syt7) (25). Namely, we were able to detect massive upregulation of Syt7 with viral overexpression of PGC-1α in C2C12 myoblasts and myotubes, but also increased protein levels in PGC-1α transgenic mice. In addition, previously published Chip-seq data from our laboratory indicate direct regulation of Syt7 by PGC-1α (26). Furthermore, we found that increase in integrin 7α (Itga7) upon exercise is dependent on PGC-1α expression, and could be responsible for modestly reduced membrane stability in PGC-1α mKO mice observed after downhill running (DHR). Having in mind the difference in membrane stability and resealing (27), it would be interesting to further explore the role of PGC-1α in these processes.

Based on our results, Syt7 would give a clear target gene to follow in order to demonstrate that its expression is the reason for the observed phenotype in the resealing (25),

given that the protein levels are reduced in PGC-1α mKO mice. It would be also worth looking at the protein levels of mitsugumin 53 (MG53) in mouse models with gain and loss of function of PGC-1α. We detected an increase MG53 on the mRNA level only in the transgenic mice, and MG53 is one of the few proteins for which a direct role in skeletal muscle membrane resealing has been demonstrated (28). In addition, it would be significant to supplement the experimental proof for reduced membrane repair with PGC-1α knock-out by looking at the primary myoblasts and fibers isolated from the mKO mice, and also to test for resealing in the contexts of injury induced by various factors. This would strengthen the findings and prove that the observed effect is also present in the physiologically closer model (*ex vivo* vs. *in vitro*). However, one needs to be careful in order to be able to distinguish between membrane leakiness caused by damage or the stretching effect (27). Therefore, membrane damage *ex vivo* can be induced by exposure to detergent solution, microelectrode penetration or bead rolling (28, 29), whereas membrane stability can be evaluated with milder protocols for stretching (e.g. FlexCell Tension system) or contraction by electrical stimulation (30-33).

With regard to the difference between membrane stability and resealing, we demonstrated that Itga7 levels are increased in wild type (WT) but not PGC-1α mKO after exercise. Itga7 is known to provide membrane stabilization and protection in cases of subsequent injury (34, 35). Therefore, it would be interesting to repeat the downhill running experiment but with two bouts of running separated by one week, and then assess sarcolemma damage in mice. Exercise is known to make muscles resistant to damage (36), and one reason for this is possibly the increase in Itga7 (35). However, PGC-1α also increases with exercise and plays a role in muscle adaptation to exercise (37). In that respect, it would be useful to complement the existing data with DHR in PGC-1α transgenic mice and see whether increased levels of PGC-1α without the exercise provide augmented stability to the membrane, or whether the protective effect of exercise can be exacerbated by overexpression of PGC-1α.

Finally, the potentially direct role of PGC-1α in membrane resealing could be supported by overexpressing PGC-1α in dysferlin knock-out ($Dysf^{-/-}$) mice (38). We should expect the overall dystrophic phenotype to be alleviated, and membrane resealing, specifically, improved. In addition, if Syt7 (25) is indeed the main factor in PGC-1α-dependent resealing, reduction and

induction of Syt7 in the muscle of genetically modified mice would result in decreased and increased capability to repair sarcolemma, respectively.

Next, we were able to delineate the influence of PGC-1α expression in the satellite cell (SC) niche, on SC activation and proliferation. SCs with higher levels of PGC-1α in the niche (muscle fiber) were able to respond to activation stimuli in a faster manner. The proliferative output of these cells was also increased compared to control mice. In Myf5-mKO mice, SC activation seemed reduced and with slower progression towards differentiated myoblast stage, although this difference was not significant. By using primary fibers from PGC-1α mouse models, we found that at least partially, increased SC proliferation with PGC-1α overexpression was due to differential expression of fibronectin in the basal lamina of muscle fibers. More specifically, we detected reduced levels of fibronectin in PGC-1α transgenic mice, and increased in Myf5-mKO mice. In addition, in the proof-of-concept experiment, we confirmed that extrinsic fibronectin reduces the proliferative output of SCs. Contrary to the results in Myf5-mKO, SC proliferative output and fibronectin levels were unchanged in human α-skeletal actin (HSA)-mKO mice.

Apart from SC activation and proliferation, another possible role of PGC-1α in the context of SCs is quiescence. In that respect, there are previous studies indicating the potential implication of PGC-1α in quiescence of stem cells, primarily hematopoietic stem cells (HSCs). It has been reported that knock-out of liver kinase B1 ($LKB1^{-/-}$) leads to depletion of HSCs, but surprisingly, this effect is not dependent on 5' AMP-activated protein kinase (AMPK) or mammalian target of rapamycin complex 1 (mTORC1) signaling. Metabolic profiling experiments determined changes in peroxisome proliferator-activated receptor (PPAR) pathways, such as downregulation in PGCs (39-41). In addition, knock-out of promyelocytic leukemia protein ($PML^{-/-}$) results in HSC depletion as well. PML together with PPARδ is responsible for HSC asymmetric division and therefore self-renewal through increased mitochondrial fatty acid oxidation (FAO) (42). In breast cancer, PML-dependent cell survival was reliant on PGC-1α deacetylation favoring PPAR signaling (43). Additionally, limited ROS production is another factor contributing to stem cell quiescence (44, 45), and PGC-1α is a known regulator of ROS metabolism through induced production of ROS-detoxifying enzymes

(10). Therefore, it would be important to investigate more closely the role of PGC-1α in SCs, both in terms of SC maintenance and activation.

Another potentially interesting finding in MCK-mTG mice is related to SC senescence. Specifically, we measured lower expression of fibroblast growth factor 2 (FGF-2) in combination with increased levels of sprouty 1 (Spry1). Myf5-mKO mice on the other hand exhibited an increase in both FGF-2 and Spry1. These measurements were carried out in 2-3 month-old mice. Spry1 is a significant regulator of SC senescence. In SCs, Spry1 is important for self-renewal and reversible quiescence, and is an inhibitor of FGF signaling (46). FGF-2 expression in the SC niche increases with age and provokes SC activation. Prolonged FGF signaling has the same effect as loss of Spry1 and results in SC depletion (47). Therefore, it would be worthwhile to study SCs in aged MCK-mTG and Myf5-mKO mice in regard to FGF signaling.

PGC-1α expression increases with exercise and leads to muscle adaptation to exercise (37). One outcome of regular endurance exercise is a fiber type switch towards the oxidative phenotype (48). Oxidative fibers are known to have more SCs than glycolytic ones (49). At the same time, acute as well as long-term exercise increases SC numbers (50-52). Although PGC-1α overexpression mimics the trained phenotype of muscles in some aspects (11), this does not extend, for example, to SC numbers. Consequently, it would be interesting to explore the effects of long-term exercise on SC numbers and behavior in PGC-1α loss and gain of function mice.

The finding that PGC-1α overexpression in fibers does not result in increased SC numbers came as a surprise to us. However, this discrepancy could be partially explained by the detected differences in fibronectin (FN) expression. We compared expression levels of several ECM/basal lamina components between oxidative and glycolytic muscles, with or without PGC-1α overexpression (Figure 4).

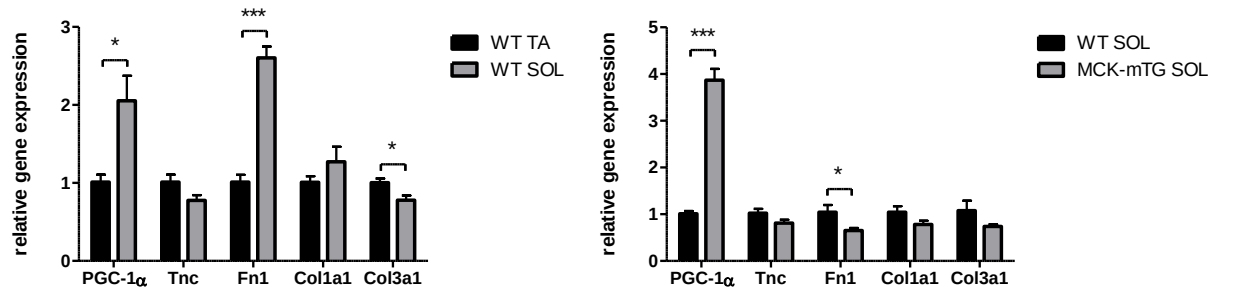

#Figure 4. Relative mRNA expression levels of genes in oxidative soleus (SOL) vs. glycolytic (TA) muscles and in oxidative muscle (SOL) from WT vs. MCK-mTG mice

#Note: for qPCR protocol, see RNA extraction and relative quantitative PCR (qPCR) in Materials and Methods section of *Project 2*

We noticed that oxidative SOL muscle has double the expression levels of PGC-1α compared to glycolytic TA, as expected, and that this is accompanied by increased FN expression levels. On the other hand, when we compared relative expression levels of the same genes in SOL muscle of WT and MCK-mTG mice, we detected even higher expression of PGC-1α in MCK-mTG, followed by a reduction in FN expression. Given the phenotype documented for LARGE^{myd} mice (53), which describes co-occurrence of increased SC numbers and elevated FN levels, we can speculate that overexpression of PGC-1α does not follow the oxidative muscle characteristics in terms of SC numbers due to the reduced FN expression.

Another exciting research direction would be to assess the outcomes of conditional PGC-1α loss and overexpression in SCs, and in that context short- and long-term effects of PGC-1α on adult SC quiescence, activation and self-renewal. There might still be some surprises for us regarding PGC-1α function in SCs. For example, we could expect that overexpression of PGC-1α in SCs might lead to increased SC cycling, activation and therefore potential SC depletion over time due to an increase in oxidative phosphorylation (OXPHOS). On the other hand, one can speculate that increased PGC-1α signaling would primarily boost FAO, which would expand SC self-renewal capacity.

Although we have only scratched the surface of PGC-1α's role in SC biology, we have demonstrated some interesting and surprising features, especially in relation to PGC-1α overexpression in fibers. Nevertheless, these indirect effects of PGC-1α might also affect SCs

themselves. Hence, it would also be essential to screen for intrinsic differences of SCs upon PGC-1α overexpression or loss in fibers. For this reason, crossing MCK-mTG mice with Pax7-GFP mice would provide easy access to the pure SC population that can be isolated by fluorescence-activated cell sorting (FACS) and analyzed *in vitro*. Our finding regarding modulation of SC behavior via PGC-1α in the niche is particularly interesting from a therapeutic point of view.

In terms of therapeutic applications, we were also interested in exploring what the effects PGC-1α overexpression in myoblasts, prior to their usage in cell transplantations, might have on muscle regeneration. In our proof-of-concept study, we aimed to induce PGC-1α expression in isolated human myoblasts, and then inject them into mice in order to monitor their behavior over time. Non-invasive observation of their survival, vascularity, migration and metabolic activity is possible with positron emission tomography (PET), which is already used in the clinic (54-56). One of the main obstacles in cell transplantation techniques is compromised cell survival due to reduced innervation and blood vessel formation (57). As PGC-1α controls both of these processes (2, 15) and has additionally been demonstrated to alleviate dystrophic conditions (2-5), improve muscle endurance (11) and diminish age-related deterioration (16), we hypothesized that the application of PGC-1α in skeletal muscle regeneration as a gene therapy treatment would prove beneficial. This project is an interdisciplinary enterprise involving three laboratories specializing in molecular biology, transplantational medicine and medical imaging.

We have reached the stage where all the optimizations have been made and standards for inducing injury and delivering treatments (cell transplantation) as well as assessing muscle functionality, have been established. We are awaiting the final results which should demonstrate if PGC-1α overexpression in myoblasts can provide a benefit in skeletal muscle regenerative medicine. We hope we will be able to answer this question by looking at muscle tissue formation and survival, as well as vascularization and innervation, both *in vivo* using PET, and *ex vivo* using isolated tissue.

Based on the results presented in this thesis, we could speculate that PGC-1α might prove to be of greater use in muscle regenerative medicine than initially thought. Fusion of transduced myoblasts with recipient myotubes would increase PGC-1α levels in the fiber, which could replicate to a certain extent the conditions seen in PGC-1α overexpressing (MCK-mTG) mice.

Therefore, we could expect to observe the positive effect on SCs and possibly stability and repair of the sarcolemma. In addition, in cases of minor injuries leading to partial myofiber necrosis, we could detect improved regeneration due to altered immune response and SC behavior. This outcome would be limited not only in size (as complete necrosis of myofibers would result in loss of PGC-1α expression from the transgene), but also in time, due to the limited duration of the transgene expression from the adenovirus (58).

If the results concerning combined gene and cell therapy (PGC-1α overexpression in human myoblasts) in mice are positive, the next step would be to translate this into humans, and therefore the first task would be to establish a safe way of PGC-1α induction in myoblasts. For this, another vehicle, with a reduced propensity to induce immune response would be optimal. Possible solutions include adeno-associated viruses (AAV) and naked DNA (59) . While AAVs have low immunogenicity and are able to transduce muscles after intramuscular (60) and systemic administration (61) and are therefore very good candidates for gene delivery *in vivo*, their propensity to transduce myoblasts *in vitro* is much reduced (62). In addition, AVVs have lower insert size capacity compared to adnoviruses, which can be a limiting factor (63). On the other hand, naked DNA transfer has long been significantly less potent delivery tool compared to viral vectors. However, this is improved using chemical (e.g. liposome) or physical (e.g. electroporation) approaches, which considerably reduce the differences in efficiency compared to viral vectors (64).

In addition, our gene therapy approach would be combined with autologous stem cell therapy in patients, again, in order to prevent immune reaction. This approach would be potentially applicable for intramuscular injections and therefore treating selected muscles, as lack of homing ability in intravenously injected myoblasts is the limiting factor in skeletal muscle regenerative medicine (65).

Our findings are overall in line with the existing body of literature on the therapeutic potential of PGC-1α in the context of muscular dystrophies. The results presented here further contribute to the understanding of the multifaceted role of PGC-1α overexpression in the mouse model of Duchenne muscular dystrophy (DMD). More specifically, our data indicate improvement of regenerative potential in addition to muscle protection. Moreover, there seems to

be a direct link between sarcolemma resealing and stability with PGC-1α expression levels, although this requires further investigation.

Exercise is not a therapeutic option in many cases of muscular disease, while in others, it is very difficult to define an exercise regimen that could improve the condition without causing more harm (66, 67). Therefore, raising PGC-1α levels might be an interesting alternative to exercise. Although PGC-1α is a nodal factor in skeletal muscle adaptation to endurance exercise, its induction does not fully mimic the effects of exercise. For example, we detected reduced SC numbers in PGC-1α transgenic mice, while endurance exercise increases their number. However, more important than numbers might be the myogenic capacity of SCs, which increases with endurance exercise (51), while PGC-1α overexpression in muscle seems to improve SC activation and proliferation.

We should emphasize that although we have discovered several important roles of PGC-1α in skeletal muscle regeneration and repair, many more questions have emerged as a consequence. Therefore, future research could provide a more complete and clear picture of the ways in which we can exploit PGC-1α for therapeutic purposes in muscle regenerative medicine and muscular dystrophies, by answering some of these newly posed questions.

9.1 References

1. Murray, J., and Huss, J. M. (2011) Estrogen-related receptor alpha regulates skeletal myocyte differentiation via modulation of the ERK MAP kinase pathway. *Am J Physiol Cell Physiol* **301**, C630-645
2. Handschin, C., Kobayashi, Y. M., Chin, S., Seale, P., Campbell, K. P., and Spiegelman, B. M. (2007) PGC-1alpha regulates the neuromuscular junction program and ameliorates Duchenne muscular dystrophy. *Genes & development* **21**, 770-783
3. Selsby, J. T., Morine, K. J., Pendrak, K., Barton, E. R., and Sweeney, H. L. (2012) Rescue of dystrophic skeletal muscle by PGC-1α involves a fast to slow fiber type shift in the mdx mouse. *PloS one* **7**, e30063-e30063
4. Hollinger, K., Gardan-Salmon, D., Santana, C., Rice, D., Snella, E., and Selsby, J. T. (2013) Rescue of dystrophic skeletal muscle by PGC-1α involves restored expression of dystrophin-associated protein complex components and satellite cell signaling. *American journal of physiology. Regulatory, integrative and comparative physiology* **305**, R13-23
5. Chan, M. C., Rowe, G. C., Raghuram, S., Patten, I. S., Farrell, C., and Arany, Z. (2014) Post-natal induction of PGC-1alpha protects against severe muscle dystrophy independently of utrophin. *Skeletal Muscle* **4**, 2-2
6. Sandri, M., Lin, J., Handschin, C., Yang, W., Arany, Z. P., Lecker, S. H., Goldberg, A. L., and Spiegelman, B. M. (2006) PGC-1alpha protects skeletal muscle from atrophy by suppressing FoxO3 action and atrophy-specific gene transcription. *Proceedings of the National Academy of Sciences of the United States of America* **103**, 16260-16265
7. Handschin, C., and Spiegelman, B. M. (2008) The role of exercise and PGC1alpha in inflammation and chronic disease. *Nature* **454**, 463-469
8. Handschin, C., Chin, S., Li, P., Liu, F., Maratos-Flier, E., Lebrasseur, N. K., Yan, Z., and Spiegelman, B. M. (2007) Skeletal muscle fiber-type switching, exercise intolerance, and myopathy in PGC-1alpha muscle-specific knock-out animals. *The Journal of biological chemistry* **282**, 30014-30021
9. Eisele, P. S., Salatino, S., Sobek, J., Hottiger, M. O., and Handschin, C. (2013) The peroxisome proliferator-activated receptor γ coactivator 1α/β (PGC-1) coactivators repress the transcriptional activity of NF-κB in skeletal muscle cells. *The Journal of biological chemistry* **288**, 2246-2260
10. St-Pierre, J., Drori, S., Uldry, M., Silvaggi, J. M., Rhee, J., Jager, S., Handschin, C., Zheng, K., Lin, J., Yang, W., Simon, D. K., Bachoo, R., and Spiegelman, B. M. (2006) Suppression of reactive oxygen species and neurodegeneration by the PGC-1 transcriptional coactivators. *Cell* **127**, 397-408
11. Lin, J., Wu, H., Tarr, P. T., Zhang, C.-Y., Wu, Z., Boss, O., Michael, L. F., Puigserver, P., Isotani, E., Olson, E. N., Lowell, B. B., Bassel-Duby, R., and Spiegelman, B. M. (2002) Transcriptional co-activator PGC-1 alpha drives the formation of slow-twitch muscle fibres. *Nature* **418**, 797-801
12. Wu, Z., Puigserver, P., Andersson, U., Zhang, C., Adelmant, G., Mootha, V., Troy, A., Cinti, S., Lowell, B., Scarpulla, R. C., and Spiegelman, B. M. (1999) Mechanisms controlling mitochondrial biogenesis and respiration through the thermogenic coactivator PGC-1. *Cell* **98**, 115-124

13. Vega, R. B., Huss, J. M., and Kelly, D. P. (2000) The coactivator PGC-1 cooperates with peroxisome proliferator-activated receptor alpha in transcriptional control of nuclear genes encoding mitochondrial fatty acid oxidation enzymes. *Mol Cell Biol* **20**, 1868-1876
14. Wende, A. R., Huss, J. M., Schaeffer, P. J., Giguere, V., and Kelly, D. P. (2005) PGC-1alpha coactivates PDK4 gene expression via the orphan nuclear receptor ERRalpha: a mechanism for transcriptional control of muscle glucose metabolism. *Mol Cell Biol* **25**, 10684-10694
15. Arany, Z., Foo, S.-Y., Ma, Y., Ruas, J. L., Bommi-Reddy, A., Girnun, G., Cooper, M., Laznik, D., Chinsomboon, J., Rangwala, S. M., Baek, K. H., Rosenzweig, A., and Spiegelman, B. M. (2008) HIF-independent regulation of VEGF and angiogenesis by the transcriptional coactivator PGC-1alpha. *Nature* **451**, 1008-1012
16. Wenz, T., Rossi, S. G., Rotundo, R. L., Spiegelman, B. M., and Moraes, C. T. (2009) Increased muscle PGC-1alpha expression protects from sarcopenia and metabolic disease during aging. *Proc Natl Acad Sci U S A* **106**, 20405-20410
17. McCroskery, S., Thomas, M., Platt, L., Hennebry, A., Nishimura, T., McLeay, L., Sharma, M., and Kambadur, R. (2005) Improved muscle healing through enhanced regeneration and reduced fibrosis in myostatin-null mice. *Journal of cell science* **118**, 3531-3541
18. Pelosi, L., Giacinti, C., Nardis, C., Borsellino, G., Rizzuto, E., Nicoletti, C., Wannenes, F., Battistini, L., Rosenthal, N., Molinaro, M., and Musarò, A. (2007) Local expression of IGF-1 accelerates muscle regeneration by rapidly modulating inflammatory cytokines and chemokines. *FASEB journal : official publication of the Federation of American Societies for Experimental Biology* **21**, 1393-1402
19. Tidball, J. G. (2005) Inflammatory processes in muscle injury and repair. 345-353
20. Ceafalan, L. C., Popescu, B. O., and Hinescu, M. E. (2014) Cellular Players in Skeletal Muscle Regeneration. *BioMed research international* **2014**, 957014-957014
21. Chargé, S. B. P., and Rudnicki, M. a. (2004) Cellular and molecular regulation of muscle regeneration. *Physiological reviews* **84**, 209-238
22. Armstrong, R. B., Warren, G. L., and Warren, J. A. (1991) Mechanisms of exercise-induced muscle fibre injury. *Sports Med* **12**, 184-207
23. McCully, K. K., and Faulkner, J. A. (1985) Injury to skeletal muscle fibers of mice following lengthening contractions. *J Appl Physiol (1985)* **59**, 119-126
24. Chamberlain, J. S., Jaynes, J. B., and Hauschka, S. D. (1985) Regulation of creatine kinase induction in differentiating mouse myoblasts. *Mol Cell Biol* **5**, 484-492
25. Chakrabarti, S., Kobayashi, K. S., Flavell, R. a., Marks, C. B., Miyake, K., Liston, D. R., Fowler, K. T., Gorelick, F. S., and Andrews, N. W. (2003) Impaired membrane resealing and autoimmune myositis in synaptotagmin VII-deficient mice. *The Journal of cell biology* **162**, 543-549
26. Baresic, M., Salatino, S., Kupr, B., van Nimwegen, E., and Handschin, C. (2014) Transcriptional network analysis in muscle reveals AP-1 as a partner of PGC-1alpha in the regulation of the hypoxic gene program. *Mol Cell Biol* **34**, 2996-3012
27. Allen, D. G., and Whitehead, N. P. (2011) Duchenne muscular dystrophy - What causes the increased membrane permeability in skeletal muscle? *The international journal of biochemistry & cell biology* **43**, 290-294
28. Cai, C., Masumiya, H., Weisleder, N., Matsuda, N., Nishi, M., Hwang, M., Ko, J.-K., Lin, P., Thornton, A., Zhao, X., Pan, Z., Komazaki, S., Brotto, M., Takeshima, H., and

Ma, J. (2009) MG53 nucleates assembly of cell membrane repair machinery. *Nature cell biology* **11**, 56-64
29. Reddy, A., Caler, E. V., and Andrews, N. W. (2001) Plasma membrane repair is mediated by Ca(2+)-regulated exocytosis of lysosomes. *Cell* **106**, 157-169
30. Passey, S., Martin, N., Player, D., and Lewis, M. P. (2011) Stretching skeletal muscle in vitro: does it replicate in vivo physiology? *Biotechnology letters* **33**, 1513-1521
31. Tsivitse, S. K., Mylona, E., Peterson, J. M., Gunning, W. T., Pizza, F. X., Susan, K., and Gunning, T. (2005) Mechanical loading and injury induce human myotubes to release neutrophil chemoattractants. **43606**, 721-729
32. Manabe, Y., Miyatake, S., Takagi, M., Nakamura, M., Okeda, A., Nakano, T., Hirshman, M. F., Goodyear, L. J., and Fujii, N. L. (2012) Characterization of an acute muscle contraction model using cultured C2C12 myotubes. *PLoS One* **7**, e52592
33. Ito, A., Yamamoto, Y., Sato, M., Ikeda, K., Yamamoto, M., Fujita, H., Nagamori, E., Kawabe, Y., and Kamihira, M. (2014) Induction of functional tissue-engineered skeletal muscle constructs by defined electrical stimulation. *Sci Rep* **4**, 4781
34. Boppart, M. D., Burkin, D. J., and Kaufman, S. J. (2006) Alpha7beta1-integrin regulates mechanotransduction and prevents skeletal muscle injury. *Am J Physiol Cell Physiol* **290**, C1660-1665
35. Boppart, M. D., Volker, S. E., Alexander, N., Burkin, D. J., and Kaufman, S. J. (2008) Exercise promotes alpha7 integrin gene transcription and protection of skeletal muscle. *Am J Physiol Regul Integr Comp Physiol* **295**, R1623-1630
36. Proske, U., and Morgan, D. L. (2001) Muscle damage from eccentric exercise: mechanism, mechanical signs, adaptation and clinical applications. *J Physiol* **537**, 333-345
37. Baar, K., Wende, A. R., Jones, T. E., Marison, M., Nolte, L. a., Chen, M., Kelly, D. P., and Holloszy, J. O. (2002) Adaptations of skeletal muscle to exercise: rapid increase in the transcriptional coactivator PGC-1. *FASEB journal : official publication of the Federation of American Societies for Experimental Biology* **16**, 1879-1886
38. Bansal, D., Miyake, K., Vogel, S. S., Groh, S., Chen, C. C., Williamson, R., McNeil, P. L., and Campbell, K. P. (2003) Defective membrane repair in dysferlin-deficient muscular dystrophy. *Nature* **423**, 168-172
39. Gan, B., Hu, J., Jiang, S., Liu, Y., Sahin, E., Zhuang, L., Fletcher-Sananikone, E., Colla, S., Wang, Y. A., Chin, L., and Depinho, R. A. (2010) Lkb1 regulates quiescence and metabolic homeostasis of haematopoietic stem cells. *Nature* **468**, 701-704
40. Nakada, D., Saunders, T. L., and Morrison, S. J. (2010) Lkb1 regulates cell cycle and energy metabolism in haematopoietic stem cells. *Nature* **468**, 653-658
41. Gurumurthy, S., Xie, S. Z., Alagesan, B., Kim, J., Yusuf, R. Z., Saez, B., Tzatsos, A., Ozsolak, F., Milos, P., Ferrari, F., Park, P. J., Shirihai, O. S., Scadden, D. T., and Bardeesy, N. (2010) The Lkb1 metabolic sensor maintains haematopoietic stem cell survival. *Nature* **468**, 659-663
42. Ito, K., Carracedo, A., Weiss, D., Arai, F., Ala, U., Avigan, D. E., Schafer, Z. T., Evans, R. M., Suda, T., Lee, C. H., and Pandolfi, P. P. (2012) A PML-PPAR-delta pathway for fatty acid oxidation regulates hematopoietic stem cell maintenance. *Nat Med* **18**, 1350-1358
43. Carracedo, A., Weiss, D., Leliaert, A. K., Bhasin, M., de Boer, V. C., Laurent, G., Adams, A. C., Sundvall, M., Song, S. J., Ito, K., Finley, L. S., Egia, A., Libermann, T.,

Gerhart-Hines, Z., Puigserver, P., Haigis, M. C., Maratos-Flier, E., Richardson, A. L., Schafer, Z. T., and Pandolfi, P. P. (2012) A metabolic prosurvival role for PML in breast cancer. *J Clin Invest* **122**, 3088-3100

44. Ito, K., Hirao, A., Arai, F., Matsuoka, S., Takubo, K., Hamaguchi, I., Nomiyama, K., Hosokawa, K., Sakurada, K., Nakagata, N., Ikeda, Y., Mak, T. W., and Suda, T. (2004) Regulation of oxidative stress by ATM is required for self-renewal of haematopoietic stem cells. *Nature* **431**, 997-1002
45. Ito, K., Hirao, A., Arai, F., Takubo, K., Matsuoka, S., Miyamoto, K., Ohmura, M., Naka, K., Hosokawa, K., Ikeda, Y., and Suda, T. (2006) Reactive oxygen species act through p38 MAPK to limit the lifespan of hematopoietic stem cells. *Nat Med* **12**, 446-451
46. Shea, K. L., Xiang, W., LaPorta, V. S., Licht, J. D., Keller, C., Basson, M. A., and Brack, A. S. (2010) Sprouty1 regulates reversible quiescence of a self-renewing adult muscle stem cell pool during regeneration. *Cell Stem Cell* **6**, 117-129
47. Chakkalakal, J. V., Jones, K. M., Basson, M. A., and Brack, A. S. (2012) The aged niche disrupts muscle stem cell quiescence. *Nature* **490**, 355-360
48. Schiaffino, S., and Reggiani, C. (2011) Fiber types in mammalian skeletal muscles. *Physiological reviews* **91**, 1447-1531
49. Gibson, M. C., and Schultz, E. (1982) The distribution of satellite cells and their relationship to specific fiber types in soleus and extensor digitorum longus muscles. *Anat Rec* **202**, 329-337
50. Parise, G., McKinnell, I. W., and Rudnicki, M. a. (2008) Muscle satellite cell and atypical myogenic progenitor response following exercise. *Muscle & Nerve* **37**, 611-619
51. Shefer, G., Rauner, G., Yablonka-Reuveni, Z., and Benayahu, D. (2010) Reduced satellite cell numbers and myogenic capacity in aging can be alleviated by endurance exercise. *PLoS One* **5**, e13307
52. Dreyer, H. C., Blanco, C. E., Sattler, F. R., Schroeder, E. T., and Wiswell, R. a. (2006) Satellite cell numbers in young and older men 24 hours after eccentric exercise. *Muscle & nerve* **33**, 242-253
53. Ross, J., Benn, A., Jonuschies, J., Boldrin, L., Muntoni, F., Hewitt, J. E., Brown, S. C., and Morgan, J. E. (2012) Defects in glycosylation impair satellite stem cell function and niche composition in the muscles of the dystrophic Large(myd) mouse. *Stem cells (Dayton, Ohio)* **30**, 2330-2341
54. Facey, K., Bradbury, I., Laking, G., and Payne, E. (2007) Overview of the clinical effectiveness of positron emission tomography imaging in selected cancers. *Health Technol Assess* **11**, iii-iv, xi-267
55. Tulving, E., Kapur, S., Craik, F. I., Moscovitch, M., and Houle, S. (1994) Hemispheric encoding/retrieval asymmetry in episodic memory: positron emission tomography findings. *Proc Natl Acad Sci U S A* **91**, 2016-2020
56. Tillisch, J., Brunken, R., Marshall, R., Schwaiger, M., Mandelkern, M., Phelps, M., and Schelbert, H. (1986) Reversibility of cardiac wall-motion abnormalities predicted by positron tomography. *N Engl J Med* **314**, 884-888
57. Koning, M., Harmsen, M. C., van Luyn, M. J., and Werker, P. M. (2009) Current opportunities and challenges in skeletal muscle tissue engineering. *J Tissue Eng Regen Med* **3**, 407-415
58. Quantin, B., Perricaudet, L. D., Tajbakhsh, S., and Mandel, J. L. (1992) Adenovirus as an expression vector in muscle cells in vivo. *Proc Natl Acad Sci U S A* **89**, 2581-2584

59. Wolff, J. A., Malone, R. W., Williams, P., Chong, W., Acsadi, G., Jani, A., and Felgner, P. L. (1990) Direct gene transfer into mouse muscle in vivo. *Science* **247**, 1465-1468
60. Kessler, P. D., Podsakoff, G. M., Chen, X., McQuiston, S. A., Colosi, P. C., Matelis, L. A., Kurtzman, G. J., and Byrne, B. J. (1996) Gene delivery to skeletal muscle results in sustained expression and systemic delivery of a therapeutic protein. *Proc Natl Acad Sci U S A* **93**, 14082-14087
61. Gregorevic, P., Blankinship, M. J., Allen, J. M., Crawford, R. W., Meuse, L., Miller, D. G., Russell, D. W., and Chamberlain, J. S. (2004) Systemic delivery of genes to striated muscles using adeno-associated viral vectors. *Nat Med* **10**, 828-834
62. Ellis, B. L., Hirsch, M. L., Barker, J. C., Connelly, J. P., Steininger, R. J., 3rd, and Porteus, M. H. (2013) A survey of ex vivo/in vitro transduction efficiency of mammalian primary cells and cell lines with Nine natural adeno-associated virus (AAV1-9) and one engineered adeno-associated virus serotype. *Virol J* **10**, 74
63. Lai, C. M., Lai, Y. K., and Rakoczy, P. E. (2002) Adenovirus and adeno-associated virus vectors. *DNA Cell Biol* **21**, 895-913
64. Lu, Q. L., Bou-Gharios, G., and Partridge, T. A. (2003) Non-viral gene delivery in skeletal muscle: a protein factory. *Gene Ther* **10**, 131-142
65. Tedesco, F. S., Dellavalle, A., Diaz-Manera, J., Messina, G., and Cossu, G. (2010) Repairing skeletal muscle: regenerative potential of skeletal muscle stem cells. *J Clin Invest* **120**, 11-19
66. Lovering, R. M., Porter, N. C., and Bloch, R. J. (2005) The muscular dystrophies: from genes to therapies. *Phys Ther* **85**, 1372-1388
67. Rowe, G. C., Safdar, A., and Arany, Z. (2014) Running forward: new frontiers in endurance exercise biology. *Circulation* **129**, 798-810

10 Acknowledgments

I would like to thank my supervisor Christoph Handschin for giving me the opportunity to work on these exciting projects and for his constructive suggestions, continuous support and optimism. I would also like to express my gratitude to the Werner Siemens Foundation, which enabled me to pursue my PhD at the Biozentrum. My PhD Committee Members, Markus Rüegg and Michael Sinnreich I would like to thank for following the development of my projects, as well as Florian Bentzinger for his valuable input and suggestions.

The conclusion of the experimental part of my PhD was accelerated by the efforts of Markus Beer, who assisted by pipetting countless qPCR plates and helped with various other bits and pieces of experimental work, also contributing a healthy dose of humor.

My start in the lab was much easier thanks to Mario Barešić and Joaquin Perez Schindler, who were always there to jump in and help. Petra Eisele was my go-to person for project-related questions and was very open to discussion. In addition, I would like to thank all of the previous and current members of the Handschin lab for contributing to a friendly atmosphere.

Thanks to the unselfish assistance of Didier Montarras and Perrine Castets, I was able to learn methods concerning myofiber and satellite cell isolation and staining, which I heavily applied during my PhD work. Without Arnaud Ferry and Bilal Azakir, and their expertise that they readily shared, this thesis would lack important data on the functional recovery of muscle after injury and membrane resealing upon laser injury.

Microscopy-related questions and appropriate approaches for analyzing images, I always addressed to Oliver Biehlmaier, Alexia Loynton-Ferrand and Niko Ehrenfeuchter. Daniel Fröhlich provided support with various IT problems.

Last but not least, I would like to thank my family and friends for being there for me and especially my husband Danilo Selić for his extensive help with various computer-related matters and encouragement.